Neuropeptides in the brain of *Cataglyphis nodus* ants and their role as potential modulators of behavior

Neuropeptide im Gehirn von *Cataglyphis nodus* Ameisen und ihre Rolle als potenzielle Modulatoren von Verhalten

Doctoral thesis for a doctoral degree

at the Graduate School of Life Sciences

Julius-Maximilians-Universität Würzburg

Section Integrative Biology

submitted by

Jens Habenstein

from

Schweinfurt

Würzburg 2021

Submitted on: .....
office stamp

Members of the *Promotionskomitee*:

Chairperson: Prof. Dr. Charlotte Förster

Primary Supervisor: Prof. Dr. Wolfgang Rössler

Supervisor (second): PD Dr. Susanne Neupert

Supervisor (third): Prof. Dr. Christian Wegener

Date of Public Defense: .....

Date of Receipt of Certificate: .....

Affidavit

I hereby confirm that my thesis entitled “Neuropeptides in the brain of *Cataglyphis nodus* ants and their role as potential modulators of behavior” is the result of my own work. I did not receive any help or support from commercial consultants. All sources and / or materials applied are listed and specified in the thesis.

Furthermore, I confirm that this thesis has not yet been submitted as part of another examination process neither in identical nor in similar form.

Place, Date Signature

Eidesstattliche Erklärung

Hiermit erkläre ich an Eides statt, die Dissertation “Neuropeptides in the brain of *Cataglyphis nodus* ants and their role as potential modulators of behavior” eigenständig, d.h. insbesondere selbständig und ohne Hilfe eines kommerziellen Promotionsberaters, angefertigt und keine anderen als die von mir angegebenen Quellen und Hilfsmittel verwendet zu haben.

Ich erkläre außerdem, dass die Dissertation weder in gleicher noch in ähnlicher Form bereits in einem anderen Prüfungsverfahren vorgelegen hat.

Ort, Datum Unterschrift

Julius-Maximilians-
UNIVERSITÄT
WÜRZBURG

Graduate School
Life Sciences

"Dissertation Based on Several Published Manuscripts"

Statement of individual author contributions and of legal second publication rights

(If required please use more than one sheet)

Publication (complete reference):

Habenstein J, Amini E, Grübel K, el Jundi B, Rössler W. The brain of *Cataglyphis* ants: neuronal organization and visual projections. Journal of Comparative Neurology. 2020;528(18):3479-506.

Participated in	**Author Initials,** Responsibility decreasing from left to right				
Study Design Methods Development	WR	BeJ	JH	EA	
Data Collection	EA	KG	JH		
Data Analysis and Interpretation	JH	EA	BeJ	WR	KG
Manuscript Writing					
Writing of Introduction	JH	EA	BeJ	WR	
Writing of Materials & Methods	JH	EA	BeJ	WR	
Writing of Discussion	JH	EA	BeJ	WR	
Writing of First Draft	JH	EA	BeJ	WR	

Explanations (if applicable):

Publication (complete reference):

Habenstein J, Schmitt F, Liessem S, Ly A, Trede D, Wegener C, Predel R, Rössler W, Neupert S Transcriptomic, peptidomic and mass spectrometry imaging analysis of the brain in the ant *Cataglyphis nodus*. Journal of Neurochemistry. 2021;158(2):391-412

Participated in	**Author Initials,** Responsibility decreasing from left to right						
Study Design Methods Development	SN	JH	WR	FS	RP	CW	
Data Collection	JH	SN	SL	AL			
Data Analysis and Interpretation	JH	SN	RP	CW	WR	SL	FS
Manuscript Writing							
Writing of Introduction	JH	SN	WR	CW	RP		
Writing of Materials & Methods	JH	SN	WR	CW	RP		
Writing of Discussion	JH	SN	WR	CW	RP		
Writing of First Draft	JH	SN	WR	CW	RP		

Explanations (if applicable):

Publication (complete reference):					
Habenstein J, Thamm M, Rössler W. Neuropeptides as potential modulators of behavioral transitions in the ant *Cataglyphis nodus*. Journal of Comparative Neurology. 2021;529(12):3155-3170.					
Participated in	**Author Initials,** Responsibility decreasing from left to right				
Study Design Methods Development	JH	WR	MT		
Data Collection	JH	MT			
Data Analysis and Interpretation	JH	WR	MT		
Manuscript Writing Writing of Introduction Writing of Materials & Methods Writing of Discussion Writing of First Draft	 JH JH JH JH	 WR WR WR WR	 MT MT MT MT		

Explanations (if applicable):

The doctoral researcher confirms that she/he has obtained permission from both the publishers and the co-authors for legal second publication.

The doctoral researcher and the primary supervisor confirm the correctness of the above mentioned assessment.

Jens Habenstein Würzburg

Doctoral Researcher's Name | Date | Place | Signature

Wolfgang Rössler 

Primary Supervisor's Name | Date | Place | Signature

“Dissertation Based on Several Published Manuscripts“

Statement of individual author contributions to figures/tables/chapters included in the manuscripts

(If required please use more than one sheet)

Publication (complete reference):

Habenstein J, Amini E, Grübel K, el Jundi B, Rössler W. The brain of Cataglyphis ants: neuronal organization and visual projections. Journal of Comparative Neurology. 2020;528(18):3479-506.

Figure	**Author Initials,** Responsibility decreasing from left to right				
1	JH	EA			
2	JH	EA			
3	JH	EA			
4	JH	EA			
5	EA	JH			
6	JH				
7	EA	JH			
8	EA	JH			
9	EA	JH			
10	EA	JH			
11	JH				
12	JH				
13	EA	JH			
14	JH				
Table 1	JH				

Explanations (if applicable):

Publication (complete reference):

Habenstein J, Schmitt F, Liessem S, Ly A, Trede D, Wegener C, Predel R, Rössler W, Neupert S Transcriptomic, peptidomic and mass spectrometry imaging analysis of the brain in the ant Cataglyphis nodus. Journal of Neurochemistry. 2021;158(2):391-412

Figure	**Author Initials,** Responsibility decreasing from left to right				
1	SN				
2	JH				
3	JH	SN			
4	JH	SN			
5	JH				
Table 1	SL	SN			
Table 2	JH	SN			
Table S1	SN	JH			
Table S2	JH				
S1	JH				
S2	JH				
S3	SN	JH			
S4	SN	SL			
S5	SN				
S6	SN				
S7	SN				
S8	JH				

Explanations (if applicable):

Publication (complete reference):

Habenstein J, Thamm M, Rössler W. Neuropeptides as potential modulators of behavioral transitions in the ant *Cataglyphis nodus*. Journal of Comparative Neurology. 2021;529(12):3155-3170.

Figure	**Author Initials,** Responsibility decreasing from left to right				
1	JH				
2	JH				
3	JH				
4	JH				
5	JH				
6	JH				
Table 1	JH				
Table 2	JH				

Explanations (if applicable):

I also confirm my primary supervisor's acceptance.

Jens Habenstein Würzburg

Doctoral Researcher's Name Date Place Signature

“Since time immemorial, human beings have been fascinated, amazed, intrigued, and captivated by ants. And yet, at first glance, there is nothing particularly attractive about the tiny creatures. Unlike butterflies, they don't have wings with vivid colour patterns; they cannot boast the iridescent wing-cases seen on many beetles. Nor do they produce things which human beings like to eat or wear, such as honey or silk. They don't even chirp or sing like crickets or cicadas; and, unlike bees, they never go in for dancing. They do, however, have other characteristics which, in their way, are much more remarkable. For one thing, their social arrangements are quite extraordinary, almost unique among living creatures, and have often been compared to human society.” - LAURENT KELLER & ELISABETH GORDON (The Lives of Ants 2009)

Summary

An adequate task allocation among colony members is of particular importance in large insect societies. Some species exhibit distinct polymorphic worker classes which are responsible for a specific range of tasks. However, much more often the behavior of the workers is related to the age of the individual. Ants of the genus *Cataglyphis* (Foerster 1850) undergo a marked age-related polyethism with three distinct behavioral stages. Newly emerged ants (callows) remain more or less motionless in the nest for the first day. The ants subsequently fulfill different tasks inside the darkness of the nest for up to four weeks (interior workers) before they finally leave the nest to collect food for the colony (foragers).

This thesis focuses on the neuronal substrate underlying the temporal polyethism in *Cataglyphis nodus* ants by addressing following major objectives:

(1) Investigating the structures and neuronal circuitries of the *Cataglyphis* brain to understand potential effects of neuromodulators in specific brain neuropils.
(2) Identification and localization of neuropeptides in the *Cataglyphis* brain.
(3) Examining the expression of suitable neuropeptide candidates during behavioral maturation of *Cataglyphis* workers.

The brain provides the fundament for the control of the behavioral output of an insect. Although the importance of the central nervous system is known beyond doubt, the functional significance of large areas of the insect brain are not completely understood. In *Cataglyphis* ants, previous studies focused almost exclusively on major neuropils while large proportions of the central protocerebrum have been often disregarded due to the lack of clear boundaries. Therefore, I reconstructed a three-dimensional *Cataglyphis* brain employing confocal laser scanning microscopy. To visualize synapsin-rich neuropils and fiber tracts, a combination of fluorescently labeled antibodies, phalloidin (a cyclic peptide binding to filamentous actin) and anterograde tracers was

used. Based on the unified nomenclature for insect brains, I defined traceable criteria for the demarcation of individual neuropils. The resulting three-dimensional brain atlas provides information about 33 distinct synapse-rich neuropils and 30 fiber tracts, including a comprehensive description of the olfactory and visual tracts in the *Cataglyphis* brain. This three-dimensional brain atlas further allows to assign present neuromodulators to individual brain neuropils.

Neuropeptides represent the largest group of neuromodulators in the central nervous system of insects. They regulate important physiological and behavioral processes and have therefore recently been associated with the regulation of the temporal polyethism in social insects. To date, the knowledge of neuropeptides in *Cataglyphis* ants has been mainly derived from neuropeptidomic data of *Camponotus floridanus* ants and only a few neuropeptides have been characterized in *Cataglyphis*. Therefore, I performed a comprehensive transcriptome analysis in *Cataglyphis nodus* ants and identified peptides by using Q-Exactive Orbitrap mass spectrometry (MS) and matrix-assisted laser desorption/ionization time-of-flight (MALDI-TOF) MS. This resulted in the characterization of 71 peptides encoded on 49 prepropeptide genes, including a novel neuropeptide-like gene (fliktin). In addition, high-resolution MALDI-TOF MS imaging (MALDI-MSI) was applied for the first time in an ant brain to localize peptides on thin brain cryosections. Employing MALDI-MSI, I was able to visualize the spatial distribution of 35 peptides encoded on 16 genes.

To investigate the role of neuropeptides during behavioral maturation, I selected suitable neuropeptide candidates and analyzed their spatial distributions and expression levels following major behavioral transitions. Based on recent studies, I suggested the neuropeptides allatostatin-A (Ast-A), corazonin (Crz) and tachykinin (TK) as potential regulators of the temporal polyethism. The peptidergic neurons were visualized in the brain of *C. nodus* ants using immunohistochemistry. Independent of the behavioral stages, numerous Ast-A- and TK-immunoreactive (-ir) neurons innervate important high-order integration centers and sensory input regions with cell bodies dispersed all across the cell body rind. In contrast, only four corazonergic neurons per

hemisphere were found in the *Cataglyphis* brain. Their somata are localized in the *pars lateralis* with axons projecting to the medial protocerebrum and the retrocerebral complex. Number and branching patterns of the Crz-ir neurons were similar across behavioral stages, however, the volume of the cell bodies was significantly larger in foragers than in the preceding behavioral stages. In addition, quantitative PCR analyses displayed increased Crz and Ast-A mRNA levels in foragers, suggesting a concomitant increase of the peptide levels. The task-specific expression of Crz and Ast-A along with the presence in important sensory input regions, high-order integration center, and the neurohormonal organs indicate a sustaining role of the neuropeptides during behavioral maturation of *Cataglyphis* workers.

The present thesis contains a comprehensive reference work for the brain anatomy and the neuropeptidome of *Cataglyphis* ants. I further demonstrated that neuropeptides are suitable modulators for the temporal polyethism of *Cataglyphis* workers. The complete dataset provides a solid framework for future neuroethological studies in *Cataglyphis* ants as well as for comparative studies on insects. This may help to improve our understanding of the functionality of individual brain neuropils and the role of neuropeptides, particularly during behavioral maturation in social insects.

Zusammenfassung

Eine adäquate Aufgabenverteilung unter den Koloniemitgliedern ist in großen Insektengesellschaften von besonderer Bedeutung. Einige Arten weisen polymorphe Arbeiterklassen auf, die jeweils für einen bestimmten Aufgabenbereich zuständig sind. Viel häufiger jedoch steht das Verhalten der Arbeiterinnen im Zusammenhang mit dem Alter der Individuen. Ameisen der Gattung *Cataglyphis* (Foerster 1850) weisen einen ausgeprägten alterskorrelierten Polyethismus auf, der sich durch drei unterschiedliche Verhaltensstadien kennzeichnet. Neu geschlüpfte Ameisen (Callows) verharren den ersten Tag mehr oder weniger bewegungslos im Nest. Anschließend erfüllen die Ameisen in der Dunkelheit des Nestes bis zu vier Wochen lang verschiedene Aufgaben (Interior), bevor sie schließlich das Nest verlassen, um Nahrung für die Kolonie zu sammeln (Forager).

Diese Arbeit konzentriert sich auf die neuronalen Grundlagen, die dem alterskorrelierten Polyethismus bei *Cataglyphis nodus* Ameisen zugrunde liegt, indem folgende Hauptziele verfolgt werden:

(1) Untersuchung der Strukturen und der neuronalen Schaltkreise des *Cataglyphis*-Gehirns, um mögliche Effekte von Neuromodulatoren in spezifischen Hirnneuropilen besser zu verstehen.
(2) Identifizierung und Lokalisierung von Neuropeptiden im Gehirn von *Cataglyphis* Ameisen.
(3) Untersuchung der Expression geeigneter Neuropeptid-Kandidaten im Zuge der Verhaltensreifung von *Cataglyphis* Arbeitern.

Das Gehirn bildet die Grundlage für die Steuerung des Verhaltens von Insekten. Obwohl die tragende Rolle des zentralen Nervensystems für das Verhalten zweifelsfrei bekannt ist, sind die funktionellen Aufgaben großer Bereiche des Insektengehirns nicht vollständig erforscht. Bei *Cataglyphis* Ameisen konzentrierten sich vorangegangene

Studien fast ausschließlich auf die Hauptneuropile, während große Teile des zentralen Protocerebrums mangels klarer Abgrenzungen weitgehend unberücksichtigt geblieben sind. Daher habe ich ein dreidimensionales *Cataglyphis*-Gehirn mit Hilfe der konfokalen Laser-Scanning-Mikroskopie rekonstruiert. Um die synapsinreichen Neuropile und Nerventrakte zu visualisieren, wurde eine Kombination aus fluoreszenzgekoppelten Antikörpern, Phalloidin (ein zyklisches Peptid, das an filamentöses Aktin bindet) und anterograden Tracern verwendet. Basierend auf der einheitlichen Nomenklatur für Insektengehirne definierte ich nachvollziehbare Kriterien für die Abgrenzung der einzelnen Neuropile. Die resultierende dreidimensionale neuronale Karte liefert Informationen über 33 verschiedene synapsinreiche Neuropile und 30 Nerventrakte, einschließlich einer umfassenden Beschreibung der olfaktorischen und visuellen Trakte im *Cataglyphis*-Gehirn. Dieser dreidimensionale Hirnatlas erlaubt es darüber hinaus, die vorhandenen Neuromodulatoren einzelnen Neuropilen des Gehirns zuzuordnen.

Neuropeptide stellen die umfangreichste Gruppe an Neuromodulatoren im zentralen Nervensystem von Insekten dar. Sie regulieren wichtige physiologische Prozesse und Verhaltensweisen und wurden deshalb in jüngerer Vergangenheit mit der Regulation des alterskorrelierenden Polyethismus bei sozialen Insekten in Verbindung gebracht. Bislang wurde das Wissen über Neuropeptide bei *Cataglyphis* Ameisen hauptsächlich aus neuropeptidomischen Daten von *Camponotus floridanus* Ameisen abgeleitet und nur wenige Neuropeptide wurden bei *Cataglyphis* charakterisiert. Daher führte ich eine umfassende Transkriptomanalyse bei *Cataglyphis nodus* Ameisen durch und identifizierte Peptide mit Hilfe der Q-Exactive Orbitrap Massenspektrometrie (MS) und der Matrix-assistierte Laser Desorption-Ionisierung Time-of-Flight (MALDI-TOF) MS. Hierdurch konnten insgesamt 71 Peptide charakterisiert werden, die auf 49 Präpropeptid-Genen kodiert sind, einschließlich eines neuartigen Neuropeptid-ähnlichen Gens (Fliktin). Darüber hinaus wurde das hochauflösende MALDI-TOF MS-Imaging (MALDI-MSI) zum ersten Mal in einem Ameisenhirn angewandt, um Peptide

auf dünnen Hirnkryoschnitten zu lokalisieren. Mittels MALDI-MSI konnte ich die räumliche Verteilung von 35 Peptiden sichtbar machen, die auf 16 Genen kodiert sind.

Um die Rolle der Neuropeptide während der Verhaltensreifung zu untersuchen, wählte ich geeignete Neuropeptid-Kandidaten aus und analysierte deren räumliche Verteilung und Expressionsniveaus im Zuge wichtiger Verhaltensübergänge. Basierend auf aktuellen Studien schlug ich die Neuropeptide Allatostatin-A (Ast-A), Corazonin (Crz) und Tachykinin (TK) als mögliche Regulatoren des alterskorrelierenden Polyethismus vor. Die peptidergen Neurone wurden im Gehirn von *C. nodus* Ameisen mittels Immunhistochemie sichtbar gemacht. Unabhängig von den Verhaltensstadien innervieren die zahlreichen Ast-A- und TK-immunreaktiven (-ir) Neuronen wichtige Integrationszentren höherer Ordnung sowie sensorische Eingangsregionen, während ihre Zellkörper über die gesamte Zellkörperschicht verteilt sind. Im Gegensatz dazu wurden im *Cataglyphis*-Gehirn nur vier corazonerge Neuronen pro Hemisphäre gefunden. Ihre Somata sind in der *Pars lateralis* lokalisiert, deren Axone in das mediale Protocerebrum und den retrozerebralen Komplex projizieren. Anzahl und Verzweigungsmuster der Crz-ir Neuronen waren in allen Verhaltensstadien ähnlich, jedoch war das Volumen der Zellkörper bei Foragern signifikant größer als in den vorangegangenen Verhaltensstadien. Darüber hinaus zeigten quantitative PCR Analysen erhöhte Crz- und Ast-A mRNA-Level in Foragern, was auf einen gleichzeitigen Anstieg der Peptidspiegel schließen lässt. Die aufgabenspezifische Expression von Crz und Ast-A sowie deren Präsenz in wichtigen sensorischen Eingangsbereichen, Integrationszentren höherer Ordnung und den neurohormonellen Organen weisen auf eine tragende Rolle der Neuropeptide während der Verhaltensreifung von *Cataglyphis* Arbeiterinnen hin.

Die vorliegende Arbeit beinhaltet ein umfassendes Nachschlagewerk für die Hirnanatomie und das Neuropeptidom von *Cataglyphis* Ameisen. Zudem konnte ich demonstrieren, dass Neuropeptide geeignete Modulatoren für den alterskorrelierenden Polyethismus von *Cataglyphis* Arbeitern sind. Der komplette Datensatz bietet eine solide Grundlage für zukünftige, neuroethologische Studien an

Cataglyphis Ameisen sowie vergleichenden Studien in Insekten. Hierdurch kann unser Verständnis über die Funktionalität einzelner Hirnneuropile und die Rolle von Neuropeptiden, insbesondere während der Verhaltensreifung sozialer Insekten, in Zukunft verbessert werden.

Table of contents

1 Introduction

1.1 General introduction

There are not many creatures in the world that seem so inconspicuous at first glance and simultaneously receive that much attention from scientists from all over the world than ants. Despite their tiny brains, thousands or even millions of individuals manage to interact as a cohesive unit within a colony [Hölldobler and Wilson, 1990; 2009]. The cooperation of a large number of individuals builds the fundament of their enormous ecological success. Nowadays ants are resident almost all over the globe. They live in all kinds of habitats from the cold steppes of the tundra to the inhospitable deserts of Africa [Hölldobler and Wilson, 2009; Bolton, 2020]. In some of the most biodiverse neotropical rainforests, ants together with termites make up to 30 % of the animal biomass [Fittkau and Klinge, 1973]. On a global scale, it is estimated that ants alone account for approximately 15-20 % of the world's animal biomass [Schultz, 2000]. The sheer number of more than 300 known genera and over 11,000 species further illustrates the global ecological success of ants [Bolton, 2020].

Key to a successful cooperation of large numbers of individuals is an efficient task allocation. The individual subordinates itself to maximize the benefit for the colony. In eusocial insects such as social bees, termites, and ants, this led to the emergence of reproductive and non-reproductive castes. Here, only few reproductive animals focus on producing offspring while the majority of individuals in an insect society represent non-reproductive workers [Hölldobler and Wilson, 1990; 2009]. All workers act together as a collective to feed and defend themselves or to build a suitable nest for the colony. In this process, each worker needs to know what task it has to perform at any given time. In some ant species, fixed worker castes have evolved. In those species, workers are responsible for a specific range of tasks and differ not only in behavior but also in their morphology [Hölldobler and Wilson, 2009]. Well-known examples for this

are major and minor workers in leaf-cutting ants. Whereas major workers are responsible for foraging or the defense of the colony, minors are concerned with tasks inside of the nest, such as growing the symbiotic fungus [Wilson, 1980; 1984; Hughes et al., 2003]. However, in most ant species, task-specific polymorphic worker castes are absent [Hölldobler and Wilson, 2009]. To nevertheless cover the diversity of requirements of an insect society, workers exhibit different response thresholds to distinct stimuli. These differences modify the individual tendency to perform a certain task, resulting in a specific behavioral phenotype [Bonabeau et al., 1998; Theraulaz et al., 1998; Pankiw and Page Jr, 2000; Duarte et al., 2012]. A flexible behavior depending on incoming stimuli allows them to respond appropriately to changing external factors such as the climatic conditions, food availability, or predation pressure [Robinson, 1992]. Although individuals thereby maintain a high degree of behavioral plasticity over their lifetimes, they still often follow an innate sequence of ethocaste stages whereby the behavioral phenotype correlates with the age of the individuals (temporal polyethism). Younger individuals usually fulfill duties inside a nest while older conspecifics leave the nest to forage or defend the colony [Robinson, 1992; Hölldobler and Wilson, 2009]. Leaving the nest and entering a completely foreign environment is probably the greatest challenge in the life of an insect. This drastic behavioral transition is accompanied by diverse changes of neuronal circuits in the brain [e.g., Rössler and Groh, 2012; Fahrbach and Van Nest, 2016; Rössler, 2019]. To preserve the equilibrium within a colony, the correct timing of behavioral transitions plays a crucial role. But what mechanisms orchestrate the age-related behavioral changes in social insects? Many studies have already addressed this question and associated various neuromodulators, such as biogenic amines, hormones, and more recently, also neuropeptides with the modulation of the temporal polyethism in social insects [reviewed by: Hamilton et al., 2017]. Even though the phenomenon is known in many species, the underlying mechanisms are not yet completely understood. Ants of the genus *Cataglyphis* (Foerster 1850) exhibit distinct behavioral stages which are accompanied by remarkable neuronal changes in their brain [reviewed by: Rössler,

2019]. Therefore, *Cataglyphis* ants are favorable experimental models to address the intrinsic mechanisms underlying the temporal polyethism.

1.2 *Cataglyphis* desert ants

Around 100 different *Cataglyphis* species have been described worldwide [Agosti, 1990; Knaden et al., 2012; Bolton, 2020]. Their natural habitats extend over large parts of the Palearctic and predominantly comprise deserts, steppes, scrublands, and Mediterranean landscapes [Agosti, 1990]. *Cataglyphis* ants are perfectly adapted to hot and dry conditions. Due to long legs, their bodies are further above the ground and thus protected from hot surface temperatures of up to more than 60 degrees [Wehner and Wehner, 2011; Sommer and Wehner, 2012]. In addition, the long legs allow faster locomotion speeds and thus more efficient foraging [Hurlbert et al., 2008]. Species of the *bicolor* and *albicans* groups additionally exhibit an upward oriented gaster. This protects the internal organs from the hot ground surface and contributes to better maneuverability [Cerdá, 2001; McMeeking et al., 2012; Boulay et al., 2017]. Moreover, heat shock proteins prevent protein denaturation, allowing the animals to be exposed to greater heat for longer periods without dying [Gehring and Wehner, 1995; Willot et al., 2017].

In addition to morphology and physiology, the behavior of *Cataglyphis* ants has also adapted to the specific conditions of their habitat [reviewed by: Boulay et al., 2017]. In particular during very hot summer days, *Cataglyphis* avoid the midday heat and shift their foraging activities to cooler times of the day [Wehner and Wehner, 2011]. *Cataglyphis* feed mainly on dead arthropods whereby they benefit from the harsh circumstances of the habitat [Wehner et al., 1983]. Due to high temperature and scattered food sources, *Cataglyphis* forage solitarily and do not use trail pheromones to recruit conspecifics [Ruano et al., 2000]. To find their way back to the nest over long distances of up to more than 350 meters [Ronacher, 2008; Buehlmann et al., 2014], the ants employ a remarkable navigational toolkit. Path integration is considered as one of the most important components for their navigation. When searching for food,

direction and distance of the covered path are integrated and a home vector is calculated continuously. The directional information is derived from celestial cues, e.g., the polarization pattern, the position of the sun or the spectral gradient [Wehner, 1997; Wehner and Müller, 2006; Lebhardt and Ronacher, 2014; 2015], whereas information about the distance is obtained by integrating steps and the optical flow [Wittlinger et al., 2006; Pfeffer and Wittlinger, 2016; Wolf et al., 2018]. Together, this information allows foragers to return to their nest in an almost straight line even without further landmarks in the landscape [reviewed by: Ronacher, 2008]. As the computation of a long-distance home vector is vulnerable to cumulative errors [Knaden and Wehner, 2006], *Cataglyphis* ants can additionally use a variety of other stimuli guiding them back to their nest. If available, panoramic features of the environment serve as landmarks for the animals [Wehner and Räber, 1979; Fleischmann et al., 2016]. In addition, olfactory signals, magnetic fields, vibrational signals, and wind can be used for navigation [Müller and Wehner, 2007; Steck et al., 2009; Buehlmann et al., 2012; Buehlmann et al., 2015].

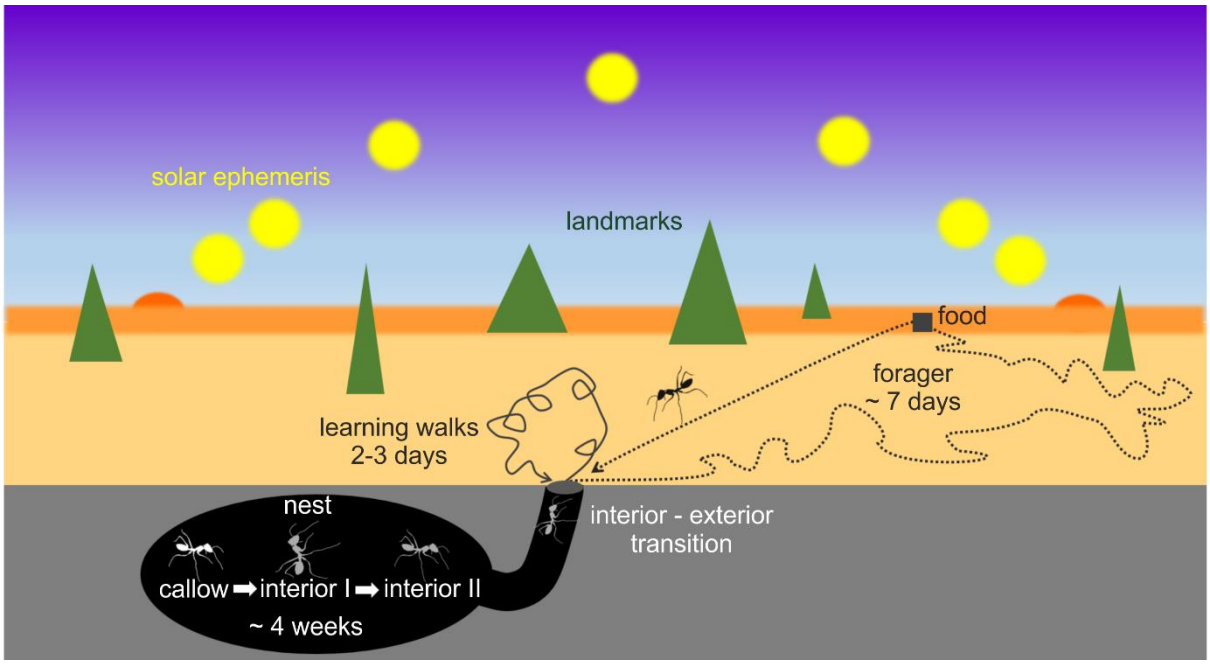

Figure 1: Temporal polyethism in *Cataglyphis* ants. *Cataglyphis* worker undergo several interior stages (callows, interior I, interior II) before they leave the dark nest after approximately 4 weeks. After performing learning walks for up to 3 days, the ants go on long-ranged foraging trips until they die after ~ 7 more days. During learning walks the ants calibrate their navigational toolkit (e.g., solar ephemeris, landmark positions). Adapted from Rössler (2019).

Before *Cataglyphis* workers become excellent navigators and start to forage, they go through several age-related behavioral stages inside of the nest [Schmid-Hempel and Schmid-Hempel, 1984; Figure 1]. Freshly eclosed *Cataglyphis* (callows) are morphologically already fully grown ants. Callows remain largely motionless in the nest and are easily recognizable by a pale pigmentation of their cuticle. After approximately 24 hours, *Cataglyphis* workers serve as repletes (interior I) for the colony. In this period shortly after hatching, the membrane of the cuticle is more elastic and allows to store larger amounts of food. Since interior I workers do not perform any other tasks and their mobility is limited by the swollen gaster, they remain mostly inactive for up to two weeks. Subsequently, workers (interior II) become more active and perform all kinds of indoor duties, such as brood care or nest maintenance [Schmid-Hempel and Schmid-Hempel, 1984; for reviews see: Wehner and Rössler, 2013; Rössler, 2019]. Often before the interior-forager transition occurs, the ants leave the nest for the first time for digging or waste disposal walks. During these short walks, Interior II workers deposit soil or waste particles only a few centimeters out of the nest and immediately return to the secure nest entrance [Fleischmann et al., 2017]. Around four weeks after hatching, naïve ants perform a sequence of learning walks on 2-3 consecutive days before they finally start to forage [Fleischmann et al., 2016; Fleischmann et al., 2017; Figure 1]. Learning walks are typically arranged in circular arcs with ascending radius around the nest entrance. They are important to acquire non-inheritable information about the environment and conditions outside of the nest [Fleischmann et al., 2016; Grob et al., 2017; for reviews see: Collett and Zeil, 2018; Rössler, 2019]. During learning walks, the ants turn back towards the inconspicuous nest entrance using a geomagnetic compass [Fleischmann et al., 2018]. This allows to store the visual information of the panoramic scenery from different heading directions towards their nest. Concomitantly, the learning walks are used to calibrate the daily and seasonally changing course of the sun [reviewed by: Collett and Zeil, 2018; Rössler, 2019; Figure 1]. These adaptations to the new habitat are accompanied by several neuronal modifications in the *Cataglyphis* brain [Stieb et al., 2010; Stieb et al., 2012; Schmitt et al., 2016; Grob et al., 2017]. Once the ants have adjusted their navigational toolkit, they

start foraging. After interior-forager transition, they have a life expectancy of about seven more days [Schmid-Hempel and Schmid-Hempel, 1984]. Despite the extensive neuroethological knowledge, the intrinsic mechanisms underlying the temporal polyethism are still largely unexplored in *Cataglyphis*.

1.3 The *Cataglyphis* brain

The behavior of insects is controlled by the central nervous system [Matthews and Matthews, 2009]. To understand physiological and behavioral processes, it is therefore necessary to know the neuronal substrate underlying these processes. Similar to other observations across species, the requirements of specific habitats and behaviors are reflected in the size and structure of the associated brain neuropils in ants [Gronenberg and Hölldobler, 1999; Gronenberg, 2008]. The ant brain is subdivided into various neuropils that differ in form and functionality (see Figure 2 for an overview of the *Cataglyphis* brain). Essentially, sensory input regions as well as high-order processing and integration sites can be distinguished [reviewed by: Gronenberg, 2008]. The first visual integration center in the ant brain, the optic lobe (OL), consists of lamina, medulla, and lobula. In *Cataglyphis*, the processing of visual stimuli, such as sky polarization patterns or visual landmarks, is of particular importance for navigation [for reviews see: Wehner, 2003; Wehner and Rössler, 2013]. Therefore, the OLs are proportionally larger in the *Cataglyphis* brain than in many other ant species [Gronenberg and Hölldobler, 1999]. Since large parts of intraspecific communication occurs by pheromones in ants, the processing of olfactory information plays a crucial role in most species [Hölldobler, 1999; Jackson and Ratnieks, 2006]. Olfactory stimuli are transmitted from receptors on the antenna via receptor neurons to the glomeruli of the antennal lobe (AL). The AL is the primary olfactory input region and simultaneously the first important odor processing center in the ant brain [Zube et al., 2008; Rössler and Zube, 2011]. Gustatory cues are perceived by chemosensory receptors which are present in several parts of the insect body including the tarsi, the mouth parts, and the antenna [for reviews see: Mitchell et al., 1999; Dahanukar et al.,

2005]. In addition to olfactory and gustatory receptors, the antenna also houses mechanosensory receptors. The latter are located in the Johnston`s organ, an important chordotonal organ of insects. The Johnston`s organ plays a crucial role in the perception of wind, vibration, and gravity [Field and Matheson, 1998; Yack, 2004]. In *Cataglyphis* ants, the Johnston`s organ has additionally been suggested as a potential site for magnetoreception [Fleischmann et al., 2018; Grob et al., 2021]. All non-olfactory receptor neurons of the antenna project to the antennal mechanosensory and motor center (AMMC) and other sensory input regions of the central adjoining neuropils (CANP) [Grob et al., 2021].

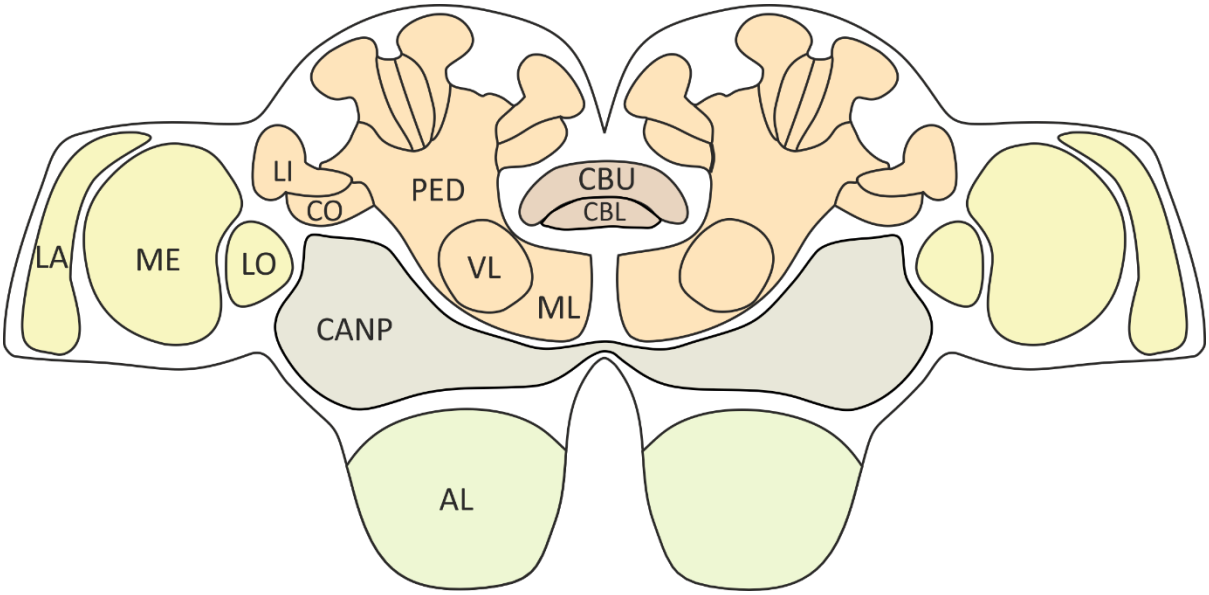

Figure 2: Schematic frontal overview of the *Cataglyphis* brain. The first sensory processing center for visual information are the optic lobes (OL). The OLs comprise three neuropils: the lamina (LA), the medulla (ME), and the lobula (LO). The antennal lobes (AL) receive primary olfactory input from the antenna. Mushroom body (MB) and central complex (CX) are high-order processing and integration sites. The CX consists of an upper (CBU) and lower unit of the central body (CBL), the protocerebral bridge and the noduli (both not shown in the Figure). The MB is subdivided into the calyces, the pedunculus (PED), the vertical - (VL), and the medial lobe (ML). The calyces receive olfactory (lip, LI) and visual information (collar, CO) from the primary sensory processing neuropils. The intrinsic MB neurons (Kenyon cells) innervate the PED and project into the VL and the ML. Protocerebral neuropils which lack clear demarcations are termed central adjoining neuropils (CANP).

After the sensory stimuli are processed in the primary input neuropils, they are transmitted to high-order integration centers of the brain. An important integration center is the mushroom body (MB). The MB consists of medial and lateral calyces, the pedunculus (PED), the vertical-, and the medial lobe. The calyx is a major input region of the MB and can be further subdivided into lip (LI) and collar (CO) in ants. The LI receives olfactory information from the AL, the CO visual information from afferent projections of the OL. The PED mainly houses the many neurites of Kenyon cells, and the lobes are considered as the primary output region of the MB [Gronenberg, 1999; 2001]. In Hymenoptera, the MB is associated with learning and memorizing olfactory and visual information and occupies large proportions of the brain [e.g., Menzel, 1999; 2001; Szyszka et al., 2008; Farris, 2013; 2016]. The function of the MB, as an important learning and memory center, requires a substantial degree of neuronal plasticity. In *Cataglyphis*, structural modifications as well as volume increases could be related to the interior-forager transition [Kühn-Bühlmann and Wehner, 2006; Stieb et al., 2010; Stieb et al., 2012; Grob et al., 2017]. The number of synapses in the calyx increases significantly after learning walks under the full light spectrum from previously naïve workers [Grob et al., 2017]. The MB is therefore proposed as the substrate for learning and memorizing the visual features of the panoramic scenery in *Cataglyphis*.

The central complex (CX) is an unpaired high-order processing and integration center in the middle of the brain and, similar to the MB, of great importance to understand insect behavior [Pfeiffer and Homberg, 2014; Honkanen et al., 2019]. The CX comprises the upper and lower unit of the central body, the protocerebral bridge and the paired noduli. It is regarded as the neuronal substrate of insect navigation and associated with the integration of terrestrial and celestial information, the orientation in space, and motor output [for reviews see: Turner-Evans and Jayaraman, 2016; Honkanen et al., 2019]. Since optical flow information and sky polarization pattern are integrated in the CX, the CX is thought to play a decisive role in path integration [Collett and Collett, 2017; Stone et al., 2017]. Sky compass information is transmitted from the ME via the anterior optic tubercle (AOTU) to the bulbs of the lateral complex (LX) before they are

finally forwarded by GABAergic projections of tangential neurons to the lower unit of the central body [Homberg et al., 2011; el Jundi et al., 2014; Pfeiffer and Homberg, 2014]. In *Cataglyphis* ants, CX and giant synapses within the LX bulbs undergo structural modifications during the interior-forager transition. An increase in the number of giant synapses in the LX bulbs was detected after first light exposure, especially to UV light, and an increase of the CX volume was found after the completion of learning walks [Schmitt et al., 2016; Grob et al., 2017]. These findings support the postulated relevance of both neuropils for celestial navigation in *Cataglyphis* ants reflected by their neuronal plasticity during the interior-exterior transition.

Neuronal studies in *Cataglyphis* are mostly restricted to the well-defined brain regions while other neuropils of the central protocerebrum received less attention in the past. These neuropils, termed CANP, are not demarcated from each other by prominent glial borders and thus, a clear assignment of individual neuropils is challenging. The CANP surround the MB and represent a significant proportion of the insect's brain volume [e.g., Brandt et al., 2005; Ito et al., 2014; Immonen et al., 2017]. Due to their size and input from various sensory information into these regions, the CANPs are thought play important roles in processing and integrating different sensory modalities up to the generation of an adequate behavioral output [e.g., Heinze and Reppert, 2012; Ito et al., 2014; Immonen et al., 2017; von Hadeln et al., 2018; Grob et al., 2021]. To understand the behavior of *Cataglyphis* ants on a neuronal level, it is therefore important to identify and localize the individual regions of CANP and the underlying neuronal circuitry in the brain. This will open up a differentiated insight into the participation of the CANP in physiological processes and behavior and therefore, the potential function of neuromodulators in this brain region.

1.4 Regulation of the temporal polyethism

The regulation of temporal polyethism is a major interest in social insect research. Since diverse internal and external factors orchestrate the behavioral output of social insects, the generation of a certain behavioral stage is a highly complex process (see Figure 3 for an overview). Environmental factors, such as food availability, climate, colony size or demography may influence the timing and quality of behavioral transitions [Robinson, 1992; Yang, 2006; Mersch, 2016]. Although the role of these factors is undisputed, they are not very promising candidates for mediating a particular sequence of behavioral stages. In search for possible mechanisms, several studies linked nutrition and the associated metabolic system with temporal polyethism [reviewed by: Hamilton et al., 2017]. It has been shown that strong nutrient deprivations accelerate the onset of foraging in honey bees [Schulz et al., 1998]. Moreover, the lipid loss in fat bodies is associated with the interior-exterior transition [Toth et al., 2005; Toth and Robinson, 2005]. Due to the close physiological connection with nutrition [Okamoto and Yamanaka, 2015; Lin and Smagghe, 2019], insulin also receives attention in this context. This assumption is supported by studies showing that the gene expression of insulin is related to different behavioral stages of honey bee workers [Whitfield et al., 2003; Ament et al., 2011]. However, the typical correlation between nutrition and insulin signaling is no longer present in adult honey bee workers. Whereas the stable lipid loss shortly before the animals leave the nest is still related to insulin, nutrition and diets only play subordinate roles. Instead, the insulin release of old honey bee worker is controlled by other factors, such as the egg yolk precursor protein vitellogenin (VG) [Ament et al., 2011; Wheeler et al., 2015]. Recent studies, therefore, have suggested that neuromodulators and hormones, such as biogenic amines, neuropeptides, juvenile hormone (JH), and VG are more likely to control behavioral transitions in social insects than insulin or their nutritional physiology [reviewed by: Hamilton et al., 2017].

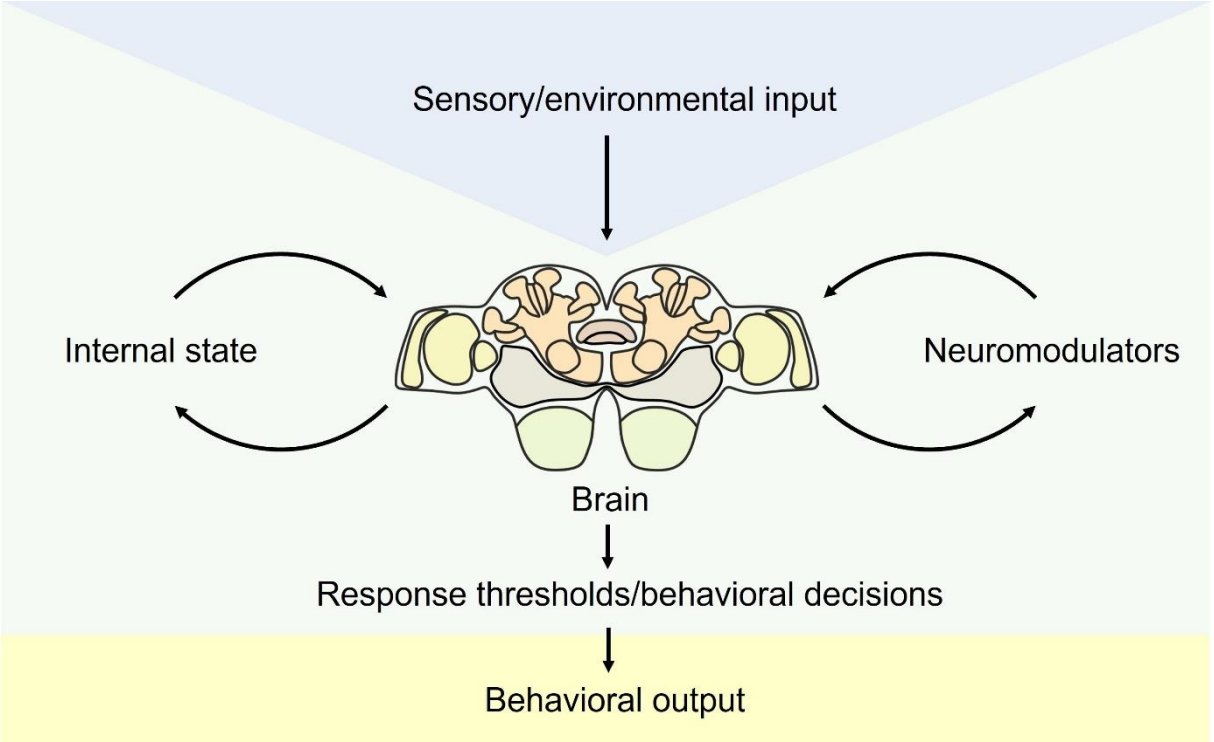

Figure 3: Schematic model describing the emergence of a behavior in social insects. Behavioral output is influenced by various internal and external factors, preserving a high degree of behavioral plasticity. External sensory input (e.g., visual- or olfactory cues) can lead to response threshold overshoots and thus to behavioral changes. External stimuli such as light exposure can further induce sustained neuronal modifications in the brain. The internal state (e.g., saturation, motivation) depends on diverse factors, such as previous experiences, nutrition, or metabolic factors. Both internal state and neuromodulators (e.g., neuropeptides, biogenic amines, hormones) have mutual relationships with neuronal processes in the brain. The interplay of all components results in individual response thresholds and behavioral decisions. Response thresholds and behavioral decisions may differ widely among age-related behavioral stages, resulting in different behavioral phenotypes.

In particular, the role of a dynamic relationship between JH and VG on the onset of foraging has been a target of numerous studies. JH is produced in the *corpora allata* and serves as a general pacemaker during behavioral maturation [Robinson et al., 1989; Robinson and Vargo, 1997]. Treatments with JH or JH analogues lead to precocious foraging in the honey bee, *Apis mellifera* [Robinson, 1985; Jassim et al., 2000] and wasps [Giray et al., 2005; Shorter and Tibbetts, 2009], and induce premature forager-like behavior in the leaf-cutting ant, *Acromyrmex octospinosus* [Norman and Hughes, 2016]. On the contrary, VG acts as a natural repressor of JH in honey bees. Here, VG suppresses the biosynthesis of JH and thus, might indirectly delay the onset of foraging [Guidugli et al., 2005; reviewed by: Harwood et al., 2017]. Although it is known that JH accelerates the interior-forager transition, JH is not essential for the

behavioral changes [reviewed by: Hamilton et al., 2017]. Honey bees , for example, also forage during winter, when their JH level is very low [Huang and Robinson, 1995]. Moreover, even in the absence of JH (after extraction of the *corpora allata*) honey bee workers are able to develop into regular foragers [Sullivan et al., 2000]. Therefore, it remains unclear how diverse behavioral programs are regulated during the behavioral transitions.

Given the complexity of behavioral control and the variety of altered behaviors associated with behavioral transitions in social insects, a crosstalk of different neuromodulators seems obvious. Neuropeptides represent the largest and most diverse group of messenger molecules. Due to their importance in a variety of physiological and behavioral processes [Nässel, 2000; Nässel and Winther, 2010; Kastin, 2013; Nässel and Zandawala, 2019], neuropeptides are highly promising candidates for orchestrating behavioral transitions in social insects. Mature neuropeptides are bioactive cell-cell signaling molecules that can act as neuromodulators at a local level or as neurohormones at a more global level. They are processed from larger precursor proteins (preproproteins) at specific cleavage sites and after further post-translational modification they obtain their bioactive relevance [for reviews see: Fricker, 2012; Nässel and Zandawala, 2019]. As a result of their participation in behaviors that change during behavioral maturation (e.g., locomotion, metabolism, feeding behavior), several neuropeptides have come into focus as potential regulators for the temporal polyethism of social Hymenoptera, such as honey bees or ants [e.g., Pratavieira et al., 2014; Gospocic et al., 2017; Schmitt et al., 2017; Han et al., 2021]. These studies identified three promising neuropeptide candidates in particular: allatostatin-A (Ast-A), corazonin (Crz), and tachykinin (TK). Most functional studies on these neuropeptides have been performed on *Drosophila melanogaster*. There, Ast-A is known for having regulatory functions in sleep, metabolism, feeding, and foraging behavior [Hergarden et al., 2012; Wang et al., 2012; Hentze et al., 2015; Chen et al., 2016]. Additionally, it was shown that Ast-A controls the release of prothoracicotropic hormones (PTTH) and insulin-like peptides. Via these pathways, it

has an indirect impact on growth and maturation of the fruit fly [Deveci et al., 2019]. In some insects, Ast-A is capable to serve as an inhibitor of JH biosynthesis [for reviews see: Weaver and Audsley, 2009; Verlinden et al., 2015; Bendena et al., 2020]. However, the putative allatoregulatory role of Ast-A depends on the species and has not yet been verified for ants. Across species, Ast-A has been found in the AL and is thought to modulate olfactory processes [e.g., Carlsson et al., 2010; Kreissl et al., 2010; Neupert et al., 2012; Christ et al., 2017]. Ast-A was also found in the AL of *Cataglyphis fortis* ants [Schmitt et al., 2017]. The potential function of Ast-A appears to be rather diverse in the honey bee. When injecting Ast-A into the hemolymph of honey bees, this induces aggressive behavior [Pratavieira et al., 2018], leads to impairments in appetitive olfactory learning [Urlacher et al., 2016], and modulates stress reactivity [Urlacher et al., 2019]. TK was shown to be present in various brain neuropils of *C. fortis* [Schmitt et al., 2017]. Functional studies in *Drosophila melanogaster* have demonstrated multiple roles of TK [reviewed by: Nässel et al., 2019b]. For instance, TK is involved in the modulation of nociception [Im et al., 2015], olfactory processes [Winther et al., 2006; Jung et al., 2013; Ko et al., 2015; Gui et al., 2017], lipid metabolism [Song et al., 2014], locomotion, and foraging [Winther et al., 2006; Kahsai et al., 2010] of the fruit fly. In honey bees, TK injections promote aggression [Pratavieira et al., 2018] and decrease the responsiveness of the proboscis extension response (PER) in a task-specific manner [Han et al., 2021]. Recent studies associated Crz with the task specialization in the ponerine ant *Harpegnathos saltator* [Gospocic et al., 2017]. Originally, it was proven that Crz has a cardiostimulatory effect on cockroaches [Veenstra, 1989]. Crz is a highly conserved neuropeptide in insects [Predel et al., 2007]. Unlike Ast-A and TK, only a few corazonergic neurons are found in insect brains studied so far [e.g., Veenstra and Davis, 1993; Roller et al., 2003; Verleyen et al., 2006; Predel et al., 2007; Závodská et al., 2009]. Their somata are typically located in the *pars lateralis* and project to the medial protocerebrum and the retrocerebral complex (RCC). In ants, however, the distribution of corazonergic neurons has not yet been shown. Because of its participation in metabolic [e.g., Kapan et al., 2012; Kubrak et al., 2016] and developmental processes [e.g., Tanaka et al., 2002b; Kim et al., 2004], Crz

may play a crucial role in insect maturation. This has been extensively investigated in locusts. Here, task-related morphological changes could be induced by Crz [Tawfik et al., 1999; Tanaka et al., 2002a; Maeno et al., 2004; Sugahara et al., 2018].

Despite the importance of neuropeptides in controlling behavior, research on neuropeptides in *Cataglyphis* ants is still in its infancy. Initial studies have already tried to link neuropeptides to behavioral transitions in *Cataglyphis* workers [Schmitt et al., 2017], but were restricted to a limited number of known neuropeptides in the *Cataglyphis* brain. Comprehensive peptidomic studies as well as brain localization, quantification, and manipulation studies are therefore necessary to determine the precise role of neuropeptides in the ants' behavior.

2 Thesis outline

Cataglyphis desert ants offer ideal experimental access to study temporal polyethism in an insect society. Their ecology [Schmid-Hempel and Schmid-Hempel, 1984; reviewed by: Wehner and Rössler, 2013] and the accompanying neuronal modifications in the brain [Stieb et al., 2010; Stieb et al., 2012; Schmitt et al., 2016; Grob et al., 2017; reviewed by: Rössler, 2019] have been the target of numerous studies. The present thesis aims to investigate the neuronal basis of temporal polyethism in *Cataglyphis* workers and the role of neuropeptides in this context. In particular, this thesis is focused on the following main questions:

- How is the brain of *Cataglyphis* ants organized in distinct synaptic neuropils?
- How are the brain neuropils interconnected by neuronal tracts? What is the precise organization of visual and olfactory input tracts?
- Which neuropeptides exist in the *Cataglyphis* brain and in which brain neuropils are individual neuropeptides localized?
- Do expression and spatial distribution of the neuropeptides Ast-A, Crz, and TK differ between behavioral stages suggesting a potential role in the regulation of behavioral transitions?

In this thesis these questions will be addressed in following three main chapters:

1. Neuronal organization of the *Cataglyphis* brain
   In the first part of my thesis, the neuronal organization of the brain of *C. nodus* ants was investigated and a detailed three-dimensional atlas was created using immunohistochemistry, tracing techniques, confocal imaging, and computer-guided 3D reconstruction. Brain neuropils and boundaries were defined based on traceable and reproducible criteria, e.g., by using prominent fiber tracts as fixed landmarks. To improve our understanding of the interplay between numerous brain neuropils, the brain fiber bundles system was examined. This includes a comprehensive analysis of the three-dimensional organization of

primary olfactory and visual fibers. The three-dimensional brain atlas provides the basis to assign neuropeptides to individual brain neuropils in the subsequent parts of this thesis.

2. Neuropeptides in the *Cataglyphis* brain

   To explore the role of individual neuropeptides in behavior, it is important to get an overview of the existing neuropeptides and their localization in the ants' brain. The second part of the study was aiming at creating a comprehensive neuropeptidomic dataset in *C. nodus* ants. To achieve this, a transcriptome analysis was performed, and the neuropeptides were identified by mass spectrometrical approaches in the ant brain. Additionally, the spatial distribution of neuropeptides was analyzed by performing mass spectrometry imaging (MSI) in 14 µm thin brain cryosections.

3. Are Ast-A, Crz, and TK regulators of the temporal polyethism in *Cataglyphis*?

   In the third section, the three selected candidate neuropeptide modulators Ast-A, Crz and TK were examined at different age-related behavioral stages in *C. nodus* ants. Immunostainings were used to localize peptidergic neurons in the brain and to highlight differences between individual behavioral stages. Further, the mRNA level of the three neuropeptides following the behavioral transitions was quantified by using quantitative real-time polymerase chain reaction (qPCR) analyses. Based on these findings and taking other social insects into consideration, the putative participation of the neuropeptides in the behavioral maturation of *Cataglyphis* worker is discussed.

Manuscript I

The brain of *Cataglyphis* ants: Neuronal organization and visual projections

Jens Habenstein, Emad Amini, Kornelia Grübel, Basil el Jundi, Wolfgang Rössler

Journal of Comparative Neurology (2020) 528(18):3479-506.

Abstract:

Cataglyphis ants are known for their outstanding navigational abilities. They return to their inconspicuous nest after far-reaching foraging trips using path integration, and whenever available, learn and memorize visual features of panoramic sceneries. To achieve this, the ants combine directional visual information from celestial cues and panoramic scenes with distance information from an intrinsic odometer. The largely vision-based navigation in *Cataglyphis* requires sophisticated neuronal networks to process the broad repertoire of visual stimuli. Although *Cataglyphis* ants have been subjected to many neuroethological studies, little is known about the general neuronal organization of their central brain and the visual pathways beyond major circuits. Here, we provide a comprehensive, three-dimensional brain atlas of synapse-rich neuropils in the brain of *Cataglyphis nodus* including major connecting fiber systems. In addition, we examined neuronal tracts underlying the processing of visual information in more detail. This study revealed a total of 33 brain neuropils and 30 neuronal fiber tracts including six distinct tracts between the optic lobes and the cerebrum. We also discuss the importance of comparative studies on insect brain architecture for a profound understanding of neuronal networks and their function.

Manuscript II

Transcriptomic, peptidomic, and mass spectrometry imaging analysis of the brain in the ant *Cataglyphis nodus*

Jens Habenstein, Franziska Schmitt, Sander Liessem, Alice Ly, Dennis Trede, Christian Wegener, Reinhard Predel, Wolfgang Rössler, Susanne Neupert

Journal of Neurochemistry (2021) 158(2):391-412

Abstract:

Behavioral flexibility is an important cornerstone for the ecological success of animals. Social *Cataglyphis nodus* ants with their age-related polyethism characterized by age-related behavioral phenotypes represent a prime example for behavioral flexibility. We propose neuropeptides as powerful candidates for the flexible modulation of age-related behavioral transitions in individual ants. As the neuropeptidome of *C. nodus* was unknown, we collected a comprehensive peptidomic data set obtained by transcriptome analysis of the ants' central nervous system combined with brain extract analysis by Q-Exactive Orbitrap mass spectrometry (MS) and direct tissue profiling of different regions of the brain by matrix-assisted laser desorption/ionization time-of-flight (MALDI-TOF) MS. In total, we identified 71 peptides with likely bioactive function, encoded on 49 neuropeptide-, neuropeptide-like, and protein hormone prepropeptide genes, including a novel neuropeptide-like gene (fliktin). We next characterized the spatial distribution of a subset of peptides encoded on 16 precursor proteins with high resolution by MALDI MS imaging (MALDI MSI) on 14 µm brain sections. The accuracy of our MSI data were confirmed by matching the immunostaining patterns for tachykinins with MSI ion images from consecutive brain sections. Our data provide a solid framework for future research into spatially resolved qualitative and quantitative peptidomic changes associated with stage-specific behavioral transitions and the functional role of neuropeptides in *Cataglyphis* ants.

Manuscript III

Neuropeptides as potential modulators of behavioral transitions in the ant *Cataglyphis nodus*

Jens Habenstein, Markus Thamm, Wolfgang Rössler

Journal of Comparative Neurology (2021) 529(12):3155-3170.

Abstract:

Age-related behavioral plasticity is a major prerequisite for the ecological success of insect societies. Although ecological aspects of behavioral flexibility have been targeted in many studies, the underlying intrinsic mechanisms controlling the diverse changes in behavior along the individual life history of social insects are not completely understood. Recently, the neuropeptides allatostatin-A, corazonin and tachykinin have been associated with the regulation of behavioral transitions in social insects. Here, we investigated changes in brain localization and expression of these neuropeptides following major behavioral transitions in *Cataglyphis nodus* ants. Our immunohistochemical analyses in the brain revealed that the overall branching pattern of neurons immunoreactive (ir) for the three neuropeptides is largely independent of the behavioral stages. Numerous allatostatin-A- and tachykinin-ir neurons innervate primary sensory neuropils and high-order integration centers of the brain. In contrast, the number of corazonergic neurons is restricted to only four neurons per brain hemisphere with cell bodies located in the *pars lateralis* and axons extending to the medial protocerebrum and the retrocerebral complex. Most interestingly, the cell-body volumes of these neurons are significantly increased in foragers compared to freshly eclosed ants and interior workers. Quantification of mRNA expression levels revealed a stage-related change in the expression of allatostatin-A and corazonin mRNA in the brain. Given the presence of the neuropeptides in major control centers of the brain and the neurohemal organs, these mRNA-changes strongly suggest an

important modulatory role of both neuropeptides in the behavioral maturation of *Cataglyphis* ants.

3 Manuscript I: The brain of *Cataglyphis* ants: Neuronal organization and visual projections

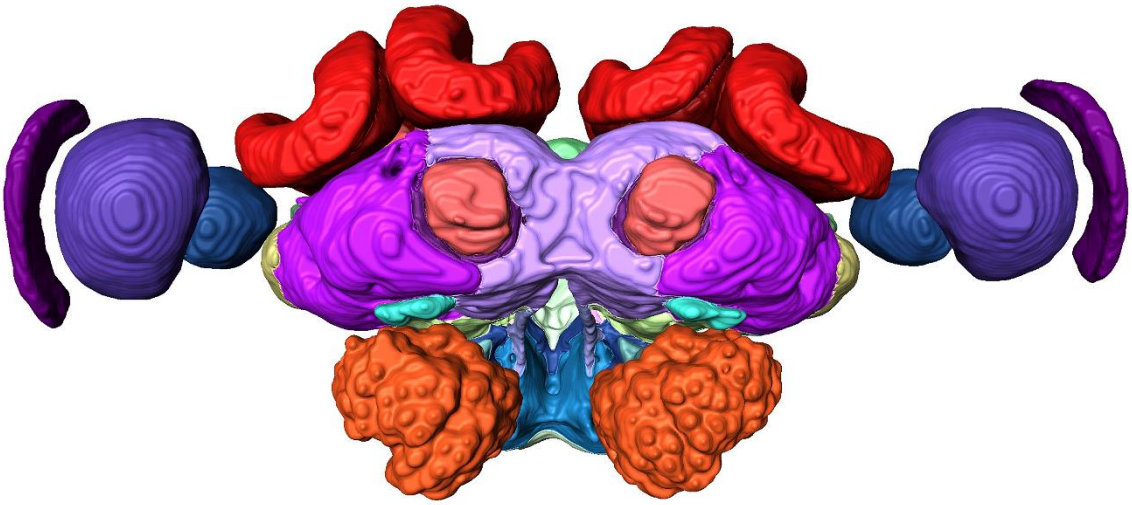

Received: 23 February 2020 | Revised: 15 April 2020 | Accepted: 20 April 2020

DOI: 10.1002/cne.24934

RESEARCH ARTICLE

JCN RESEARCH IN SYSTEMS NEUROSCIENCE THE JOURNAL OF COMPARATIVE NEUROLOGY WILEY

The brain of *Cataglyphis* ants: Neuronal organization and visual projections

Jens Habenstein[1] | Emad Amini[2] | Kornelia Grübel[1] | Basil el Jundi[1] | Wolfgang Rössler[1]

[1]Biocenter, Behavioral Physiology and Sociobiology (Zoology II), University of Würzburg, Würzburg, Germany

[2]Biocenter, Neurobiology and Genetics, University of Würzburg, Würzburg, Germany

Correspondence
Basil el Jundi and Wolfgang Rössler, Biocenter, Behavioral Physiology and Sociobiology (Zoology II), University of Würzburg, Am Hubland, Würzburg 97074, Germany.
Email: basil.el-jundi@uni-wuerzburg.de (B. J.) and roessler@biozentrum.uni-wuerzburg.de (W. R.)

Funding information
Deutsche Forschungsgemeinschaft, Grant/Award Numbers: INST 93/829-1, Ro1177/7-1

Peer Review
The peer review history for this article is available at https://publons.com/publon/10.1002/cne.24934.

Abstract

Cataglyphis ants are known for their outstanding navigational abilities. They return to their inconspicuous nest after far-reaching foraging trips using path integration, and whenever available, learn and memorize visual features of panoramic sceneries. To achieve this, the ants combine directional visual information from celestial cues and panoramic scenes with distance information from an intrinsic odometer. The largely vision-based navigation in *Cataglyphis* requires sophisticated neuronal networks to process the broad repertoire of visual stimuli. Although *Cataglyphis* ants have been subjected to many neuroethological studies, little is known about the general neuronal organization of their central brain and the visual pathways beyond major circuits. Here, we provide a comprehensive, three-dimensional neuronal map of synapse-rich neuropils in the brain of *Cataglyphis nodus* including major connecting fiber systems. In addition, we examined neuronal tracts underlying the processing of visual information in more detail. This study revealed a total of 33 brain neuropils and 30 neuronal fiber tracts including six distinct tracts between the optic lobes and the cerebrum. We also discuss the importance of comparative studies on insect brain architecture for a profound understanding of neuronal networks and their function.

Abbreviations: 5-HT, serotonin; AL, antennal lobe; AMMC, antennal mechanosensory and motor center; AN, antennal nerve; AOT, anterior optic tract; AOTU, anterior optic tubercle; ATL, antler; ASOT, anterior superior optic tract; AVLP, anterior ventrolateral protocerebrum; BU, bulb; CA, calyx; CAN, cantle; CANP, central adjoining neuropil; CB, central body; CBL, central body lower division; CBU, central body upper division; CL, clamp; CO, collar; CRE, crepine; CRG, cerebral ganglion; CX, central complex; FLA, flange; GNG, gnathal ganglion; hVLPF, horizontal ventrolateral protocerebrum fascicle; IB, inferior bridge; IFS, inferior fiber system; INP, inferior neuropil; IOC, inferior optic commissure; IT, isthmus tract; KC, Kenyon cell; LA, lamina; LAL, lateral accessory lobe; LALC, lateral accessory lobe commissure; l-ALT, lateral antennal lobe tract; LCA, lateral calyx; LEF, lateral equatorial fascicle; LI, lip; LH, lateral horn; LO, lobula; LX, lateral complex; m-ALT, medial antennal lobe tract; MB, mushroom body; MBDL, median bundle; ME, medulla; MEF, medial equatorial fascicle; ML, medial lobe; ml-ALT, mediolateral antennal lobe tract; mTUTUT, medial tubercle-tubercle tract; NGS, normal goat serum; NO, noduli; OCT, optical calycal tract; OL, optic lobe; ORN, olfactory receptor neuron; PB, protocerebral bridge; PBS, phosphate-buffered saline; PCT, protocerebral-calycal tract; PED, pedunculus; PENP, periesophageal neuropils; PLF, posterior lateral fascicle; PLP, posterolateral protocerebrum; POC, posterior optic commissure; PRW, prow; PS, posterior slope; PVLP, posterior ventrolateral protocerebrum; SAD, saddle; SFS, superior fiber system; SIP, superior intermediate protocerebrum; SLP, superior lateral protocerebrum; SLPT, superior lateral protocerebral tract; SMP, superior medial protocerebrum; SNP, superior neuropil; SOC, serpentine optic commissure; SPL, serpentine layer; sPLPC, superior posterolateral protocerebrum commissure; TUBUT, tubercle-bulb tract; VL, vertical lobe; VLNP, ventrolateral neuropil; VLP, ventrolateral protocerebrum; VMNP, ventromedial neuropil; vTUTUT, ventral tubercle-tubercle tract; VX, ventral complex.

Jens Habenstein and Emad Amini are co-first authors.

Basil el Jundi and Wolfgang Rössler are senior authors.

KEYWORDS
3D reconstruction, ant brain, antennal lobes, central complex, insect, mushroom bodies, optical tracts

1 | INTRODUCTION

Ants of the genus *Cataglyphis* (Foerster 1850) are thermophilic and live in arid zones of Central and North Africa, the Mediterranean, Middle East, and in Central Asia. Their natural habitats comprise deserts, steppes, and Mediterranean landscapes (Agosti, 1990). Due to high surface temperatures and scarce food sources, *Cataglyphis* ants are solitary foragers and do not employ pheromone trails to recruit nestmates (Ruano, Tinaut, & Soler, 2000). The ants predominantly rely on visual cues during far-reaching foraging trips that may span over remarkable distances (reviewed by: Wehner, 2003; Buehlmann, Graham, Hansson, & Knaden, 2014; Huber & Knaden, 2015). Even in environments that lack distinct panoramic features, *Cataglyphis* foragers find their way back to their nest along an almost straight line using path integration (for reviews, see Ronacher, 2008; Wehner, 2009). For path integration, the distance and directional information have to be continuously updated (and stored) during outbound trips. In *Cataglyphis*, the distance information is encoded by a stride-integration mechanism in combination with optic-flow perception (Pfeffer & Wittlinger, 2016; Wittlinger, Wehner, & Wolf, 2006; Wolf, Wittlinger, & Pfeffer, 2018), and the directional information by celestial cues such as the polarization pattern, the position of the sun, and the spectral gradient (Lebhardt & Ronacher, 2014, 2015; Wehner, 1997; Wehner & Muller, 2006). Even though path integration works without any landmark information, *Cataglyphis* ants use the panoramic skyline and visual landmarks of their surroundings, whenever available, to minimize errors (Collett, Dillmann, Giger, & Wehner, 1992; Wehner, Hoinville, Cruse, & Cheng, 2016; Wehner, Michel, & Antonsen, 1996; Wehner & Räber, 1979). The combination of path integration and landmark guidance generates a robust navigational compass (Knaden & Wehner, 2005) and provides a most successful form of navigation. More recently, *Cataglyphis nodus* (Brullé 1833), the species in the focus of our present study, was shown to use a magnetic compass for calibrating their visual compasses during naïve learning (exploration) walks that the ants perform upon leaving the nest for the first time and before heading out on first foraging trips (Fleischmann, Grob, Müller, Wehner, & Rössler, 2018; reviewed by: Grob, Fleischmann, & Rössler, 2019).

Both path integration and landmark guidance require sophisticated processing and storage of different visual information in the relatively small brain of the ants. Recent studies have mainly focused on two visual pathways—one projects to the central complex (CX), the other to the mushroom bodies (MBs) (for reviews, see Grob et al., 2019; Rössler, 2019). The CX pathway is highly conserved across insects and has been shown to integrate skylight cues such as polarized light and the sun in the brains of locusts (Heinze, 2014; Homberg, 2004; Homberg, Heinze, Pfeiffer, Kinoshita, & el Jundi, 2011; Homberg, Hofer, Pfeiffer, & Gebhardt, 2003), fruit flies (Sancer et al., 2019; Warren, Giraldo, & Dickinson, 2019), dung beetles (el Jundi, Warrant, Pfeiffer, & Dacke, 2018; Immonen, Dacke, Heinze, & el Jundi, 2017), monarch butterflies (Heinze, Florman, Asokaraj, el Jundi, & Reppert, 2013; Heinze & Reppert, 2011), several bee species (Held et al., 2016; Pfeiffer & Kinoshita, 2012; Stone et al., 2017; Zeller et al., 2015), and *Cataglyphis* ants (Grob, Fleischmann, Grübel, Wehner, & Rössler, 2017; Schmitt, Stieb, Wehner, & Rössler, 2016). In all insects investigated so far, sky-compass information is received by photoreceptors in the compound eyes and transmitted from the medulla (ME) of the optic lobe (OL) via the anterior optic tract (AOT) to the anterior optic tubercle (AOTU). Further neuronal projections connect the AOTU to the lateral complex (LX) and, from there, to the CX. The CX integrates different celestial cues (el Jundi, Pfeiffer, Heinze, & Homberg, 2014; Heinze & Homberg, 2007; Homberg et al., 2011) with other sensory information and represents a high-order center for motor control in insects (Guo & Ritzmann, 2013; Martin, Guo, Mu, Harley, & Ritzmann, 2015; Seelig & Jayaraman, 2015; Strauss, 2002). The second pathway to the MB transmits the visual information to be processed in many parallel microcircuits involved in learning and memory formation (for reviews, see Heisenberg, 2003; Menzel, 2014) as well as multisensory integration of stimuli (Kirkhart & Scott, 2015; Lin, Lai, Chin, Chen, & Chiang, 2007; Liu, Wolf, Ernst, & Heisenberg, 1999). As a special feature in Hymenoptera, projection neurons of the ME form a prominent anterior superior optic tract (ASOT) that projects to the collar (CO) region of the MB calyces in both hemispheres of ants (Ehmer & Gronenberg, 2004; Grob et al., 2017; Gronenberg, 1999, 2001; Yilmaz et al., 2016) and bees (Ehmer & Gronenberg, 2002; Gronenberg, 2001; Mobbs, 1984).

Most previous studies focused on these two visual pathways, while a comprehensive description of further visual tracts, their target neuropils in the central brain, and physiological relevance are largely missing in Hymenoptera. The reason for this, most likely, is because many of their target regions in the cerebrum, an area termed central adjoining neuropil (CANP), lack clear boundaries between the enclosed individual neuropil regions. Although the neuropils of the CANP have gained less attention, they probably play as much a role in the processing of visual information as the previously established neuropils, such as the AOTU, MB, or CX. For a similar reason, and to be able to assign other attributes to distinct brain regions, a consortium of insect neuroanatomists introduced a systematic nomenclature for all neuropils and fiber tracts of the insect brain using *Drosophila* as a model insect (Ito et al., 2014). Further studies created 3D maps of the brains of the monarch butterfly (Heinze & Reppert, 2012), the ant *Cardiocondyla obscurior* (Bressan et al., 2015), the dung beetle *Scarabaeus*

lamarcki (Immonen et al., 2017), and, more recently, the desert locust *Schistocerca gregaria* (von Hadeln, Althaus, Häger, & Homberg, 2018).

In this study, we provide a comprehensive map of synapse-rich neuropils and major connecting fiber tracts including all visual pathways in the brain of the thermophilic ant *Cataglyphis nodus*. By means of immunohistochemical staining and anterograde fluorescent tracing, we were able to define and reconstruct 25 paired and 8 unpaired synapse-rich neuropils and found an overall number of 30 connecting fiber tracts. We further labeled and described six major optical tracts and commissures and their projections into the central brain. This extensive neuronal circuitry demonstrates the complexity of the visual system of *Cataglyphis* ants and emphasizes the importance of further studies to understand the complex processing of visual navigational information in the insect brain.

2 | MATERIAL AND METHODS

2.1 | Animals

Cataglyphis nodus colonies were collected at Schinias National Park, Greece (38°80′N, 24°01′E), and Strofylia National Park, Greece (38°15′N, 21°37′E), and transferred to Würzburg. The ants were kept under a 12 hr/12 hr day/night cycle in a climate chamber with constant temperature (24°C) and humidity (30%). The animals had permanent access to water and were fed with honey water (1:2) and dead cockroaches twice per week. For all neuroanatomical studies, *Cataglyphis* workers of unknown age and previous experiences were randomly chosen from queenless colonies.

Please note that in some previous publications, the species name *Cataglyphis nodus* was *Cataglyphis noda*, to match the species with the feminine gender of the genus (for details see Rössler, 2019). As the term *nodus* (latin) is a masculine noun, it should stay unchanged, in opposition to the name of the genus. This is in accordance with Articles 11.9.1.2 and 34.2.1 of the International Code of Zoological Nomenclature of 1999 (B. Bolton, pers. comm.). We therefore use *C. nodus*, as suggested in Rössler (2019).

2.2 | Antibody characterization

To visualize the synaptic neuropils and fiber tracts in *Cataglyphis*, we used a monoclonal antibody to synapsin (SYN-ORF1, mouse@synapsin; kindly provided by E. Buchner and C. Wegener, University of Würzburg, Germany) and fluorescently labeled Alexa Fluor® 488-phalloidin (Invitrogen, Carlsbad, CA; Cat# A12379). The presence of synapsin in presynaptic terminals is highly conserved among invertebrates (Hofbauer et al., 2009; Klagges et al., 1996). The specificity of the antibody has been characterized in *Drosophila* (Klagges et al., 1996) and in the honey bee *Apis mellifera* (Pasch, Muenz, & Rössler, 2011) and its affinity was confirmed in numerous neuroanatomical studies on diverse insect species (Groh & Rössler, 2011; Immonen et al., 2017; von Hadeln et al., 2018) including *Cataglyphis* ants (Schmitt, Stieb, et al., 2016; Schmitt, Vanselow, Schlosser, Wegener, & Rössler, 2016; Stieb, Hellwig, Wehner, & Rössler, 2012; Stieb, Muenz, Wehner, & Rössler, 2010). Phalloidin is a cyclic peptide originating from the fungus *Amanita phalloides*, which binds to filamentous actin, for example, in dendritic tips (Dancker, Low, Hasselbach, & Wieland, 1975; Frambach, Rössler, Winkler, & Schürmann, 2004), and axonal processes (Rössler, Kuduz, Schürmann, & Schild, 2002). It has recently been used to study brain structures in *Cataglyphis* (Schmitt, Stieb, et al., 2016; Stieb et al., 2010). The combination of fluorescently labeled phalloidin and anti-synapsin increased the contrast of tissue structures and, thus, allowed for a more accurate demarcation of the borders within the CANP.

For additional information about the neuropil boundaries and substructures, we used a polyclonal anti-serotonin antibody (rabbit@5-HT; Immunostar, Hudson, WI; Cat# 20080). The specificity of the anti-serotonin antibody was previously tested in dung beetles (Immonen et al., 2017) and its functionality has been demonstrated in diverse insect species (Dacks, Christensen, & Hildebrand, 2006; Falibene, Rössler, & Josens, 2012; Hoyer, Liebig, & Rössler, 2005; Watanabe, Shimohigashi, & Yokohari, 2014; Zieger, Bräunig, & Harzsch, 2013). We used Alexa Fluor® 568-goat@rabbit (Molecular Probes, Eugene, OR; Cat# A11011) and CF633 goat@mouse (Biotium, Hayward, CA; Cat# 20121) as fluorescently labeled secondary antibodies.

2.3 | Immunohistochemistry

Ants were anesthetized on ice before the head was cutoff and fixed in dental wax coated dishes. A small window was cut between the compound eyes of the head, and the brain tissue was dissected out and covered in ice-cold ant ringer saline (127 mM NaCl, 7 mM KCl, 2 mM CaCl2, 7.7 M Na2HPO4, 3.8 M KH2PO4, 4 mM TES, and 3.5 mM trehalose; pH 7.0). For whole-mount staining, the brains were fixated in 4% formaldehyde (FA) in phosphate-buffered saline (PBS) overnight at 4°C. Brains were washed in PBS (3 × 10 min) on the next day and afterward treated with PBS containing Triton-X (2% PBST for 10 min, 0.2% PBST for 2 × 10 min) to facilitate the penetration of the antibodies. After pre-incubation with 2% normal goat serum (NGS) in 0.2% PBST (4°C, overnight), samples were incubated in the primary antibody solution (1:50 anti-synapsin, 2% NGS in 0.2% PBST) for 4 days at 4°C (Table 1). They were rinsed in PBS (3 × 20 min) followed by an incubation in the primary polyclonal antiserum against 5-HT (1:4000 anti-5-HT, 1% NGS in 0.2% PBST) for another 4 days at 4°C. Subsequently, the brains were incubated in the secondary antibody solution (1:250) and phalloidin (1:200) combined with 1% NGS in PBS for 3 days at 4°C. The brains were then washed in PBS (4 × 20 min) and post-fixed overnight in 4% FA in PBS at 4°C. After rinsing with PBS, the samples were dehydrated in an ethanol series (30, 50, 70, 90, 95, 100, and 100% for 3–4 min each step), cleared in methyl salicylate (35 min; M-2047; Sigma Aldrich, Steinheim, Germany) and mounted in Permount (Fisher Scientific, Schwerte, Germany; Cat# 15820100).

TABLE 1 Primary antibodies

Antibody	Immunogen	Manufacturer; species; clonality; Cat #; RRID	Dilution
Synapsin	*Drosophila* Synapsin glutathione-S-transferase fusion protein	E. Buchner, Theodor-Boveri-Institute, University of Würzburg, Germany; mouse; monoclonal; Cat # 3C11 (SYNORF1); RRID: AB_528479	1:50
Serotonin (5-HT)	5-HT coupled to bovine serum albumin with paraformaldehyde	Immunostar, Hudson, WI; rabbit; polyclonal; Cat # 20080; RRID: AB_572263	1:4,000

2.4 | Neuronal tracing

All neuronal tracings were done by using combinations of tetramethylrhodamine-biotin dextran (Microruby, 3,000 MW, lysine fixable; Molecular Probes, Eugene, OR, D-7162) and Alexa Fluor 488 dextran (10,000 MW, lysine fixable; Molecular Probes, Eugene, OR, D-22910). To trace the visual and olfactory tracts, the animals were anesthetized on ice, mounted on a holder and the head and antennae were fixed by using dental wax. A square window was cut into the head capsule, and trachea and glands were removed. Subsequently, the brain was rinsed with ant ringer saline before the fluorescent tracer was injected with a glass capillary into the neuropil of interest. To distinguish between tracts that were stained through injections into the ME and lobula (LO) of the same OL, different fluorescent tracers were used. In addition, the olfactory tracts were analyzed in a different set of brain samples by injecting Microruby into the antennal lobes (ALs). After injection, the injection site was rinsed in ant ringer saline and the head capsule was resealed to avoid dehydration of the brain. For anterograde staining of the antennal nerves (ANs), the antennae were cut close to their base and Microruby was added on the antennae stump. In all cases, the animals were stored in humidified chambers in the darkness for 5 hr to allow the dye to be transported. The brains were afterward dissected and fixated in 4% FA in PBS overnight at 4°C. To visualize the neuropils that are innervated by the visual tracts, the corresponding brains were additionally incubated with anti-synapsin antibody as described above. Finally, all brains were rinsed in PBS (5 × 10 min), dehydrated in an ethanol series (30, 50, 70, 90, 95, 100, 100, and 100%; each step 10 min), cleared in methyl salicylate (35 min), and embedded in Permount.

2.5 | Laser scanning confocal microscopy and image processing

Brain samples were scanned with a confocal laser scanning microscope (either Leica TCS SP2 or Leica TCS SP8, Leica Microsystems AG, Wetzlar, Germany) using a 20× water immersion objective (20.0 × 0.7/0.75 NA). The fluorophores were excited with a wavelength of 488 nm for phalloidin and Alexa Fluor 488 dextran, 568 nm for anti-5-HT and Microruby, and 633 nm for anti-synapsin. All samples were scanned at a step size of 4–6 μm in z-direction and at a resolution of 1,024 × 1,024 pixels in xy-direction. Image stacks were processed using ImageJ (ImageJ 1.52p; Wayne Rasband, NIH, Bethesda, MD) and CorelDRAW X8 (Version 20.1.0.708, Corel Corporation, Ottawa, ON, Canada). If necessary, contrast was adjusted in ImageJ. Pairwise 2D-stitching was performed with the stitching plugin in ImageJ (Preibisch, Saalfeld, & Tomancak, 2009).

2.6 | 3D reconstruction and labeling

Three-dimensional (3D) reconstructions of neuropils and fiber tracts were based on anti-synapsin, anti-5-HT, and phalloidin labeling using the software Amira 2019.1 (FEI, Visualization Sciences Group; Hillsboro, OR; http://thermofisher.com/amira-avizo). In anti-synapsin staining, only synapse-rich regions are stained while most fiber bundles appear as dark regions. On the other hand, phalloidin staining highlights differences of f-actin distributions between fiber tracts and neuropils. The combination of both techniques in whole-mount brains enabled us to better visualize the contours of individual fiber tracts and neuropils. Voxels of the structures of interest were manually labeled in two dimensions in the segmentation editor and, afterward, interpolated using the interpolation tool. The interpolated contours were double checked and manually corrected in case of deviations from the gray values of the image stack. The corresponding 3D models were generated using the SurfaceGen module.

We followed the unified nomenclature for insect brain introduced by Ito et al. (2014) to define known neuropils and fiber tracts. For undescribed structures, we introduced new terms while accurately following the general rules of the nomenclature (Ito et al., 2014). To define the borders of the brain regions of the CANPs, clearly identifiable fiber tracts and neuropils were used as landmarks. In addition, visible structural alterations of the brain tissue and/or serotonergic innervation patterns were used to discriminate between individual neuropils, similar to the technique introduced by Immonen et al. (2017) and Heinze and Reppert (2012). In some cases, no apparent distinction between neuropils was possible. In these cases, the borders were defined based on traceable and reproducible landmark criteria.

The orientation of the *Cataglyphis* brain relative to its body axis is tilted by about 90° in comparison to that of, for example, *Drosophila* (Ito et al., 2014; Pereanu, Kumar, Jennett, Reichert, & Hartenstein, 2010). Consequently, anterior in *Drosophila* appears as dorsal in *Cataglyphis*, posterior as ventral. As the different orientation can be misleading in comparison with other insect brains, this should be kept in mind, especially considering the nomenclature of individual neuropils and their position in the brain (e.g., the superior neuropils [SNPs] are in the anterior brain region in *Cataglyphis*).

3 | RESULTS

3.1 | General layout of the *Cataglyphis* brain

The central brain of Hymenoptera is organized bilaterally, and the protocerebrum, deutocerebrum, and tritocerebrum are fused into one cerebral ganglion (CRG) with less distinct borders (Dettner & Peters, 2011). In *Cataglyphis*, the CRG on its two lateral ends is enclosed by (compared to many other ant species) relatively large OLs (Figure 1a–d,f,g). The distal regions of the OLs are directly attached to the compound eye's retina. The most conspicuous structures of the CRG are the calyces (CAs) of the MBs, which are located at the dorsal tip of the brain

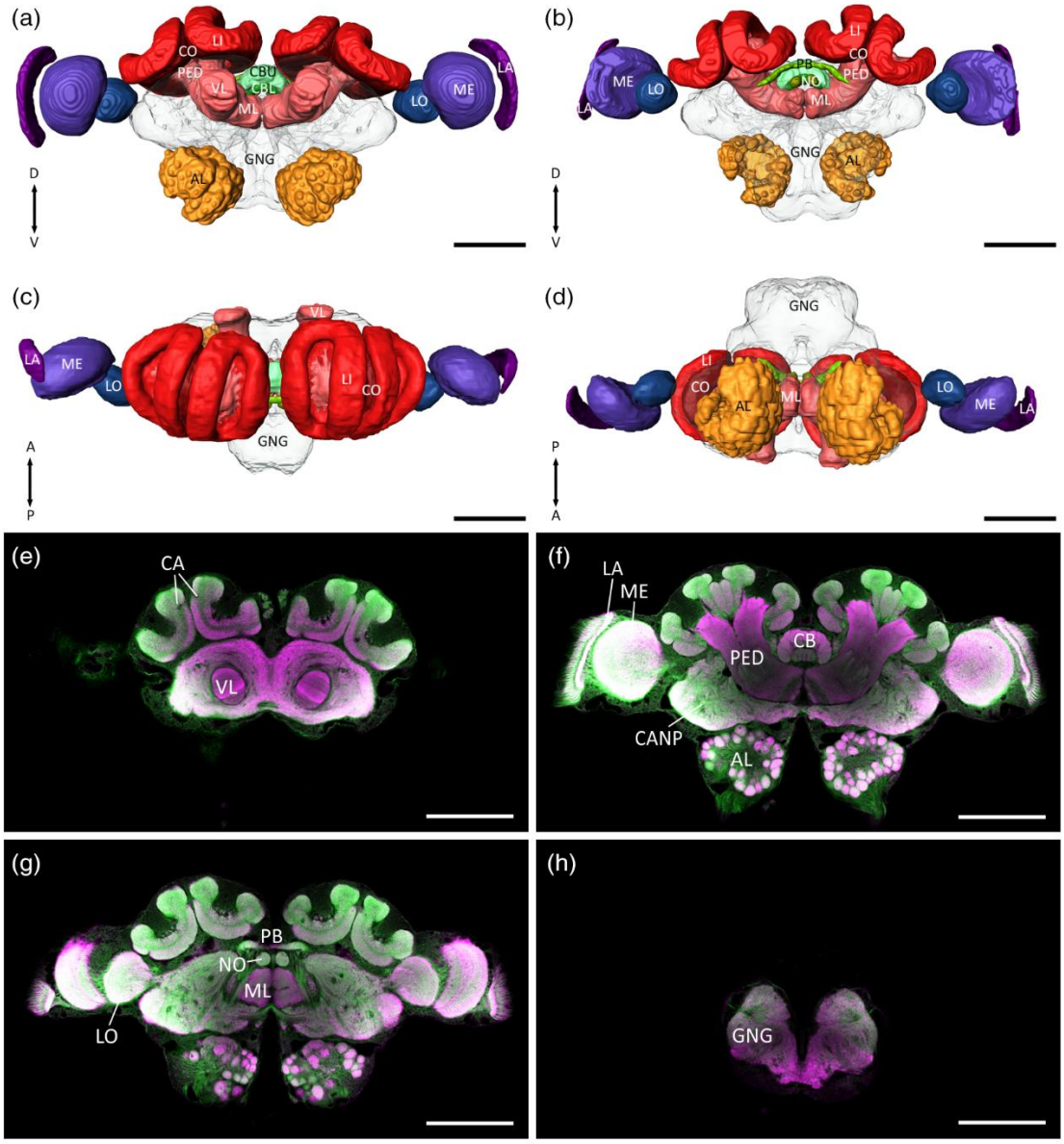

FIGURE 1 General layout of the *Cataglyphis nodus* brain. (a–d) Surface reconstructions of the well-defined brain neuropils include the antennal lobes (ALs), the mushroom bodies (MBs), the optic lobes (OLs), and the central complex (CX). The reconstruction of the neuropils is visualized from different views: (a) anterior, (b) posterior, (c) dorsal, and (d) ventral. The MB can be further subdivided into the calyces (CA), which comprise the collar (CO) and lip (LI), the pedunculus (PED), and the medial and vertical lobes (ML and VL). The CX consists of the central body (CB), the protocerebral bridge (PB), and the noduli (NO), and the optic lobes comprise the lamina (LA), medulla (ME), and lobula (LO). The central adjoining neuropils (CANP, gray) and the gnathal ganglion (GNG, green) are shown as transparent structures. (e–h) Examples of confocal images from anterior (e) to posterior (h) of the whole brain. The preparation was double-stained with anti-synapsin (magenta) and phalloidin (green) to ensure the highest contrast of the fiber bundles and neuropils. Scale bars = 200 μm [Color figure can be viewed at wileyonlinelibrary.com]

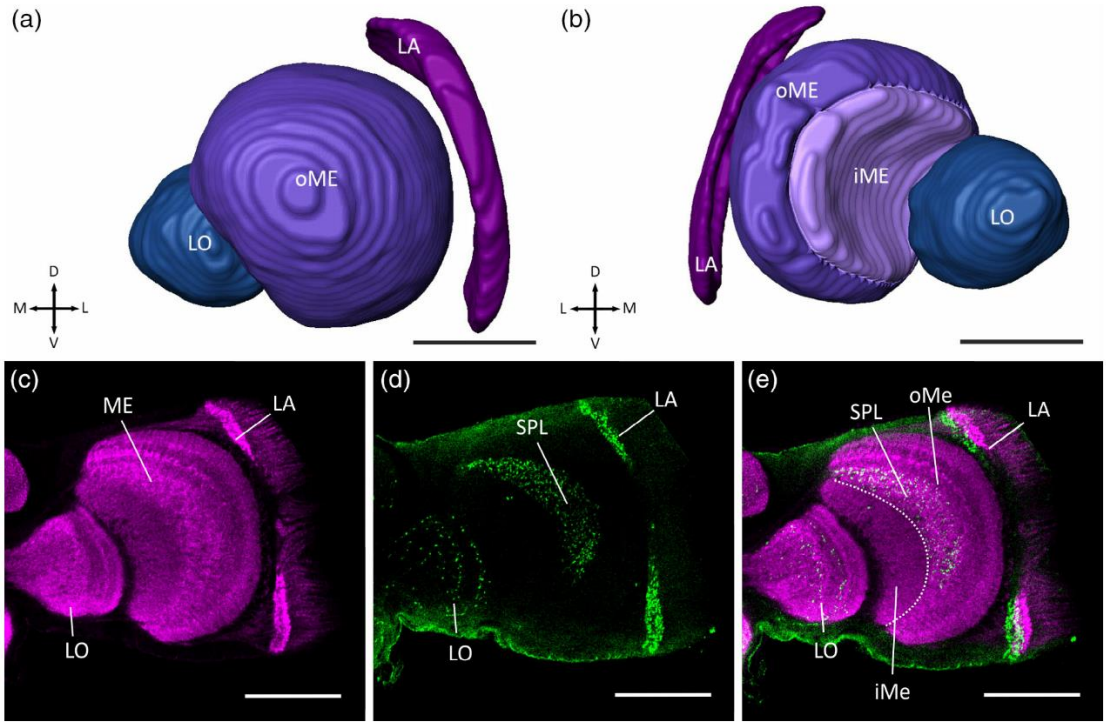

FIGURE 2 The optic lobes of *Cataglyphis nodus*. (a, b) Three-dimensional reconstruction of the optic lobes. The optic lobes consist of the lamina (LA), medulla (ME), and lobula (LO). The medulla can be further subdivided into an inner (iME) and outer medulla (oME): (a) anterior view and (b) posterior view. (c–e) Confocal images of the optic lobes based on anti-synapsin (c, magenta), anti-serotonin (d, green) labeling, or both (e). The serpentine layer (SPL) demarcates the border between iME and oME. Scale bars = 100 μm [Color figure can be viewed at wileyonlinelibrary.com]

(Figure 1a–c,e–g). The ALs contain olfactory glomeruli (Figure 1f,g) and extend to the most ventral regions of the CRG. As in all hymenopteran species (Dettner & Peters, 2011), the gnathal ganglion (GNG) is fused ventrally to the CRG and demarcates the posterior end of the central brain (Figure 1a–d,h). In insects, the GNG comprises three neuromeres: the mandibular, maxillary and labial ganglia, which are fused into one brain region (Scholtz & Edgecombe, 2006). Several neuropils of the central brain are surrounded by glial cells and, thus, exhibit well-defined boundaries. This applies to the ALs, the neuropils of the CX, the MBs, and the neuropils of the OLs—and is consistent with anatomical studies in other insects (Adden, Wibrand, Pfeiffer, Warrant, & Heinze, 2020; Brandt et al., 2005; Bressan et al., 2015; el Jundi, Huetteroth, Kurylas, & Schachtner, 2009; Groothuis, Pfeiffer, el Jundi, & Smid, 2019; Heinze & Reppert, 2012; Immonen et al., 2017; Ito et al., 2014; von Hadeln et al., 2018). The general shape and structural characteristics of these neuropils in the brain of *Cataglyphis nodus* are also similar to the findings in the honey bee (Brandt et al., 2005). The MB and the CX are surrounded by the CANP, which make up a considerable proportion of the *Cataglyphis* brain (Figure 1e–g).

3.2 | Sensory input regions

In contrast to the majority of ant species (Gronenberg, 2008), the OLs represent the largest sensory input area in the brain of *Cataglyphis* (Figure 1). They serve as primary processing centers before the visual information is transferred via projection neurons to high-order processing and integration sites (reviewed by Rössler, 2019). From distal to medial, the OLs consist of the lamina (LA), the ME, and the LO (Figure 2a–c). Based on anti-synapsin and 5-HT staining, the ME can be further subdivided into the inner medulla (iME) and outer medulla (oME). A relatively prominent layer of serotonergic processes demarcates the proximal boundary between the oME and iME (Figure 2d,e). Although tracings indicate that visual information from the dorsal rim area is transmitted via separate paths along dorsal parts of the LA and ME (Grob et al., 2017), no structural features of a distinct dorsal rim area can be localized within the ME or the LA, unlike to what has been shown in some other insects (el Jundi, Pfeiffer, & Homberg, 2011; Pfeiffer & Kinoshita, 2012; Schmeling, Tegtmeier, Kinoshita, & Homberg, 2015; Zeller et al., 2015).

The ALs process the olfactory information from olfactory receptor neurons (ORNs) housed in sensilla on the insect antenna. ORN axons project into the glomeruli of the AL. The ALs of *Cataglyphis nodus* contain around 226 olfactory glomeruli (Figure 1a,b,d,f,g) (for glomerulus numbers, see Stieb, Kelber, Wehner, & Rössler, 2011).

3.3 | High-order processing centers

The MBs are very prominent neuropils in the *Cataglyphis* central brain (Figure 1). The neuroanatomy of the MBs is typical for

Aculeata: each MB consists of a cup-shaped medial and lateral calyx (MCA and LCA), a pedunculus (PED), as well as a medial lobe (ML) and a vertical lobe (VL) (Figures 1 and 3). The MCA and LCA form major input regions of the MB and receive olfactory as well as visual information from afferent projection neurons of the primary sensory neuropils. In *Cataglyphis* each calyx can be subdivided into two subneuropils: the lip (LI) and collar (CO) (Figure 3a,b,d–g). Both LI and CO exhibit characteristic microglomerular structures (Figure 3e–g). Numerous microglomeruli in the visual (LI) and olfactory (CO) subregions of the MB calyx provide thousands of parallel microcircuits forming a rich neuronal substrate for memory formation (Stieb et al., 2012; for reviews, see Rössler, 2019; Groh & Rössler, 2020). In comparison to many other (mostly olfactory guided) ant species (Gronenberg, 1999, 2001), the visual CO is relatively prominent in the *Cataglyphis* MB (Figure 3d–g), further supporting the prominent role of vision. The axons of MB intrinsic neurons (Kenyon cells [KCs]) innervate the PED and terminate in the ML and VL (Figure 3a,b,d,e–g), which are the major output regions

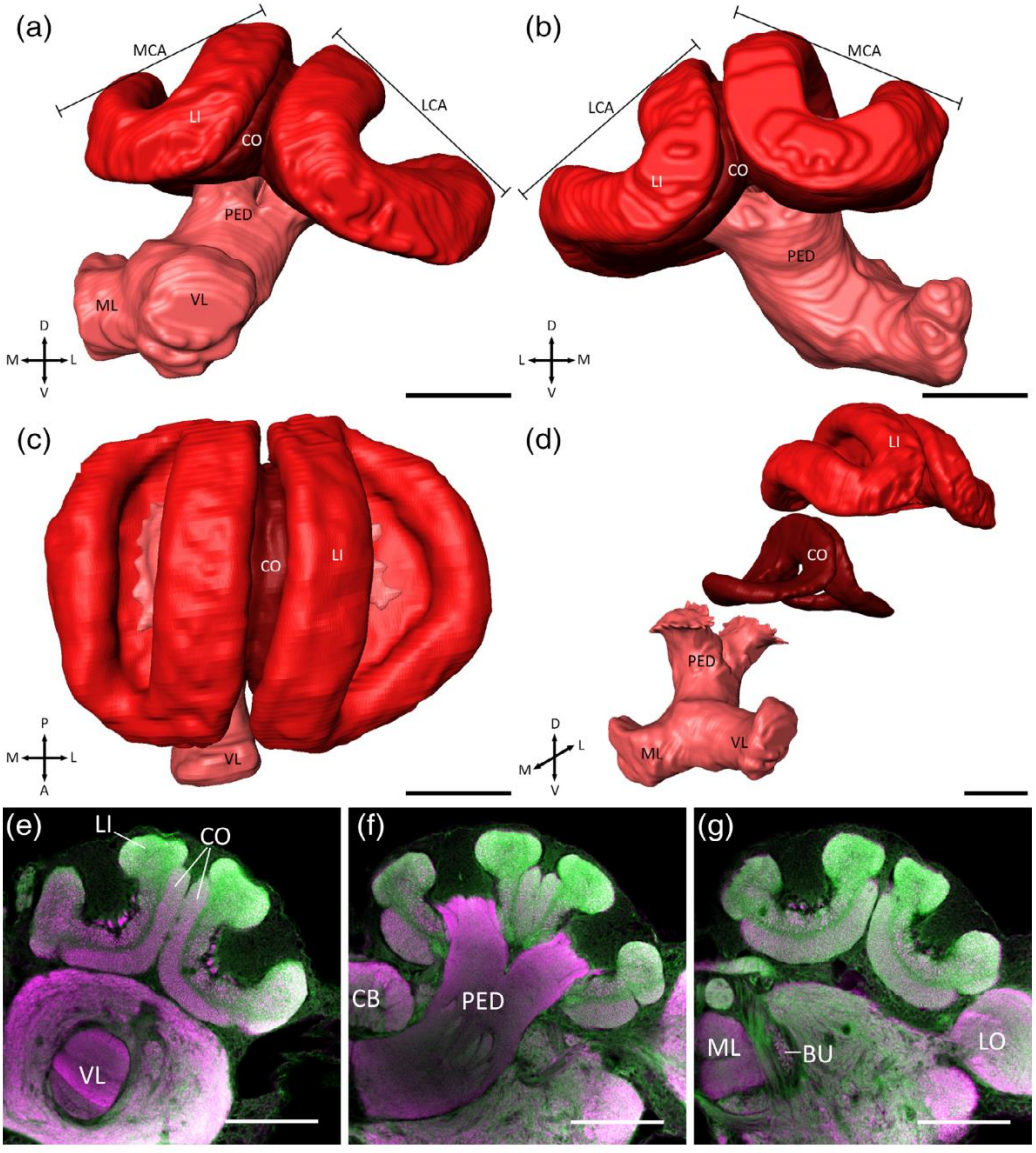

FIGURE 3 The mushroom body (MB) of *Cataglyphis nodus*. The MB consists of the pedunculus (PED), medial and vertical lobes (ML and VL), and the medial and lateral calyces (MCA and LCA). The calyces can be further subdivided into collar (CO) and lip (LI). (a–d) Three-dimensional reconstruction of the MB. (a) Anterior view, (b) posterior view, (c) dorsal view, and (d) oblique anteromedial view of the distinct neuropils of the MB. (e–g) Confocal images of the MB from anterior (e) to posterior (g) of a whole-mount preparation (anti-synapsin: magenta; phalloidin: green). Scale bars = 100 μm. BU, bulb; LO, lobula [Color figure can be viewed at wileyonlinelibrary.com]

of the MBs (Farris, 2005; Li & Strausfeld, 1997; Strausfeld, Homburg, & Kloppenberg, 2000; Strausfeld, Sinakevitch, Brown, & Farris, 2009). In *Cataglyphis*, the ML is in the inferior region of the brain, ventral to the CX (Figure 3f,g), while the VL extends in a perpendicular angle toward the anterior brain surface and forms, together with SNPs, the anteriormost structures of the brain (Figure 3a,d,e). On its lateral side, the VL is connected to the calyces by the protocerebral-calycal tract (PCT), which represents an intrinsic feedback circuit of the MB (Figure 5a,e). GABAergic PCT-neurons have been characterized most extensively in honey bees (Grünewald, 1999; Haehnel & Menzel, 2010; Mobbs, 1982) and may be a general feature of hymenopteran MBs.

Sky-compass information converges in the CX before being passed on to premotor centers (Schmitt, Stieb, et al., 2016; Grob et al., 2017; reviewed by: Rössler, 2019). As in other insects, the CX is positioned at the brain midline (Figure 1). It is composed of four distinct neuropils: the upper (CBU) and lower division (CBL) of the central body (CB), the paired noduli (NO), and the protocerebral bridge (PB) (Figure 4). The CBU is often referred to as the fan-shaped body and the CBL as ellipsoid body. The anteriormost neuropil of the CX is the CBU. To its posterior end, it mounts dorsally on top of the CBL. Both neuropils are located medial to the pedunculi and superior to the MLs of the MBs (Figure 7e–h). More posterior in the brain lies the PB (Figure 7i–k). The only paired structures of the CX in ants are the NO (Figures 4b,d, and 7i).

3.4 | Central adjoining neuropils

In contrast to the major neuropils, the individual regions within the CANP are mostly unsheathed by glial processes and possess less distinct borders in the insect brain (Ito et al., 2014). To define neuropil boundaries, we used prominent fiber bundles as discernable landmarks, as it has also been done in previous work on other insects (Heinze & Reppert, 2012; Immonen et al., 2017; von Hadeln et al., 2018). We first localized and reconstructed the fiber tracts in the *Cataglyphis* brain (Figure 5) to further determine the ambiguous areas of the CANP. The output pathways of the ALs have been studied in detail, in particular in honey bees and are described as a dual olfactory pathway (Kirschner et al., 2006; reviewed by: Galizia & Rössler, 2010; Rössler & Brill, 2013). In *Cataglyphis*, we found five output tracts, termed antennal lobe tracts (ALTs), which transfer the olfactory information via projection neurons to higher brain regions: the medial (m-ALT), the lateral (l-ALT), and three mediolateral tracts (ml-ALT; Figure 6a). The ml-ALTs are considerably thinner and extend their arborizations into some CANP: the ventrolateral neuropils (VLNP), the superior intermediate protocerebrum (SIP) and the lateral horn (LH, Figure 6a,c). In contrast, the m-ALT and the l-ALT are two of the largest fiber bundles in the entire brain. Both tracts project into the ipsilateral LI and LH (Figure 6a, b). While the m-ALT first passes through the LI of the CA (and afterward into the LH), the l-ALT enters the LH first (Figure 6a,b), similar to the findings in the honey bee and in *Camponotus floridanus* (Kirschner et al., 2006; Zube, Kleineidam, Kirschner, Neef, & Rössler, 2008).

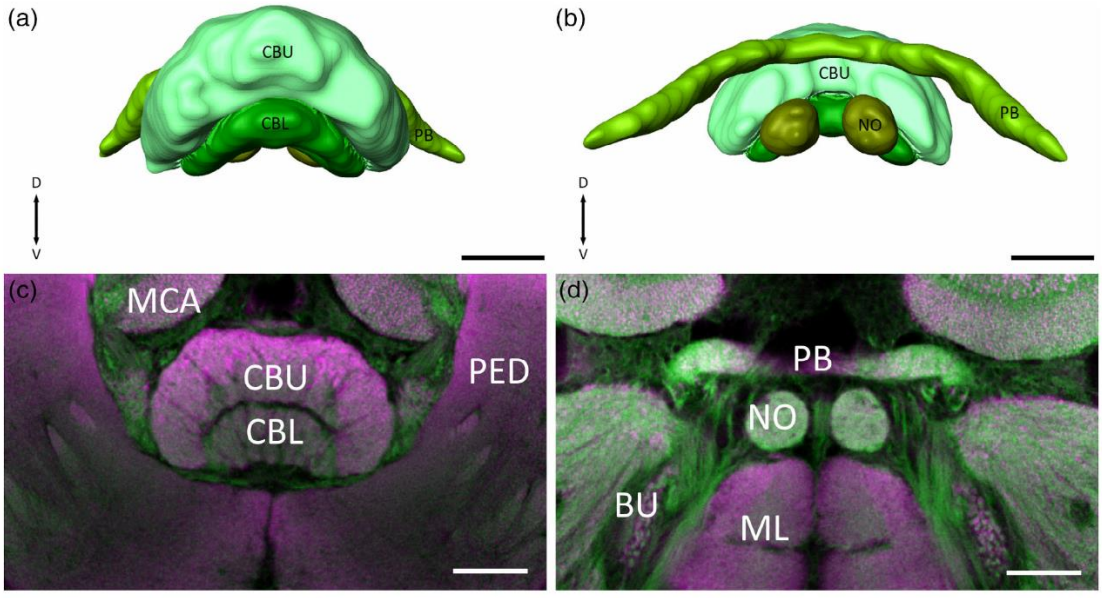

FIGURE 4 The central complex (CX) of *Cataglyphis nodus*. The CX consists of the upper (CBU) and lower divisions (CBL) of the central body, the protocerebral bridge (PB), and the paired noduli (NO). (a, b) Three-dimensional reconstructions of the central complex: (a) anterior view and (b) posterior view. (c, d) Confocal images of the CX from anterior (c) to posterior (d) in a whole-mount preparation. The preparation was double-stained with anti-synapsin (magenta) and phalloidin (green). Scale bars = 50 μm. BU, bulb; MCA, medial calyx; ML, medial lobe; PED, pedunculus [Color figure can be viewed at wileyonlinelibrary.com]

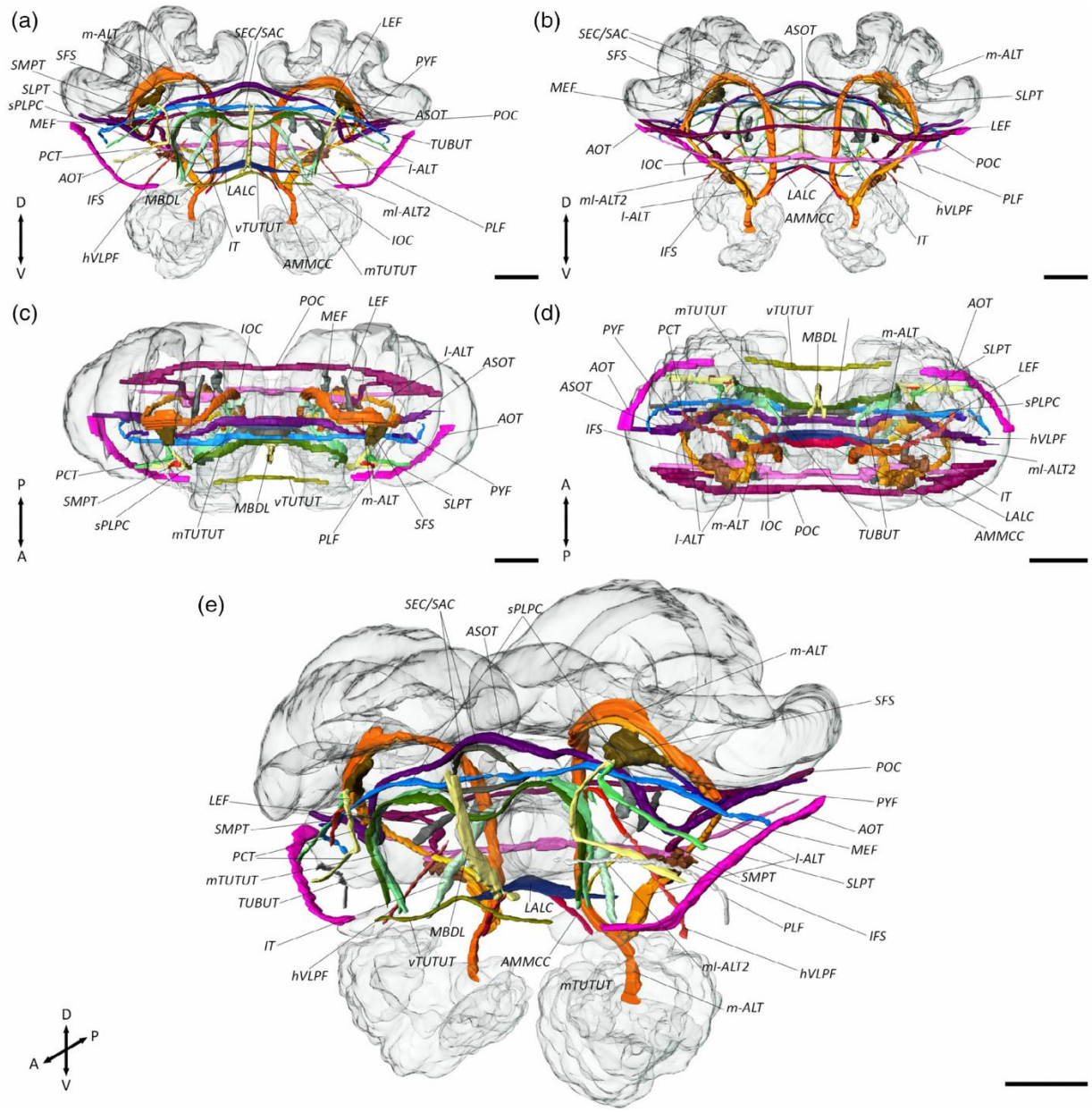

FIGURE 5 Three-dimensional reconstruction of important fiber bundles in the *Cataglyphis nodus* brain. Only tracts and commissures that could be clearly localized and identified based on anti-synapsin and f-actin phalloidin staining were reconstructed. The mushroom bodies, the central complex, and the antennal lobes are shown in transparent. (a) Anterior view; (b) posterior view; (c) dorsal view; (d) ventral view; (e) oblique anterolateral view. Scale bars = 100 μm. AMMCC, antennal mechanosensory and motor center commissure; AOT, anterior optic tract; ASOT, anterior superior optic tract; hVLPF, horizontal ventrolateral protocerebrum fascicle; IFS, inferior fiber system; IOC, inferior optic commissure; IT, isthmus tract; LALC, lateral accessory lobe commissure; l-ALT, lateral antennal lobe tract; LEF, lateral equatorial fascicle; m-ALT, medial antennal lobe tract; MBDL, median bundle; MEF, medial equatorial fascicle; ml-ALT, mediolateral antennal lobe tract; mTUTUT medial tubercle-tubercle tract; PCT, protocerebral-calycal tract; PLF, posterior lateral fascicle; POC, posterior optic commissure; PYF, pyriform fascicle; SEC/SAC, superior ellipsoid/arch commissure; SFS, superior fiber system; SLPT, superior lateral protocerebrum tract; SMPT, superior medial protocerebrum tract; sPLPC, superior posterolateral protocerebrum commissure; TUBUT, tubercle-bulb tract; vTUTUT, ventral tubercle-tubercle tract [Color figure can be viewed at wileyonlinelibrary.com]

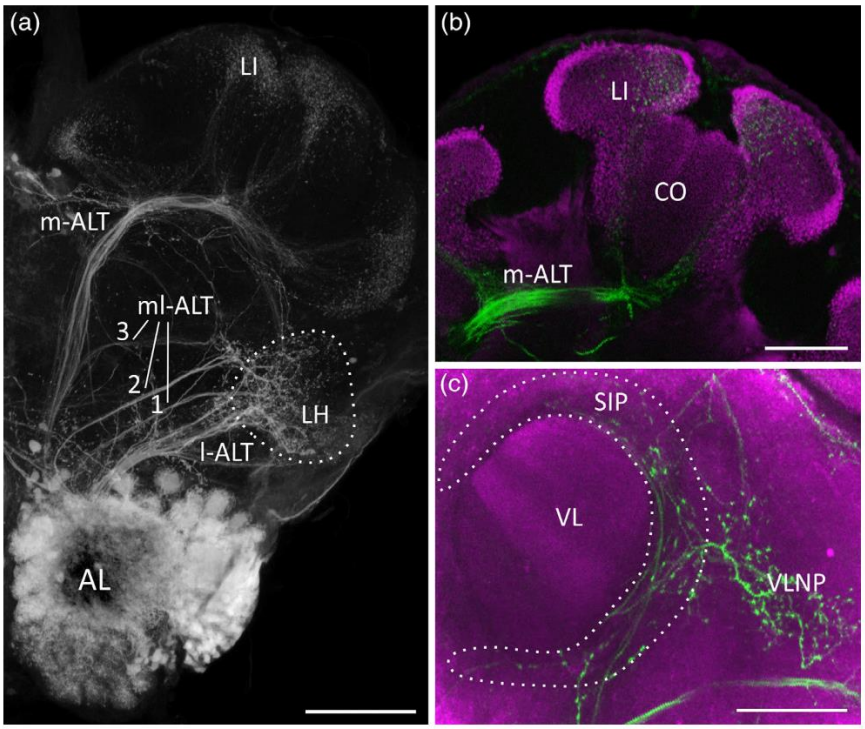

FIGURE 6 Projections from the antennal lobes (ALs) into the central brain. Anterograde staining was obtained by microruby injections (gray/green) into the AL. The pre-synapses are visualized with anti-synapsin labeling (magenta; b, c). (a) Overview of the antennal lobe tracts. The medial antennal lobe tract (m-ALT) and lateral antennal lobe tract (l-ALT) project into the lateral horn (LH) and the lip (LI) of the mushroom body (MB). The mediolateral antennal lobe tracts (ml-ALT) 1–3 project into different parts of the central adjoining neuropils including the LH. Z-projection from a stack of 27 images with 5 μm step size. (b) Projections of the ALTs into the LI. Z-projection from a stack of seven images with 5 μm step size. (c) Projections of the ALTs into the ventrolateral neuropils and the superior intermediate protocerebrum. Z-projection from a stack of 11 images with 5 μm step size. Scale bars = 100 μm (a) and 50 μm (b, c) [Color figure can be viewed at wileyonlinelibrary.com]

With the help of these tracts as crucial landmarks, the CANP can be subdivided in different brain regions that include the AOTU, the LX, the SNP, the inferior neuropils (INP), the ventromedial neuropils (VMNP), the LH, the VLNP, and the periesophageal neuropils (PENP). Overall, we defined 15 paired and 5 unpaired neuropils in the central adjoining brain region (Figures 7 and 8).

3.5 | Anterior optic tubercle

The AOTU is an important high-order visual processing center in insects. As demonstrated in previous studies on locusts, butterflies and honey bees, the AOTU is involved in processing polarized-light information (el Jundi & Homberg, 2012; Heinze & Reppert, 2011; Pfeiffer, Kinoshita, & Homberg, 2005) and chromatic cues (Kinoshita, Pfeiffer, & Homberg, 2007; Mota, Gronenberg, Giurfa, & Sandoz, 2013; Pfeiffer & Homberg, 2007). In *Cataglyphis*, the AOTU is located superficially in the ventrolateral brain region (Figures 7a,b and 8a) and can be subdivided into two compartments: the upper and the lower subunits (Figure 9a). Projection neurons of the tubercle-bulb tract (TUBUT) transmit the visual information from the AOTU to the ipsilateral bulb (BU, Figure 9a). Before the axons finally terminate in the BU, they project around the VL superiorly and pass by the SIP, the antler (ATL), and the clamp (CL). In addition, the AOTUs of both hemispheres are interconnected by the medial tubercle-tubercle tract (mTUTUT) and the ventral tubercle-tubercle tract (vTUTUT, Figure 9a). The mTUTUT neurons originate from the TUBUT. After passing the VL, they bifurcate from the TUBUT and cross the midline through the ATL, anteroventral to the CBU. In contrast to the mTUTUT neurons, the vTUTUT neurons connect the upper subunits along an almost straight course at the inferiormost border of the superior medial protocerebrum (SMP). Similar intertubercle tracts have been previously described in honey bees (Mota, Yamagata, Giurfa, Gronenberg, & Sandoz, 2011), bumblebees (Pfeiffer & Kinoshita, 2012), and locusts (el Jundi et al., 2011; el Jundi & Homberg, 2012; Pfeiffer et al., 2005), implying a general characteristic of the interconnection of the AOTUs.

3.6 | Lateral complex

The LX consists of the lateral accessory lobe (LAL) and the bulb (BU) in *Cataglyphis*. The BU is recognizable by its very large

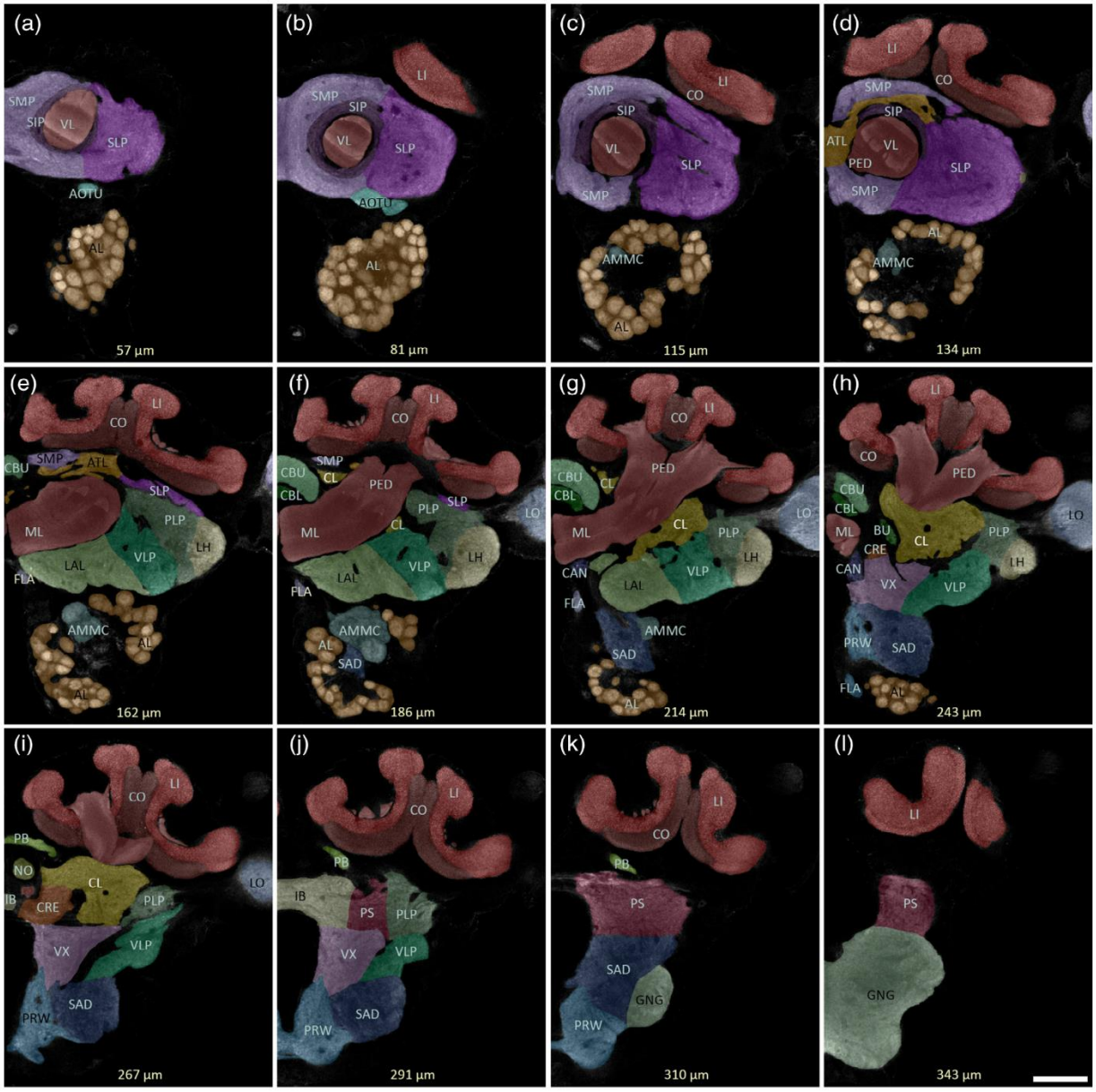

FIGURE 7 Confocal images (anterior view) of the neuropils of the central brain of *Cataglyphis nodus*. The optical sections (anti-synapsin staining) are shown from anterior (a) to posterior (l). Individual neuropils were labeled with transparent colors to demarcate their boundaries. Scale bar = 100 µm. AL, antennal lobe; AMMC, antennal mechanosensory and motor center; AOTU, anterior optic tubercle; ATL, antler; BU, bulb; CAN, cantle; CBL, central body lower division; CBU, central body upper division; CL, clamp; CO, collar; CRE, crepine; FLA, flange; GNG, gnathal ganglion; IB, inferior bridge; LAL, lateral accessory lobe; LH, lateral horn; LI, lip; LO, lobula; ML, medial lobe; NO, noduli; PB, protocerebral bridge; PED, pedunculus; PLP, posterolateral protocerebrum; PRW, prow; PS, posterior slope; SAD, saddle; SIP, superior intermediate protocerebrum; SLP, superior lateral protocerebrum; SMP, superior medial protocerebrum; VL, vertical lobe; VLP ventrolateral protocerebrum; VX, ventral complex [Color figure can be viewed at wileyonlinelibrary.com]

microglomerular synaptic structures (Figures 3g and 4d) and presents a prominent synaptic relay of the sky-compass pathway (el Jundi et al., 2018; Grob et al., 2017; Heinze & Reppert, 2011; Held et al., 2016; Homberg et al., 2003; Pfeiffer & Kinoshita, 2012; Schmitt, Stieb, et al., 2016). The BU receives sensory information from the AOTU by extrinsic neurons innervating the TUBUT (Figure 9a). The *Cataglyphis* brain exhibits only one single BU per hemisphere which is positioned ventrolateral to the CB (Figure 7h). Its medial border is demarcated by the isthmus tract (IT), which connects the LAL with the CB (Figure 9a). The LAL lies inferior to the PED and the CL and more

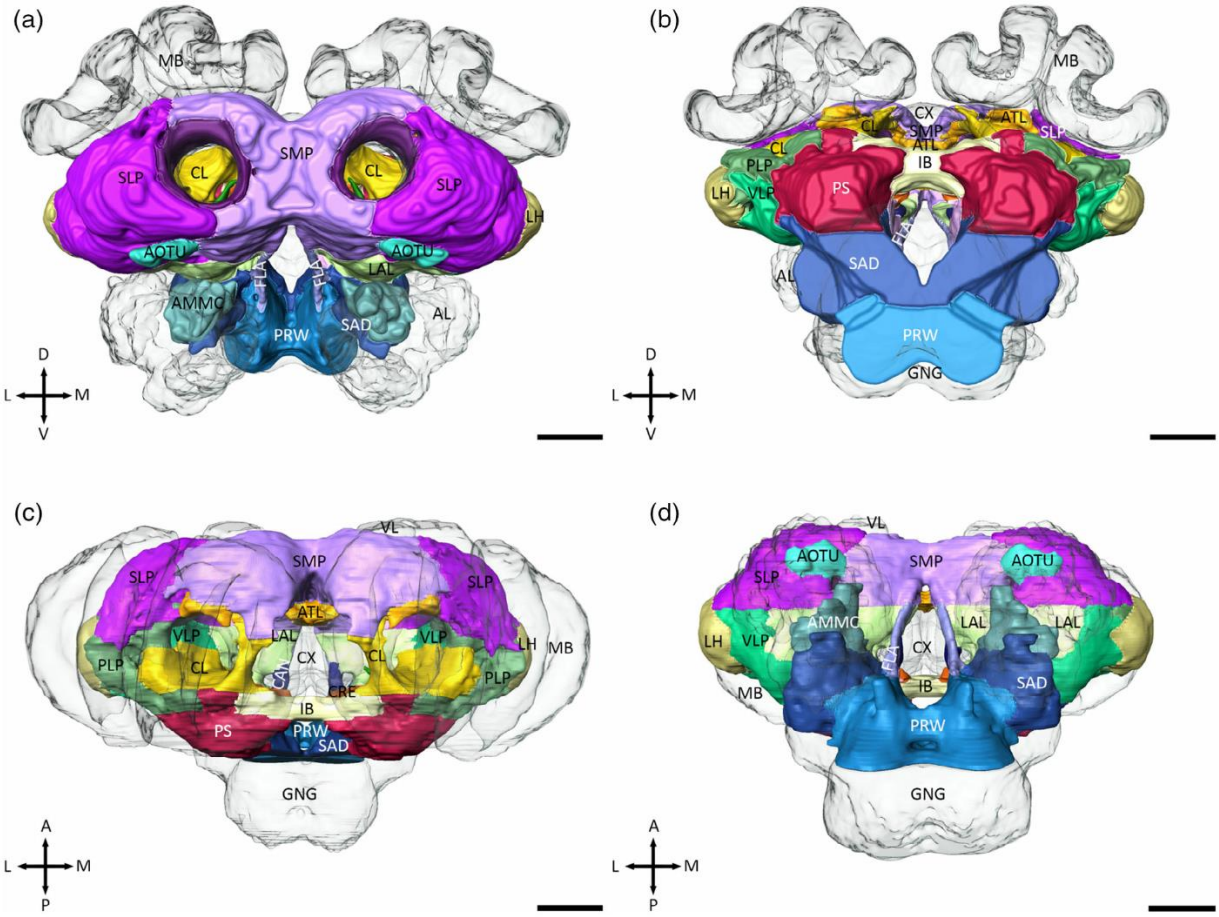

FIGURE 8 Three-dimensional reconstruction of the central adjoining neuropils. The reconstructions of the neuropils were based on anti-5-HT, anti-synapsin, and f-actin phalloidin staining. Antennal lobes (AL), mushroom bodies (MB), and central complex (CX) are shown in transparent. (a) Anterior view. (b) Posterior view. (c) Dorsal view. (d) Ventral view. Scale bars = 100 μm. AMMC, antennal mechanosensory and motor center; ATL, antler; CAN, cantle; CL, clamp; CRE, crepine; FLA, flange; GNG, gnathal ganglion; IB, inferior bridge; LAL, lateral accessory lobe; LH, lateral horn; LI, lip; PLP, posterolateral protocerebrum; PRW, prow; PS, posterior slope; SAD, saddle; SIP, superior intermediate protocerebrum; SLP, superior lateral protocerebrum; SMP, superior medial protocerebrum; VLP ventrolateral protocerebrum [Color figure can be viewed at wileyonlinelibrary.com]

posterior, inferior to the BU (Figure 7e–g). The inferior border is defined by thick glial processes and its medial border by the m-ALT (Figure 9a). To its lateral side, the LAL is flanked by the ventrolateral protocerebrum (VLP, Figure 7e–g). The horizontal ventrolateral protocerebrum fascicle (hVLPF) and the inferior fiber system (IFS) demarcate the boundary between these two neuropils (Figure 9a). As the anterior border between the LAL and the SMP appears to be very ambiguous, the border was set at the level of the anteriormost part of the superior fiber system (SFS). The LALs of both hemispheres are interconnected by the LAL commissure (Figure 9a).

3.7 | Superior neuropils

The superior lateral protocerebrum (SLP), the superior intermediate protocerebrum (SIP), and the superior medial protocerebrum (SMP) form the superior neuropils (SNP). In *Cataglyphis*, the SNP are the anteriormost region of the brain (Figures 7a–f and 8a,c,d). The largest neuropils of the SNP are the SMP and the SLP. The SLP demarcates the anterolateral border of the brain and extends between the MB calyces and the AL/AOTU all across the anteriormost part of the central brain. To its medial side, the TUBUT and the PCT define the boundaries of the SMP and the SIP (Figure 9b). The superior lateral protocerebral tract (SLPT) outlines the posteroinferior boundary of the SLP to the neighboring posterolateral protocerebrum (PLP, Figures 7e,f and 9b). In contrast to dung beetles (Immonen et al., 2017), we found only one branch of the SLPT, which runs from the lateral cell body rind to the SFS (Figure 5). The SMP expands to the anteriormost part of the brain across the midline and encloses in a cup-shaped manner on both hemispheres the SIP, the VLs, and the anterolateral part of the ATL (Figures 7a–f and 9b). More posteriorly, the median bundle (MBDL) and the posteromedial part of the ATL

separate the neuropil of both hemispheres (Figures 7d and 9b). Dorsal and anteroventral, respectively, the neuropil is ensheathed by a thick layer of glial cells (Figure 7a–d). TUBUT, PCT, SFS, and AOTU demarcate the lateral borders of the SMP (Figures 7a,b and 9b). While SMP and SLP occupy relatively large areas in the brain, the SIP is much smaller. It surrounds the VL in the anteriormost region of the brain and is encircled by the SLP, the SMP, and, more posteriorly, by the ATL and the anteriormost edge of the PLP (Figures 7a–d and 9b). As this neuropil is interspersed by many efferent neurons of the VL and the LX, it is recognizable by its less homogenous and intense

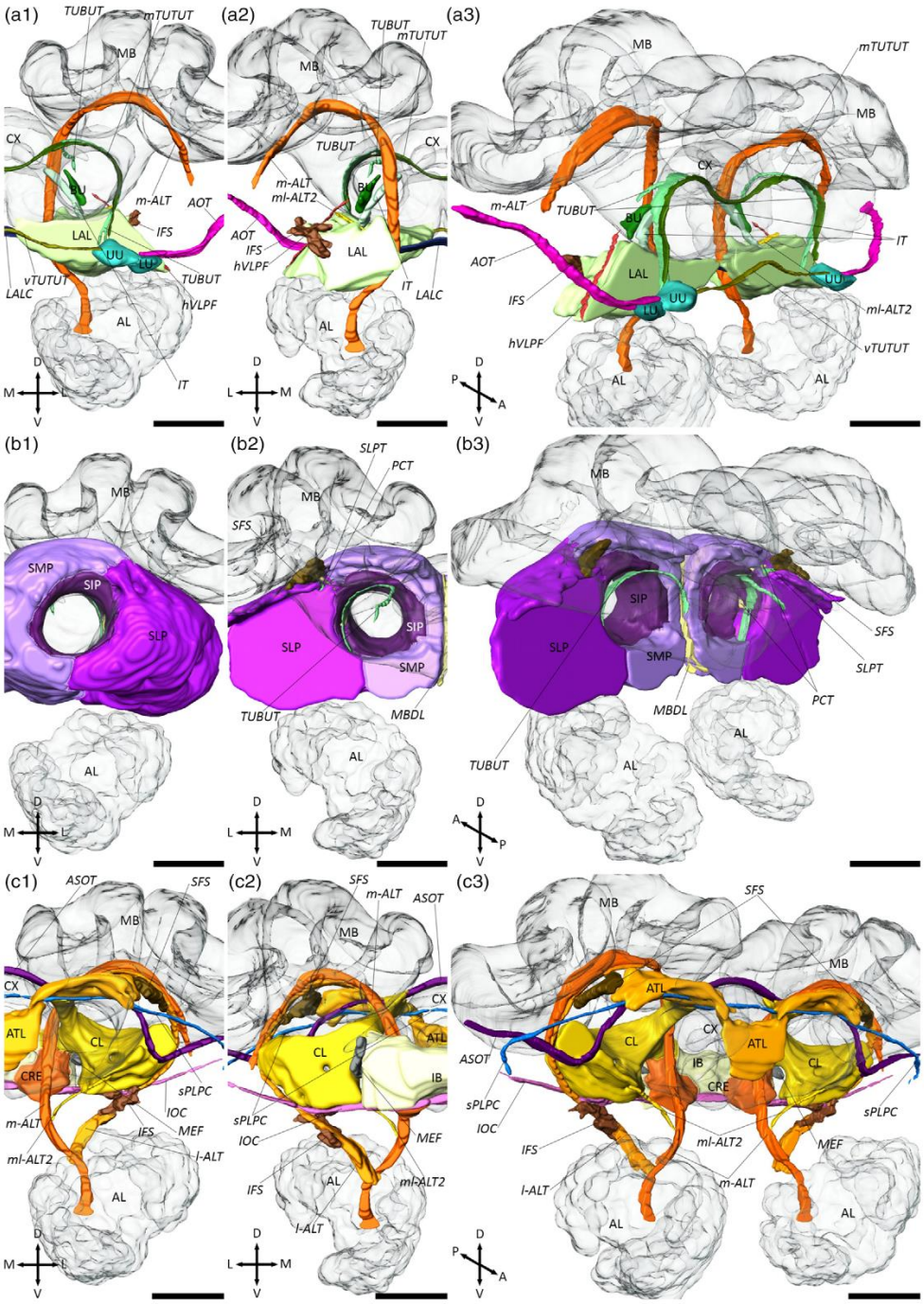

FIGURE 9 Legend on next page.

synapsin-immunoreactivity (-ir). In honey bees, this brain region has been termed ring neuropil, which is characterized by the innervation of the projection neurons from the ml-ALTs (Abel, Rybak, & Menzel, 2001; Kirschner et al., 2006).

3.8 | Inferior neuropils

The inferior neuropils (INP) occupy the medial brain region around the PED and the ML and lie posterior to the SNP and medial to the VLNP (Figures 7d–i and 8). They comprise the brain areas crepine (CRE), clamp (CL), inferior bridge (IB), and antler (ATL). The ATL and is the anteriormost neuropil of the INP. As in dung beetles (Immonen et al., 2017), the ATL extends across the midline up to the SFS and the posteromedial edge of the SLP (Figure 7d–f). The shape of the ATL is closely associated with the processes of the superior posterolateral protocerebrum commissure (sPLPC, Figure 9c). The posterior end of the ATL is delineated by a clear glial boundary (Figure 7e,f). Its dorsal and ventral borders are enclosed by the SMP and the SIP (Figure 7d). Since the ATL and most of the neighboring neuropils are obviously contiguous, we defined the borders based on slight differences in the anti-synapsin-ir. More posteriorly in the brain are the CRE, CL, and IB located. The CL is wrapped around the posterior part of the PED and is flanked by the m-ALT and the l-ALT (Figure 9c). It extends from the CBU (dorsomedial) up to the dorsal edge of the LAL (anterior), the ventral complex (VX, posterior), and the VLNP (Figure 7f–i). The CL is separated from the neighboring SMP (superior), ATL (anterolateral), CBU (medial), m-ALT (medial), BU (medial), CRE (medial), NO (posteromedial), and the lateral MB calyx (dorsolateral, Figure 7f–i) by thick glial processes. In contrast, most boundaries to the ventral and lateral adjoining neuropils are continuous and were marked by the help of several fiber bundles: the ASOT (anterolateral), the l-ALT (lateral), the ml-ALT 2 (anteroventral), the medial equatorial fascicle (MEF, posteromedial), the IFS, and the inferior optic commissure (IOC; both ventral, Figure 9c). The CRE wraps around the ventral and lateral sides of the posterior tip of the medial lobes (Figure 7h,i). In *Drosophila*, this neuropil is heavily innervated by MB extrinsic neurons (Tanaka, Tanimoto, & Ito, 2008). It is surrounded by the BU and the CL (lateral), the VX (ventral), and the IB (posterior, Figure 7h–j). On its posterior end, the boundaries of CL and CRE to the IB and the posterior slope (PS) appear rather contiguous. We therefore used the posterior tip of the MLs to set the posterior end of these neuropils. The posteriormost subregion of the INP is the IB. First identified in *Musca domestica* (Strausfeld, 1976), the IB is an unpaired neuropil, which is stretched across the midline. Together with the PS and the PLP, the IB forms the dorsalmost part of the posterior cerebrum in *Cataglyphis* (Figure 7j). The IB is laterally separated from the PS by the MEF. The ventral boundary of the IB and the VX, in turn, is defined by the IOC, respectively (Figures 7j and 9c).

3.9 | Lateral horn

The LH is one of the most prominent neuropils of the CANP. It receives direct sensory input from all ALTs (Figure 6a) and demarcates the lateral border of the cerebrum (Figures 7d–h and 8). The boundaries of the LH were determined based on the innervation by projection neurons traced along the ALTs. In addition, the LH can be distinguished by its brighter synapsin-ir in comparison to its adjacent neuropils. Medial to the LH lie the SLP, the PLP, and more ventral, the VLP (Figures 7d–h and 10a).

3.10 | Ventrolateral neuropils

The ventrolateral neuropils (VLNP) consist of the ventrolateral protocerebrum (VLP) and the posterolateral protocerebrum (PLP). They are located posterior to the SNP and ventrolateral to the INP (Figures 7e–j and 8b–d). The VLNP covers a large area in the *Cataglyphis* brain, expanding from the AL up to the OL and from the anteriormost part of the SFS up to the posteriormost regions of the IFS and lateral equatorial fascicle (LEF, Figures 7e–j and 10a). While the boundaries on the superior and inferior sides are obviously separated by extensive glial sheaths, the medial/lateral, and anterior/posterior junctions to neighboring neuropils are very often contiguous (Figure 7e–j). In *Drosophila*, the VLP is divided into an anterior (anterior ventrolateral protocerebrum [AVLP]) and posterior part (posterior

FIGURE 9 Three-dimensional reconstruction of individual central adjoining neuropils and associated fiber bundles. Antennal lobes (AL), mushroom bodies (MB), and central complex (CX) are shown in transparent. All neuropils are shown from anterior (1), posterior (2), and anterolateral (a3, c3), or posterolateral (b3). (a) Lateral complex (LX), anterior optic tubercle (AOTU), and associated fiber bundles. The LX can further be divided into the bulb (BU) and lateral accessory lobe (LAL). The AOTU consist of an upper (UU) and lower unit (LU). For the demarcation of the neuropils, the horizontal ventrolateral protocerebrum fascicle (hVLPF), the isthmus tract (IT), the inferior fiber system (IFS), the lateral accessory lobe commissure (LALC), the medial antennal lobe tract (m-ALT), the medial tubercle-tubercle tract (mTUTUT), the mediolateral antennal lobe tract 2 (ml-ALT *2*), the tubercle-bulb tract (TUBUT), and the ventral tubercle-tubercle tract (vTUTUT) were used. (b) Superior neuropils and associated fiber bundles. The superior neuropils consist of the superior intermediate protocerebrum (SIP), the superior lateral protocerebrum (SLP), and the superior medial protocerebrum (SMP). The median bundle (MBDL), the protocerebral-calycal tract (PCT), the superior lateral protocerebrum tract (SLPT), and the TUBUT were used as landmarks to define the boundaries of the superior neuropils. (c) Inferior neuropils and associated fiber bundles. The inferior neuropils comprise the antler (ATL), the clamp (CL), the crepine (CRE), and the inferior bridge (IB). Important fiber bundles for the demarcation of these neuropils are the inferior fiber system (IFS), the inferior optic commissure (IOC), lateral antennal lobe tract (l-ALT), the medial equatorial fascicle (MEF), the ml-ALT 2, the superior fiber system (SFS), and the superior posterolateral protocerebrum (sPLPC). Scale bars = 100 μm [Color figure can be viewed at wileyonlinelibrary.com]

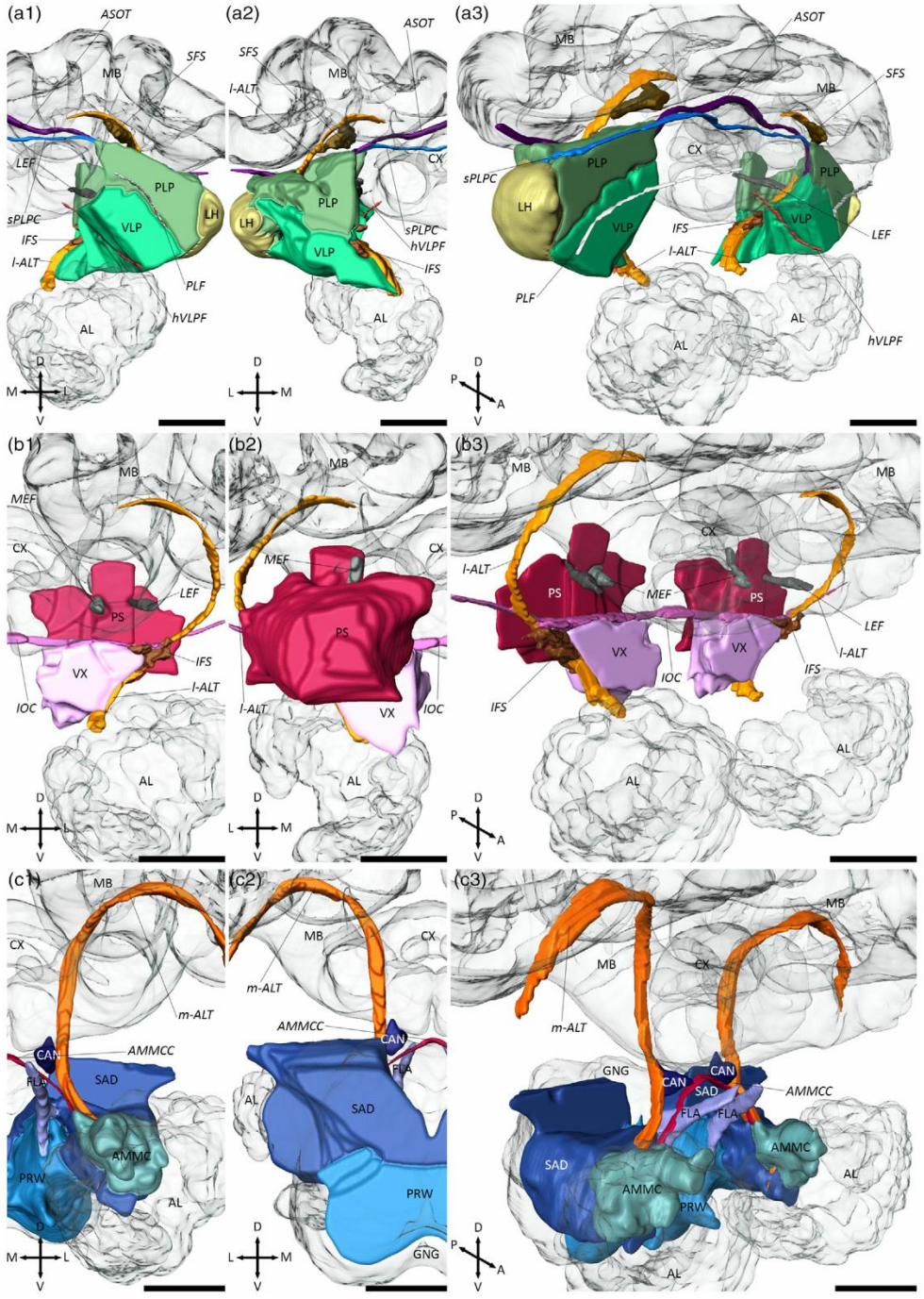

FIGURE 10 Three-dimensional reconstruction of individual central adjoining neuropil groups and associated fiber bundles (continuing from Figure 9). All neuropil groups are shown in anterior (1), posterior (2), and anterolateral view (3). (a) Ventrolateral neuropils (VLNP), lateral horn (LH), and associated fiber bundles. The posterolateral protocerebrum and the ventrolateral protocerebrum form the VLNP. The anterior superior optic tract (ASOT), the inferior fiber system (IFS), the lateral antennal lobe tract (l-ALT), the lateral equatorial fascicle (LEF), the superior posterolateral protocerebrum commissure (sPLPC), and the horizontal ventrolateral protocerebrum fascicle (hVLPF) are used to define the boundaries of the neuropils. (b) Ventromedial neuropils (VMNPs) and associated fiber bundles. The posterior slope (PS) and the ventral complex are the VMNP in the *Cataglyphis* brain. To demarcate the borders of the VMNP, the l-ALT, the IFS, the inferior optic commissure (IOC), the LEF, and the medial equatorial fascicle (MEF) were used. (c) Periesophageal neuropils (PENP) and associated fiber bundles. The PENP consist of the antennal mechanosensory and motor center (AMMC), the cantle (CAN), the flange (FLA), the prow (PRW), and the saddle (SAD). Important fiber bundles as landmarks for the demarcation of the PENP are the medial antennal lobe tract (m-ALT) and the antennal mechanosensory and motor center commissure (AMMCC). Scale bars = 100 μm [Color figure can be viewed at wileyonlinelibrary.com]

ventrolateral protocerebrum [PVLP]) based on a more glomerular structure of the PVLP in comparison with the AVLP (Ito et al., 2014; Otsuna & Ito, 2006). However, no structural differences could be recognized in this region in *Cataglyphis*, and thus, the neuropil was not further divided into subregions. Unlike in dung beetles (Immonen et al., 2017), the VLP is not characterized by an enriched serotonergic innervation. We therefore defined the borders based on several fiber bundles: the ASOT (superior), the posterior lateral fascicle (PLF, superolateral), the l-ALT (superomedial), the hVLPF, and the IFS (both medial, Figure 10a). The PLP is demarcated by the sPLPC (superior), the PLF (inferomedial) the ASOT (anteromedial), the l-ALT (medial), and the LEF (posteromedial, Figure 10a). Lateral to the VLNPs is the LH attached (Figure 7e–h).

3.11 | Ventromedial neuropils

Ventral complex (VX) and posterior slope (PS) form the ventromedial neuropils (VMNP) of the *Cataglyphis* brain. They are located posterior to the INP and flank the esophagus on both hemispheres of the brain (Figures 7h–l and 8b,c). Because of a lack of unambiguous landmarks, VX and PS were not further divided into subcompartments (namely vest, gorget, and epaulette; superior and inferior PS). The IFS is the most important landmark to localize the VX in the brain of *Cataglyphis*. It defines the anterior and posterior end of the neuropil and demarcates, together with the l-ALT, the lateral borders to the VLP (Figure 10b). In addition, the IOC serves as an apparent dorsal boundary to the neighboring CRE, BU, CL, and more posterior, IB and PS (Figures 7h–j and 10b). In contrast, the ventral boundaries to the prow (PRW) and the saddle (SAD) are rather contiguous but due to a more intense synapsin-ir of the PRW still is clearly recognizable (Figure 7h–j). The PS starts at the level of the IB and is situated at its anteriormost part between IB and PLP, whereas LEF and MEF form the lateral and medial borders (Figures 7j and 10b). More posterior, the PS expands from the esophagus to the lateral edge of the cerebrum. The SAD and the GNG are localized ventral to the PS (Figure 7k,l).

3.12 | Periesophageal neuropils

The periesophageal neuropils (PENP) in the *Cataglyphis* brain comprises the regions of the cantle (CAN), flange (FLA), prow (PRW), and the saddle (SAD), which houses the antennal mechanosensory and motor center (AMMC). These neuropils form the ventralmost region of the brain around the esophagus between the AL and the GNG (Figures 7e–k and 8). The AMMC is the most prominent and probably best studied neuropil of the PENP. It receives primary mechanosensory input from the antennae, providing information about position and movement of the antennae (Ai, Nishino, & Itoh, 2007; Ehmer & Gronenberg, 1997; Homberg, Christensen, & Hildebrand, 1989; Kamikouchi et al., 2009), and gustatory input in a variety of insects (Farris, 2008; Jørgensen, Kvello, Almaas, & Mustaparta, 2006; Miyazaki & Ito, 2010). To accurately define the borders of the AMMC, in particular to the SAD, we performed AN backfills (Figure 11). In *Cataglyphis*, the AMMC is adjacent to glomeruli of the AL and more posteriorly it merges smoothly into the SAD (Figure 7c–g). The SAD is a relatively large neuropil and is situated between the LAL and the AL (Figure 7g). More posteriorly, it lies beneath the VX, the VLP and superolateral to the PRW (Figure 7h–j). In its posteriormost region, the neuropil is connected across the midline and its boundaries to the adjacent PS (superior) and the GNG (posterolateral) appear rather contiguous (Figures 7k and 10c). In contrast to the SAD, the CAN is a very small and paired neuropil with clear borders (Figures 7g,h and 10c). In *Cataglyphis*, it fills out a triangular-shaped area in between of the ML (superior), the m-ALT (lateral), and the esophagus (medial, Figure 7g,h and 10c). The ventral boundary of the CAN is defined by the AMMC commissure which interconnects the AMMCs of both hemispheres (Figure 10c). Neighboring neuropils are the LAL (lateral), the VX (inferolateral), the SAD (inferolateral), and the FLA (ventral, Figure 7g,h). Unlike in *Drosophila* (Ito et al., 2014), the FLA is heavily surrounded by thick glial processes in *Cataglyphis*. Due to its bar-shaped structure and unambiguous borders, it is easily distinguishable from the surrounding neuropils such as the LAL and the SAD (both lateral). It emerges at the root of the MBDL, where it extends lateral from the esophagus and extends up to the anterior tip of the PRW (Figures 7e–h, 8a,d, and 10c). The last and most ventral structure of the PENP is the PRW. The structure of this neuropil appears brighter in the anti-synapsin staining than in the remaining adjoining neuropils. Its neighbors are the VX (superior), the FLA (anterior), the SAD (superolateral), and the GNG (posterolateral, Figures 7h–l and 8a,d).

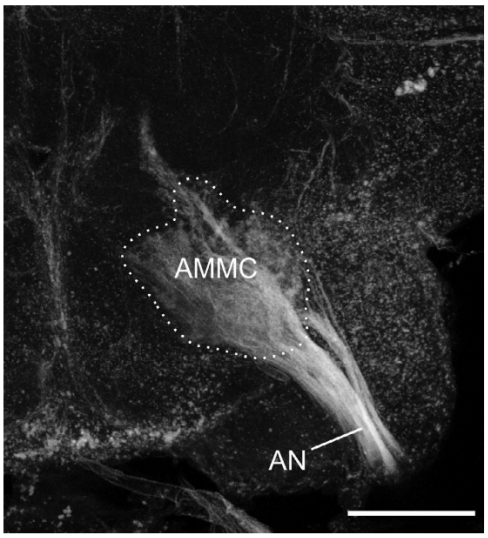

FIGURE 11 Projection of the antennal nerve (AN) into the antennal mechanosensory and motor center (AMMC). Microruby was used for the anterograde staining. Z-projection from a stack of 21 images with 5 μm step size. Scale bar = 100 μm

3.13 | Visual fibers

To generate an overview of all visual tracts and commissures and their target neuropils, we used neuronal tracer injections into the ME and LO and projected them into the map of synapsin-rich neuropils in the *Cataglyphis* brain. One of the most prominent visual fiber bundles in Hymenoptera is the ASOT to the lateral and medial calyces of the MBs. The ASOT forms side branches into the ipsilateral and contralateral CO of the MB calyces (Figures 12a–c,h, 13, and 14b). The ASOT predominantly comprises OL neurons of the ME but also houses a small number of neurons originating from the LO (Figure 12a–c). In contrast to our findings, in honey bees the LO projections run in a separate tract (LO tract) before they join the ASOT (Ehmer & Gronenberg, 2002; Mobbs, 1984). The ASOT can be found anterior in the brain and exhibits a characteristic course through the brain with a sharp bend lateral to the PED, just before it passes the VLs superiorly and crosses the midline dorsal to the CX (Figures 12a–c,h, 13, and 14b). In *Cataglyphis*, the ASOT is not the only visual fiber tract with projections into the MBs. Our tracer injections revealed a second fiber tract of unknown identity that runs anterior to the ASOT and dorsal to the SLP, which we termed optical calycal tract (OCT). The OCT interconnects the ME and LO with the ipsilateral MB CO but, in contrast to the ASOT, does not project into the contralateral brain hemisphere (Figures 12a–c, 13, and 14a).

In addition to these two fiber bundles, we found further tracts and commissures that project into different regions of the central brain or interconnect the OLs. We identified a very thin and serpentine shaped commissure—the serpentine optic commissure (SOC) (Figure 12h), which has also been described in the honey bee (Hertel & Maronde, 1987; Hertel, Schäfer, & Maronde, 1987). The general shape of this extremely thin commissure has strong similarities to the ASOT. In contrast to the ASOT, the SOC is situated slightly more posteriorly in the brain and consists of fibers from only a few neurons, which project from the ME and LO to their contralateral counterparts without any further arborizations into other neuropils (Figures 12a–c,h, 13, and 14b). The SOC neurons enter the central brain either ventrally to the ASOT (anterior in the brain) or more posteriorly, together with the neurons of the posterior optic commissure (POC) (Figure 12h). All SOC neurons merge at the inferolateral edge of the CL before they together pass the PE through the CL and cross the midline anterior to the CBU slightly ventral to the ASOT (Figures 12h and 14b).

Another very prominent tract in all insect brains investigated so far is the AOT (Figures 12a–c,g, 13, and 14a). In *Cataglyphis*, the AOT is situated inferolaterally of the SLP and anteriorly to the LH. Among others, it transfers information from the sky polarization pattern from the OLs to the AOTU (el Jundi et al., 2011; Pfeiffer & Kinoshita, 2012; Zeller et al., 2015). In *Cataglyphis*, the AOT is accompanied by additional neurons that pass the AOTU and run into the VX (Figures 12g, 13, and 14a). Both subunits of the AOTU as well as the VX are supplied by projection neurons of the ME and the LO (Figure 12a–c,g).

In addition, we found two further commissures, the POC and the IOC. Both commissures have previously been reported in honey bees (DeVoe, Kaiser, Ohm, & Stone, 1982; Hertel et al., 1987; Hertel & Maronde, 1987; Mobbs, 1984) and in the ant *Camponotus rufipes* (Yilmaz et al., 2016). In *Cataglyphis*, POC and IOC contain projection neurons of the ME and the LO (Figure 12d–f). The POC is the thickest visual fiber bundle in the *Cataglyphis* brain and easily recognizable in the immunostaining, even without any further anterograde tracing. After the commissure emerges from the OLs, it enters the cerebrum just ventral to the posterior part of the LCA and exhibits many ramifications into the VLNPs (Figures 12d–f, 13, and 14c). From there, the POC runs inferior to the calyces and superior to the PLP before it bifurcates into two relatively thick branches. One neuronal bundle exits the commissure ventrally and innervates the VMNPs (Figures 12d–f, 13, and 14c). The remaining neurons of the POC continue along a more or less straight line in between the CA and the PS before they cross the midline above the IB (Figure 12d–f). Close to the midline, some of these neurons bifurcate into the ocellar tracts (Figure 12i). The IOC lies inferior to the POC (Figures 12d–f, 13, and 14c). In *Cataglyphis*, this commissure separates PLP (superior) and VLP (inferior) as well as CL/CRE (superior) and VX (inferior) before it crosses the midline of the brain. Lateral to the l-ALT, many neurons of the IOC leave the commissure ventrally and innervate the VLNPs. In addition, the IOC gives rise to medial arborizations into the VX (Figures 12d–f, 13, and 14c).

4 | DISCUSSION

In this study, we examined the brain of the worker caste in the thermophilic ant *Cataglyphis nodus*, a favorable experimental model for the study of long-distance navigation. These ants are perfectly adapted to harsh environments with very high ground temperatures and scattered food resources, which they predominantly find during largely visually guided foraging trips. Overall, we reconstructed 25 paired and 8 unpaired synapse-rich neuropils, defined 30 fiber tracts, among them 6 fiber tracts that provide new insights into the complexity of the visual system of the ants. A comparably detailed description of an insect brain that also includes the brain regions of the CANP currently exists only for the fruit fly *Drosophila melanogaster* (Ito et al., 2014; Pereanu et al., 2010), the monarch butterfly *Danaus plexippus* (Heinze & Reppert, 2012), the ant *Cardiocondyla obscurior* (Bressan et al., 2015), the dung beetle *Scarabaeus lamarcki* (Immonen et al., 2017) and the desert locust *Schistocerca gregaria* (von Hadeln et al., 2018). The orientation, structure, and overall layout of the *Cataglyphis* brain show large similarities with the honey bee brain (Brandt et al., 2005; Ribi, Senden, Sakellariou, Limaye, & Zhang, 2008) and appears similar across ant species, at least for the major neuropils like AL, MB, OL, and other distinct and easy recognizable neuropils. However, marked differences in relative volumes are present, for example like small optic neuropils in highly olfactory ants such as *Atta* or *Pheidole* (Groh, Kelber, Grübel, & Rössler, 2014; Ilieş, Muscedere, & Traniello, 2015), less visual *Camponotus* species (Yilmaz et al., 2016),

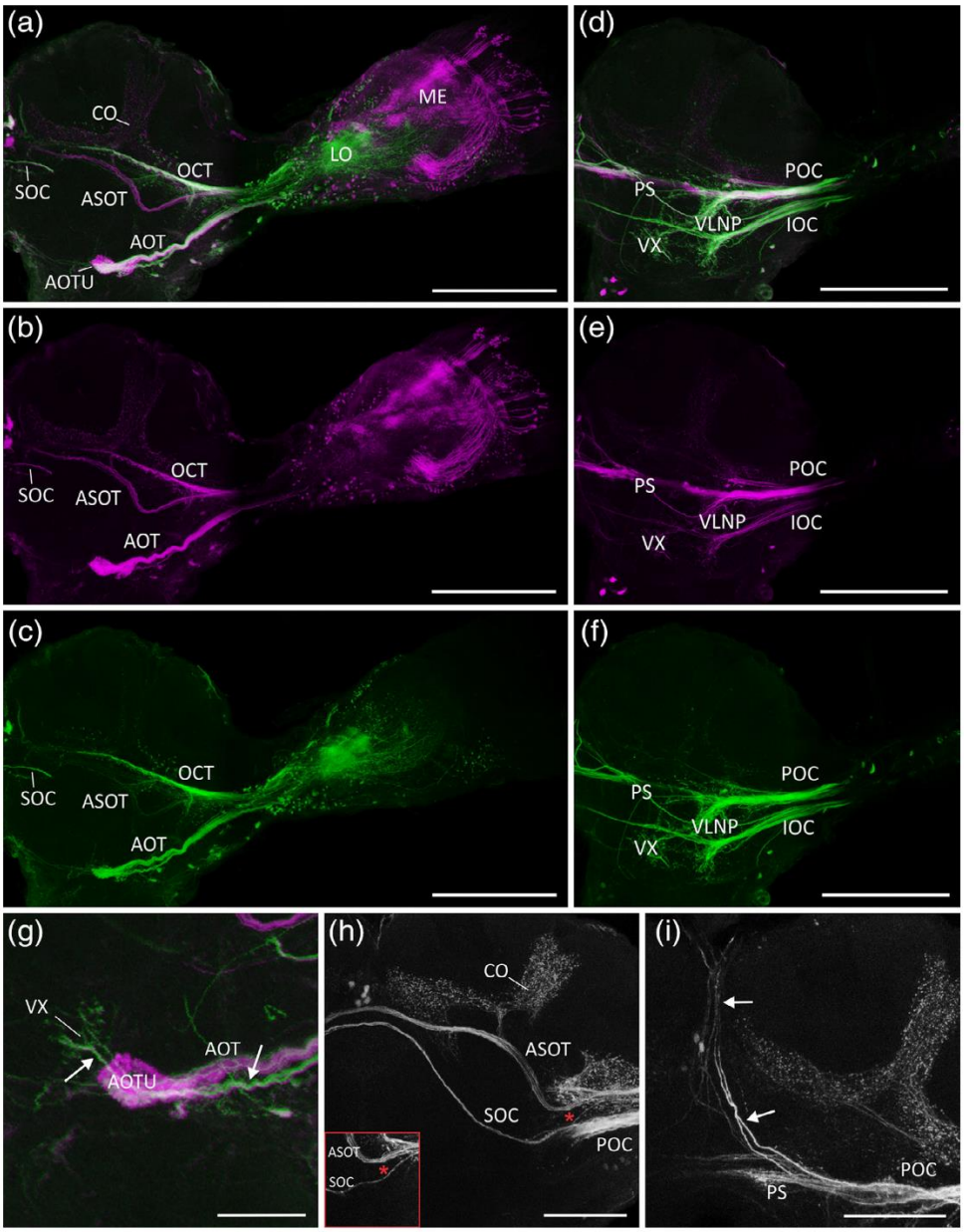

FIGURE 12 Visual projections from the optic lobes into the central brain. Anterograde staining obtained from dye injections into the medulla (ME; microruby in magenta or gray) and lobula (LO; Alexa 488 dextran in green). (a–c) Visual fiber bundles of the ME (a, b) and the LO (a, c) located in the anterior brain. Anterior optic tract (AOT), anterior superior optic tract (ASOT), optical calycal tract (OCT), and superior optic commissure (SOC) comprise all projection neurons from ME and LO. The ASOT and the OCT project into the collar (CO) of the mushroom body and the AOT into the anterior optic tubercle (AOTU). Z-projection from a stack of 20 images with 5 µm step size. Scale bars = 200 µm. (d–f) Visual fiber bundles of the ME (d, e) and LO (d, f) located in the posterior brain. The inferior (IOC) and posterior (POC) optic commissure comprise both neurons from ME and LO and project into the ventrolateral neuropils (VLNP) and the ventral complex (VX). In addition, the POC exhibits projections into the posterior slope (PS). Z-projection from a stack of 14 images with 5 µm step size. Scale bars = 200 µm. (g) The AOT is accompanied by some neurons, which run into deeper layers of the brain and innervate there the ventral complex (neurons are indicated by white arrows). Z-projection from a stack of 24 images with 5 µm step size. Scale bar = 50 µm. (h) The SOC exhibits no projections into the protocerebrum. The SOC neurons originate either from the POC or ventral to the ASOT (indicated by the asterisk, inset). Z-projection from a stack of 13 images or eight images (inset) with 5 µm step size. Scale bar = 100 µm. (i) The POC is accompanied by some neurons with projections to the ocellar tracts (indicated by white arrows). Z-projection from a stack of 10 images with 5 µm step size. Scale bar = 100 µm [Color figure can be viewed at wileyonlinelibrary.com]

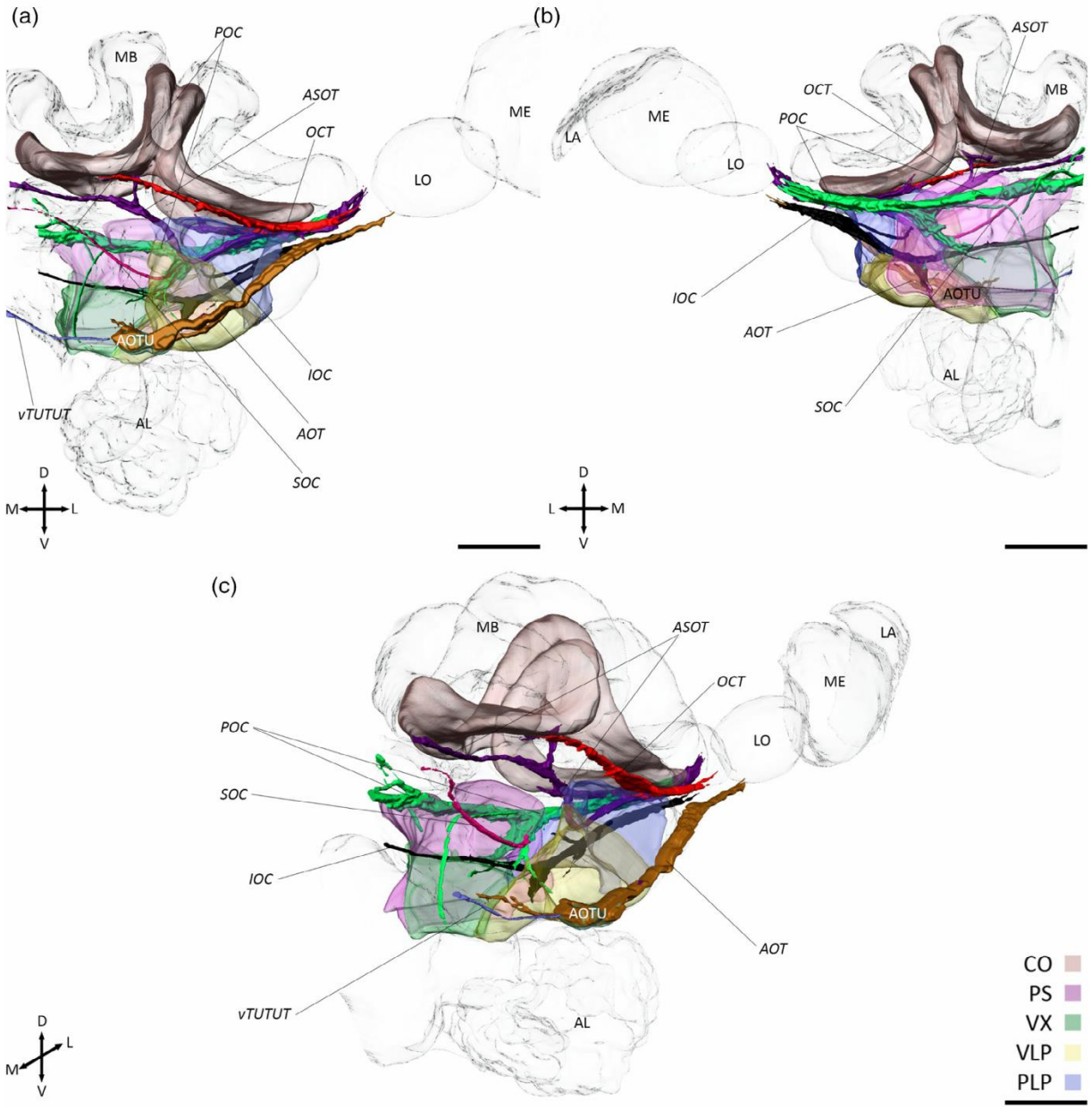

FIGURE 13 Surface reconstructions of the visual fiber bundles and their target neuropils. The surface reconstructions of the fiber bundles are based on anterograde staining and in case of the neuropils on anti-synapsin labeling. Two major optic tracts (AOT, Anterior optic tract; OCT, Optical calycal tract) and four optic commissures (ASOT, anterior superior optic tract; IOC, inferior optic commissure; POC, posterior optic commissure; SOC, serpentine optic commissure) were found. The OCT projects into the collar (CO) of the ipsilateral mushroom body and the AOT into the anterior optic tubercle (AOTU). The AOTUs are interconnected by the ventral tubercle-tubercle tract (vTUTUT). In addition, the AOT is accompanied by some neurons which project into the ventral complex (VX). The SOC is the only commissure without any ramifications into the cerebrum. The ASOT exhibits arborizations into the CO, the IOC into the posterolateral protocerebrum (PLP), the ventrolateral protocerebrum (VLP) and the ventral complex (VX), and the POC into the PLP, the VLP, the VX, and the posterior slope (PS). (a) Anterior view. (b) Posterior view. (c) Anteromedial oblique view. Scale bars = 100 μm. LA, lamina; LO, lobula; ME, medulla [Color figure can be viewed at wileyonlinelibrary.com]

or *Cardiocondyla obscurior* (Bressan et al., 2015). A most striking difference is the orientation of the brain. While the central brains of other insects, including dipterans, lepidopterans, and coleopterans (el Jundi et al., 2009; Heinze & Reppert, 2012; Immonen et al., 2017; Ito et al., 2014) tilt during the metamorphic development by 90° (Huetteroth, el Jundi, el Jundi, & Schachtner, 2010), the brains of

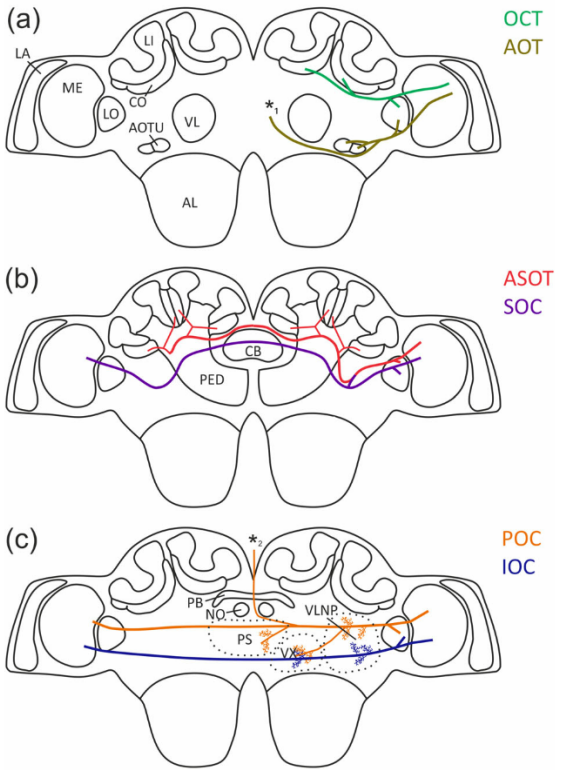

FIGURE 14 Schematic drawing of the visual fiber bundles of the *Cataglyphis nodus* brain. The overview of the optical tracts and commissures based on anterograde staining received from dye injections into the medulla (ME; microruby) and lobula (LO; Alexa 488 dextran). (a) The optical calycal tract (OCT) and the anterior optic tract (AOT) are situated in the anterior part of the brain. The OCT projects into the ipsilateral collars (CO) of the mushroom bodies (MB) and the AOT into the ipsilateral anterior optic tubercle (AOTU). Both tracts receive input from the medulla (ME) and lobula (LO). The AOT is additionally accompanied by some neurons, which run into deeper layers of the brain, innervating the ventral complex (VX, indicated by asterisk 1). (b) The anterior superior optic tract (ASOT) and the serpentine optic commissure (SOC) are situated more posteriorly than AOT and OCT but still relatively far anterior in the brain. The SOC connects the ME and LO with their contralateral counterparts. The ASOT has ramifications into the ipsi- and contralateral COs. (c) The posterior optic commissure (POC) and the inferior optic commissure (IOC) are situated in the posterior part of the brain. Both commissures connect the MEs and LOs between the hemispheres. The POC has ramifications into the dorsal region of the ventrolateral neuropils (VLNP), the ventral complex (VX), and the posterior slope (PS). In addition, some neurons, which accompany the POC, connect the optic lobes with the ocelli (indicated by asterisk 2); the IOC innervates the ventrolateral part of the VLNP and the VX. AL, antennal lobe; CB, central body; LA, lamina; LI, lip; NO, noduli; PB, protocerebral bridge; PED, pedunculus [Color figure can be viewed at wileyonlinelibrary.com]

hymenopterans do not undergo such a modification. Thus, the central brain of, for example, ants, honey bees, wasps, and also hemimetabolous insects like locusts (Brandt et al., 2005; Groothuis et al., 2019; Kurylas, Rohlfing, Krofczik, Jenett, & Homberg, 2008) are oriented perpendicular compared to, for example, the fly brain. It was therefore not trivial to compare and identify similar brain regions in the ant brain using those described in the fly brain. Nevertheless, our description of the neuropils, tracts, fibers and commissures can serve as a reliable base for the brains of other ant species, bees, and wasps.

4.1 | Mushroom bodies and visual input

Cataglyphis ants, like honey bees, possess very prominent and complex MBs (Figures 1 and 3): each MB consists of a medial and a lateral calyx, and each of these calyces, in turn, can further be subdivided into a CO and LI region. This subdivision most likely is a consequence of the high importance of visual memory, in addition to olfactory memory (Gronenberg, 1999; Hertel & Maronde, 1987; Mobbs, 1984; Paulk & Gronenberg, 2008; Yilmaz et al., 2016). Therefore, the MBs in *Cataglyphis* represent a truly multimodal integration center (Figures 6a,b and 12a–c,h) (Gronenberg, 1999, 2001). The expansion of visual innervation of the MB calyx in species along the hymenopteran lineage first occurs in species with parasitoid lifestyles as well as in all social species, and, therefore, was interpreted as a trait that co-occurred with advanced spatial orientation (Farris & Schulmeister, 2010). The importance of the MBs for learning and memory has been extensively demonstrated in honey bees (Erber, Masuhr, & Menzel, 1980; Menzel, 1999, 2001; Szyszka, Galkin, & Menzel, 2008) and can be assumed to serve a similar function in *Cataglyphis*. Although the exact number of KCs of the MBs in *Cataglyphis* is not known, it can be assumed to be very high compared to many other insects. For example, the MB of the ant *Camponotus rufipes* houses around 130,000 KC (Ehmer & Gronenberg, 2004). As the visual MB COs in *Cataglyphis* have large volumes and contain an estimated total number of ~400,000 microglomeruli (Grob et al., 2017; Grob et al., 2019), compared to ~160,000 in *Camponotus rufipes* (C. Groh, personal communication), we assume that the total number of associated KCs may be even higher in *Cataglyphis*. Therefore, KC numbers in *Cataglyphis* MBs are likely as high as in *Camponotus* with a decent number of KCs associated with the large CO region (Figure 3) (Gronenberg & Hölldobler, 1999). However, as the relationship between KC numbers and microglomeruli may differ between ant species, this requires further investigations. Comparison with honey bees suggest that the KC numbers are of the same order (340,000 KCs) (Rössler & Groh, 2012; Strausfeld, 2002; Witthöft, 1967) and much higher than in *Drosophila* MBs (2,500 KC) (Fahrbach, 2006). The discrepancy between *Drosophila* and aculeate hymenopteran MBs most likely concerns differences in navigational abilities and the socio-ecological context of social Hymenoptera. As outlined above, the correlation between advanced spatial orientation with the visual input and expansion of the MBs in higher Hymenoptera was proposed in several studies (Farris, 2013, 2015; Farris & Schulmeister, 2010).

Our study shows that several fibers and commissures transfer visual input into the MBs of *Cataglyphis nodus*, which likely causes the relatively large CO region containing a high number of input synaptic complexes (microglomeruli) (Grob et al., 2017; Stieb et al., 2012). The

large MBs, in general, and the substantial amount of visual input into the CO are in line with the excellent abilities of *Cataglyphis nodus* and other *Cataglyphis* species to form visual memories for landmarks and/or panoramic sceneries as shown or highlighted more recently (Fleischmann, Christian, Müller, Rössler, & Wehner, 2016; Fleischmann et al., 2018; for reviews, see Rössler, 2019; Zeil & Fleischmann, 2019). *Cataglyphis* foragers have to learn the visual features of their nest surroundings in order to find their way to their nest entrance when homing back from foraging trips (Cruse & Wehner, 2011; Wehner & Menzel, 1969; Wehner & Räber, 1979). Several studies suggest that the latter is achieved by taking snapshots of the panorama during specific learning walks when the ants leave their nest for the first time (Fleischmann, Grob, Wehner, & Rössler, 2017; Müller & Wehner, 1988). This visual information, most likely, is stored in the vast number of associative visual microcircuits that involve many thousands of KCs. It appears counterintuitive, however, that the basal ring, a substructure known from honey bees, is not a distinct structure in *Cataglyphis* MBs, especially as the basal ring is known as a multimodal sensory input region integrating visual and olfactory stimuli (Gronenberg, 1999, 2001). However, also in other ant species, the basal ring is largely reduced, possibly absent, or indistinguishable from the CO (Ehmer & Gronenberg, 2004; Gronenberg, 1999). The reasons for this remain unclear.

4.2 | Antennal lobes and dual olfactory pathway

Recent studies showed that the ALs of *C. nodus* workers contain about 226 glomeruli, which is in a similar range to other *Cataglyphis* species such as *C. fortis* (∼198) and *C. bicolor* (∼249) (Stieb et al., 2011). However, this number is substantially smaller compared to high glomeruli numbers in other ant species, such as *Camponotus floridanus* (∼434) (Zube et al., 2008), *Camponotus japonicus* (∼438) (Nishikawa et al., 2008), the wood ant *Formica rufibarbis* (∼373) (Stieb et al., 2011), or the high numbers in leaf cutting ants, for example *Atta vollenweideri* (Kelber, Rössler, Roces, & Kleineidam, 2009). The reduced number of glomeruli might reflect the different ecology of *Cataglyphis* ants that, compared to all other species mentioned above, primarily rely on visual information instead of pheromonal cues during foraging (Ruano et al., 2000; reviewed by: Wehner, 2003). On the other hand, studies have shown that *Cataglyphis* do use olfactory cues during cross wind orientation while searching for food (Buehlmann et al., 2014; Steck, Hansson, & Knaden, 2011). However, both the role of pheromones and food odors may be minor compared to ants with reduced visual capabilities. In any case, compared to non-social insects, for example, *Drosophila* (∼40) (Laissue et al., 1999; Stocker, Lienhard, Borst, & Fischbach, 1990; Wong, Wang, & Axel, 2002), lepidopterans (∼ 50–70) (Masante-Roca, Gadenne, & Anton, 2005; Montgomery & Ott, 2015; Varela et al., 2009), and dung beetles (∼ 85) (Immonen et al., 2017), the number of olfactory glomeruli in *Cataglyphis* still are comparatively high most likely due to social interactions and communication inside the nest using cuticular hydrocarbon cues (Hölldobler & Wilson, 1990).

We also found that *Cataglyphis* possess a dual olfactory pathway, similar to the previously described feature in various other higher hymenopterans (Brill, Meyer, & Rössler, 2015; Couto, Lapeyre, Thiéry, & Sandoz, 2016; Kirschner et al., 2006; Rössler & Zube, 2011; Zube et al., 2008). Like in other Hymenoptera, projection neurons of different subpopulations of glomeruli and projection neurons form the major tracts m-ALT, l-ALT, and the three thinner ml-ALTs in *Cataglyphis* (Figure 6a). This feature appears more complex compared to most other insect species, with a smaller number of AL output tracts (reviewed by Galizia & Rössler, 2010). Functional studies suggest that both parallel processing and coincidence coding are employed within this system leading to enhanced coding capabilities for these insects with highly complex olfactory environments and behaviors (Brill et al., 2013; Brill et al., 2015; Carcaud, Giurfa, & Sandoz, 2015; Müller, Abel, Brandt, Zöckler, & Menzel, 2002; Rössler & Brill, 2013).

4.3 | Optic lobes

The OLs in the *Cataglyphis* brain are relatively large in comparison to other ant species (Figure 1) (Gronenberg & Hölldobler, 1999). Enlarged OLs are otherwise typically present in winged, reproductive castes or visually hunting ants, which underpins the high relevance of visual stimuli for visually based navigation in *Cataglyphis* workers. The OLs of *Cataglyphis* show the typical structure with LA, ME, and LO (Figure 2) (Brandt et al., 2005; Gronenberg, 2008; Gronenberg & Hölldobler, 1999). In contrast to Diptera, Coleoptera, Lepidoptera, or Trichoptera, *Cataglyphis* possess one coherent LO instead of an LO complex that consists of two distinct areas: LO and LO plate. In many insects, the LO plate is a center for motion vision that encodes optic-flow information (Hausen, 1976; Hausen, 1984; Joesch, Plett, Borst, & Reiff, 2008). However, studies in *Cataglyphis bicolor* have shown that the ants perceive optic-flow information and use it for distance estimations (Pfeffer & Wittlinger, 2016). This raises the question how optic-flow information is processed in the ant brain, more explicitly whether the LO can further be subdivided into different functional subregions, similar to what has been shown for the praying mantis and the locust (Kurylas et al., 2008; Rosner, von Hadeln, Salden, & Homberg, 2017) or in other hymenopteran species (Paulk & Gronenberg, 2008; Strausfeld, 2012).

4.4 | Central complex, anterior optic tubercle, and lateral complex

In *Cataglyphis*, the AOTU comprises an upper and a lower subunit which seems to be highly conserved in all insects studied so far (el Jundi et al., 2010; Heinze & Reppert, 2012; Immonen et al., 2017; Montgomery, Merrill, & Ott, 2016; Mota et al., 2011; Strausfeld & Okamura, 2007; von Hadeln et al., 2018). In all insects, sky-compass neurons project into the lower subunit of the AOTU whereas the upper division is associated with chromatic, unpolarized-light vision (Mota et al., 2011; Mota et al., 2013; Pfeiffer & Kinoshita, 2012; Zeller

et al., 2015). In *Cataglyphis*, the AOTUs on both sides are connected via the TUBUT (Figure 9c) and transmit sky-compass information to the BU, similar to what has been shown in other insects studied so far (el Jundi & Homberg, 2010; Heinze & Reppert, 2012; Pfeiffer et al., 2005).

While the boundaries of the LAL of the LX, a region that mediates motor output to the ventral nerve cord (Namiki & Kanzaki, 2016; Turner-Evans & Jayaraman, 2016), are more difficult to align, the BUs are easily recognizable in *Cataglyphis* due to the existence of large microglomerular synaptic structures (Figures 3g and 4d). These microglomeruli gate sky compass and other visual information before entering the lower unit of the CB via tangential neurons (Heinze & Reppert, 2012; Pfeiffer & Homberg, 2007; Seelig & Jayaraman, 2013). Interestingly, precocious stimulation of the ants with UV-light was shown to cause an increase in the number of microglomeruli in the BUs of *Cataglyphis fortis* indicating a substantial level of structural plasticity in these synaptic circuits (Schmitt, Stieb, et al., 2016). *Cataglyphis* has only one BU per hemisphere, like *Drosophila* (Seelig & Jayaraman, 2013), monarch butterflies (Heinze et al., 2013), and dung beetles (el Jundi et al., 2018) while locusts and honey bees possess two distinct BUs or groups of microglomerular complexes (el Jundi et al., 2014; Heinze & Homberg, 2008; Mota et al., 2016; Träger, Wagner, Bausenwein, & Homberg, 2008; von Hadeln et al., 2018). The reason for these differences are currently not known.

We could also define the IT in *Cataglyphis*. Via this tract, among others, visual information from the BUs of the LX is transferred to the CX as has been demonstrated in various insects (el Jundi et al., 2014; Homberg et al., 2011; Schmitt, Stieb, et al., 2016; Sun et al., 2017). The overall layout of the CX in *Cataglyphis* (Figures 1 and 4) appears similar to other insect species such as dung beetles (el Jundi et al., 2018; Immonen et al., 2017), bees (Brandt et al., 2005; Pfeiffer & Kinoshita, 2012), *Drosophila* (Ito et al., 2014; Pereanu et al., 2010), monarch butterflies (Heinze et al., 2013), and locusts (Heinze, Gotthardt, & Homberg, 2009; von Hadeln et al., 2018). Future studies using additional markers and single neuron labeling are needed to reveal the fine structure of the different components of the CX. However, the prominent input from the sky-compass system and similarities in general layout are highly suggestive for an important role of the CX in path integration in *Cataglyphis* ants, especially in the light of recent studies on the neuronal network that encodes the current and desired directions in the CX network (Seelig & Jayaraman, 2015; Stone et al., 2017; Green, Vijayan, Pires, Adachi, & Maimon, 2019).

4.5 | Central adjoining neuropils

Even though the function of most areas within the CANP is largely unknown, the use of genetic tools in *Drosophila* promoted functional studies of the neuronal circuits in this brain region. For instance, novel calcium imaging tools in behaving flies could demonstrate the participation of different neuropils of the CANP in walking behavior (Aimon et al., 2019). To better relate and compare studies in other insects with *Cataglyphis*, we subdivided the CANP into subunits using glial boundaries, fiber tracts, f-actin phalloidin staining as well as synapsin-ir and 5-HT-ir as criteria for defining borders. This first map of the CANP will allow us to study these brain regions in more detail in the future, particularly for investigating the distribution of neurotransmitters, neuromodulators, individual neurons and circuits, or gene expression profiles and compare these features directly with the situation in other insects.

Most of the described neuropils within the CANP of *Drosophila* do also exist in the brain of *Cataglyphis* (Figures 7 and 8). Since the enormous MBs of *Cataglyphis* occupy large parts of the central brain, the location and the size of the CANP components differ in some cases compared to the CANP in *Drosophila* and other insects investigated for this region so far. For instance, the CRE encases the complete ML of the MB in *Drosophila* (Ito et al., 2014) but appears much smaller and only around the tip of the ML in *Cataglyphis* (Figure 7h,i). Nevertheless, the general layout and location of the CANP components in *Cataglyphis* are very similar to other insects and appear as diverse as in dung beetles, fruit flies, locusts, and monarch butterflies (Heinze & Reppert, 2012; Immonen et al., 2017; Ito et al., 2014; von Hadeln et al., 2018). However, due to the lack of clear landmarks, we did not further subdivide some brain areas within the CANP of *Cataglyphis*. This concerns the CL, the PS, the ventrolateral complex (VX), and the VLP. Using the present template as a basis, the use of more diverse molecular markers might open up new insight into subdivisions in the future.

Our anterograde staining highlighted some subdivisions of the CANP in *Cataglyphis*, which largely correspond with previous investigations in other Hymenoptera (Zube et al., 2008; reviewed by: Galizia & Rössler, 2010; Rössler & Zube, 2011) and *Drosophila* (Tanaka, Endo, & Ito, 2012; Tanaka, Suzuki, Dye, Ejima, & Stopfer, 2012). Thus, the LH, the SIP (referred as "ring neuropil" in previous studies) and the VLNP receive olfactory information from the ALs (Figure 6). In addition, the VLNP and the VMNP receive visual input from the OLs (Figures 12a–g, 13, and 14), which is consistent with data from honey bees (Hertel & Maronde, 1987; Maronde, 1991; Milde, 1988), bumblebees (Paulk, Phillips-Portillo, Dacks, Fellous, & Gronenberg, 2008), and *Drosophila* (Namiki, Dickinson, Wong, Korff, & Card, 2018; Otsuna & Ito, 2006; Panser et al., 2016; Strausfeld, 1976; Wu et al., 2016). In flies, both brain regions are associated with the detection of directed motion and looming of objects (Ibbotson, Maddess, & DuBois, 1991; Klapoetke et al., 2017; Okamura & Strausfeld, 2007; Wicklein & Strausfeld, 2000; Wu et al., 2016). These very conserved findings across species illustrate the importance and behavioral relevance of distinct CANP structures as high-order integration centers in the insect brain.

4.6 | Visual projections in *Cataglyphis*

We confirmed two major optical tracts and four optic commissures in *Cataglyphis*. The anteriormost tract is the AOT (Figure 12a–c, 13, and 14a). The AOT seems to be a most conserved optic tract in insects. It

has been described in diverse insect orders such as Blattodea (Reischig & Stengl, 2002; Rosner et al., 2017), Coleoptera (Immonen et al., 2017), Diptera (Adden et al., 2019; Fischbach & Lyly-Hünerberg, 1983; Omoto et al., 2017; Power, 1943; Strausfeld, 1976), Lepidoptera (Collett, 1972; Strausfeld & Blest, 1970), Orthoptera (Homberg et al., 2003; Pfeiffer et al., 2005), and Hymenoptera including different *Cataglyphis* species (Grob et al., 2017; Held et al., 2016; Mota et al., 2011; Pfeiffer & Kinoshita, 2012; Schmitt, Stieb, et al., 2016). The AOT relays optic motion information (Collett, 1972; DeVoe et al., 1982; Paulk et al., 2008) as well as chromatic and polarization cues (Kinoshita et al., 2007; Mota et al., 2011; Pfeiffer et al., 2005) to the AOTU. In *Cataglyphis*, the AOT consists of projection neurons from the ME and LO (Figure 12a–c). Surprisingly, we also found that a few isolated neurons accompany the AOT but arborize into the VX instead of the AOTU (Figure 12g). Whether these neurons transmit similar information or completely different visual properties than other AOT-neurons requires future functional studies.

The OCT exclusively projects into the ipsilateral COs in the *Cataglyphis* brain (Figures 12a–c, 13, and 14a). To our knowledge, this tract has not been described before in any insect. Three different optic tracts, the ASOT, the anterior inferior optic tract (AIOT) and the LO tract (LOT) are known in honey bees (Ehmer & Gronenberg, 2002; Mobbs, 1984). In *Cataglyphis*, we did not find any evidence for a distinct AIOT or LOT. Instead, a very small subset of LO neurons join the ASOT formed by dorsal and ventral medullar neurons (Grob et al., 2017) and project into the calyces of both hemispheres (Figure 14b). The ASOT has exclusively been described in Hymenoptera, whereas other insects possess a prominent anterior optical commissure that we could not find in *Cataglyphis*—the great commissure (GC) (Immonen et al., 2017; Ito et al., 2014; Strausfeld, 1976; von Hadeln et al., 2018).

We also identified a commissure that exclusively interconnects the OLs in the *Cataglyphis* brain—the SOC (Figures 12a–c,h, 13, and 14b), which has previously been described in the brains of the cockroach *Leucophaea maderae* (Loesel & Homberg, 2001; Reischig & Stengl, 2002), crickets (Honegger & Schürmann, 1975; Tomioka, Nakamichi, & Yukizane, 1994) and the honey bee (Hertel & Maronde, 1987). In all of these insects, the SOC comprises only very few neurons originating from the LO and ME, which is consistent with our findings in *Cataglyphis* (Figure 12a–c). These neurons might respond to moving objects and play a role in tracking of objects as it has been shown in other insects (Hertel & Maronde, 1987; Loesel & Homberg, 2001).

The POC and the IOC are situated more posteriorly in the *Cataglyphis* brain. Here, the POC is a very prominent commissure. It was described in numerous insect species including Hymenoptera (Hertel & Maronde, 1987; Honegger & Schürmann, 1975; Immonen et al., 2017; Ito et al., 2014; Reischig & Stengl, 2002; von Hadeln et al., 2018; Yilmaz et al., 2016). In contrast, the IOC has only been described in few insect species such as the cockroach *Leucophaea maderae* (Reischig & Stengl, 2002), crickets (Honegger & Schürmann, 1975), and Hymenoptera (Hertel & Maronde, 1987; Mobbs, 1984; Paulk et al., 2008; Yilmaz et al., 2016). These tracts transfer, among others, information from the OL to the VMNPs and the VLNPs. Electrophysiological recordings in bees showed that these neurons, for the most part, are achromatic (Hertel & Maronde, 1987; Paulk, Dacks, Phillips-Portillo, Fellous, & Gronenberg, 2009). Further results associated the neurons of the POC with the localization of stationary targets, while the IOC neurons respond to directional movements of objects (Hertel & Maronde, 1987; Maronde, 1991).

ACKNOWLEDGMENTS

We would like to thank the Greek government and the management boards of the Schinias and Strofylia National Park for the permission to excavate and transfer the *Cataglyphis* ants to Germany. We especially thank Maria Trivourea, Vasiliki Orfanou, and Georgia Karamperou for the warm welcome and their support during our field work. We are very grateful to Christos Georgiadis for his longstanding cooperation, administrative help, and for guiding us to the *Cataglyphis* nests. We also thank the field assistants who defied the heat in the field and helped to excavate the *Cataglyphis* nests. Special thanks go to Erich Buchner and Christian Wegener for kindly providing the anti-synapsin antibody. The study was financially supported by the German Research Foundation (DFG), DFG Ro1177/7-1 and DFG equipment grant INST 93/829-1, both to W. R.

CONFLICT OF INTEREST

The authors declare no conflicts of interest.

AUTHOR CONTRIBUTIONS

Wolfgang Rössler, Basil el Jundi, Jens Habenstein, and Emad Amini contributed to study concept and design. Emad Amini, Kornelia Grübel, and Jens Habenstein contributed to preparation and acquisition of data. Jens Habenstein contributed to drafting of the manuscript. Emad Amini, Basil el Jundi, and Wolfgang Rössler contributed to critical review of the manuscript. Wolfgang Rössler obtained funding. All authors contributed to analyses and interpretation of data, and approved the final version of the manuscript for submission.

DATA AVAILABILITY STATEMENT

Three-dimensional data of the brain of Cataglyphis nodus are available at the Insect Brain Database website (https://www.insectbraindb.org/).

REFERENCES

Abel, R., Rybak, J., & Menzel, R. (2001). Structure and response patterns of olfactory interneurons in the honeybee, *Apis mellifera*. *Journal of Comparative Neurology*, *437*(3), 363–383.

Adden, A., Wibrand, S., Pfeiffer, K., Warrant, E., & Heinze, S. (2020). The brain of a nocturnal migratory insect, the Australian Bogong moth. *Journal of Comparative Neurology*. https://doi.org/10.1002/cne.24866

Agosti, D. (1990). Review and reclassification of Cataglyphis (Hymenoptera, Formicidae). *Journal of Natural History*, *24*(6), 1457–1505.

Ai, H., Nishino, H., & Itoh, T. (2007). Topographic organization of sensory afferents of Johnston's organ in the honeybee brain. *Journal of Comparative Neurology*, *502*(6), 1030–1046.

Aimon, S., Katsuki, T., Jia, T., Grosenick, L., Broxton, M., Deisseroth, K., … Greenspan, R. J. (2019). Fast near-whole–brain imaging in adult

Drosophila during responses to stimuli and behavior. *PLoS Biology*, *17*(2), e2006732.

Brandt, R., Rohlfing, T., Rybak, J., Krofczik, S., Maye, A., Westerhoff, M., … Menzel, R. (2005). Three-dimensional average-shape atlas of the honeybee brain and its applications. *Journal of Comparative Neurology*, *492*(1), 1–19.

Bressan, J., Benz, M., Oettler, J., Heinze, J., Hartenstein, V., & Sprecher, S. G. (2015). A map of brain neuropils and fiber systems in the ant Cardiocondyla obscurior. *Frontiers in Neuroanatomy*, *8*, 166.

Brill, M. F., Rosenbaum, T., Reus, I., Kleineidam, C. J., Nawrot, M. P., & Rössler, W. (2013). Parallel processing via a dual olfactory pathway in the honeybee. *Journal of Neuroscience*, *33*(6), 2443–2456.

Brill, M. F., Meyer, A., & Rössler, W. (2015). It takes two—Coincidence coding within the dual olfactory pathway of the honeybee. *Frontiers in Physiology*, *6*, 208.

Buehlmann, C., Graham, P., Hansson, B. S., & Knaden, M. (2014). Desert ants locate food by combining high sensitivity to food odors with extensive crosswind runs. *Current Biology*, *24*(9), 960–964.

Carcaud, J., Giurfa, M., & Sandoz, J.-C. (2015). Differential combinatorial coding of pheromones in two olfactory subsystems of the honey bee brain. *Journal of Neuroscience*, *35*(10), 4157–4167.

Collett, T. (1972). Visual neurones in the anterior optic tract of the privet hawk moth. *Journal of Comparative Physiology*, *78*(4), 396–433.

Collett, T. S., Dillmann, E., Giger, A., & Wehner, R. (1992). Visual landmarks and route following in desert ants. *Journal of Comparative Physiology A*, *170*(4), 435–442.

Couto, A., Lapeyre, B., Thiéry, D., & Sandoz, J. C. (2016). Olfactory pathway of the hornet Vespa velutina: New insights into the evolution of the hymenopteran antennal lobe. *Journal of Comparative Neurology*, *524*(11), 2335–2359.

Cruse, H., & Wehner, R. (2011). No need for a cognitive map: Decentralized memory for insect navigation. *PLoS Computational Biology*, *7*(3), e1002009.

Dacks, A. M., Christensen, T. A., & Hildebrand, J. G. (2006). Phylogeny of a serotonin-immunoreactive neuron in the primary olfactory center of the insect brain. *Journal of Comparative Neurology*, *498*(6), 727–746.

Dancker, P., Low, I., Hasselbach, W., & Wieland, T. (1975). Interaction of Actin with phalloidin: Polymerization and stabilization of F-Actin. *Biochimica et Biophysica Acta*, *400*(2), 407–414.

Dettner, K., & Peters, W. (2011). *Lehrbuch der Entomologie*. Heidelberg: Springer Spektrum.

DeVoe, R. D., Kaiser, W., Ohm, J., & Stone, L. S. (1982). Horizontal movement detectors of honeybees: Directionally-selective visual neurons in the lobula and brain. *Journal of Comparative Physiology*, *147*(2), 155–170.

Ehmer, B., & Gronenberg, W. (1997). Proprioceptors and fast antennal reflexes in the ant Odontomachus (Formicidae, Ponerinae). *Cell and Tissue Research*, *290*(1), 153–165.

Ehmer, B., & Gronenberg, W. (2002). Segregation of visual input to the mushroom bodies in the honeybee (*Apis mellifera*). *Journal of Comparative Neurology*, *451*(4), 362–373.

Ehmer, B., & Gronenberg, W. (2004). Mushroom body volumes and visual interneurons in ants: Comparison between sexes and castes. *Journal of Comparative Neurology*, *469*(2), 198–213.

el Jundi, B., Huetteroth, W., Kurylas, A. E., & Schachtner, J. (2009). Anisometric brain dimorphism revisited: Implementation of a volumetric 3D standard brain in Manduca sexta. *Journal of Comparative Neurology*, *517*(2), 210–225.

el Jundi, B., Heinze, S., Lenschow, C., Kurylas, A., Rohlfing, T., & Homberg, U. (2010). The locust standard brain: A 3D standard of the central complex as a platform for neural network analysis. *Frontiers in Systems Neuroscience*, *3*, 21.

el Jundi, B., & Homberg, U. (2010). Evidence for the possible existence of a second polarization-vision pathway in the locust brain. *Journal of Insect Physiology*, *56*(8), 971–979.

el Jundi, B., Pfeiffer, K., & Homberg, U. (2011). A distinct layer of the medulla integrates sky compass signals in the brain of an insect. *PLoS One*, *6*(11), e27855.

el Jundi, B., & Homberg, U. (2012). Receptive field properties and intensity-response functions of polarization-sensitive neurons of the optic tubercle in gregarious and solitarious locusts. *Journal of Neurophysiology*, *108*(6), 1695–1710.

el Jundi, B., Pfeiffer, K., Heinze, S., & Homberg, U. (2014). Integration of polarization and chromatic cues in the insect sky compass. *Journal of Comparative Physiology A*, *200*(6), 575–589.

el Jundi, B., Warrant, E. J., Pfeiffer, K., & Dacke, M. (2018). Neuroarchitecture of the dung beetle central complex. *Journal of Comparative Neurology*, *526*(16), 2612–2630.

Erber, J., Masuhr, T., & Menzel, R. (1980). Localization of short-term memory in the brain of the bee, *Apis mellifera*. *Physiological Entomology*, *5*(4), 343–358.

Fahrbach, S. E. (2006). Structure of the mushroom bodies of the insect brain. *Annual Review of Entomology*, *51*, 209–232.

Falibene, A., Rössler, W., & Josens, R. (2012). Serotonin depresses feeding behaviour in ants. *Journal of Insect Physiology*, *58*(1), 7–17.

Farris, S. M. (2005). Evolution of insect mushroom bodies: Old clues, new insights. *Arthropod Structure & Development*, *34*(3), 211–234.

Farris, S. M. (2008). Tritocerebral tract input to the insect mushroom bodies. *Arthropod Structure & Development*, *37*(6), 492–503.

Farris, S. M., & Schulmeister, S. (2010). Parasitoidism, not sociality, is associated with the evolution of elaborate mushroom bodies in the brains of hymenopteran insects. *Proceedings of the Royal Society B: Biological Sciences*, *278*(1707), 940–951.

Farris, S. M. (2013). Evolution of complex higher brain centers and behaviors: Behavioral correlates of mushroom body elaboration in insects. *Brain, Behavior and Evolution*, *82*(1), 9–18.

Farris, S. M. (2015). Evolution of brain elaboration. *Philosophical Transactions of the Royal Society B: Biological Sciences*, *370*(1684), 20150054.

Fischbach, K., & Lyly-Hünerberg, I. (1983). Genetic dissection of the anterior optic tract of *Drosophila melanogaster*. *Cell and Tissue Research*, *231*(3), 551–563.

Fleischmann, P. N., Christian, M., Müller, V. L., Rössler, W., & Wehner, R. (2016). Ontogeny of learning walks and the acquisition of landmark information in desert ants, *Cataglyphis fortis*. *Journal of Experimental Biology*, *219*(19), 3137–3145.

Fleischmann, P. N., Grob, R., Wehner, R., & Rössler, W. (2017). Species-specific differences in the fine structure of learning walk elements in Cataglyphis ants. *Journal of Experimental Biology*, *220*(13), 2426–2435.

Fleischmann, P. N., Grob, R., Müller, V. L., Wehner, R., & Rössler, W. (2018). The geomagnetic field is a compass cue in Cataglyphis ant navigation. *Current Biology*, *28*(9), 1440, e1442–1444.

Frambach, I., Rössler, W., Winkler, M., & Schurmann, F. W. (2004). F-Actin at identified synapses in the mushroom body neuropil of the insect brain. *Journal of Comparative Neurology*, *475*(3), 303–314.

Galizia, C. G., & Rössler, W. (2010). Parallel olfactory systems in insects: Anatomy and function. *Annual Review of Entomology*, *55*, 399–420.

Green, J., Vijayan, V., Pires, P. M., Adachi, A., & Maimon, G. (2019). A neural heading estimate is compared with an internal goal to guide oriented navigation. *Nature Neuroscience*, *22*(9), 1460–1468.

Grob, R., Fleischmann, P. N., Grübel, K., Wehner, R., & Rössler, W. (2017). The role of celestial compass information in Cataglyphis ants during learning walks and for neuroplasticity in the central complex and mushroom bodies. *Frontiers in Behavioral Neuroscience*, *11*, 226.

Grob, R., Fleischmann, P. N., & Rössler, W. (2019). Learning to navigate–how desert ants calibrate their compass systems. *E-Neuroforum*, *25*(2), 109–120.

Groh, C., & Rössler, W. (2011). Comparison of microglomerular structures in the mushroom body calyx of neopteran insects. *Arthropod Structure & Development*, *40*(4), 358–367.

Groh, C., Kelber, C., Grübel, K., & Rössler, W. (2014). Density of mushroom body synaptic complexes limits intraspecies brain miniaturization in highly polymorphic leaf-cutting ant workers. *Proceedings of the Royal Society B: Biological Sciences*, *281*(1785), 20140432.

Groh, C., & Rössler, W. (2020). Analysis of synaptic microcircuits in the mushroom bodies of the honeybee. *Insects*, *11*(1), 43.

Gronenberg, W. (1999). Modality-specific segregation of input to ant mushroom bodies. *Brain, Behavior and Evolution*, *54*(2), 85–95.

Gronenberg, W., & Hölldobler, B. (1999). Morphologic representation of visual and antennal information in the ant brain. *Journal of Comparative Neurology*, *412*(2), 229–240.

Gronenberg, W. (2001). Subdivisions of hymenopteran mushroom body calyces by their afferent supply. *Journal of Comparative Neurology*, *435*(4), 474–489.

Gronenberg, W. (2008). Structure and function of ant (hymenoptera: Formicidae) brains: Strength in numbers. *Myrmecological News*, *11*, 25–36.

Groothuis, J., Pfeiffer, K., el Jundi, B., & Smid, H. M. (2019). The Jewel wasp standard brain: Average shape atlas and morphology of the female Nasonia vitripennis brain. *Arthropod Structure & Development*, *51*, 41–51.

Grünewald, B. (1999). Physiological properties and response modulations of mushroom body feedback neurons during olfactory learning in the honeybee, *Apis mellifera*. *Journal of Comparative Physiology A*, *185*(6), 565–576.

Guo, P., & Ritzmann, R. E. (2013). Neural activity in the central complex of the cockroach brain is linked to turning behaviors. *Journal of Experimental Biology*, *216*(6), 992–1002.

Haehnel, M., & Menzel, R. (2010). Sensory representation and learning-related plasticity in mushroom body extrinsic feedback neurons of the protocerebral tract. *Frontiers in Systems Neuroscience*, *4*, 161.

Hausen, K. (1976). Functional characterization and anatomical identification of motion sensitive neurons in the lobula plate of the blowfly Calliphora erythrocephala. *Zeitschrift für Naturforschung c*, *31*(9–10), 629–634.

Hausen, K. (1984). The lobula-complex of the fly: Structure, function and significance in visual behaviour. In *Photoreception and vision in invertebrates* (pp. 523–559). Berlin, Heidelberg: Springer.

Heinze, S., & Homberg, U. (2007). Maplike representation of celestial E-vector orientations in the brain of an insect. *Science*, *315*(5814), 995–997.

Heinze, S., & Homberg, U. (2008). Neuroarchitecture of the central complex of the desert locust: Intrinsic and columnar neurons. *Journal of Comparative Neurology*, *511*(4), 454–478.

Heinze, S., Gotthardt, S., & Homberg, U. (2009). Transformation of polarized light information in the central complex of the locust. *Journal of Neuroscience*, *29*(38), 11783–11793.

Heinze, S., & Reppert, S. M. (2011). Sun compass integration of skylight cues in migratory monarch butterflies. *Neuron*, *69*(2), 345–358.

Heinze, S., & Reppert, S. M. (2012). Anatomical basis of sun compass navigation I: The general layout of the monarch butterfly brain. *Journal of Comparative Neurology*, *520*(8), 1599–1628.

Heinze, S., Florman, J., Asokaraj, S., El Jundi, B., & Reppert, S. M. (2013). Anatomical basis of sun compass navigation II: The neuronal composition of the central complex of the monarch butterfly. *Journal of Comparative Neurology*, *521*(2), 267–298.

Heinze, S. (2014). Polarized-light processing in insect brains: recent insights from the desert locust, the monarch butterfly, the cricket, and the fruit fly. In *Polarized light and polarization vision in animal sciences* (pp. 61–111). Berlin, Heidelberg: Springer.

Heisenberg, M. (2003). Mushroom body memoir: From maps to models. *Nature Reviews Neuroscience*, *4*(4), 266–275.

Held, M., Berz, A., Hensgen, R., Muenz, T. S., Scholl, C., Rössler, W., … Pfeiffer, K. (2016). Microglomerular synaptic complexes in the sky-compass network of the honeybee connect parallel pathways from the anterior optic tubercle to the central complex. *Frontiers in Behavioral Neuroscience*, *10*, 186.

Hertel, H., Schäfer, S., & Maronde, U. (1987). The physiology and morphology of visual commissures in the honeybee brain. *Journal of Experimental Biology*, *133*(1), 283–300.

Hertel, H., & Maronde, U. (1987). Processing of visual information in the honeybee brain. In *Neurobiology and behavior of honeybees* (pp. 141–157). Berlin, Heidelberg: Springer.

Hofbauer, A., Ebel, T., Waltenspiel, B., Oswald, P., Chen, Y.-C., Halder, P., … Buchner, E. (2009). The Wuerzburg hybridoma library against drosophila brain. *Journal of Neurogenetics*, *23*(1–2), 78–91.

Hölldobler, B., & Wilson, E. O. (1990). *The ants*. Berlin, Heidelberg: Springer-Verlag.

Homberg, U., Christensen, T. A., & Hildebrand, J. G. (1989). Structure and function of the deutocerebrum in insects. *Annual Review of Entomology*, *34*(1), 477–501.

Homberg, U., Hofer, S., Pfeiffer, K., & Gebhardt, S. (2003). Organization and neural connections of the anterior optic tubercle in the brain of the locust, Schistocerca gregaria. *Journal of Comparative Neurology*, *462*(4), 415–430.

Homberg, U. (2004). In search of the sky compass in the insect brain. *Naturwissenschaften*, *91*(5), 199–208.

Homberg, U., Heinze, S., Pfeiffer, K., Kinoshita, M., & el Jundi, B. (2011). Central neural coding of sky polarization in insects. *Philosophical Transactions of the Royal Society B*, *366*(1565), 680–687.

Honegger, H.-W., & Schürmann, F. (1975). Cobalt sulphide staining of optic fibres in the brain of the cricket, Gryllus campestris. *Cell and Tissue Research*, *159*(2), 213–225.

Hoyer, S. C., Liebig, J., & Rössler, W. (2005). Biogenic amines in the ponerine ant *Harpegnathos saltator*: Serotonin and dopamine immunoreactivity in the brain. *Arthropod Structure & Development*, *34*(4), 429–440.

Huber, R., & Knaden, M. (2015). Egocentric and geocentric navigation during extremely long foraging paths of desert ants. *Journal of Comparative Physiology A*, *201*(6), 609–616.

Huetteroth, W., El Jundi, B., El Jundi, S., & Schachtner, J. (2010). 3D-reconstructions and virtual 4D-visualization to study metamorphic brain development in the sphinx moth Manduca sexta. *Frontiers in Systems Neuroscience*, *4*, 7.

Ibbotson, M., Maddess, T., & DuBois, R. (1991). A system of insect neurons sensitive to horizontal and vertical image motion connects the medulla and midbrain. *Journal of Comparative Physiology A*, *169*(3), 355–367.

Ilieș, I., Muscedere, M. L., & Traniello, J. F. (2015). Neuroanatomical and morphological trait clusters in the ant genus Pheidole: Evidence for modularity and integration in brain structure. *Brain, Behavior and Evolution*, *85*(1), 63–76.

Immonen, E. V., Dacke, M., Heinze, S., & el Jundi, B. (2017). Anatomical organization of the brain of a diurnal and a nocturnal dung beetle. *Journal of Comparative Neurology*, *525*(8), 1879–1908.

Ito, K., Shinomiya, K., Ito, M., Armstrong, J. D., Boyan, G., Hartenstein, V., … Vosshall, L. B. (2014). A systematic nomenclature for the insect brain. *Neuron*, *81*(4), 755–765.

Joesch, M., Plett, J., Borst, A., & Reiff, D. F. (2008). Response properties of motion-sensitive visual interneurons in the lobula plate of *Drosophila melanogaster*. *Current Biology*, *18*(5), 368–374.

Jørgensen, K., Kvello, P., Almaas, T. J., & Mustaparta, H. (2006). Two closely located areas in the suboesophageal ganglion and the tritocerebrum receive projections of gustatory receptor neurons located on the antennae and the proboscis in the moth Heliothis virescens. *Journal of Comparative Neurology*, *496*(1), 121–134.

Kamikouchi, A., Inagaki, H. K., Effertz, T., Hendrich, O., Fiala, A., Göpfert, M. C., & Ito, K. (2009). The neural basis of drosophila gravity-sensing and hearing. *Nature*, *458*(7235), 165–171.

Kelber, C., Rössler, W., Roces, F., & Kleineidam, C. J. (2009). The antennal lobes of fungus-growing ants (Attini): Neuroanatomical traits and evolutionary trends. *Brain, Behavior and Evolution*, *73*(4), 273–284.

Kinoshita, M., Pfeiffer, K., & Homberg, U. (2007). Spectral properties of identified polarized-light sensitive interneurons in the brain of the desert locust Schistocerca gregaria. *Journal of Experimental Biology*, *210*(8), 1350–1361.

Kirkhart, C., & Scott, K. (2015). Gustatory learning and processing in the drosophila mushroom bodies. *Journal of Neuroscience*, *35*(15), 5950–5958.

Kirschner, S., Kleineidam, C. J., Zube, C., Rybak, J., Grünewald, B., & Rössler, W. (2006). Dual olfactory pathway in the honeybee, *Apis mellifera*. *Journal of Comparative Neurology*, *499*(6), 933–952.

Klagges, B. R., Heimbeck, G., Godenschwege, T. A., Hofbauer, A., Pflugfelder, G. O., Reifegerste, R., … Buchner, E. (1996). Invertebrate synapsins: A single gene codes for several isoforms in drosophila. *Journal of Neuroscience*, *16*(10), 3154–3165.

Klapoetke, N. C., Nern, A., Peek, M. Y., Rogers, E. M., Breads, P., Rubin, G. M., … Card, G. M. (2017). Ultra-selective looming detection from radial motion opponency. *Nature*, *551*(7679), 237–241.

Knaden, M., & Wehner, R. (2005). Nest mark orientation in desert ants Cataglyphis: What does it do to the path integrator? *Animal Behaviour*, *70*(6), 1349–1354.

Kurylas, A. E., Rohlfing, T., Krofczik, S., Jenett, A., & Homberg, U. (2008). Standardized atlas of the brain of the desert locust, Schistocerca gregaria. *Cell and Tissue Research*, *333*(1), 125–145.

Laissue, P., Reiter, C., Hiesinger, P., Halter, S., Fischbach, K., & Stocker, R. (1999). Three-dimensional reconstruction of the antennal lobe in *Drosophila melanogaster*. *Journal of Comparative Neurology*, *405*(4), 543–552.

Lebhardt, F., & Ronacher, B. (2014). Interactions of the polarization and the sun compass in path integration of desert ants. *Journal of Comparative Physiology A*, *200*(8), 711–720.

Lebhardt, F., & Ronacher, B. (2015). Transfer of directional information between the polarization compass and the sun compass in desert ants. *Journal of Comparative Physiology A*, *201*(6), 599–608.

Li, Y., & Strausfeld, N. J. (1997). Morphology and sensory modality of mushroom body extrinsic neurons in the brain of the cockroach, *Periplaneta americana*. *Journal of Comparative Neurology*, *387*(4), 631–650.

Lin, H.-H., Lai, J. S.-Y., Chin, A.-L., Chen, Y.-C., & Chiang, A.-S. (2007). A map of olfactory representation in the drosophila mushroom body. *Cell*, *128*(6), 1205–1217.

Liu, L., Wolf, R., Ernst, R., & Heisenberg, M. (1999). Context generalization in drosophila visual learning requires the mushroom bodies. *Nature*, *400*(6746), 753.

Loesel, R., & Homberg, U. (2001). Anatomy and physiology of neurons with processes in the accessory medulla of the cockroach *Leucophaea maderae*. *Journal of Comparative Neurology*, *439*(2), 193–207.

Maronde, U. (1991). Common projection areas of antennal and visual pathways in the honeybee brain, *Apis mellifera*. *Journal of Comparative Neurology*, *309*(3), 328–340.

Martin, J. P., Guo, P., Mu, L., Harley, C. M., & Ritzmann, R. E. (2015). Central-complex control of movement in the freely walking cockroach. *Current Biology*, *25*(21), 2795–2803.

Masante-Roca, I., Gadenne, C., & Anton, S. (2005). Three-dimensional antennal lobe atlas of male and female moths, Lobesia botrana (Lepidoptera: Tortricidae) and glomerular representation of plant volatiles in females. *Journal of Experimental Biology*, *208*(6), 1147–1159.

Menzel, R. (1999). Memory dynamics in the honeybee. *Journal of Comparative Physiology A*, *185*(4), 323–340.

Menzel, R. (2001). Searching for the memory trace in a mini-brain, the honeybee. *Learning & Memory*, *8*(2), 53–62.

Menzel, R. (2014). The insect mushroom body, an experience-dependent recoding device. *Journal of Physiology*, *108*(2–3), 84–95.

Milde, J. J. (1988). Visual responses of interneurones in the posterior median protocerebrum and the central complex of the honeybee *Apis mellifera*. *Journal of Insect Physiology*, *34*(5), 427–436.

Miyazaki, T., & Ito, K. (2010). Neural architecture of the primary gustatory center of *Drosophila melanogaster* visualized with GAL4 and LexA enhancer-trap systems. *Journal of Comparative Neurology*, *518*(20), 4147–4181.

Mobbs, P. (1982). The brain of the honeybee *Apis mellifera*. I. the connections and spatial organization of the mushroom bodies. *Philosophical Transactions of the Royal Society of London B, Biological Sciences*, *298* (1091), 309–354.

Mobbs, P. (1984). Neural networks in the mushroom bodies of the honeybee. *Journal of Insect Physiology*, *30*(1), 43–58.

Montgomery, S. H., & Ott, S. R. (2015). Brain composition in Godyris zavaleta, a diurnal butterfly, reflects an increased reliance on olfactory information. *Journal of Comparative Neurology*, *523*(6), 869–891.

Montgomery, S. H., Merrill, R. M., & Ott, S. R. (2016). Brain composition in Heliconius butterflies, posteclosion growth and experience-dependent neuropil plasticity. *Journal of Comparative Neurology*, *524*(9), 1747–1769.

Mota, T., Yamagata, N., Giurfa, M., Gronenberg, W., & Sandoz, J.-C. (2011). Neural organization and visual processing in the anterior optic tubercle of the honeybee brain. *Journal of Neuroscience*, *31*(32), 11443–11456.

Mota, T., Gronenberg, W., Giurfa, M., & Sandoz, J.-C. (2013). Chromatic processing in the anterior optic tubercle of the honey bee brain. *Journal of Neuroscience*, *33*(1), 4–16.

Mota, T., Kreissl, S., Carrasco, D. A., Lefer, D., Galizia, G., & Giurfa, M. (2016). Synaptic organization of microglomerular clusters in the lateral and medial bulbs of the honeybee brain. *Frontiers in Neuroanatomy*, *10*, 103.

Müller, D., Abel, R., Brandt, R., Zöckler, M., & Menzel, R. (2002). Differential parallel processing of olfactory information in the honeybee, *Apis mellifera* L. *Journal of Comparative Physiology A*, *188*(5), 359–370.

Müller, M., & Wehner, R. (1988). Path integration in desert ants, *Cataglyphis fortis*. *Proceedings of the National Academy of Science of the USA*, *85*(14), 5287–5290.

Namiki, S., & Kanzaki, R. (2016). Comparative neuroanatomy of the lateral accessory lobe in the insect brain. *Frontiers in Physiology*, *7*, 244.

Namiki, S., Dickinson, M. H., Wong, A. M., Korff, W., & Card, G. M. (2018). The functional organization of descending sensory-motor pathways in drosophila. *Elife*, *7*, e34272.

Nishikawa, M., Nishino, H., Misaka, Y., Kubota, M., Tsuji, E., Satoji, Y., … Yokohari, F. (2008). Sexual dimorphism in the antennal lobe of the ant *Camponotus japonicus*. *Zoological Science*, *25*(2), 195–205.

Okamura, J. Y., & Strausfeld, N. J. (2007). Visual system of calliphorid flies: Motion-and orientation-sensitive visual interneurons supplying dorsal optic glomeruli. *Journal of Comparative Neurology*, *500*(1), 189–208.

Omoto, J. J., Keleş, M. F., Nguyen, B.-C. M., Bolanos, C., Lovick, J. K., Frye, M. A., & Hartenstein, V. (2017). Visual input to the drosophila central complex by developmentally and functionally distinct neuronal populations. *Current Biology*, *27*(8), 1098–1110.

Otsuna, H., & Ito, K. (2006). Systematic analysis of the visual projection neurons of *Drosophila melanogaster*. I. Lobula-specific pathways. *Journal of Comparative Neurology*, *497*(6), 928–958.

Panser, K., Tirian, L., Schulze, F., Villalba, S., Jefferis, G. S., Buehler, K., & Straw, A. D. (2016). Automatic segmentation of Drosophila neural compartments using GAL4 expression data reveals novel visual pathways. *Current Biology*, *26*(15), 1943–1954.

Pasch, E., Muenz, T. S., & Rössler, W. (2011). CaMKII is differentially localized in synaptic regions of Kenyon cells within the mushroom bodies of the honeybee brain. *Journal of Comparative Neurology*, *519*(18), 3700–3712.

Paulk, A. C., Phillips-Portillo, J., Dacks, A. M., Fellous, J.-M., & Gronenberg, W. (2008). The processing of color, motion, and stimulus timing are anatomically segregated in the bumblebee brain. *Journal of Neuroscience*, *28*(25), 6319–6332.

Paulk, A. C., & Gronenberg, W. (2008). Higher order visual input to the mushroom bodies in the bee, *Bombus impatiens*. *Arthropod Structure & Development*, *37*(6), 443–458.

Paulk, A. C., Dacks, A. M., Phillips-Portillo, J., Fellous, J.-M., & Gronenberg, W. (2009). Visual processing in the central bee brain. *Journal of Neuroscience*, *29*(32), 9987–9999.

Pereanu, W., Kumar, A., Jennett, A., Reichert, H., & Hartenstein, V. (2010). Development-based compartmentalization of the Drosophila central brain. *Journal of Comparative Neurology*, *518*(15), 2996–3023.

Pfeffer, S. E., & Wittlinger, M. (2016). Optic flow odometry operates independently of stride integration in carried ants. *Science*, *353*(6304), 1155–1157.

Pfeiffer, K., Kinoshita, M., & Homberg, U. (2005). Polarization-sensitive and light-sensitive neurons in two parallel pathways passing through the anterior optic tubercle in the locust brain. *Journal of Neurophysiology*, *94*, 3903–3915.

Pfeiffer, K., & Homberg, U. (2007). Coding of azimuthal directions via time-compensated combination of celestial compass cues. *Current Biology*, *17*(11), 960–965.

Pfeiffer, K., & Kinoshita, M. (2012). Segregation of visual inputs from different regions of the compound eye in two parallel pathways through the anterior optic tubercle of the bumblebee (*Bombus ignitus*). *Journal of Comparative Neurology*, *520*(2), 212–229.

Power, M. E. (1943). The brain of *Drosophila melanogaster*. *Journal of Morphology*, *72*(3), 517–559.

Preibisch, S., Saalfeld, S., & Tomancak, P. (2009). Globally optimal stitching of tiled 3D microscopic image acquisitions. *Bioinformatics*, *25*(11), 1463–1465.

Reischig, T., & Stengl, M. (2002). Optic lobe commissures in a three-dimensional brain model of the cockroach *Leucophaea maderae*: A search for the circadian coupling pathways. *Journal of Comparative Neurology*, *443*(4), 388–400.

Ribi, W., Senden, T. J., Sakellariou, A., Limaye, A., & Zhang, S. (2008). Imaging honey bee brain anatomy with micro-X-ray-computed tomography. *Journal of Neuroscience Methods*, *171*(1), 93–97.

Ronacher, B. (2008). Path integration as the basic navigation mechanism of the desert ant *Cataglyphis fortis* (Forel, 1902) (Hymenoptera: Formicidae). *Myrmecological News*, *11*, 53–62.

Rosner, R., von Hadeln, J., Salden, T., & Homberg, U. (2017). Anatomy of the lobula complex in the brain of the praying mantis compared to the lobula complexes of the locust and cockroach. *Journal of Comparative Neurology*, *525*(10), 2343–2357.

Rössler, W., Kuduz, J., Schürmann, F. W., & Schild, D. (2002). Aggregation of F-actin in olfactory glomeruli: A common feature of glomeruli across phyla. *Chemical Senses*, *27*(9), 803–810.

Rössler, W., & Zube, C. (2011). Dual olfactory pathway in hymenoptera: Evolutionary insights from comparative studies. *Arthropod Structure & Development*, *40*(4), 349–357.

Rössler, W., & Groh, C. (2012). Plasticity of synaptic microcircuits in the mushroom-body calyx of the honey bee. In *Honeybee neurobiology and behavior* (pp. 141–153). Dordrecht, Heidelberg, London New York: Springer.

Rössler, W., & Brill, M. F. (2013). Parallel processing in the honeybee olfactory pathway: Structure, function, and evolution. *Journal of Comparative Physiology A*, *199*(11), 981–996.

Rössler, W. (2019). Neuroplasticity in desert ants (hymenoptera: Formicidae)–importance for the ontogeny of navigation. *Myrmecological News*, *29*, 1–20.

Ruano, F., Tinaut, A., & Soler, J. J. (2000). High surface temperatures select for individual foraging in ants. *Behavioral Ecology*, *11*(4), 396–404.

Sancer, G., Kind, E., Plazaola-Sasieta, H., Balke, J., Pham, T., Hasan, A., … Wernet, M. F. (2019). Modality-specific circuits for skylight orientation in the fly visual system. *Current Biology*, *29*(17), 2812–2825.

Schmeling, F., Tegtmeier, J., Kinoshita, M., & Homberg, U. (2015). Photoreceptor projections and receptive fields in the dorsal rim area and main retina of the locust eye. *Journal of Comparative Physiology A*, *201*(5), 427–440.

Schmitt, F., Stieb, S. M., Wehner, R., & Rossler, W. (2016). Experience-related reorganization of giant synapses in the lateral complex: Potential role in plasticity of the sky-compass pathway in the desert ant *Cataglyphis fortis*. *Developmental Neurobiology*, *76*(4), 390–404.

Schmitt, F., Vanselow, J. T., Schlosser, A., Wegener, C., & Rossler, W. (2016). Neuropeptides in the desert ant *Cataglyphis fortis*: Mass spectrometric analysis, localization, and age-related changes. *Journal of Comparative Neurology*, *525*, 901–918.

Scholtz, G., & Edgecombe, G. D. (2006). The evolution of arthropod heads: Reconciling morphological, developmental and palaeontological evidence. *Development Genes and Evolution*, *216*(7–8), 395–415.

Seelig, J. D., & Jayaraman, V. (2013). Feature detection and orientation tuning in the Drosophila central complex. *Nature*, *503*(7475), 262.

Seelig, J. D., & Jayaraman, V. (2015). Neural dynamics for landmark orientation and angular path integration. *Nature*, *521*(7551), 186.

Steck, K., Hansson, B. S., & Knaden, M. (2011). Desert ants benefit from combining visual and olfactory landmarks. *Journal of Experimental Biology*, *214*(8), 1307–1312.

Stieb, S. M., Muenz, T. S., Wehner, R., & Rössler, W. (2010). Visual experience and age affect synaptic organization in the mushroom bodies of the desert ant *Cataglyphis fortis*. *Developmental Neurobiology*, *70*(6), 408–423.

Stieb, S. M., Kelber, C., Wehner, R., & Rössler, W. (2011). Antennal-lobe organization in desert ants of the genus Cataglyphis. *Brain, Behavior and Evolution*, *77*(3), 136–146.

Stieb, S. M., Hellwig, A., Wehner, R., & Rössler, W. (2012). Visual experience affects both behavioral and neuronal aspects in the individual life history of the desert ant *Cataglyphis fortis*. *Developmental Neurobiology*, *72*(5), 729–742.

Stocker, R., Lienhard, M., Borst, A., & Fischbach, K. (1990). Neuronal architecture of the antennal lobe in *Drosophila melanogaster*. *Cell and Tissue Research*, *262*(1), 9–34.

Stone, T., Webb, B., Adden, A., Weddig, N. B., Honkanen, A., Templin, R., … Heinze, S. (2017). An anatomically constrained model for path integration in the bee brain. *Current Biology*, *27*(20), 3069–3085. e3011.

Strausfeld, N. J., & Blest, A. (1970). Golgi studies on insects Part I. The optic lobes of Lepidoptera. *Philosophical Transactions of the Royal Society of London B, Biological Sciences*, *258*(820), 81–134.

Strausfeld N. J. (1976). *Atlas of an insect brain*. Berlin, Heidelberg, New York: Springer.

Strausfeld, N. J., Homburg, U., & Kloppenberg, P. (2000). Parallel organization in honey bee mushroom bodies by peptidergic Kenyon cells. *Journal of Comparative Neurology*, *424*(1), 179–195.

Strausfeld, N. J. (2002). Organization of the honey bee mushroom body: Representation of the calyx within the vertical and gamma lobes. *Journal of Comparative Neurology*, *450*(1), 4–33.

Strausfeld, N. J., & Okamura, J. Y. (2007). Visual system of calliphorid flies: Organization of optic glomeruli and their lobula complex efferents. *Journal of Comparative Neurology*, *500*(1), 166–188.

Strausfeld, N. J., Sinakevitch, I., Brown, S. M., & Farris, S. M. (2009). Ground plan of the insect mushroom body: Functional and evolutionary implications. *Journal of Comparative Neurology*, *513*(3), 265–291.

Strausfeld, N. J. (2012). *Arthropod brains: Evolution, functional elegance, and historical significance*. Cambridge, MA: Belknap Press of Harvard University Press.

Strauss, R. (2002). The central complex and the genetic dissection of locomotor behaviour. *Current Opinion in Neurobiology*, *12*(6), 633–638.

Sun, Y., Nern, A., Franconville, R., Dana, H., Schreiter, E. R., Looger, L. L., … Jayaraman, V. (2017). Neural signatures of dynamic stimulus selection in Drosophila. *Nature Neuroscience*, *20*(8), 1104–1113.

Szyszka, P., Galkin, A., & Menzel, R. (2008). Associative and non-associative plasticity in Kenyon cells of the honeybee mushroom body. *Frontiers in Systems Neuroscience*, *2*, 3.

Tanaka, N. K., Tanimoto, H., & Ito, K. (2008). Neuronal assemblies of the Drosophila mushroom body. *Journal of Comparative Neurology*, *508*(5), 711–755.

Tanaka, N. K., Suzuki, E., Dye, L., Ejima, A., & Stopfer, M. (2012). Dye fills reveal additional olfactory tracts in the protocerebrum of wild-type Drosophila. *Journal of Comparative Neurology*, *520*(18), 4131–4140.

Tanaka, N. K., Endo, K., & Ito, K. (2012). Organization of antennal lobe-associated neurons in adult *Drosophila melanogaster* brain. *Journal of Comparative Neurology*, *520*(18), 4067–4130.

Tomioka, K., Nakamichi, M., & Yukizane, M. (1994). Optic lobe circadian pacemaker sends its information to the contralateral optic lobe in the cricket Gryllus bimaculatus. *Journal of Comparative Physiology A*, *175*(4), 381–388.

Träger, U., Wagner, R., Bausenwein, B., & Homberg, U. (2008). A novel type of microglomerular synaptic complex in the polarization vision pathway of the locust brain. *Journal of Comparative Neurology*, *506*(2), 288–300.

Turner-Evans, D. B., & Jayaraman, V. (2016). The insect central complex. *Current Biology*, *26*(11), R453–R457.

Varela, N., Couton, L., Gemeno, C., Avilla, J., Rospars, J.-P., & Anton, S. (2009). Three-dimensional antennal lobe atlas of the oriental fruit moth, Cydia molesta (Busck) (Lepidoptera: Tortricidae): Comparison of male and female glomerular organization. *Cell and Tissue Research*, *337*(3), 513–526.

von Hadeln, J., Althaus, V., Häger, L., & Homberg, U. (2018). Anatomical organization of the cerebrum of the desert locust Schistocerca gregaria. *Cell and Tissue Research*, *374*(1), 39–62.

Warren, T. L., Giraldo, Y. M., & Dickinson, M. H. (2019). Celestial navigation in Drosophila. *Journal of Experimental Biology*, *222*(Suppl 1), jeb186148.

Watanabe, H., Shimohigashi, M., & Yokohari, F. (2014). Serotonin-immunoreactive sensory neurons in the antenna of the cockroach *Periplaneta americana*. *Journal of Comparative Neurology*, *522*(2), 414–434.

Wehner, R., & Menzel, R. (1969). Homing in the ant *Cataglyphis bicolor*. *Science*, *164*(3876), 192–194.

Wehner, R., & Räber, F. (1979). Visual spatial memory in desert ants, *Cataglyphis bicolor* (Hymenoptera: Formicidae). *Experientia*, *35*(12), 1569–1571.

Wehner, R., Michel, B., & Antonsen, P. (1996). Visual navigation in insects: Coupling of egocentric and geocentric information. *Journal of Experimental Biology*, *199*(1), 129–140.

Wehner, R. (1997). The ant's celestial compass system: Spectral and polarization channels. In *Orientation and communication in arthropods* (pp. 145–185). Berlin, Heidelberg: Springer.

Wehner, R. (2003). Desert ant navigation: How miniature brains solve complex tasks. *Journal of Comparative Physiology A*, *189*(8), 579–588.

Wehner, R., & Muller, M. (2006). The significance of direct sunlight and polarized skylight in the ant's celestial system of navigation. *Proceedings of the National Academy of Sciences of the United States of America*, *103*(33), 12575–12579.

Wehner, R. (2009). The architecture of the desert ant's navigational toolkit (Hymenoptera: Formicidae). *Myrmecological News*, *12*(September), 85–96.

Wehner, R., Hoinville, T., Cruse, H., & Cheng, K. (2016). Steering intermediate courses: Desert ants combine information from various navigational routines. *Journal of Comparative Physiology A*, *202*(7), 459–472.

Wicklein, M., & Strausfeld, N. J. (2000). Organization and significance of neurons that detect change of visual depth in the hawk moth Manduca sexta. *Journal of Comparative Neurology*, *424*(2), 356–376.

Witthöft, W. (1967). Absolute anzahl und verteilung der zellen im him der honigbiene. *Zeitschrift für Morphologie der Tiere*, *61*(1), 160–184.

Wittlinger, M., Wehner, R., & Wolf, H. (2006). The ant odometer: Stepping on stilts and stumps. *Science*, *312*(5782), 1965–1967.

Wolf, H., Wittlinger, M., & Pfeffer, S. E. (2018). Two distance memories in desert ants—Modes of interaction. *PLoS One*, *13*(10), e0204664.

Wong, A. M., Wang, J. W., & Axel, R. (2002). Spatial representation of the glomerular map in the Drosophila protocerebrum. *Cell*, *109*(2), 229–241.

Wu, M., Nern, A., Williamson, W. R., Morimoto, M. M., Reiser, M. B., Card, G. M., & Rubin, G. M. (2016). Visual projection neurons in the Drosophila lobula link feature detection to distinct behavioral programs. *Elife*, *5*, e21022.

Yilmaz, A., Lindenberg, A., Albert, S., Grübel, K., Spaethe, J., Rössler, W., & Groh, C. (2016). Age-related and light-induced plasticity in opsin gene expression and in primary and secondary visual centers of the nectar-feeding ant *Camponotus rufipes*. *Developmental Neurobiology*, *76*(9), 1041–1057.

Zeil, J., & Fleischmann, P. N. (2019). The learning walks of ants (Hymenoptera: Formicidae). *Myrmecological News*, *29*, 93–110.

Zeller, M., Held, M., Bender, J., Berz, A., Heinloth, T., Hellfritz, T., & Pfeiffer, K. (2015). Transmedulla neurons in the sky compass network of the honeybee (*Apis mellifera*) are a possible site of circadian input. *PLoS One*, *10*(12), e0143244.

Zieger, E., Bräunig, P., & Harzsch, S. (2013). A developmental study of serotonin-immunoreactive neurons in the embryonic brain of the Marbled Crayfish and the Migratory Locust: Evidence for a homologous protocerebral group of neurons. *Arthropod Structure & Development*, *42*(6), 507–520.

Zube, C., Kleineidam, C. J., Kirschner, S., Neef, J., & Rössler, W. (2008). Organization of the olfactory pathway and odor processing in the antennal lobe of the ant *Camponotus floridanus*. *Journal of Comparative Neurology*, *506*(3), 425–441.

How to cite this article: Habenstein J, Amini E, Grübel K, B el Jundi, Rössler W. The brain of *Cataglyphis* ants: Neuronal organization and visual projections. *J Comp Neurol*. 2020;1–28. https://doi.org/10.1002/cne.24934

4 Manuscript II: Transcriptomic, peptidomic and mass spectrometry imaging analysis of the brain in the ant *Cataglyphis nodus*

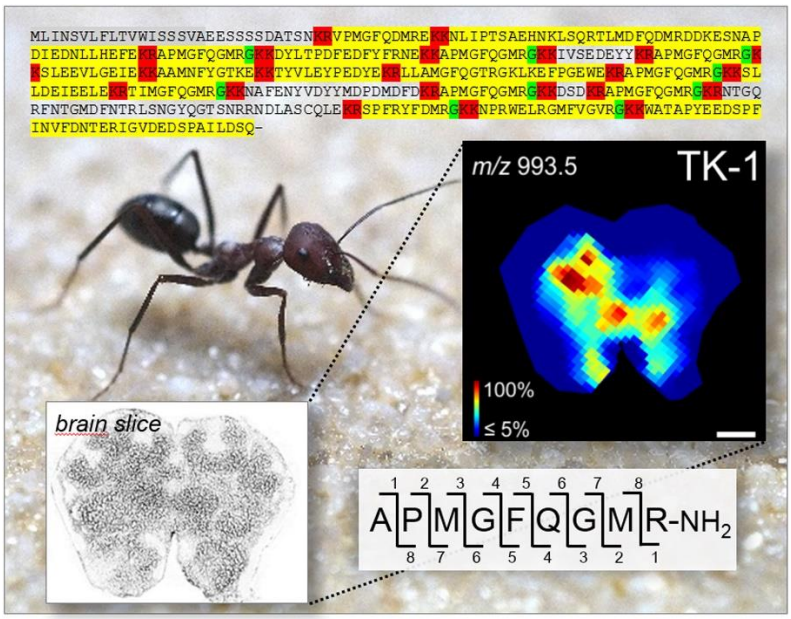

Received: 14 December 2020 | Revised: 5 March 2021 | Accepted: 8 March 2021

DOI: 10.1111/jnc.15346

ORIGINAL ARTICLE

Journal of Neurochemistry JNC WILEY

Transcriptomic, peptidomic, and mass spectrometry imaging analysis of the brain in the ant *Cataglyphis nodus*

Jens Habenstein[1] | Franziska Schmitt[1] | Sander Liessem[2] | Alice Ly[3] | Dennis Trede[4] | Christian Wegener[5] | Reinhard Predel[2] | Wolfgang Rössler[1] | Susanne Neupert[2,6]

[1]Behavioral Physiology and Sociobiology (Zoology II), University of Würzburg, Würzburg, Germany

[2]Department of Biology, Institute for Zoology, University of Cologne, Cologne, Germany

[3]Bruker Daltonik GmbH, Bremen, Germany

[4]SCiLS, Zweigniederlassung Bremen der Bruker Daltonik GmbH, Bremen, Germany

[5]Theodor-Boveri-Institute, Neurobiology and Genetics, Würzburg Insect Research, University of Würzburg, Würzburg, Germany

[6]Department of Biology, University of Kassel, Kassel, Germany

Correspondence
Susanne Neupert, Department for Biology, Animal Physiology, University of Kassel, Heinrich-Plett-Strasse 40, 34132 Kassel, Germany
Email: mail@susanne-neupert.de

Jens Habenstein
Biocenter, Behavioral Physiology and Sociobiology (Zoology II), University of Würzburg, Am Hubland, 97,074 Würzburg, Germany.
Email: jens.habenstein@.uni-wuerzburg.de

Funding information
The study was supported by following projects financed by the German Research Foundation (DFG): DFG Ro1177/7-1 (to WR), SFB 1047 (Insect Timing, Project B6, to WR), DFG NE 911/5-1 (to SN), Equipment grant PR 766/11-1 (Großgeräteinitative, to RP, CW, WR), by the European Commission (Grant number 634361, to RP), and the Graduate School for Biological Sciences, Cologne (DFG-RTG 1960: Neural Circuit Analysis of the Cellular and Subcellular Level (to SL) and RTG-NCA1980 (to SL)).

Abstract

Behavioral flexibility is an important cornerstone for the ecological success of animals. Social *Cataglyphis nodus* ants with their age-related polyethism characterized by age-related behavioral phenotypes represent a prime example for behavioral flexibility. We propose neuropeptides as powerful candidates for the flexible modulation of age-related behavioral transitions in individual ants. As the neuropeptidome of *C. nodus* was unknown, we collected a comprehensive peptidomic data set obtained by transcriptome analysis of the ants' central nervous system combined with brain extract analysis by Q-Exactive Orbitrap mass spectrometry (MS) and direct tissue profiling of different regions of the brain by matrix-assisted laser desorption/ionization time-of-flight (MALDI-TOF) MS. In total, we identified 71 peptides with likely bioactive function, encoded on 49 neuropeptide-, neuropeptide-like, and protein hormone prepropeptide genes, including a novel neuropeptide-like gene (*fliktin*). We next characterized the spatial distribution of a subset of peptides encoded on 16 precursor proteins with high resolution by MALDI MS imaging (MALDI MSI) on 14 μm brain sections. The accuracy of our MSI data were confirmed by matching the immunostaining patterns for tachykinins with MSI ion images from consecutive brain sections. Our data provide a solid framework for future research into spatially resolved qualitative

Abbreviations: AKH, adipokinetic hormone; AL, antennal lobe; Ast-A, allatostatin-A; Ast-C, -CC, -CCC, allatostatin-C, -CC, -CCC; AT, allatotropin; CB, central body; CCAP, crustacean cardioactive peptide; CHCA, α-cyano-4-hydroxycinnamic acid; Crz, corazonin; DH-31, calcitonin-like diuretic hormone-31; DH-44, corticotropin releasing factor-like diuretic hormone-44; DHB, 2,5–dihydroxybenzoic acid; EH, eclosion hormone; ETH, ecdysis triggering hormone; Flik, fliktin; FMRF, Phe-Met-Arg-Phe; GNG, gnathal ganglion; IDL, IDL-containing peptide; ILP, insulin-like peptide; ITG, ITG-like peptide; ITO, indium tin oxide; ITP, ion transport peptide; MALDI, matrix-assisted laser desorption/ionization; MB, mushroom body; MS, mass spectrometry; MSI, mass spectrometry imaging; NP, neuroparsin; NPLP, neuropeptide-like precursor; NVP, NVP-containing peptide; OL, optic lobe; Orc, orcokinin; PBS, phosphate-buffered saline; PDF, pigment dispersing factor; PI, pars intercerebralis; PK, pyrokinin; PL, pars lateralis; PP, precursor peptide; PTM, posttranslational modification; PTTH, prothoracicotropic hormone; PVK, periviscerokinin; RCC, retrocerebral complex; RRID, Research Resource Identifier; SK, sulfakinin; sNPF, short neuropeptide F; TIC, total ion count; TK, tachykinin-related peptide; TOF, time-of-flight.

and quantitative peptidomic changes associated with stage-specific behavioral transitions and the functional role of neuropeptides in *Cataglyphis* ants.

KEYWORDS

Cataglyphis nodus brain, MALDI imaging, neuropeptides, neuropeptidomics, social insect, transcriptomics

1 | INTRODUCTION

Insect societies operate as cohesive units, even though individual colony members may express very different behavioral phenotypes contributing to diverse tasks (Hölldobler & Wilson, 1990). To ensure a dynamic and successful interplay of the insects within a colony, task allocation needs to be orchestrated in response to various internal and external cues (for reviews see: Beshers & Fewell, 2001; Robinson, 1992). External cues such as the availability of food, stimuli that signal the need for a specific task, or the demographic composition of the colony, directly affect the task performance and can induce short-term task switches (Gordon, 1989, reviewed by: Robinson, 1992, Yang, 2006). In addition, individuals follow innate behavioral patterns. These are often related to age. For example, young individuals fulfill tasks inside the nest, whereas older individuals primarily perform completely different and riskier tasks outside the nest (for reviews see: Hölldobler & Wilson, 1990; Oster & Wilson, 1978).

Age-related behavioral plasticity in social insects was shown to be associated with changes in diverse neuromodulators and hormones (reviewed by: Hamilton et al., 2016). Variations in biogenic amine levels (Wagener-Hulme et al., 1999, Seid & Traniello, 2005, reviewed by: Kamhi & Traniello, 2013), juvenile hormone titers (Bloch et al., 2002; Ddolezal et al., 2012; Robinson, 1987), and vitellogenin levels (Amdam & Omholt, 2003; Gospocic et al., 2017; Kohlmeier et al., 2018) at the transition from interior worker to forager are prominent examples. However, the causal contribution of these messenger molecules to changes in specific behaviors were discussed controversially (Huang & Robinson, 1995, Sullivan et al., 2000, Scholl et al., 2014, reviewed by: Hamilton et al., 2016). Recent studies, therefore, started to focus on neuropeptides as potential regulators of specific behavioral patterns and their transitions in social Hymenoptera (*e.g.* Takeuchi et al., 2003, Brockmann et al., 2009, Pratavieira et al., 2014, 2018; Han et al., 2015, Schmitt et al., 2017, Gospocic et al., 2017).

Neuropeptides represent a very large and diverse group of intercellular messenger molecules. They are processed from larger precursor proteins (preproprotein) by a set of dedicated enzymes that cleave the proprotein at specific sites (Fricker, 2012; Pauls et al., 2014), and typically act as neurohormones or neuromodulators (for reviews see: Fricker, 2012; Nässel & Zandawala, 2019; Schoofs et al., 2017). Neuropeptides orchestrate diverse behaviors as well as physiological and developmental processes (for reviews see: Fricker, 2012; Kastin, 2013; Nässel & Zandawala, 2019). In insects, neuropeptides modulate for instance general locomotor activity (Kahsai, Martin et al., 2010), feeding (Ko et al., 2015, Chen et al., 2016, reviewed by: Schoofs et al., 2017), or olfactory memory (Knapek et al., 2013; Urlacher et al., 2016; Winther et al., 2006). Neuropeptides such as corazonin (Crz), tachykinin-related peptides (TK), or short neuropeptide *F* (sNPF) show different expression levels (protein/RNA) related to age, tasks or internal and behavioral stages in honey bees (Gospocic et al., 2017; Pratavieira et al., 2018; Takeuchi et al., 2003), wasps, and ants (Gospocic et al., 2017). In the same line, the distribution of allatostatin-A (Ast-A) and TK exhibit age-related changes within multisensory integration centers in the brain of the honey bee (Pratavieira et al., 2014) and *Cataglyphis* ants (Schmitt et al., 2017). These studies are highly suggestive for a key role of neuropeptides in the flexible regulation of distinct behavioral phenotypes in social insects, particularly at the transition from nursing behavior inside the dark nest to the performance of outdoor foraging. The marked behavioral transitions in thermophilic ants of the genus *Cataglyphis* Foerster, 1,850 (Hymenoptera, Formicidae) provide an excellent experimental model to investigate mechanisms of neuronal plasticity underlying age-related behavioral plasticity (Rössler, 2019). After several interior stages with tasks inside the darkness of the nest which last about four weeks, the ants leave the nest for the first time to perform learning walks close to the nest entrance under bright sunlight for 2–3 days (Fleischmann et al., 2017, 2018). Immediately after completing their learning walks, the ants start to search for food by performing primarily visually guided foraging trips that may span over remarkable distances of up to several hundred meters (reviewed in Ronacher, 2008; Rössler, 2019; Wehner, 2009).

To start to investigate the molecular mechanisms underlying such behavioral flexibility, genomics and transcriptomic data from various ant species are available (e.g. Warner et al., 2019; Wurm et al., 2011). Furthermore, neuropeptidergic data sets from the carpenter ant *Camponotus floridanus* (Schmitt et al., 2015) and the closely related desert ant *Cataclyphis fortis* (Schmitt et al., 2017) exist, however, comparable genetic and biochemical data in the important experimental model ant *C. nodus* are missing so far. Recently, a three-dimensional brain atlas was published for this ant by mapping 33 synapse-rich neuropil regions and 30 interconnecting fiber tracts, among them are six parallel visual pathways (Habenstein et al., 2020; neuronal cell bodies are mostly on the cortex of the brain and were excluded). This first comprehensive neuroanatomical analysis of an ant brain revealed a highly complex compartmentalization of neuronal processes in a small brain. Until now, however, nothing is known

about the distribution of signaling molecules such as neuropeptides within the *C. nodus* brain. As a prerequisite to better understand the functional role of neuropeptides within the neurocircuits in the nervous system of this social insect model, we here started by analyzing the transcriptome of the *C. nodus* brain for neuropeptide sequences. We found 49 identified protein sequences from 31 genes encoding neuropeptides and neuropeptide-like substances. Next, we analyzed brain extracts of *C. nodus* by Q-Exactive Orbitrap MS and individual neuronal tissue samples by direct tissue profiling using MALDI-TOF MS to determine the actual set of processed neuroactive compounds including post-translational modifications (PTM). The most common PTMs in insects are the C-terminal amidation of the hydroxyl group of glycine, cyclization of the N-terminal glutamine and aspartate to pyroglutamic acid, formation of disulfide bridges formed between thiol groups in two cysteine residues and sulfation. The combination of MS methods had previously been successfully used by us to characterize the neuropeptidome of other insects, including ants (e.g. Liessem et al., 2018; Predel et al., 2018; Schmitt et al., 2015). Altogether, we identified 71 potential bioactive neuropeptides via mass matches in the brain of *C. nodus* whereas 56 peptides are confirmed by fragmentation experiments. Then, we localized subsets of the identified neuropeptides to specific brain compartments and neuropils in the brain by mass spectrometric imaging (MALDI-MSI).

In insects, MSI has been used for the first time for neuropeptide imaging from neuronal tissue samples of the cricket *Acheta domesticus* by a MALDI- ion trap (Verhaert et al., 2007). Previously, Pratavieira et al., (2014, 2018) used MALDI-TOF MSI to analyze developmental and state-dependent changes in the neuropeptide composition and distribution in the honey bee brain, yet these studies, although being successful, were restricted to a limited set of detected neuropeptides. Here, based on previously published protocols for neuropeptidergic MSI analysis of invertebrate tissue samples (e.g. Chen & Li, 2010; Ly et al., 2019; Pratavieira et al., 2014), we optimized and further developed sample preparation steps for MALDI-MSI of ant brains, and evaluated their accuracy comparing TK immunostaining and MALDI-MSI ion signal patterns on consecutive brain sections. Overall, we were able to obtain molecular images for peptides encoded on 16 genes.

The results of our comprehensive peptidomic study together with the MALDI-MSI procedure optimized for ant brains now open the possibility to correlate brain-wide peptidomic changes and test their function on modulation of dynamic behavioral phenotypes in manipulation experiments, in particular behaviors associated with polyethism in social insects like *C. nodus* ants.

2 | EXPERIMENTAL PROCEDURES

2.1 | Animals

C. nodus colonies were collected at Schinias National Park, Greece (38°15' N, 24°03' E) and transported to the Biocenter of the University of Würzburg. In Würzburg, the ants were kept in a climate chamber under 12:12 hr day/night conditions at 28°C and 20%–30% relative humidity. The animals had infinite access to water and were fed with dead cockroaches and honey diluted in water (1:2). For all studies, *Cataglyphis* workers were taken from queenless colonies. Age and previous experiences of individuals were unknown. Since all animals were picked arbitrarily, no randomization as well as no blinding was performed to allocate individual subjects in the study. In all experiments, adult ant brains were used without a specific sample size calculation. A number of at least four animals were tested in each experimental approach. This study was carried out in accordance with the Greek and German laws. Institutional ethics approval was not required for this study. The study was not pre-registered.

2.2 | Classification of analytes

In this study, we used the term neuropeptide for shorter peptide molecules of a length up to 45 aa produced by neuronal and endocrine cells and from larger preproproteins that contain a signal peptide and canonical prohormone convertase processing sites, and which are known in insects to execute functions as neuromodulator or hormone via G-protein-coupled receptor (GCPR)-signaling. Neuropeptide-like peptides are here defined as peptides which fulfilled most of the above criteria but for which the functions or receptors are unknown. Protein hormones are peptides larger than 45 aa which are produced by neuronal and endocrine cells from larger preproproteins that contain at least a signal peptide, and which are known in insects to be secreted into the haemolymph to regulate processes in distant target organs. Precursor peptides (PP) are biologically inactive shorter peptide sequences produced during preproprotein processing which cannot be turned into an active form by posttranslational modification.

2.3 | Transcriptome analysis

- *RNA extraction*: Whole brains of *C. nodus* workers ($n = 12$) were preserved in TRIzol (Life Technologies Inc.) at 4°C according to the manufacturer´s recommendation. RNA analysis was implemented in Agilent 2,100 Bioanalyzer.
- *Library construction and transcriptome sequencing*: Libraries were sequenced using the Illumina Truseq RNA Sample Preparation Kit (Illumina) and sequencing was done using an Illumina TruSeq PE Cluster Kit v3 and an Illumina TruSeq 31 SBS Kit v3—HS on an Illumina HiSeq 4,000 sequencer with a paired-end by the Gene Expression Affymetrix facility at the CMMC at the University of Cologne (Germany). The library was sequenced for 100 bp paired-ends, which were stored as FASTQ files.
- De novo *assembly*: Raw data were initially filtered by removing adapters, reads with more than 5% of unknown bases and reads with low quality sequences (reads having more than 20% bases with quality value lower or equal to 10). Subsequently transcripts were de novo assembled using Trinity (v2.2.0) (Grabherr

et al., 2011; Haas et al., 2013) and Bridger (v2014-12-01) (Chang et al., 2015) with default options. De-novo assembly quality was assessed using TransRate (v1.0.3, Smith-Unna et al., 2016). The resulting RAW reads were filtered, by removing adapter sequences, contamination and low-quality reads using Trimmomatic 0.38 (Bolger et al., 2014) and submitted to NCBI (Sequence Read Archives (SRA): SRR10955559, BioProject: PRJNA602618, BioSample: SAMN13899910, Transcriptome Shotgun Assembly (TSA): pending for release. The quality of the assembly was subsequently assessed with TransRate: 106,977,131 bases and 76,048 contigs were included in the assembly. The N50 length, that is the largest contigs size at which 50% of bases are contained in contigs of at least this length, is 2,952.

- *Compiling of Precursor Sequences*: The tBLASTn algorithm from the BLAST + suite command-line tool (v2.4.0.) (Camacho et al., 2009) was used to conduct database searches for *C. nodus* neuropeptide precursor sequences. As reference queries, selected sequences of known insect neuropeptide precursors from different non-pterygote hexapods (Derst et al., 2016) and pterygote insects such as the honey bee *Apis mellifera* (Hummon et al., 2006), the yellow fever mosquito *Aedes agyptii* (Predel et al., 2010), the stick insect *Carausius morosus* (Liessem et al., 2018) and the two closely related ant species *Camponotus floridanus* (Schmitt et al., 2015) and *Cataglyphis fortis* (Schmitt et al., 2017) were used. Identified sequences were translated into proteins using ExPASy translate tool (http://web.expasy.org/translate/, Swiss Institute of Bioinformatics, Switzerland) (Gasteiger et al., 2003). Signal peptides (SP) were predicted using the SignalP 4.1 server (www.cbs.dtu.dk/services/SignalP/. Technical University of Denmark, Denmark). If no SP could be predicted or no stop codon was present, precursors were considered as incomplete. Cleavage sites, potential neuropeptides, and precursor peptides (PPs) were calculated by the NeuroPred server (http://stagbeetle.animal.uiuc.edu/cgi-bin/neuropred.py) and were manually assigned based on Veenstra (2000).

2.4 | Tissue preparation for mass spectrometry

Ants were anesthetized on ice and decapitated. Head capsules were opened and covered with ice-cold physiological insect saline (128 mM NaCl, 2.7 mM KCl, 2 mM $CaCl_2$, 1.2 mM $NaHCO_3$, pH 7.25).

- *Direct tissue profiling (n = 15)*: Brains with attached *corpora cardiaca* and *corpora allata* (retrocerebral complex) and gnathal ganglion (GNG) were removed and transferred into a drop of fresh saline. *Corpora cardiaca* and *corpora allata*, small parts of different brain areas and GNG were separately dissected and transferred using a glass capillary fitted to a tube with a mouth piece into a drop of water placed on a sample plate for MALDI-TOF MS analysis as described in Schachtner et al., (2010). Immediately after transfer, water was removed around the sample and the tissue was allowed to dry before matrix application. Only tissue samples that were not contaminated by other tissues such as fat were chosen for MS profiling.
- *Tissue extraction (in total n = 95)*: We made eight different sample sets, consisting of 2 × 20, 1 × 15, 3 × 10, and 2 × 5 brains/GNGs. Each sample set was collected in 30 µl extraction solution containing 50% methanol, 49% H_2O, and 1% formic acid (FA) on ice. Tissue samples were homogenized using an ultrasonic bath (Transonic 660/H; Elma Schmidbauer GmbH) for 5 min on ice and then treated using an ultrasonic-finger (BandelinSono HD 200; Bandelin Electronic GmbH) three times for 5 s. Afterwards, the samples were centrifuged for 15 min at 13,000 rpm at 4°C. The supernatants were separated and then evaporated in a vacuum concentrator to remove methanol. Extracts were stored at −20°C until use.
- *MALDI-MSI (for protocol optimization: n = around 500 brain sections from around 100 brains; for final experiments: n = 12 brain sections [3 sections from 4 brains])*: Heads were fixed in wax-coated dishes and the head capsule was opened. To minimize peptide-release during the preparation, we rinsed the brains with ice-cold artificial ant saline solution (127 mM NaCl, 7 mM KCl, 1.5 mM CaCl2, 0.8 mM Na2HPO4, 0.4 mM KH2PO4, 4.8 mM TES, 3.2 mM trehalose, pH 7.0) and analyzed only brains for which the isolation procedure did not exceed 10 min. The brain was removed, rinsed in distilled water for a few seconds and embedded in gelatin (Dr. Oetker Gelatine Gold extra, Germany). For neuropeptide imaging experiments, gelatin is the embedding substrate of choice because it does not produce interfering signals in the neuropeptide mass range (m/z 600–4,000), unlike polymer-containing embedding media (Chen et al., 2009; Chen & Li, 2010; Khatib-Shahidi et al., 2006). Confirming Chen & Li, 2010, 100 mg/ml gelatin in water resulted in highly reproducible consecutive brain sections with high-quality mass spectra containing neuropeptide signals. For that, 100 mg/ml gelatin was completely dissolved in distilled water at 50°C and poured into 5 × 5 × 10 mm custom-made tinfoil cups. The cups were filled to two-third and the gelatin was allowed to cool down to around 30°C. To compare the spatial distribution of neuropeptides between different sections within or between brains, reproducible positioning of the samples prior to sectioning is required. To achieve this, each isolated brain was pushed with the anterior surface down in warm gelatin close to the bottom of the tinfoil cup. Next, the brain was slowly entirely covered with warm gelatin, after remaining water had been carefully removed with a glass capillary to avoid salt crystal formation during subsequent snap-freezing to −57°C on the cryobar device provided in the cryotom CryoStar NX50 (ThermoFisher Scientific). Appropriate section thickness, cutting angle, and sample cutting temperature are crucial parameters for high quality, reproducible brain tissue sections (e.g. Buchberger et al., 2018; Ly et al., 2019; Yang & Caprioli, 2011). Therefore, we tested different tissue cutting angles (5° to 25°), cutting temperatures (−30°C to −5°C), and brain section thicknesses (10 to 25 µm). The most efficient

neuropeptide detection was achieved in 14 μm brain sections produced with a cutting angle of 10° at −10°C, which was described as the optimal procedure for MSI analysis of cockroach neuroendocrine tissue (Ly et al., 2019). Using these parameters, we sliced the brain into 14 μm thick sections using a CryoStar NX50 and thaw-mounted them on indium tin oxide coated glass slides (ITO slides; Delta Technologies Limited). Dehydrating the samples in a desiccator evacuated to 300 mbar for at least two days prior to the rinsing procedure (n = 18) considerably improved the signal to noise ratio for neuropeptide detection in the ant brain sections (see Figure S1). We therefore dehydrated the tissue sections in a desiccator at 300 mbar with a drying agent (blue silica gel) at room temperature in the dark for at least two days until use.

2.5 | Matrix application

• *Direct tissue profiling:* 10 mg/ml 2,5–dihydroxybenzoic acid (DHB, Sigma-Aldrich, Steinheim, Germany) dissolved in 20% acetonitrile/1% FA/79% water (Fluka) or 10mg/ml α-cyano-4-hydroxycinnamic acid (CHCA; Sigma-Aldrich) dissolved in 60% ethanol, 36% acetonitrile, 4% water were used as matrix stock solutions. Dried tissue samples were covered with either 0.1 μl DHB solution or 0.1 μl of a mixture of one part CHCA stock solution and three parts 50% methanol/water using a 0.1–2.5 μl Eppendorf pipette (Eppendorf AB). Only after DHB application, spots were blow-dried with a commercially available hair dryer to form homogeneous crystals.

• *MSI:* Before matrix application, transmitted light-microscopy images of brain sections were acquired using the PALM Robo-software (V.4.6.0.4) on a PALM Microbeam (Zeiss Corporate) as orientation template for subsequent MALDI-MSI experiments. We applied a rinsing pipeline to remove lipids and increase neuropeptide signals followed existing protocols for the honey bee brain (Pratavieira et al., 2018; Pratavieira et al., 2014) or cockroach RCC sections (Ly et al., 2019) with slight modifications. The best coverage of neuropeptides detection from ant brain sections was obtained by rinsing with 70% ethanol followed by absolute ethanol for 20 s respectively. After each rinsing step, the ethanol was immediately removed by applying a constant compressed air flow for 30 s, which resulted in an additional improvement of neuropeptide detection by a more homogeneous matrix crystal formation afterwards (Figure S2). After the rinsing procedure, samples were dried again using 300 mbar vacuum for 30 min in a desiccator at room temperature in darkness to maximize the solvent removal before matrix application. Matrix application was performed as described by Ly et al., 2019 with slight modifications. In our experiments, the best results were obtained using 5 mg/ml CHCA dissolved in 50% acetonitrile and 1% FA. Matrix coating was performed at a velocity of 900 mm/min, a Z-position of 25 mm, 7 layers with a layer dependent flow rate (layer 1:10 μl/min, layer 2:20 μl/min, layer 3:40 μl/min, layer 4–7:60 μl/min) using a SunCollect Sprayer (SunChrom GmbH). All settings were adjusted using the SunCollect V. 1.7.52 software package.

2.6 | MALDI-TOF MS

Mass spectra were acquired manually using an ultrafleXtreme TOF/TOF mass spectrometer (Bruker Daltonik GmbH) in reflector positive ion mode in a mass range of 600–10,000 Da. Instrument settings were optimized for the mass range of 600–4,000 Da and 3,000–10,000 Da respectively. Proteins or peptide with a predicted ion mass above 10,000 Da were not analyzed in this study. For calibration, the following synthetic peptide mixture was used: proctolin, *Drosophila melanogaster* (Drm)- sNPF-1$^{4-11}$, *Locusta migratoria* periviscerokinin-1 (PVK-1), *Periplaneta americana* (Pea)-FMRFa-12, *Manduca sexta* allatotropin (AT), Drm-IPNa, Pea-SKN and glucagon for the mass range at m/z 600–4,000 and a mixture of glucagon, bovine insulin-A, and ubiquitin for the mass range at m/z 3,000–10,000 was used. Laser fluency was adjusted to provide an optimal signal-to-noise ratio. The obtained data were processed using FlexAnalysis V.3.4 software package. MS/MS was performed with LIFT technology. LIFT acceleration was set at 1 kV. The number of laser shots used to obtain a spectrum varied from 2,000 to 20,000, depending on ion signal quality. For MS/MS experiments, we also used an ABI 4,800 proteomics analyzer (Applied Biosystems). MS/MS fragment spectra were acquired manually in gas-off mode and processed and handled using DataExplorer V.4.10 software package. Peptide identities were verified by comparison of masses of theoretical (http://prospector.ucsf.edu) and experimentally obtained fragments.

2.7 | MALDI-TOF MSI

MALDI-MSI data were acquired in reflector positive ion mode either on the ultrafleXtreme TOF/TOF mass spectrometer or on a rapifleX TOF/TOF Tissuetyper mass spectrometer (both Bruker Daltonik GmbH). Settings for imaging analysis by ultrafleXtreme instrument were: m/z 600–4,000 detection range, 2 kHz Bruker smartbeam-II laser with a laser repetition rate of 1,000 Hz, 1,500 shots per spot, a 15 μm laser-spot size (laser focus diameter setting small) and a 15 μm lateral step size. Recordings using rapifleX instrument are set as following: mass range at m/z 600–3,200, 500 laser shots were accumulated using a Smartbeam 3D Nd:YAG (355 nm) at a frequency of 5,000 Hz and a sample rate of 1.25 GS/s with baseline subtraction (TopHat) during acquisition. The instrument was calibrated using peptide calibration standard II (Bruker Daltonik GmbH) spotted onto the matrix-coated ITO glass slide, taking care that the spot did not obscure the tissue. Ion images were generated using SCiLS Lab MVS software version 2020a (RRID:SCR_014426, Bruker Daltonik GmbH) with the data normalized to the total ion count (TIC). To allow for better comparison between preparations, we used only brain sections that were not

damaged and originated from nearly the same cutting level within each brain. We only analyzed sections of the anterior brain regions between the mushroom bodies (MB) and the central bodies (CB). More posterior brain sections were excluded in subsequent analyses. Raw data (Bruker DAT files) were uploaded and preprocessed in SCiLS Lab and underwent spatial-segmentation analysis using a bisecting-k-means with correlation as distance measure (Trede et al., 2012). The default pipeline was used with the following modifications: weak denoizing and an accuracy of mass matching for peptide assignment at ±0.05%. The lower indication limits for neuropeptide distributions were manually adjusted according to varying strengths of ion signal intensities of different neuropeptides to exclude baseline noises. Overall mass spectra of brain sections were generated with Bruker flexImaging V. 3.4. software package. Mass spectra of individual spots were analyzed with Bruker flexAnalysis V. 3.4. software package.

2.8 | Quadrupole Orbitrap MS Coupled to Nanoflow HPLC

Before injecting the samples into the nanoLC system, extracts were desalted using self-packed Stage Tip C18 (IVA Analysentechnik e.K.) spin columns (Rappsilber et al., 2007). For analysis, peptides were separated on an EASY nanoLC 1,000 UPLC system (Thermo Fisher Scientific) using RPC18 columns 50 cm (fused Silica tube with ID 50 ± 3 µm, OD 150 ± 6 µm, Reprosil 1.9 µm, pore diameter 60 Å, Dr. Maisch, Ammerbuch-Entringen) and a binary buffer system (A: 0.1% FA, B: 80% ACN, 0.1% FA) as described for *Cimex* samples (Predel et al., 2018). Running conditions were as follows: linear gradient from 2% to 62% B in 110 min, 62–75% B in 30 min, and final washing from 75% to 95% B in 6 min (45°C, flow rate 250 nl/min). Finally, the gradients were re-equilibrated for 4 min at 5% B. The HPLC was coupled to a Q-Exactive Plus (Thermo Scientific) mass spectrometer. MS data were acquired in a top-10 data-dependent method dynamically choosing the most abundant peptide ions from the respective survey scans in a mass range of 300–3,000 m/z for HCD fragmentation. Full MS^1 acquisitions ran with 70,000 resolution, with automatic gain control target (AGC target) at 3e6 and maximum injection time at 80 ms. HCD spectra were measured with a resolution of 35,000, AGC target at 3e6, maximum injection time at 240 ms, 28 eV normalized collision energy, and dynamic exclusion set at 25 s. The instrument was run in peptide recognition mode (i.e. from two to eight charges), singly charged and unassigned precursor ions were excluded. Raw data were analyzed with PEAKS Studio 10.5 (BSI). Neuropeptides were searched against an internal database comprising *C. nodus* neuropeptide precursor sequences with parent mass error tolerance of 0.1 Da and fragment mass error tolerance of 0.2 Da. Setting enzymes: none was selected because samples were not digested. The false discovery rate (FDR) was enabled by a decoy database search as implement in PEAKS 10.5. Following posttranslational modification (PTM) were selected: C-terminal amidation as fixed PTM and oxidation at methionine, N-terminal acetylation, pyroglutamate from glutamine, pyroglutamate from glutamic acid, sulfation of tyrosine, serine, and threonine, as well as disulfide bridges as variable PTMs. In each run a maximum of three variable PTMs per peptide were allowed. Fragment spectra with a peptide score (−10 lgP) equivalent to a *p*-value of ~1%, were manually reviewed.

2.9 | Immunohistochemistry

Brain sections were prepared as described above and fixated with 4% formaldehyde in 0.1 M phosphate-buffered saline (PBS) overnight at 4°C. After fixation, the sections were rinsed with PBS (3 × 10 min) and pre-incubated in PBS, containing 2% normal goat serum (NGS, Jackson ImmunoResearch Laboratories) for one hour at room temperature. Subsequently, the brain sections were incubated in tachykinin-related peptide antiserum (rabbit anti-LemTKRP-1, kindly provided by Dick Nässel, RRID: AB_2315469) at a concentration of 1:2,500 diluted in PBS with 0.2 Triton-X100, 2% NGS and 0.02% NaN_3 for two hours at room temperature. Afterwards, brain sections were rinsed with 0.1 M PBS three times for 10 min and finally incubated in a mixture of goat anti-rabbit Alexa Fluor 488 (RRID:AB_143165, Thermo Fisher Scientific) at a concentration of 1:250 and CF 633 phalloidin (Catalogue number: 00046; BIOTREND Chemikalien) at a concentration of 1:200 diluted in 0.1 M PBS, containing 1% NGS, as secondary antisera for two hours at room temperature. Phalloidin was used to label filamentous actin (F-actin) (Dancker et al., 1975) in neurons throughout the ant brain, which helps to delineate synaptic neuropils and neuronal fiber tracts in the brain (Habenstein et al., 2020). Then, the samples were rinsed in 0.1 M PBS two times for 10 min and transferred into 60% glycerol in PBS for 30 min at room temperature. Finally, the brain sections were mounted in 80% glycerol in 20% PBS on microscopic slides and coverslips were sealed with nail polish.

2.9.1 | Confocal laser scanning microscopy

Samples were scanned as image stacks with an optical thickness of 0.5–1.5 µm at a resolution of 1,024 × 1,024 pixels using a Leica TCS SP2 AOBS confocal laser-scanning microscope equipped with a 10.0 × 0.4 NA objective (Leica Microsystems AG). Alexa Fluor 488 was excited at 488 nm using an argon/krypton laser and CF 633 phalloidin was excited at 633 nm using a diode laser. Each slice of the stack was scanned 3–4 times and averaged to reduce background noises. Serial optical sections were processed with Fiji (RRID:SCR_002285, ImageJ 1.50e, Wayne Rasband; NIH], Schindelin et al., 2012). In double stained preparations, the different channels were merged with the use of pseudocolors. The final figures were exported and processed to adjust brightness and contrast using CorelDraw Graphics Suite X8 (V. 18.0.0.448; Corel Corporation).

3 | RESULTS

3.1 | Transcriptomics

The transcriptome of *C. nodus* brain tissues ($n = 4$) was assembled into contigs by Trinity followed by BLAST searches using known neuropeptide prepropeptide genes from different insects (Hummon et al., 2006; Liessem et al., 2018; Predel et al., 2010; Schmitt et al., 2015, 2017). In total, a set of 49 *C. nodus* prepropeptide sequences subdivided into 30 complete neuropeptide genes, 7 complete neuropeptide-like genes and, 11 complete, and 1 non-complete protein hormone gene were yielded that likely originate from 42 different genes (Table 1, Figure S3). For the genes encoding agatoxin-like peptide (ALP), CAPA/PVKs, neuropeptide-like precursor-1 (NPLP-1), CCHamide-1, CCHamide-2, and insulin-like peptide-2 (ILP-2), alternatively spliced mRNAs were found. Orthologs of further neuropeptide precursors included in the BLAST search (adipokinetic hormone/corazonin-related peptide [ACP], myoinhibitory peptide [MIP], Ast-C, EFLamide, calcitonin-A, B, natalisin/WAARamide, RYamide, proctolin, insect kinin, HanSolin, RFLamide, and trypto-pyrokinin) were not found, neither in the assembled transcriptome data nor by searching in the transcript raw data using homolog insect peptide sequences (see Table 1).

3.2 | Neuropeptidomics

3.2.1 | Brain extract analysis by Q Exactive Orbitrap MS for peptide identification

For chemical identification of transcriptome-predicted peptides and additional precursor peptides (PP), we used the *C. nodus* precursor sequences as database and analyzed brain extracts by ESI-Q Exactive Orbitrap MS followed by PEAKS 10.5 software package. This resulted in sequence identification of products from 16 genes encoding single neuropeptides or neuropeptide-like molecules (adipokinetic hormone [AKH], ALP, AT, allatostatin-CCC [Ast-CCC], calcitonin-like diuretic hormone-31 [DH-31], corticotropin releasing factor-like diuretic hormone [DH-44], CCHamide-2_a, Crz; IDL-containing peptide [IDL], ITG-like peptide [ITG], ion transport peptide [ITP], ITP-like, myosuppressin [Ms], pigment dispersing factor [PDF], sNPF, SIFamide), and peptides from nine genes containing multiple copies (Ast-A, CAPA-PVK, extended FMRFamides, NPLP-1, NVP-containing peptide [NVP], orcokinin [Orc], pyrokinin [PK], sulfakinin [SK], TK; see Table 2, Figure S4). We also identified five novel peptides in the brain extracts using de novo sequencing algorithms provides in PEAKS 10.5 software. These peptides show no sequence similarities to known neuropeptides or neuropeptide-like molecules in insects. Consequently, we used NBCI Protein BLAST search against the novel identified peptide sequences which revealed sequence matches to peptides encoded on the uncharacterized protein precursor of various different ant species such as *Solenopsis invicta* (protein LOC105202364; Accession No. XP_011169138.1), *Formica exsecta* (protein LOC115241177; Accession No. XP_029672667.1), *Camponotus floridana* (protein LOC105254232; Accession No: EFN65144) or *Lasius niger* (protein RF55_8265; Accession No. KMQ91825.1 (Figure S5). Additionally, we found a high sequence similarity between the novel *C. nodus* protein precursor with a protein precursor predicted as stress-response protein in the ant *V. emeryi* (Accession No. XP_011877808). However, this record is predicted by automated computational analysis and derived from a genomic sequence (NW_011967229.1) annotated using gene prediction method: Gnomon from the *V. emeryi* genome, without any functional evidence in stress regulation in the ant. Recently, a neuropeptide gene designated as PaOGS36577 was described in the cockroach *P. americana* by genomics and peptidomics-based strategies, however, without any functional evidence or information about the distribution of the encoded peptides within the brain (Zeng et al., 2021). As tribute for the first evidence of product processing from theses protein precursors within the brain in the ant *C. nodus*, we named the novel peptides Fliktin (Flik) after the impulsive and clumsy inventor ant Flik from the animation movie A Bug´s Life.

3.2.2 | Direct tissue profiling by MALDI-TOF MS

We analyzed several brain areas, portions of the GNG, and the retrocerebral complex (RCC), a peripheral neurohormone storage and release site of insects, which is connected to the brain. The primary objectives were (a) to localize peptides identified by Q Exactive Orbitrap MS experiments to defined brain areas or the RCC, and (b) to find further neuropeptides in the mass range 600–10,000 Da (Table S1,S2) which could not be identified by brain extract MS analysis. Representative mass spectra of the different neuronal regions are shown in Figure 1 and Figure S6, S7. Analysis of portions of the *pars intercerebralis* (PI, $n = 12$), the median protocerebral region in the insect brain where mainly neurosecretory cells are located, revealed the presence of products from 27 genes (Table S1). The most abundant peptides originated from seven neuropeptide genes (*ast-A*, *ast-CCC*, *crz*, *ms*, *snpf*, *orc*, *tk*), two neuropeptide-like genes (*nplp-1*, *nvp*) and one protein hormone gene (*itg*). In addition, ion signals of the novel Flik peptides could also be detected (Figure 1a, Table S1). Potential bioactive molecules produced in the PI are transported via the *nervi corporis cardiaci* (NCC-1) to the RCC. The RCC consists of both nervous and endocrine structures. Mass spectrometrydata obtained from RCC preparation ($n = 15$) revealed ion signals of products from 19 genes (Table S1). The most distinct ion signals mass-matched peptides encoded by the genes *alp*, *ast-CCC*, *crz*, *dh-44*, *ms*, *nvp*, and *flik* (Figure 1b,c). Subsequent fragmentation experiments confirmed the peptide sequences of AKH (as sodium adduct AKH $[M + Na]^+$: *m/z* 1,141.6) Crz (*m/z* 1,369.8), Ast-A-6 (*m/z* 1,427.8), ALP-$1_{a/b}$ (*m/z* 4,861.1), Ast-CCC (*m/z* 1,650.8), extended FMRFa-3 (*m/z* 1,222.6), TK-2 (*m/z* 1,039.5), TK-3 (*m/z* 1,217.6), and TK-4 (*m/z* 1715.9) (Figure S4). Direct profiling of the MB ($n = 4$), centers for learning and memory in insects, confirmed the presence of products from 17 genes (Table S1), with peptides of six genes (*ast-A*, *itg*, *idl*, *nplp-1*, *nvp*, *and tk*)

TABLE 1 Prepropeptide genes for neuropeptides, neuropeptide-like molecules, and protein hormones identified in the transcriptome of *Cataglyphis nodus* brain. Different transcripts are marked with subscript characters (*e.g.*, CCHamide-1_a, CCHamide-1_b)

Designation	Source	Accession	Complete
Neuropeptide genes			
Adipokinetic hormone	TRINITY_DN1080_c0_g1_i1	MN996797	+
Allatotropin	TRINITY_DN31792_c0_g1_i1	MN996792	+
Allatostatin-A	TRINITY_DN14240_c0_g1_i1	MN996769	+
Allatostatin-CC	TRINITY_DN13459_c0_g1_i1	MN996793	+
Allatostatin-CCC	TRINITY_DN10970_c0_g1_i1	MN996771	+
Arginine–vasopressin-like peptide/ Inotocin	TRINITY_DN26862_c0_g1_i1	MN996787	+
Calcitonin-like diuretic hormone–31	TRINITY_DN13546_c0_g1_i1	MN996801	+
$CAPA_a$/Periviscerokinin	TRINITY_DN8747_c0_g1_i1	MN996766	+
$CAPA_b$/Periviscerokinin	TRINITY_DN8747_c0_g2_i1	MN996767	+
CCHamide–1_a	TRINITY_DN15956_c0_g1_i1	MN996776	+
CCHamide–1_b	TRINITY_DN15956_c0_g1_i4	MN996777	+
CCHamide–2_a	TRINITY_DN10059_c0_g1_i1	MN996783	+
CCHamide–2_b	TRINITY_DN10059_c0_g1_i2	MN996784	+
CNMamide	TRINITY_DN10563_c0_g1_i2	MN996802	+
Corazonin	TRINITY_DN31041_c0_g1_i1	MN996775	+
Corticotropin releasing factor-like diuretic hormone	TRINITY_DN15881_c0_g1_i1	MN996782	+
Crustacean cardioactive peptide	TRINITY_DN31220_c0_g1_i1	MN996773	+
Ecdysis triggering hormone	TRINITY_DN2946_c0_g1_i1	MN996768	+
Elevenin	TRINITY_DN15212_c0_g1_i1	MN996762	+
Extended FMRFamide	TRINITY_DN14605_c0_g1_i1	MN996772	+
Myosuppressin	TRINITY_DN14195_c0_g1_i1	MN996806	+
Neuropeptide F	TRINITY_DN14055_c0_g1_i1	MN996770	+
Orcokinin	TRINITY_DN14752_c0_g1_i1	MN996788	+
Pigment dispersing factor	TRINITY_DN23971_c0_g1_i1	MN996807	+
Pyrokinin	TRINITY_DN9819_c0_g1_i1	MN996789	+
short neuropeptide F	TRINITY_DN16538_c0_g11_i1	MN996779	+
SIFamide	TRINITY_DN5040_c0_g2_i1	MN996785	+
Sulfakinin	TRINITY_DN9919_c0_g1_i1	MN996781	+
Tachykinin-related peptide	TRINITY_DN16581_c0_g1_i2	MN996780	+
Trissin	TRINITY_DN14132_c0_g2_i1	MN996805	+
Neuropeptide-like genes			
Agatoxin-like-peptide–1_a	TRINITY_DN14927_c0_g1_i1	MN996764	+
Agatoxin-like-peptide–1_b	TRINITY_DN14927_c0_g2_i1	MN996765	+
Fliktin	TRINITY_DN18124_c1_g1_i2	MN996812	+
Neuropeptide-like precursor–1_a (NPLP–1_a)	TRINITY_DN18383_c1_g1_i2	MN996809	+
Neuropeptide-like precursor–1_b (NPLP–1_b)	TRINITY_DN18383_c1_g1_i3	MN996810	+
Neuropeptide-like precursor–1_c (NPLP–1_c)	TRINITY_DN18383_c1_g1_i1	MN996808	+
NVP-like peptides	TRINITY_DN18939_c7_g1_i1	MN996799	+
Protein hormone genes			
Bursicon-*alpha*	TRINITY_DN17815_c6_g2_i1	MN996790	+
Bursicon-*beta*	TRINITY_DN17815_c2_g1_i1	MN996813	(+)
Eclosion hormone	TRINITY_DN20318_c0_g1_i1	MN996774	+

(Continues)

TABLE 1 (Continued)

Designation	Source	Accession	Complete
IDL-containing peptide	TRINITY_DN12956_c0_g8_i1	MN996800	+
ITG-like peptide	TRINITY_DN17809_c3_g1_i1	MN996791	+
Insulin-like peptide−1	TRINITY_DN18145_c0_g1_i1	MN996811	+
Insulin-like peptide−2_a	TRINITY_DN16229_c0_g1_i2	MN996804	+
Insulin-like peptide−2_b	TRINITY_DN16229_c0_g1_i1	MN996803	+
Ion transport peptide-like	TRINITY_DN12575_c0_g1_i2	MN996796	+
Ion transport peptide	TRINITY_DN12575_c0_g1_i1	MN996795	+
Neuroparsin	TRINITY_DN863_c0_g1_i1	MN996794	+
Prothoracicotropic hormone	TRINITY_DN5171_c0_g1_i1	MN996778	+

Note: Precursor sequences are listed in Supporting Information S3, which also consider partial sequences (+). Precursor sequences were annotated and submitted to GenBank ((BioProject: PRJNA602618, BioSample: SAMN13899910, Sequence Read Archive (SRA): SRP10955559).

showing the highest ion signal intensities (Figure 1d). Measurements of the optic lobe (OL) region ($n = 8$), which contains the first synaptic relay for visual information and parts of the central circadian clock in insects, exposed peptide precursor products from 17 genes (Table S1). The most prominent ion signals belonged to putative neuroactive substances encoded by the *ast-a-*, *itg-*, *idl-*, *tk-*, *nplp-1-*, *orc*, *pdf-*, and *sifamide* gene (Figure 1e). Analysis of the antennal lobe (AL, $n = 10$), the first synaptic relay of olfactory information, revealed the presence of neuropeptides from 18 different precursor genes (Table S1) with prominent ion signals for products of *snpf-*, *tk-* *dh-31-* *and* *nplp-1-* gene (Figure 1f). Furthermore, the predicted ion mass of trissin (*m/z* 3,024.3), CCHamide-$1_{a,b}$, 2_b, CCAP, elevenin and PTTH-PPs were detected by mass matches (see Table 2). Distinct ion signal intensities corresponding to extended FMRFa were observed in preparations of the GNG ($n = 6$) which allowed the validation of the peptide sequence of extended FMRFa-3 (Figure S6, S7). Transcriptome-predicted sequences for bursicon-alpha, bursicon-beta, EH, ETH, ILP-$2_{a,b}$, NP, and neuropeptide F were neither identified by Q Exactive Orbitrap MS nor by direct tissue profiling. In line with the lack of respective transcripts in our *C. nodus* brain transcriptomic data set, peptidomics did not support the presence of ACP, MIP, Ast-C, calcitonin-A, B, HanSolin, natalisin/WAARamides, RFLa, RYamide, proctolin, insect kinin, and tryptopyrokinin.

3.3 | MALDI-TOF MSI

3.3.1 | Sample preparation and reproducibility of neuropeptide detection in *C. nodus* brain sections

In the last decade, MALDI-TOF MSI has moved into the center stage for untargeted analysis of the spatial distribution of molecule species such as neuropeptides in tissue samples. The availability of more sensitive, robust and precise mass spectrometers improved the detection of putative neuropeptides directly from tissue sections. As a first step to uncover potential functions of neuropeptides in age-related polyethism and during distinct behavioral stages in ants, we optimized available MSI protocols (*e.g.* Chen & Li, 2010, Pratavieira et al., 2014, Ly et al., 2019) for neuropeptide detection in the *C. nodus* brain to gain comprehensive information of the spatial distribution of these signaling molecules in the tiny ant brain. We evaluated different experimental steps including sample preparation, tissue embedding material, tissue thickness, tissue rinsing procedure, tissue storage, matrix composition and matrix application tools for *C. nodus* brain sections as described in the experimental procedures (see 2.4, 2.5 and 2.7).

In our study, we used two commercially available mass spectrometer for MSI analysis. To evaluate the reproducibility of our optimized MSI for neuropeptide detection, we compared twelve brain sections analyzed either on an ultrafleXtreme (nine brain sections) or rapifleX (three brain sections) instrument based on the detectable number of neuropeptides as well as the quality of ion signal intensities. Resulting overall mass spectra from all 12 brain section revealed good signal to noise ratios, high quality ion signal intensities for the detection of putative bioactive mature neuropeptides and a nearly identical number of detectable neuropeptides per brain slide (Figure S8).

3.3.2 | Spatial distribution of neuropeptides in the ant brain: MALDI- MSI

Among the characterized *C. nodus* brain neuropeptides, we were able to visualize the spatial distribution of 35 peptides encoded on 16 precursor genes (*ast-A*, *at*, *capa*, *crz*, *dh-31*, *fmrf*, *idl*, *inotocin*, *itg*, *ms*, *nplp-1*, *nvp*, *orc*, *snpf*, *tk*, *flik*) in 14 µm thin sections using our optimized MALDI- MSI protocol. Figure 2 shows typical peptide ion maps in brain sections. Signals for Ast-A, IDL, Flik, inotocin, Orc, and TK were most prominent in the MBs, whereas products from the *capa* and the *dh-31* genes were almost exclusively detectable in the ALs in these sections. Furthermore, ion maps of Flik, ITG, NPLP-1, TK, Orc, and sNPF revealed distinct peptide presences in the AL. Dorsal to the ALs, Ast-A, IDL, ITG, FMRFa, myosuppressin, NPLP-1, NVP, Flik, sNPF, Orc, and TK were mapped with distinct ion

TABLE 2 Alphabetic list of mature neuropeptides, neuropeptide-like, protein hormones, and precursor peptides (PP) of *C. nodus* brain and retrocerebral complex (RCC) samples analyzed using three different mass spectrometrical approaches

Designation	Sequence	m/z $[M+H]^+$,	MS	MS[b]	MSI
Adipokinetic hormone (AKH)					
AKH	pQLNFSTGWGQ-NH_2	1,119.55	+	+	–*
Agatoxin-like-peptide$_a$ (ALP_a)					
ALP_a	ACIRRGGNCDHRPKDCCYSSSCRCNLWGSNCQCQRMGLFQ KW-NH_2	4,861.11	+	–	–[a]
Agatoxin-like-peptide$_b$ (ALP_b)					
ALP_b	ACIRRGGNCDHRPKDCCYSSSCRCNLWGSNCQCQRMGLFQ KW-NH_2	4,861.11	+	–	–[a]
Allatotropin (AT)					
AT	GFKPEYISTAIGF-NH_2	1,428.75	+	(+)	+
Allatostatin-A (AST-A)					
Ast-A-1	LPLYNFGI-NH_2	935.53	+	+	+
Ast-A-2	TRPFSFGI-NH_2	923.51	+	+	+
Ast-A-3	LRDYRFGI-NH_2	1,038.58	+	+	+
Ast-A-4	GGQPFSFGI-NH_2	908.46	+	+	–
Ast-A-5	PNDVIGPKYLLSL-NH_2	1,427.83	+	–	–
Ast-A-PP-1	AVEEAPSSSLHIPRLNPLSSSLEGYDKPSE-OH	3,209.60	+	+	–
Ast-A-PP-2	AYAYISEY-OH	979.44	+	–	+
Allatostatin-CCC (AST-CCC)					
Ast-CCC	SYWKQCAFNAVSCF-NH_2	1,650.73	+	+	–
Ast-CCC-PP	MPTTDTDKDRLLNTVDLIDDDGSIETALINYLFTKQIV-OH	4,297.18	+	–	–[a]
Allatostatin-CC (Ast-CC)					
Ast-CC	GQAKGQVYWRCYFNAVTCF-OH	2,238.04	+	–	–
Arginine–vasopressin-like peptide/Inotocin					
Inotocin	CLITNCPRG-NH_2	973.49	+	–	+
Calcitonin-like diuretic hormone-31 (DH-31)					
DH-31	GLDLGLSRGFSGSQAAKHLMGLAAANYAGGP-NH_2	2,986.53	+	+	+
DH-31-PP	IPHSHESYWDQQDDMDRDEFLDILSRLSRTVMNRPEMENS -OH	4,892.21	+	(+)	–[a]
DH-31-PP$^{1\text{-}28}$	IPHSHESYWDQQDDMDRDEFLDILSRLS-OH	3,447.55	+	(+)	–
DH-31-PP$^{30\text{-}40}$	TVMNRPEMENS-OH	1,307.57	+	+	+
$CAPA_a$/Periviscerokinin (PVK)					
$CAPA_a$-PVK-1	SAGLVPYPRI-NH_2	1,071.63	+	+	+
$CAPA_a$-PVK-2	ALGMINVPRV-NH_2	1,068.63	+	–	+
$CAPA_a$-PK	NTQGQGGYTPRL-NH_2	1,290.65	+	+	–
$CAPA_a$-PVK-PP-1(Q)	QKLKAND-OH	816.46	+	+	–
$CAPA_a$-PVK-PP-1 (pQ)	pQKLKAND-OH	799.46	+	+	–
$CAPA_a$-PVK-PP-2	NSEISSISRSE-OH	1,208.58	+	+	+
$CAPA_b$/Periviscerokinin (PVK)					
$CAPA_b$-PVK-1	SAGLVPYPRI-NH_2	1,071.63	+	+	+
$CAPA_b$-PVK-2	ALGMINVPRV-NH_2	1,068.63	+	–	+
$CAPA_b$-PK	NTQGQGGYTPRL-NH_2	1,290.65	+	+	–
$CAPA_b$-PVK-PP-1	SVGQQFESAREGQKLKAND-OH	2092.04	+	–	–
$CAPA_b$-PVK-2-PP-2	NSEISSISRSE-OH	1,208.58	+	+	+

(Continues)

TABLE 2 (Continued)

Designation	Sequence	m/z $[M+H]^+$,	MS	MS[b]	MSI
CCHamide-1					
CCHa-1	SCLSYGHSCWGAH-NH_2	1,404.57	+	–	–
CCHamide-2_a					
CCHa-2_a	GGCASFGHSCFGGH-NH_2	1,320.52	–	+	–
CNMamide					
CNMa	HGTNTVSYMSLCHFKICNM-NH_2	2,182.98	+	–	–
Corazonin (Crz)					
Crz	pQTFQYSRGWTN-NH_2	1,369.65	+	+	+
Crz-PP	SEFPSSPEISTAGYERINNGDLNRLKMLIHGSTDEQPLIIHCDFV DKLRNFLQTDNYAPQLHREKGPNLDY-OH	8,170.03	+	–	–[a]
Corticotropin releasing factor-like Diuretic hormone (DH-44)					
DH-44	IGSLSIVNNLDVLRQRVLLELARRKQEQDLRQIQENRRVLENI -NH_2	5,136.93	+	(+)	–[a]
DH-44-PP-1	APLSSYERRDMSDDGPKIFLLMDERIPELENEILGNDLGSDVTR T-OH	5,107.50	+	–	–[a]
DH-44-PP-2	SVPGSDAGRIARSGKSRNDRDRPAVSNRIEWIEEDDPLFRGSQ DGRMARVQANELRLL-OH	6,519.33	+	–	–[a]
Crustacean cardioactive peptide (CCAP)					
CCAP	PFCNAFTGC-NH_2	956.39	+	–	–
Ecdysis triggering hormone (ETH)					
ETH-1	DEVPAFFLKIAKMKTLPRV-NH_2	2,202.28	–*		
ETH-2	SGRFEDFFYKAEKHIPRI-NH_2	2,239.18	–*		
Elevenin					
Elevenin-1	VDCERNPYDRSCRGAQI-OH	1979.90	+	–	–
Elevenin-2	LEQIDQQDVYMDY-OH	1659.72	+	–	–
Extended FMRFamide					
FMRFa-1	SNMGSSFIRF-NH_2	1,144.56	+	–	+
FMRFa-2	WKSPDVVIRF-NH_2	1,245.71	+	+	–
FMRFa-2^{3-10}	SPDVVIRF-NH_2	931.54	+	+	–
FMRFa-3	GKNDLNFIRF-NH_2	1,222.67	+	+	+
FMRFa-PP-1	SILKDDSSLRIFKESPNEFEYVV-OH	2,715.39	+	(+)	+
FMRFa-PP-2	TDLDDRKEDTESKE-OH	1,680.76	+	(+)	–
FMRFa-PP-3	GQSFDNSALDNEIDSKVSRHPRW-OH	2,658.27	+	(+)	–
Fliktin (Flik)					
Flik-1	SLDAADTPEYYNDLHSF-OH	1957.84	–	+	–
Flik-2	NVNGRYPIGREFGNY-OH	1755.86	+	+	+
Flik-3	LTKRYPVA-OH	947.57	+	+	+
Flik-4	SPRPTQTKLKTTDP-OH	1569.86	+	+	+[b]
Flik-4^{1-9}	SPRPTQTKL-OH	1,027.59	+	+	+
Flik-5	ATFTAGHNTQNQDDEWMLQ-OH	2,206.95	–	+	–
IDL-containing peptide					
IDL	IDLSRFYGHINT-OH	1,435.73	+	+	+
Insulin-like peptide-1 (ILP-1)					
ILP-1-PP	DGYPQFNPK-OH	1,065.50	+	–	–
Ion transport peptide-like (ITP-like)					

(Continues)

TABLE 2 (Continued)

Designation	Sequence	m/z $[M+H]^+$,	MS	MS[b]	MSI
ITP-like-PP	ATLNGHPL-NH_2	821.46	+	+	–
Ion transport peptide (ITP)					
ITP-PP	ATLNGHPL-NH_2	821.46	+	+	–
ITP	SFFDIQCKGVYDKSIFARLDRICEDCYNLFREPQLHMLCKQDCF STQYFTSCIQALLLEDEKERLQEMVEYL-NH_2	8,691.13	+	–	–[a]
ITG-like peptide					
ITG	ITGQGNRLF-OH	1,005.55	+	+	+
Myosuppressin (Ms)					
Ms (pQ)	pQDVDHVFLRF-NH_2	1,257.66	+	+	+
Ms (Q)	QDVDHVFLRF-NH_2	1,274.66	+	+	+
Ms-PP	AMPLQCNSGFLEELPPRLRKICVAIARIWDAREMNDFVDNREY RENLPRYDSSV-OH	6,394.17	+	–	–[a]
Neuropeptide-like precursor-1 (NPLP-1)					
NPLP-1–1	NVGSLARDFALPK-NH_2	1,386.79	+	+	+
NPLP-1–2	HIASVAREYGLPS-NH_2	1,398.75	+	+	+[b]
NPLP-1–3	NIGSLARQSMMPLG-NH_2	1,473.77	+	+	+
NPLP-1–4	NIASLARYDMLPQN-NH_2	1604.82	+	+	+
NPLP-1–5	NVAALARDSSLPY-NH_2	1,375.73	+	+	+
NPLP-1–6	YLGSLARNGGYQTVREYDD-NH_2	2,176.04	+	+	+
NPLP-1–7	SIASLARNADWPGIV-OH	1569.84	+	+	+
NPLP-1–8	GRMTSGRIIARVLNRH-NH_2	1836.06	+	–	+
NPLP-1–9	FSRSPRYLVERS-NH_2	1,495.81	+	–	–
NVP-like peptides					
NVP-1	ADQAMKPKS-OH	975.49	–	+	–
NVP-2	TQEMLMFGNQQNRQANAAASESFTSNAE-OH	3,075.35	+	(+)	–
NVP-3	LVSTTQQPVQAQV-OH	1,398.76	+	–	+[b]
NVP-4	SVPFYQEPRF-OH	1,269.63	+	+	+
NVP-5	MQSYDPYSTAQLQLSSQPRSYQYPHRVVY-OH	3,492.66	+	+	–
Orcokinin (Orc)					
Orc-1	GPVQGASNAVQQDTYASPADLAILARYLENRNAGNRNLDGY LLRQT-OH	4,974.52	+	(+)	–[a]
Orc-2	RGLDSLSGATFGEN-OH	1,423.68	+	+	+
Orc-3	YVPLRRFGAISLQPGNFDEIDRSVFDRFS-OH	3,401.74	+	(+)	–
Orc-3$^{16-29}$	NFDEIDRSVFDRFS-OH	1746.81	+	(+)	–
Orc-4	NIDEIDTAFDSFF-OH	1533.67	–	+	–
Orc-5	NFDEIDRAGWSGFV-OH	1612.74	+	+	+
Orc-6	LNNYLADRQ-NH_2	1,105.57	+	+	+
Pigment dispersing factor (PDF)					
PDF	NSELINSLLSLPKNMHNA-NH_2	1994.05	+	(+)	–
Prothoracicotropic hormone (PTTH)					
PTTH-PP-1	EGPGQVLSIGRWKEQVVAPEFLLDDREDITSNRNAFFYED-OH	4,640.27	+	–	–[a]
PTTH-PP-2	SFRPEGLGEQV-OH	1,218.61	+	–	–
Pyrokinin (PK)					
PK-1	TTAQEITSGMWFGPRL-NH_2	1793.90	+	–	–
PK-2 (Q)	QQTQFTPRL-NH_2	1,117.61	+	–	–

(Continues)

TABLE 2 (Continued)

Designation	Sequence	m/z $[M + H]^+$,	MS	MS[b]	MSI
PK-2 (pQ)	pQQTQFTPRL-NH_2	1,100.61	+	+	–
PK-3	GSDEELFSYGDATDRNEIEENDRLLPPIFAPRL-NH_2	3,777.84	+	(+)	–
PK-4	RVSWIPSPRL-NH_2	1,209.72	+	+	–
PK-PP-1	EYELRETPNGGSNDNRSPSNEFGSCIEGKCT-OH	3,388.45	+	–	–
PK-PP-2 (Q)	QSRSVSRKI-OH	1,060.62	+	–	–
PK-PP-2 (pQ)	pQSRSVSRKI-OH	1,043.62	+	–	–
Short neuropeptide F (sNPF)					
sNPF	SQRSPSLRLRF-NH_2	1,345.78	+	–	+
$sNPF^{4-11}$	SPSLRLRF-NH_2	974.59	+	+	+
sNPF-PP-1	TENYMDYGEEMAEKTPADNIHEFYRLLLQRNALDNAGFGSIPL EHLMI-OH	5,569.65	+	(+)	–[a]
sNPF-PP-2	SGPHISARDLARPVGAAAGYNDNN-OH	2,423.18	+	(+)	+
SIFamide					
SIFa	YKKPPFNGSIF-NH_2	1,296.71	+	+	–
Sulfakinin (SK)					
SK-1	pQQLDDYGHMRF-NH_2	1,391.64	+	–	–
SK-2	SNGDDEEYGHSRF-NH_2	1511.64	+	+	–
SK-2	SNGDDEEY(SO_3)GHSRF-NH_2	1,590.61	–	+	–
Tachykinin-related peptide (TKRP)					
TK-1 (6×)	APMGFQGMR-NH_2	993.48	+	+	+
TK-2	TIMGFQGMR-NH_2	1,039.52	+	+	+
TK-3	SPFRYFDMR-NH_2	1,217.59	+	+	+
TK-4	NPRWELRGMFVGVR-NH_2	1715.93	+	+	–
TK-PP-1	VPMGFQDMRE-OH	1,209.54	+	+	–
TK-PP-2	NLIPTSAEHNKLSQRTLMDFQDMRDDKESNAPDIEDNLLHEF E-OH	5,056.37	+	+	–[a]
TK-PP-3	DYLTPDFEDFYFRNE-OH	1970.84	+	(+)	+
TK-PP-4	SLEEVLGEIE-OH	1,117.56	+	–	–
TK-PP-5	AAMNFYGTKE-OH	1,131.51	+	+	–
TK-PP-6	TYVLEYPEDYEKRLLAMGFQGTRGKLKEFPGEWE-OH	4,080.02	+	–	–[a]
$TK\text{-}PP\text{-}6^{1-11}$	TYVLEYPEDYE-OH	1,420.62	+	–	–
$TK\text{-}PP\text{-}6^{14-34}$	LLAMGFQGTRGKLKEFPGEWE-OH	2,394.23	+	+	–
TK-PP-7	SLLDEIEELE-OH	1,189.58	+	+	–
Trissin					
Trissin	VSCDQCGRECADICGTRQFRACCFNNM-OH	3,024.20	+	–	–

Note: Direct tissue profiling by MALDI-TOF mass spectrometry (MS) with subsequent MSMS fragmentation experiments and brain tissue extraction analyzed by ESI-Q-TOF MS were used for peptide sequence confirmation (bracket: a part of the peptide amino acid sequence is confirmed). Because of the lack of basic amino acids, AKH is detected as sodium $[M + Na]^+$ and potassium $[M + K]^+$ adducts. MSI was applied for selected neuropeptide spatial distribution within fresh-frozen 14 µm thin brain sections.

[a]Out of detection range in MSI experiments.

[b]Peptide distribution is inferred by mass matches.

*Not produced from neurons of the brain.

intensities. The ion map of Crz showed a unique distribution pattern as only ion signals in the region of the *pars lateralis* (PL), a neuroendocrine center in insects, were found. In the region of the CB, neuropeptides encoded on the *dh-31*, *itg*, *myosuppressin*, *nvp*, *orc*, and *tk* genes were observed.

Insect neuropeptides are contained either as a single copy (*e.g.* AT, Crz, myosuppressin) or as multiple copies (paracopies, *e.g.* Ast-A, extended FMRFamides, TKs, PKs) within the precursor proteins. In MALDI-TOF mass spectrometric diagrams, the ion signal intensities of paracopies show constant relative patterns which resulted in

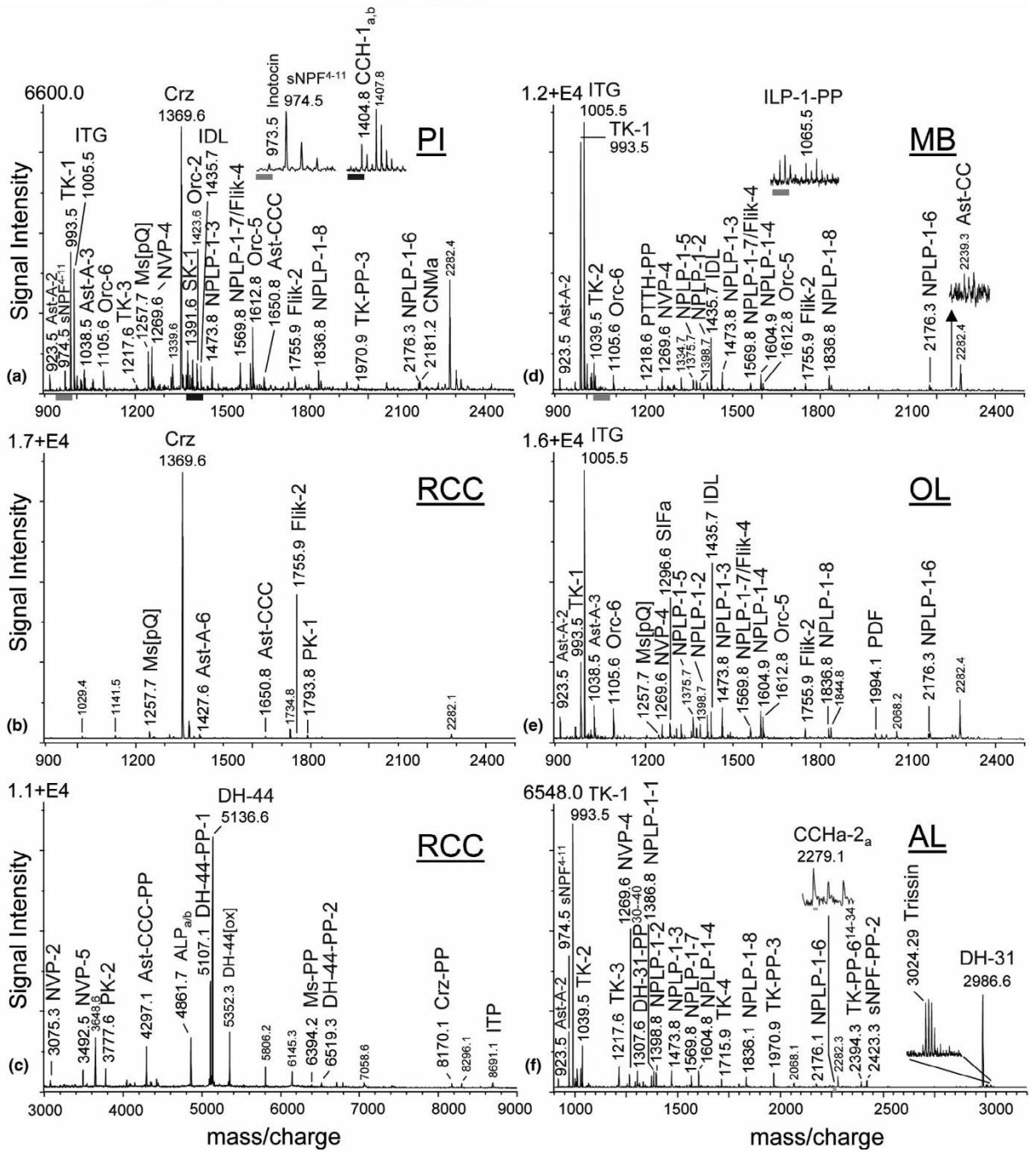

FIGURE 1 Representative MALDI-TOF mass spectra (direct tissue profiling) obtained from preparations of (a) cell population of the *pars intercerebralis* (PI, $n = 12$ samples from 12 brains), (b) the retrocerebral complex (RCC, $n = 15$ samples from 15 animals) in the mass range m/z 900–2,500, (c) the RCC in the mass range m/z 3,000–9,000, (d) a portion of the mushroom body (MB, $n = 4$ samples from 4 brains), (e) an optic lobe (OL, $n = 8$ samples from 8 brains) and (f) an antennal lobe (AL, $n = 10$ samples from 10 brains). Ion signals are marked and represent single charged peptides $[M + H]^+$. Ast-A, allatostatin-A; Ast-CCC, allatostatin-CCC; DH-31, calcitonin-like diuretic hormone-31; DH-44, corticotropin-releasing factor-like diuretic hormone-44; Crz, corazonin; IDL, IDL-containing peptide; ITG, ITG-like peptide; ITP, ion transport peptide; Ms, myosuppressin; TK, tachykinin-related peptide; NVP, NVP-containing peptide; NPLP-1, neuropeptide-like precursor 1; Orc, orcokinin; Flik-fliktin; PDF, pigment dispersing factor; PK, pyrokinin; PP, precursor peptide; sNPF, short neuropeptide F; SK, sulfakinin

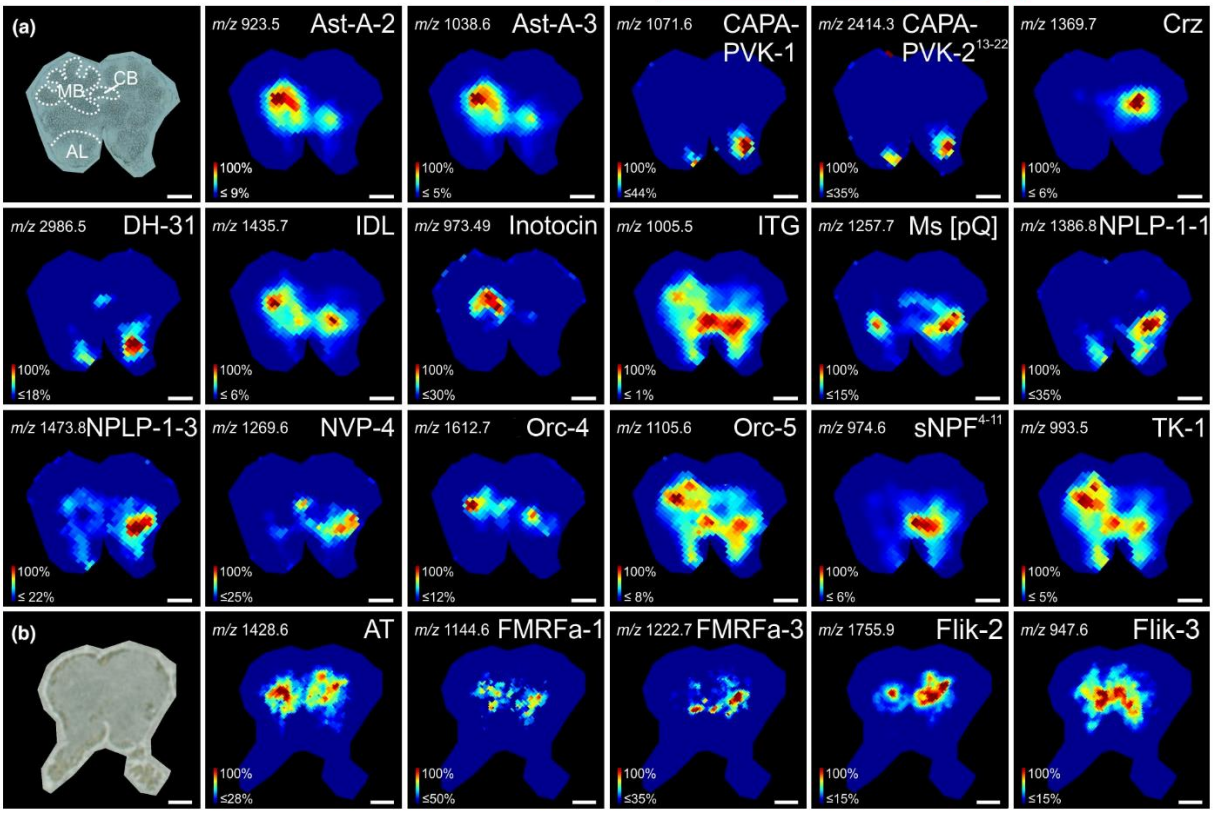

FIGURE 2 MALDI-MSI ion maps show the spatial distribution of 22 peptides from 16 genes in two exemplary ant brain sections recorded using the (a) UltrafleXtreme (first section) and (b) rapifleX MS instrument (second section). The accuracy of mass matching for peptide assignment was settled at ±0.05%. Ast-A, allatostatin-A; AT, allatotropin; DH-31, calcitonin-like diuretic hormone-31; Crz, corazonin; CAPA-PVK, CAPA/periviscerokinin; FMRFa, extended FMRFamides; IDL, IDL-containing peptide; ITG, ITG-like peptide; ITP, ion transport peptide; Ms myosuppressin; TK, tachykinin-related peptide; NVP, NVP-containing peptide; NPLP-1, neuropeptide-like precursor 1; Orc, orcokinin; Flik, fliktin; PP, precursor peptide; sNPF, short neuropeptide F. Scale bars = 200 μm

similar spatial distributions in imaging ion maps as shown exemplarily for TKs in Figure 3a. The spatial distribution of three mature neuropeptides (TK-1, -2, -3) and one precursor protein (TK-PP-3), all encoded on the *tk*-gene, were detected in a single brain section. Each *tk*-gene product has a different amino acid sequence (Table 2) which resulted in a different molecule ionization efficiency in MALDI-TOF MS and, thus, different ion signal intensities in resulting mass spectra (Figure 3b,c). Ion maps of TK-4 and TK-PP-1, -2, -4 to -8 were not visualized in this section, likely because their ion intensities were either too low or the ion mass (TK-PP-2, *m/z* 5,056.4) was out of the detection range.

To interpret the large dataset resulting from each single brain imaging analysis, we applied bisecting k-means segmentation clustering using SCILS Lab. The result of the segmentation analysis is a binary hierarchical tree containing nested sub regions, each defined by a unique composition of different ion signals within the mass spectrum. A representing spatial segmentation analysis of a single ant brain section is shown in Figure 4. The analyzed ants MSI dataset could be compartmentalized into certain clusters which enabled the assignment of subdivided regions of the protocerebrum, the PL (left side) and the MB (right side) as well as the neuropil region of the deutocerebrum, the ALs.

3.3.3 | Spatial distribution of neuropeptides in the ant brain: MALDI-MSI and immunostaining

The immunostaining pattern of TK is well-characterized for the brain of *Cataglyphis* (Schmitt et al., 2017). To evaluate the precision of our MALDI-MSI neuropeptide data set, we therefore performed immunostainings against TK combined with MALDI-MSI in consecutive brain sections (Figure 5). To visualize neuroanatomical landmarks in the brain, we co-stained the brain sections with fluorophore-conjugated phalloidin as a general label for neuronal tissue that helps to delineate neuropil regions and fiber connections in brain regions that are devoid of cell bodies. TK-*like* immunoreactivity was found throughout the brain sections, with very distinct labeling in the CB, the MB, and the AL (Figure 5 [S1, S3, S5]) as previously described (Schmitt et al., 2017). MALDI-MSI and TK-*like* immunoreactivity data illustrated very well the

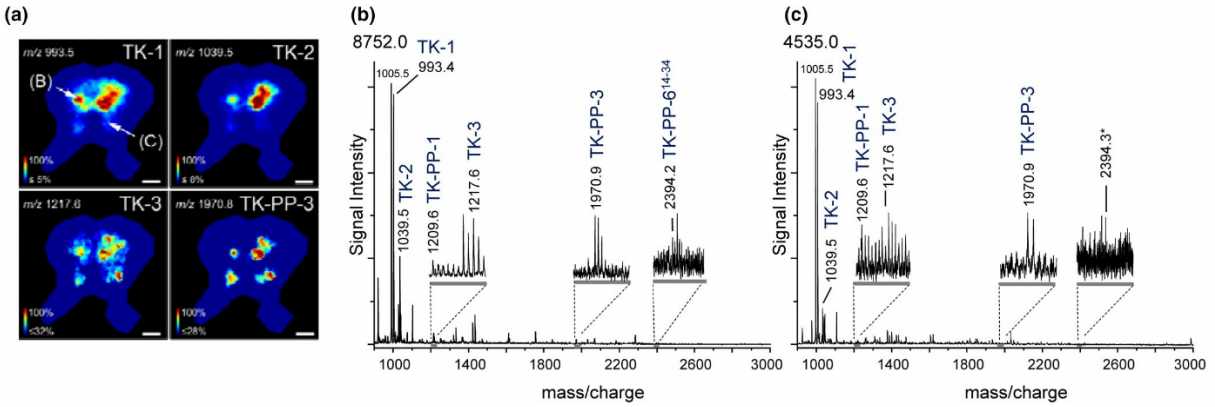

FIGURE 3 MALDI-MSI ion maps demonstrating the spatial distribution of products from *tachykinin-related peptide* (*tk*) gene analyzed from a *C. nodus* brain section (thickness: 14 µm) recorded using the rapifleX MS instrument. The *tk*-gene encodes four different tachykinin-related peptides (TK) and eight TK-PPs. (a) Ion signal intensity of three TKs (TK-1, -2, -3) and TK-PP-3 was sufficient to be visualized in these MALDI-MSI spectra. The accuracy of mass matching for peptide assignment was settled at ±0.05%. Minimum intensity was defined individually for each ion of interest to ignore smaller peaks in the baseline which could be cause in false positive ion distribution. Scale bar: 200 µm. (b, c) Mass spectra obtained by MSI showing the relative signal intensities of TK paracopies processed from the *tk*-gene at different neuronal regions of the brain. The absence of an ion signal representing TK-PP-6^{14-34} in (c) (marked with an asterisk) is a result of the lower signal intensity of TK paracopies at this spot relative to the analyzed region in B. The analyzed spots are indicated in (a) by white arrows

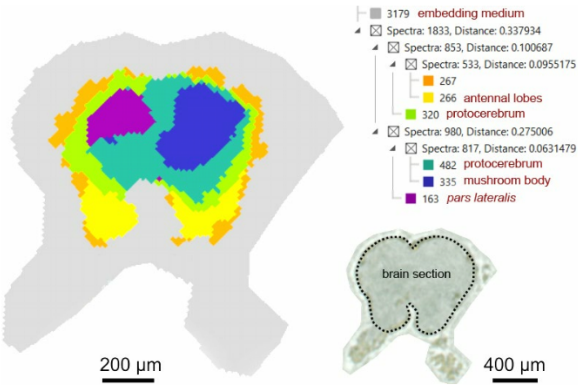

FIGURE 4 Spatial segmentation analysis based on MS imaging data measured from a single brain section using the rapifleX MS instrument. The color-coded levels in the segmentation dendrogram reveal different regions of the protocerebrum including the right neuropil area of the mushroom body and the lateral neurosecretory area, the *pars lateralis* as well as the deutocerebral neuropil region, the antennal lobes. The statistical evaluation of our MSI data showing division of *C. nodus* brain in different neuropil brain regions, which is consistent with the recently described neuroanatomical organization of the *Cataglyphis* brain (Habenstein et al., 2020)

spatial distribution of TKs throughout consecutive brain sections, as illustrated by ion maps for TK-1 (Figure 5 [S2, S4, S6]). Slight mismatches between MALDI-MSI and the immunostaining data are attributable to the different brain regions in consecutive section as well as to the nature of evaluation methods underlying the two distinct methods (MALDI-MSI and immunohistochemistry). The immunohistochemical images (Figure 5 [S1, S3, S5]) do not display relative differences of the TK abundances. Consequently, TK occurs in bright green wherever the antibody binds in a certain quantity. In contrast, MALD-MSI images (Figure 5 [S2, S4, S6]) display the relative signal intensity of the analyte throughout the brain sections. For instance, we detected TK also in the AL using MALDI-MSI. However, the detected expression (ion signal intensity) of TK was considerably lower than in other parts in the brain. We found the highest TK levels in the mushroom body (indicated in red) whereas the TK level in the AL was in most cases only 0.1%–10% (indicated in dark to light blue) of it. Throughout consecutive serial sections of the MB, a slightly asymmetric distribution of TK-1 and TK-*like* immunoreactivity between the right and the left cerebral hemisphere was observed in more posteriorly located brain layers. Overall, the largely coherent findings using both visualization methods show that the applied MALDI-MSI procedure is suitable to detect and localize neuropeptides at high spatial resolution, even within small subcompartments of the *C. nodus* brain.

4 | DISCUSSION

Our study presents a comprehensive chemical as well as spatial characterization of the peptidome from the small brain of the ant *C. nodus*, obtained by a combination of transcriptomic and different MS approaches (see Table S2).

4.1 | *C. nodus* brain transcriptome

The transcriptome from adult *C. nodus* worker brains revealed 49 precursor proteins belonging to 27 neuropeptides, 4

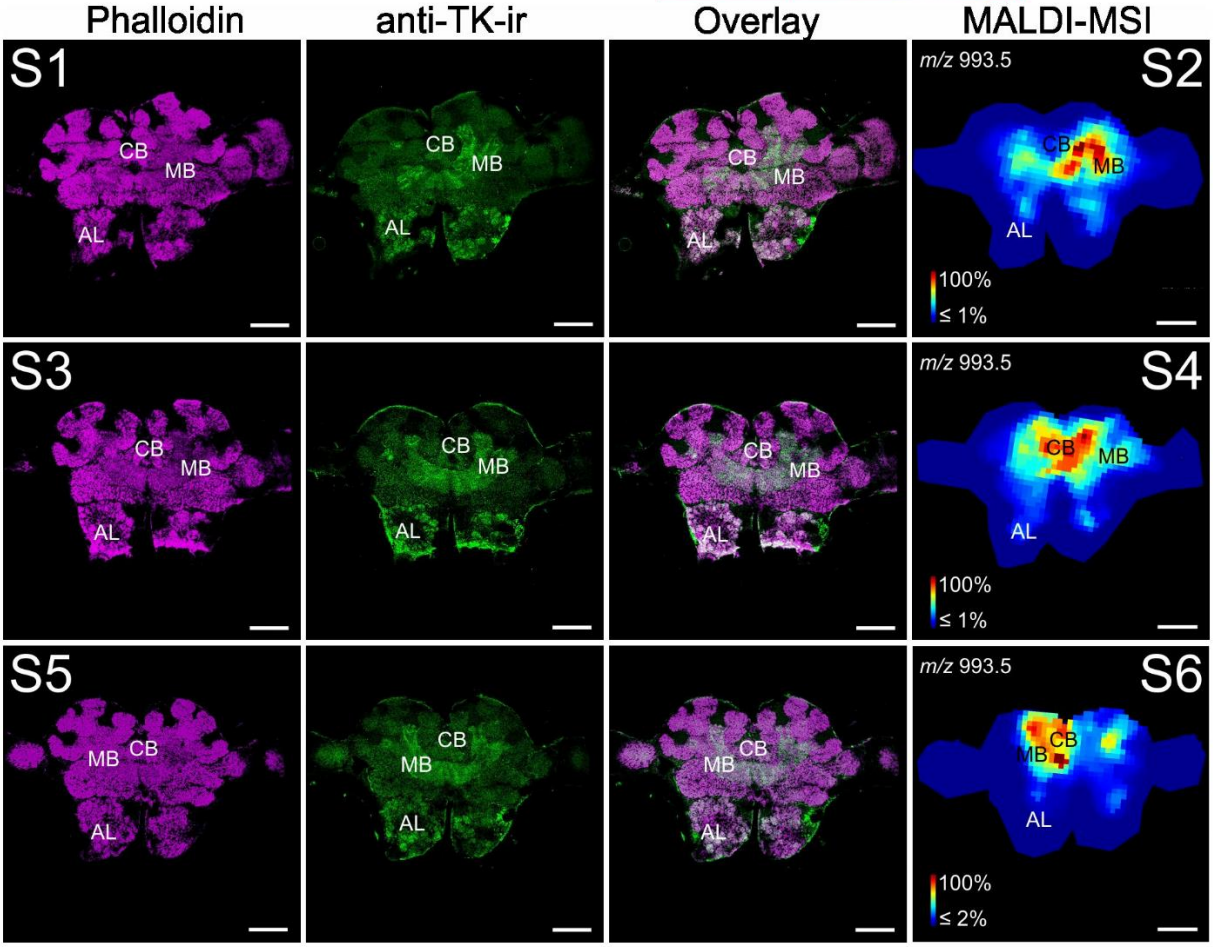

FIGURE 5 Distribution of tachykinin-related peptides (TK) analyzed in six consecutive brain sections (S1–S6) using immunohistochemistry and MALDI-MSI by the ultrafleXtreme MS instrument. The 14 μm brain sections are ordered from anterior to posterior (S1–S6). (S1, S3 and S5) Double-immunofluorescence stainings of anti-TK like-ir (green) and phalloidin labeling (magenta). F-actin labeling with phalloidin was used to identify specific neuropil regions in the brain such as the mushroom body (MB), the central body (CB) and the glomeruli of the antennal lobes (AL). Anti-TK labeling reveals the presence of anti-TK-ir in the MB, CB and the glomeruli of the AL, shifting from the right to the left hemisphere in consecutive serial sections (green). (S2, S4 and S6) Molecular images of TK-1 (*m/z* 993.5) using mass spectrometry imaging revealed the spatial distribution of TK-1 in the MB, CB as well as in the glomeruli of the AL with a similar shift from right to left in consecutive sections as shown with immunostaining. The accuracy of mass matching for peptide assignment was set to ±0.05%. Scale bars = 200 μm

neuropeptide-like, and 11 protein hormone genes (Table 1). We found that six of these precursors were translated from alternatively spliced mRNAs (*alp*, *capa*, *nplp-1*, *cch-1 cch-2*, *ilp-2*, *itp*) which potentially results in differences in the amino acid sequence of some peptides. In insects, alternatively spliced neuropeptide mRNAs are not unusual and were also found in *e.g.* the stick insect *C. morosus* (Liessem et al., 2018), locusts, termites (Veenstra, 2014), kissing bugs (Sterkel et al., 2012), and ants (Choi et al., 2014). Longer and shorter *capa* transcripts were previously described for other insects including the cockroach *P. americana* (Neupert et al., 2014), the fire ant *Solenopsis invicta* (Choi et al., 2014) and the stick insect *C. morosus* (Liessem et al., 2018). Cell-specific transcripts of CAPA peptides in individual *capa*-neurons have not been observed in cockroaches (Eckert et al., 2002; Neupert et al., 2014; Pollák et al., 2005), but were suggested for the fire ant *S. invicta* (Choi et al., 2014) and may thus also exist for the related *C. nodus*. The novel neuropeptide-like gene *fliktin* with protein sequence similarities to uncharacterized protein precursors from other ants contains five non-amidated peptides. BLAST searches revealed highly sequence similarities of the *fliktin* gene with a *V. emeryi* protein precursor predicted as stress-response protein NST-1 by automated computational analysis and annotation from the *V. emeryi* genome and a potential neuropeptide gene designated as PaOGS36577 from the cockroach *P. americana* (Zeng et al., 2021). Furthermore, using the same annotation method as described for *V. emeryi*, an NST-1 precursor (Acc.-No. XP_033313739) was predicted from the bumblebee *Bombus bifarius*. For these insects, functional studies of the NST-1 or PaOGS36577 gene are lacking.

Transcripts for 13 insect neuropeptide genes described from other insects (*acp*, *mip*, *ast-c*, *calcitonin-a*, *-b*, *efla*, *hansolin*, *natalisin/waara*, *rya*, *proctolin*, *insect kinin*, *rfla*, and *tryptopyrokinin*) could not be found in the assembled brain transcriptome data of *C. nodus*. Genes for these neuropeptide precursors were also not found in other ant species (Nygaard et al., 2011; Schmitt et al., 2015). Our data thus supports a general absence of these peptides in ants (Formicidae), although they occur in at least some non-formicid hymenopteran species - with exception of MIP and calcitonin (Chang et al., 2018; Hummon et al., 2006) which seem to be generally missing in hymenopteran genomes.

4.2 | MS characterization of putative mature neuropeptides, neuropeptide-like, and protein hormones

To characterize the potential bioactive peptides processed from the 49 predicted precursor proteins from the brain transcriptome, we applied brain extract analysis by Q-Exactive Orbitrap MS and direct tissue profiling by MALDI-TOF MS. For most of the prepropeptide genes, we identified all predicted and likely bioactive neuropeptides by comparing calculated peptide fragments with the resulting fragmentation pattern generated by MS^2 of the ion of interest. This also includes five products from the novel *flik* gene, three of which were detected in the RCC by direct tissue profiling which indicates likely a potential hormonal function in *C. nodus*. For a few prepropeptides, predicted mature neuropeptides were confirmed by mass match only. The protein hormones ILP-1 and PTTH were not confirmed by mass spectrometry but identification of adjoining PPs indicated at least the processing of the respective prepropeptide. Furthermore, we did not detect ETH peptides in our brain samples. This is not surprising as ETH in insects is expressed exclusively in epi/peritracheal cells (Inka cells) attached to the surface of the major tracheal trunk (O'Brien & Taghert, 1998; Zitnan et al., 2003). The protein hormones NPF-1, NP, EH, bursicon alpha, and beta also did not yield positive hits. Their predicted ion mass is either above 10,000 Da and thus outside of the detection range of *m/z* 600–10,000 Da in our experiments, or their production is restricted to specific developmental time windows (e.g. EH).

4.3 | Molecular imaging of mature neuropeptides in *C. nodus* brain sections as a tool to correlate behavioral transitions with compartment-specific changes in the neuropeptidome

As outlined in the introduction, neuropeptides are prime candidates to regulate age-specific behavioral transitions in social insects. Still very little is known about which peptide signaling pathways are involved. One way to approach this interesting question is to correlate expression of given peptides with a certain age or behavior. Measuring neuropeptide content in insect brains by immunological methods (e.g. ELISA) has since long been established, and is now increasingly performed by (semi)quantiative mass spectrometry of tissue extracts (e.g. Brockmann et al., 2009; Kunz et al., 2018; Sterkel et al., 2011) or by direct tissue profiling (*e.g.*, Wegener et al., 2011, Nagata et al., 2012, Christ et al., 2017). Yet, there is growing evidence that insect neurons of a given peptide identity do not necessarily form functionally homogenous groups and may have different functions and may act in different circuits. This seems not surprising given the comparatively low number of neurons by which insect brains fulfill astonishingly complex tasks. For example, sNPF neurons have diverse subset-specific functions in e.g. metabolic stress response (Kahsai, Kapan et al., 2010) or promotion of sleep (Shang et al., 2013). Moreover, neuropeptides are sometimes stored in excess and up-regulation and release may lead to substantial changes only at certain storage or release sites in a compartment-specific manner, especially in widely branched peptidergic neurons such as the SIFamide neurons (Dreyer et al., 2019). While not explicitly demonstrated for insect neuropeptides so far, this situation has been recently demonstrated for the other large class of neuromodulators, the biogenic amines during arousal in the honey bee brain (Ramesh & Brockmann, 2019). Thus, measuring total peptide levels over larger brain areas may mask actual changes in peptide levels that occur in either specific neurons or specific brain compartments where the peptides are released.

In our study, we used MALDI-MSI to detect the spatial distribution of mature bioactive neuropeptides and neuropeptide-like molecules within the ant brain at high spatial resolution. Different to immunolabeling, MSI enables untargeted investigation of neuropeptides in thin brain sections, and has already been used successfully to characterize age- and state-dependent changes in specific peptides in the honey bee brain (Pratavieira et al., 2014, 2018). We here optimized and standardized an MSI protocol for neuropeptide detection in ant brain sections that allows to perform similar analyses over a much broader range of peptides at high spatial resolution. For ant brains, we found that an adequate dehydration procedure of the samples in a desiccator is a crucial step to achieve sufficient neuropeptide detection. The quick removal of ethanol during the washing steps clearly improved the homogeneity of matrix crystal formation, and, thus, the reproducibility of molecular images.

The reproducibility and spatial accuracy of MALDI-MSI in small tissues has been demonstrated by comparing peptide distribution patterns obtained by immunostainings and MALDI-MSI in the neuroendocrine RCC of cockroaches (Ly et al., 2019). We now confirmed these findings for ant brain tissue and show that MSI and TK-immunostaining revealed very similar distribution patterns of TKs with pronounced labeling in the MBs, the CB and the ALs across consecutive brain tissue sections, consistent with the immunostaining pattern in the closely related ant *Cataglyphis fortis* (Schmitt et al., 2017). In general, the generated ion maps for the different neuropeptides exhibited very distinct patterns in line with our results from direct tissue profiling. For instance, in both direct tissue profiling and MALDI-MSI, CAPA/PVK and DH-31 were found in the ALs but did not occur in the MBs of the *Cataglyphis* brain. In contrast, inotocin and extended FMRFamides were exclusively found in the central brain but not in the ALs. We revealed a

pertinent pattern across various brain sections for Crz: the detection was restricted to lateral parts of the anterior brain sections (PL) and, with lower signal intensities, to parts of the medial protocerebrum. This indicates the presence of corazoninergic neurons in the PL with axonal projections to the medial protocerebrum and to the RCC where we found strong ion intensities for corazonin using direct tissue profiling. Thus, MALDI-MSI describes a morphology of corazoninergic neurons fully consistent with the highly conserved distribution in other insects including Hymenoptera such as *Apis mellifera* (Verleyen et al., 2006) and *Camponotus* ants (Schmitt et al., 2015). Importantly, the spatial reliability of our MALDI-MSI data is supported by unsupervised statistical analysis that maps out divisions in the *C. nodus* brain based on regional neuropeptide content. These divisions are fully consistent with specific neuropil regions of the *Cataglyphis* brain recently described by three-dimensional neuroanatomical reconstructions (Habenstein et al., 2020). We also used MALDI-MSI to uncover for the first time the location of products of the novel neuropeptide-like gene *flik* in an insect. This knowledge about the distribution of potential neuropeptides in the brain is an important fundamental prerequisite for future functional studies.

5 | CONCLUSION

In this study, we present a peptidomic data set for the ant *C. nodus* based on transcriptome analysis combined with three different MS approaches. This is the most comprehensive peptidomic analysis for a hymenopteran species so far. We further demonstrate that our optimized MALDI-MSI pipeline is an appropriate tool to investigate the spatial distribution of multiple neuropeptides in small ant brains. Furthermore, post-processing steps and MSI data clustering using k-means allows for correct allocation of neuropeptides to the respective neuronal region. This now sets the stage to use *C. nodus* for future studies to address brain-wide peptidomic changes correlated to age or stage- and task-specific behaviors in a social insect.

ACKNOWLEDGMENTS

We thank the Greek government and the management board of the Schinias National Park for providing access to the park and the *Cataglyphis* ants. We especially thank Maria Trivourea and Christos Georgiadis for the administrative help and the support during our field work in the national park. We further thank all field assistants who helped to excavate the *Cataglyphis* nests in Greece. We thank Claudia Groh and Kornelia Grübel (University of Würzburg) for help in brain extract sample preparation, Astrid Wilbrand-Hennes, Ursula Cullman and Christian Frese (CECAD Cologne Proteomics Facility) for Orbitrap MS analyses and Lapo Ragionieri for support in sample treatment before transcriptomic analyses. Special thanks go to Dick Nässel for kindly providing the TK antiserum. We also thank Robin Grob for providing the picture of the *Cataglyphis* ant for the graphical abstract.

All experiments were conducted in compliance with the ARRIVE guidelines.

CONFLICT OF INTEREST

The authors declare the following competing financial interest(s): A.L. and D.T. were employees of Bruker Daltonik GmbH for the duration of this study.

Open Research Badges

This article has received a badge for *Open Materials* because it provided all relevant information to reproduce the study in the manuscript. More information about the Open Practices badges can be found at https://cos.io/our-services/open-science-badges/.

ORCID

Jens Habenstein https://orcid.org/0000-0003-3589-6436
Sander Liessem https://orcid.org/0000-0002-7073-2659
Christian Wegener https://orcid.org/0000-0003-4481-3567
Reinhard Predel https://orcid.org/0000-0002-0202-6672
Wolfgang Rössler https://orcid.org/0000-0002-5195-8214
Susanne Neupert https://orcid.org/0000-0003-1562-5743

REFERENCES

Amdam, G. V., & Omholt, S. W. (2003). The hive bee to forager transition in honeybee colonies: The double repressor hypothesis. *Journal of Theoretical Biology*, *223*, 451–464. https://doi.org/10.1016/S0022-5193(03)00121-8

Beshers, S. N., & Fewell, J. H. (2001). Models of division of labor in social insects. *Annual Review of Entomology*, *46*, 413–440.

Bloch, G., Sullivan, J., & Robinson, G. (2002). Juvenile hormone and circadian locomotor activity in the honey bee *Apis mellifera*. *Journal of Insect Physiology*, *48*, 1123–1131. https://doi.org/10.1016/S0022-1910(02)00205-6

Bolger, A. M., Lohse, M., & Usadel, B. (2014). Trimmomatic: A flexible trimmer for Illumina sequence data. *Bioinformatics*, *30*, 2114–2120. https://doi.org/10.1093/bioinformatics/btu170

Brockmann, A., Annangudi, S. P., Richmond, T. A., Ament, S. A., Xie, F., Southey, B. R., Rodriguez-Zas, S. R., Robinson, G. E., & Sweedler, J. V. (2009). Quantitative peptidomics reveal brain peptide signatures of behavior. *Proceedings of the National Academy of Sciences of the United States of America*, *106*, 2383–2388. https://doi.org/10.1073/pnas.0813021106

Buchberger, A. R., DeLaney, K., Johnson, J., & Li, L. (2018). Mass spectrometry imaging: A review of emerging advancements and future insights. *Analytical Chemistry*, *90*, 240–265.

Camacho, C., Coulouris, G., Avagyan, V., Ma, N., Papadopoulos, J., Bealer, K., & Madden, T. L. (2009). BLAST+: Architecture and applications. *BMC Bioinformatics*, *10*, 421.–https://doi.org/10.1186/1471-2105-10-421

Chang, J., Zhao, J., & Tian, X. (2018). In silico prediction of neuropeptides in Hymenoptera parasitoid wasps. *PLoS One*, *13*, e0193561.–https://doi.org/10.1371/journal.pone.0193561

Chang, Z., Li, G., Liu, J., Zhang, Y., Ashby, C., Liu, D., Cramer, C. L., & Huang, X. (2015). Bridger: A new framework for de novo transcriptome assembly using RNA-seq data. *Genome Biology*, *16*, 30., https://doi.org/10.1186/s13059-015-0596-2

Chen, J., Reiher, W., Hermann-Luibl, C., Sellami, A., Cognigni, P., Kondo, S., Helfrich-Forster, C., Veenstra, J. A., & Wegener, C. (2016).

Allatostatin a signalling in *Drosophila* regulates feeding and sleep and is modulated by PDF. *PLoS Genetics*, *12*, e1006346.

Chen, R., Hui, L., Sturm, R. M., & Li, L. (2009). Three dimensional mapping of neuropeptides and lipids in crustacean brain by mass spectral imaging. *Journal of the American Society for Mass Spectrometry*, *20*, 1068–1077. https://doi.org/10.1016/j.jasms.2009.01.017

Chen, R., & Li, L. (2010). Mass spectral imaging and profiling of neuropeptides at the organ and cellular domains. *Analytical and Bioanalytical Chemistry*, *397*, 3185–3193.

Choi, M. Y., Köhler, R., Vander Meer, R. K., Neupert, S., & Predel, R. (2014). Identification and expression of capa gene in the fire ant, Solenopsis Invicta. *PLoS One*, *9*, e94274. https://doi.org/10.1371/journal.pone.0094274

Christ, P., Reifenrath, A., Kahnt, J., Hauser, F., Hill, S. R., Schachtner, J., & Ignell, R. (2017). Feeding-induced changes in allatostatin-A and short neuropeptide F in the antennal lobes affect odor-mediated host seeking in the yellow fever mosquito, Aedes aegypti. *PLoS One*, *12*, e0188243.–https://doi.org/10.1371/journal.pone.0188243

Dancker, P., Low, I., Hasselbach, W., & Wieland, T. (1975). Interaction of actin with phalloidin: Polymerization and stabilization of F-actin. *Biochimica Et Biophysica Acta (BBA) - Protein Structure*, *400*, 407–414. https://doi.org/10.1016/0005-2795(75)90196-8

Ddolezal, A. G., Brent, C. S., Hölldobler, B., & Amdam, G. V. (2012). Worker division of labor and endocrine physiology are associated in the harvester ant, *Pogonomyrmex californicus*. *Journal of Experimental Biology*, *215*, 454–460.

Derst, C., Dircksen, H., Meusemann, K., Zhou, X., Liu, S., & Predel, R. (2016). Evolution of neuropeptides in non-pterygote hexapods. *BMC Evolutionary Biology*, *16*, 51.

Dreyer, A. P., Martin, M. M., Fulgham, C. V., Jabr, D. A., Bai, L., Beshel, J., & Cavanaugh, D. J. (2019). A circadian output center controlling feeding: Fasting rhythms in *Drosophila*. *PLOS Genetics*, *15*, e1008478.

Eckert, M., Herbert, Z., Pollák, E., Molnár, L., & Predel, R. (2002). Identical cellular distribution of all abundant neuropeptides in the major abdominal neurohemal system of an insect (*Periplaneta americana*). *The Journal of Comparative Neurology*, *452*, 264–275.

Fleischmann, P. N., Grob, R., Müller, V. L., Wehner, R., & Rössler, W. (2018). The geomagnetic field is a compass cue in *Cataglyphis* ant navigation. *Current Biology*, *28*, 1440–1444.

Fleischmann, P. N., Grob, R., Wehner, R., & Rössler, W. (2017). Species-specific differences in the fine structure of learning walk elements in *Cataglyphis* ants. *Journal of Experimental Biology*, *220*, 2426–2435.

Fricker, L. D. (2012). *Neuropeptides and other bioactive peptides*. Morgan & Claypool Life Sciences.

Gasteiger, E., Gattiker, A., Hoogland, C., Ivanyi, I., Appel, R. D., & Bairoch, A. (2003). ExPASy: The proteomics server for in-depth protein knowledge and analysis. *Nucleic Acids Research*, *31*, 3784–3788. https://doi.org/10.1093/nar/gkg563

Gordon, D. M. (1989). Dynamics of task switching in harvester ants. *Animal Behaviour*, *38*, 194–204. https://doi.org/10.1016/S0003-3472(89)80082-X

Gospocic, J., Shields, E. J., Glastad, K. M., Lin, Y., Penick, C. A., Yan, H., Mikheyev, A. S., Linksvayer, T. A., Garcia, B. A., Berger, S. L., Liebig, J., Reinberg, D., & Bonasio, R. (2017). The neuropeptide corazonin controls social behavior and caste identity in ants. *Cell*, *170*(748–759), e12. https://doi.org/10.1016/j.cell.2017.07.014

Grabherr, M. G., Haas, B. J., Yassour, M., Levin, J. Z., Thompson, D. A., Amit, I., Adiconis, X., Fan, L., Raychowdhury, R., Zeng, Q., Chen, Z., Mauceli, E., Hacohen, N., Gnirke, A., Rhind, N., di Palma, F., Birren, B. W., Nusbaum, C., Lindblad-Toh, K., … Regev, A. (2011). Full-length transcriptome assembly from RNA-Seq data without a reference genome. *Nature Biotechnology*, *29*, 644–652.

Haas, B. J., Papanicolaou, A., Yassour, M., Grabherr, M., Blood, P. D., Bowden, J., Couger, M. B., Eccles, D., Li, B., Lieber, M., Macmanes, M. D., Ott, M., Orvis, J., Pochet, N., Strozzi, F., Weeks, N., Westerman, R., William, T., Dewey, C. N., … Regev, A. (2013). *De novo* transcript sequence reconstruction from RNA-seq using the Trinity platform for reference generation and analysis. *Nature Protocols*, *8*, 1494–1512. https://doi.org/10.1038/nprot.2013.084

Habenstein, J., Amini, E., Grübel, K., el Jundi, B., & Rössler, W. (2020). The brain of *Cataglyphis* ants: Neuronal organization and visual projections. *The Journal of Comparative Neurology*, *528*, 3479–3506. https://doi.org/10.1002/cne.24934

Hamilton, A., Shpigler, H., Bloch, G., Wheeler, D. E., & Robinson, G. E. (2016). *Endocrine influences on insect societies. Non-mammalian hormone-behavior systems*. Elsevier.

Han, B., Fang, Y., Feng, M., Hu, H., Qi, Y., Huo, X., Meng, L., Wu, B., & Li, J. (2015). Quantitative neuropeptidome analysis reveals neuropeptides are correlated with social behavior regulation of the honeybee workers. *Journal of Proteome Research*, *14*, 4382–4393. https://doi.org/10.1021/acs.jproteome.5b00632

Hölldobler, B., & Wilson, E. O. (1990). *The ants*. Harvard University Press.

Huang, Z. Y., & Robinson, G. (1995). Seasonal changes in juvenile hormone titers and rates of biosynthesis in honey bees. *Journal of Comparative Physiology B*, *165*, 18–28.

Hummon, A. B., Richmond, T. A., Verleyen, P., Baggerman, G., Huybrechts, J., Ewing, M. A., Vierstraete, E., Rodriguez-Zas, S. L., Schoofs, L., Robinson, G. E., & Sweedler, J. V. (2006). From the genome to the proteome: Uncovering peptides in the *Apis* brain. *Science*, *314*, 647–649. https://doi.org/10.1126/science.1124128

Kahsai, L., Kapan, N., Dircksen, H., Winther, A. M. E., & Nässel, D. R. (2010). Metabolic stress responses in Drosophila are modulated by brain neurosecretory cells that produce multiple neuropeptides. *PLoS One*, *5*, e11480. https://doi.org/10.1371/journal.pone.0011480

Kahsai, L., Martin, J. R., & Winther, A. M. (2010). Neuropeptides in the drosophila central complex in modulation of locomotor behavior. *Journal of Experimental Biology*, *213*, 2256–2265.

Kamhi, J. F., & Traniello, J. F. (2013). Biogenic amines and collective organization in a superorganism: Neuromodulation of social behavior in ants. *Brain, Behavior and Evolution*, *82*, 220–236. https://doi.org/10.1159/000356091

Kastin, A. J. (Ed.) (2013). *Handbook of Biologically active peptides*, 2nd edn. Academic Press.

Khatib-Shahidi, S., Andersson, M., Herman, J. L., Gillespie, T. A., & Caprioli, R. M. (2006). Direct molecular analysis of whole-body animal tissue sections by imaging MALDI mass spectrometry. *Analytical Chemistry*, *78*, 6448–6456.

Knapek, S., Kahsai, L., Winther, A. M., Tanimoto, H., & Nässel, D. R. (2013). short neuropeptide F acts as a functional neuromodulator for olfactory memory in kenyon cells of *Drosophila* mushroom bodies. *Journal of Neuroscience*, *33*, 5340–5345. https://doi.org/10.1523/JNEUROSCI.2287-12.2013

Ko, K. I., Root, C. M., Lindsay, S. A., Zaninovich, O. A., Shepherd, A. K., Wasserman, S. A., Kim, S. M., & Wang, J. A. (2015). Starvation promotes concerted modulation of appetitive olfactory behavior via parallel neuromodulatory circuits. *eLife*, *4*, e08298.

Kohlmeier, P., Feldmeyer, B., & Foitzik, S. (2018). Vitellogenin-like a–associated shifts in social cue responsiveness regulate behavioral task specialization in an ant. *PLOS Biology.*, *16*, e2005747. https://doi.org/10.1371/journal.pbio.2005747

Kunz, T. O., Chen, J., & Wegener, C. (2018). Metabolic labeling to quantify drosophila neuropeptides and peptide hormones. *Methods in Molecular Biology*, *1719*, 175–185.

Liessem, S., Ragionieri, L., Neupert, S., Büschges, A., & Predel, R. (2018). Transcriptomic and neuropeptidomic analysis of the stick insect, *Carausius morosus*. *Journal of Proteome Research*, *17*, 2192–2204.

Ly, A., Ragionieri, L., Liessem, S., Becker, M., Deininger, S. O., Neupert, S., & Predel, R. (2019). Enhanced coverage of insect neuropeptides in tissue sections by an optimized mass-spectrometry-imaging protocol. *Analytical Chemistry*, *91*, 1980–1988.

Nagata, S., Matsumoto, S., Nakane, T., Ohara, A., Morooka, N., Konuma, T., Nagai, C., & Nagasawa, H. (2012). Effects of starvation on brain short neuropeptide F-1, -2, and -3 levels and short neuropeptide F receptor expression levels of the Silkworm, Bombyx Mori. *Frontiers in Endocrinology*, *3*, 3. https://doi.org/10.3389/fendo.2012.00003

Nässel, D. R., & Zandawala, M. (2019). Recent advances in neuropeptide signaling in drosophila, from genes to physiology and behavior. *Progress in Neurobiology*, *179*, 101607.

Neupert, S., Derst, C., Sturm, S., & Predel, R. (2014). Identification of two Capa cDNA transcripts and detailed peptidomic characterization of their peptide products in *Periplaneta americana*. *EuPa Open Proteomics*, *3*, 195–205. https://doi.org/10.1016/j.euprot.2014.02.005

Nygaard S., Zhang G., Schiøtt M., Li C., Wurm Y., Hu H., Zhou J., Ji L., Qiu F., Rasmussen M., Pan H., Hauser F., Krogh A., Grimmelikhuijzen C. J., Wang J., & Boomsma J. J. (2011) The genome of the leaf-cutting ant Acromyrmex echinatior suggests key adaptations to advanced social life and fungus farming. *Genome Research*. *21*, 1339–1348. https://doi.org/10.1101/gr.121392.111

O'Brien, M. A., & Taghert, P. H. (1998). A peritracheal neuropeptide system in insects: Release of myomodulin-like peptides at ecdysis. *Journal of Experimental Biology*, *201*, 193–209.

Oster, G. F., & Wilson, E. O. (1978). *Caste and ecology in the social insects*. Princeton University Press.

Pauls, D., Chen, J., Reiher, W., Vanselow, J. T., Schlosser, A., Kahnt, J., & Wegener, C. (2014). Peptidomics and processing of regulatory peptides in the fruit fly *Drosophila*. *EuPA Open Proteomics*, *3*, 114–127. https://doi.org/10.1016/j.euprot.2014.02.007

Pollák, E., Eckert, M., Molnár, L., & Predel, R. (2005). Differential sorting and packaging of *capa*-gene related products in an insect. *The Journal of Comparative Neurology*, *481*, 84–95.

Pratavieira, M., da Silva Menegasso, A. R., Garcia, A. M., dos Santos, D. S., Gomes, P. C., Malaspina, O., & Palma, M. S. (2014). MALDI imaging analysis of neuropeptides in the africanized honeybee (*Apis mellifera*) brain: Effect of ontogeny. *Journal of Proteome Research*, *13*, 3054–3064.

Pratavieira, M., Menegasso, A. R. D. S., Esteves, F. G., Sato, K. U., Malaspina, O., & Palma, M. S. (2018). MALDI Imaging analysis of neuropeptides in Africanized Honeybee (*Apis mellifera*) brain: Effect of aggressiveness. *Journal of Proteome Research*, *17*, 2358–2369.

Predel, R., Neupert, S., Derst, C., Reinhardt, K., & Wegener, C. (2018). Neuropeptidomics of the bed bug *Cimex lectular*ius. *Journal of Proteome Research*, *17*, 440–454.

Predel, R., Neupert, S., Garczynski, S. F., Crim, J. W., Brown, M. R., Russell, W. K., Kahnt, J., Russell, D. H., & Nachman, R. J. (2010). Neuropeptidomics of the mosquito *Aedes aegypti*. *Journal of Proteome Research*, *9*, 2006–2015.

Ramesh, D., & Brockmann, A. (2019). Mass spectrometric quantification of arousal associated neurochemical changes in single honey bee brains and brain regions. *ACS Chemical Neuroscience*, *10*, 1950–1959.

Rappsilber, J., Mann, M., & Ishihama, Y. (2007). Protocol for micropurification, enrichment, pre-fractionation and storage of peptides for proteomics using StageTips. *Nature Protocols*, *2*, 1896–1906.

Robinson, G. E. (1987). Regulation of honey bee age polyethism by juvenile hormone. *Behavioral Ecology and Sociobiology*, *20*, 329–338. https://doi.org/10.1007/BF00300679

Robinson, G. E. (1992). Regulation of division of labor in insect societies. *Annual Review of Entomology*, *37*, 637–665. https://doi.org/10.1146/annurev.en.37.010192.003225

Ronacher, B. (2008). Path integration as the basic navigation mechanism of the desert ant *Cataglyphis fortis* (Forel, 1902) (Hymenoptera: Formicidae). *Myrmecological News*, *11*, 53–62.

Rössler, W. (2019). Neuroplasticity in desert ants (Hymenoptera: Formicidae) – importance for the ontogeny of navigation. *Myrmecological News*, *29*, 1–20.

Schachtner, J., Wegener, C., Neupert, S., & Predel, R. (2010). Direct peptide profiling of brain tissue by MALDI-TOF mass spectrometry. *Methods in Molecular Biology*, *615*, 129–135.

Schindelin, J., Arganda-Carreras, I., Frise, E., Kaynig, V., Longair, M., Pietzsch, T., Preibisch, S., Rueden, C., Saalfeld, S., Schmid, B., Tinevez, J. Y., White, D. J., Hartenstein, V., Eliceiri, K., Tomancak, P., & Cardona, A. (2012). Fiji: An open-source platform for biological-image analysis. *Nature Methods*, *9*, 676–682. https://doi.org/10.1038/nmeth.2019

Schmitt, F., Vanselow, J. T., Schlosser, A., Kahnt, J., Rössler, W., & Wegener, C. (2015). Neuropeptidomics of the carpenter ant *Camponotus floridanus*. *Journal of Proteome Research*, *14*, 1504–1514.

Schmitt, F., Vanselow, J. T., Schlosser, A., Wegener, C., & Rössler, W. (2017). Neuropeptides in the desert ant *Cataglyphis fortis*: Mass spectrometric analysis, localization, and age-related changes. *The Journal of Comparative Neurology*, *525*, 901–918.

Scholl, C., Wang, Y., Krischke, M., Mueller, M. J., Amdam, G. V., & Rössler, W. (2014). Light exposure leads to reorganization of microglomeruli in the mushroom bodies and influences juvenile hormone levels in the honeybee. *Developmental Neurobiology*, *74*, 1141–1153. https://doi.org/10.1002/dneu.22195

Schoofs, L., de Loof, A., & van Hiel, M. B. (2017). Neuropeptides as regulators of behavior in insects. *Annual Review of Entomology*, *62*, 35–52. https://doi.org/10.1146/annurev-ento-031616-035500

Seid, M. A., & Traniello, J. F. (2005). Age-related changes in biogenic amines in individual brains of the ant Pheidole dentata. *Naturwissenschaften*, *92*, 198–201. https://doi.org/10.1007/s00114-005-0610-8

Shang, Y., Donelson, N. C., Vecsey, C. G., Guo, F., Rosbash, M., & Griffith, L. C. (2013). Short neuropeptide F is a sleep-promoting inhibitory modulator. *Neuron*, *80*, 171–183. https://doi.org/10.1016/j.neuron.2013.07.029

Smith-Unna, R., Boursnell, C., Patro, R., Hibberd, J. M., & Kelly, S. (2016). TransRate: Reference-free quality assessment of de novo transcriptome assemblies. *Genome Research*, *26*, 1134–1144. https://doi.org/10.1101/gr.196469.115

Sterkel, M., Oliveira, P. L., Urlaub, H., Hernandez-Martinez, S., Rivera-Pomar, R., & Ons, S. (2012). OKB, a novel family of brain-gut neuropeptides from insects. *Insect Biochemistry and Molecular Biology*, *42*, 466–473. https://doi.org/10.1016/j.ibmb.2012.03.003

Sterkel, M., Urlaub, H., Rivera-Pomar, R., & Ons, S. (2011). Functional proteomics of neuropeptidome dynamics during the feeding process of *Rhodnius prolixus*. *Journal of Proteome Research*, *10*, 3363–3371.

Sullivan, J. P., Jassim, O., Fahrbach, S. E., & Robinson, G. E. (2000). Juvenile hormone paces behavioral development in the adult worker honey bee. *Hormones and Behavior.*, *37*, 1–14. https://doi.org/10.1006/hbeh.1999.1552

Takeuchi, H., Yasuda, A., Yasuda-Kamatani, Y., Kubo, T., & Nakajima, T. (2003). Identification of a tachykinin-related neuropeptide from the honeybee brain using direct MALDI-TOF MS and its gene expression in worker, queen and drone heads. *Insect Molecular Biology*, *12*, 291–298. https://doi.org/10.1046/j.1365-2583.2003.00414.x

Trede, D., Schiffler, S., Becker, M., Wirtz, S., Steinhorst, K., Strehlow, J., Aichler, M., Kobarg, J. H., Oetjen, J., Dyatlov, A., Heldmann, S., Walch, A., Thiele, H., Maass, P., & Alexandrov, T. (2012). Exploring three-dimensional matrix-assisted laser desorption/ionization imaging mass spectrometry data: Three-dimensional spatial segmentation of mouse kidney. *Analytical Chemistry*, *84*, 6079–6087.

Urlacher, E., Soustelle, L., Parmentier, M. L., Verlinden, H., Gherardi, M. J., Fourmy, D., Mercer, A. R., Devaud, J. M., & Massou, I. (2016). Honey bee allatostatins target galanin/somatostatin-like receptors and modulate learning: A conserved function? *PLoS One*, *11*, e0146248.– https://doi.org/10.1371/journal.pone.0146248

Veenstra, J. A. (2000). Mono- and dibasic proteolytic cleavage sites in insect neuroendocrine peptide precursors. *Archives of Insect Biochemistry and Physiology*, *43*, 49–63.

Veenstra, J. A. (2014). The contribution of the genomes of a termite and a locust to our understanding of insect neuropeptides and neurohormones. *Frontiers in Physiology*, *5*, 454.

Verhaert, P. D., Prieto Conaway, M. C., Pekar, T. M., & Miller, K. (2007). Neuropeptide imaging on an LTQ with vMALDI source: The complete 'all-in-one' peptidome analysis. *International Journal of Mass Spectrometry*, *260*, 177–184. https://doi.org/10.1016/j.ijms.2006.11.008

Verleyen, P., Baggerman, G., Mertens, I., Vandersmissen, T., Huybrechts, J., Van Lommel, A., De Loof, A., & Schoofs, L. (2006). Cloning and characterization of a third isoform of corazonin in the honey bee *Apis mellifera*. *Peptides*, *27*, 493–499. https://doi.org/10.1016/j.peptides.2005.03.065

Wagener-Hulme, C., Kuehn, J., Schulz, D., & Robinson, G. (1999). Biogenic amines and division of labor in honey bee colonies. *Journal of Comparative Physiology A*, *184*, 471–479.

Warner, M. R., Mikheyev, A. S., & Linksvayer, T. A. (2019). Transcriptomic basis and evolution of the ant nurse-larval social interactome. *PLoS Genetics*, *15*, e1008156. https://doi.org/10.1371/journal.pgen.1008156

Wegener, C., Herbert, H., Kahnt, J., Bender, M., & Rhea, J. M. (2011). Deficiency of prohormone convertase dPC2 (AMONTILLADO) results in impaired production of bioactive neuropeptide hormones in Drosophila. *Journal of Neurochemistry*, *118*, 581–595. https://doi.org/10.1111/j.1471-4159.2010.07130.x

Wehner, R. (2009). The architecture of the desert ant's navigational toolkit (Hymenoptera: 1404 Formicidae). *Myrmecological News*, *12*, 85–96.

Winther, A. M., Acebes, A., & Ferrus, A. (2006). Tachykinin-related peptides modulate odor perception and locomotor activity in *Drosophila*. *Molecular and Cellular Neurosciences*, *31*, 399–406. https://doi.org/10.1016/j.mcn.2005.10.010

Wurm, Y., Wang, J., Riba-Grognuz, O., Corona, M., Nygaard, S., Hunt, B. G., Ingram, K. K., Falquet, L., Nipitwattanaphon, M., Gotzek, D., Dijkstra, M. B., Oettler, J., Comtesse, F., Shih, C. J., Wu, W. J., Yang, C. C., Thomas, J., Beaudoing, E., Pradervand, S., … Keller, L. (2011). The genome of the fire ant *Solenopsis invicta*. *Proceedings of the National Academy of Sciences of the United States of America*, *108*, 5679–5684.

Yang, A. (2006). Seasonality, division of labor, and dynamics of colony-level nutrient storage in the ant *Pheidole morrisi*. *Insectes Sociaux*, *53*, 456–462. https://doi.org/10.1007/s00040-005-0896-3

Yang, J., & Caprioli, R. M. (2011). Matrix sublimation/recrystallization for imaging proteins by mass spectrometry at high spatial resolution. *Analytical Chemistry*, *83*, 5728–5734.

Zeng, H., Qin, Y., Du, E., Wei, Q., Li, Y., Huang, D., Wang, G., Veenstra, J. A., Li, S., & Li, N. (2021). Genomics- and peptidomics-based discovery of conserved and novel neuropeptides in the American Cockroach. *Journal of Proteome Research*, *20*, 1217–1228. https://doi.org/10.1021/acs.jproteome.0c00596

Zitnan, D., Zitnanová, I., Spalovská, I., Takác, P., Park, Y., & Adams, M. E. (2003). Conservation of ecdysis-triggering hormone signalling in insects. *Journal of Experimental Biology*, *206*, 1275–1289.

SUPPORTING INFORMATION

Additional supporting information may be found online in the Supporting Information section.

How to cite this article: Habenstein J, Schmitt F, Liessem S, et al. Transcriptomic, peptidomic, and mass spectrometry imaging analysis of the brain in the ant *Cataglyphis nodus*. *J Neurochem*. 2021;00:1–22. https://doi.org/10.1111/jnc.15346

5 Manuscript III: Neuropeptides as potential modulators of behavioral transitions in the ant *Cataglyphis nodus*

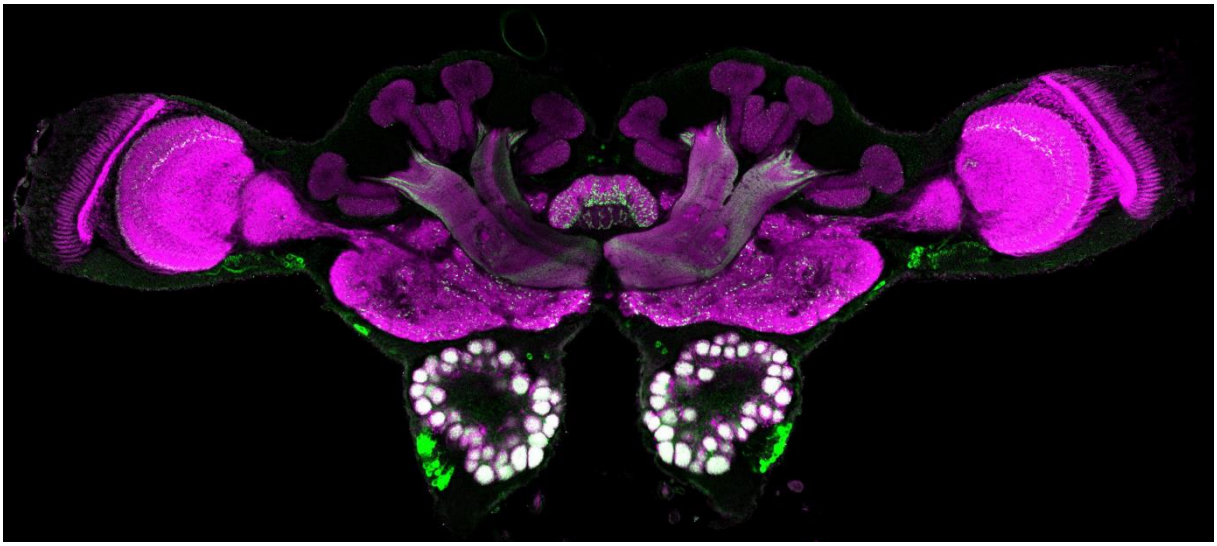

Received: 1 April 2021 | Revised: 26 April 2021 | Accepted: 29 April 2021

DOI: 10.1002/cne.25166

RESEARCH ARTICLE

JCN RESEARCH IN SYSTEMS NEUROSCIENCE THE JOURNAL OF COMPARATIVE NEUROLOGY WILEY

Neuropeptides as potential modulators of behavioral transitions in the ant *Cataglyphis nodus*

Jens Habenstein | **Markus Thamm** | **Wolfgang Rössler**

Behavioral Physiology and Sociobiology (Zoology II), Biocenter, University of Würzburg, Würzburg, Germany

Correspondence
Jens Habenstein and Wolfgang Rössler, Behavioral Physiology and Sociobiology (Zoology II), Biocenter, University of Würzburg, Am Hubland, 97074 Würzburg, Germany.
Email: jens.habenstein@uni-wuerzburg.de (J. H.) and roessler@biozentrum.uni-wuerzburg.de (W. R.)

Funding information
German Research Foundation (DFG), Grant/Award Numbers: INST 93/829-1, DFG Ro1177/7-1

Abstract

Age-related behavioral plasticity is a major prerequisite for the ecological success of insect societies. Although ecological aspects of behavioral flexibility have been targeted in many studies, the underlying intrinsic mechanisms controlling the diverse changes in behavior along the individual life history of social insects are not completely understood. Recently, the neuropeptides allatostatin-A, corazonin, and tachykinin have been associated with the regulation of behavioral transitions in social insects. Here, we investigated changes in brain localization and expression of these neuropeptides following major behavioral transitions in *Cataglyphis nodus* ants. Our immunohistochemical analyses in the brain revealed that the overall branching pattern of neurons immunoreactive (ir) for the three neuropeptides is largely independent of the behavioral stages. Numerous allatostatin-A- and tachykinin-ir neurons innervate primary sensory neuropils and high-order integration centers of the brain. In contrast, the number of corazonergic neurons is restricted to only four neurons per brain hemisphere with cell bodies located in the pars lateralis and axons extending to the medial protocerebrum and the retrocerebral complex. Most interestingly, the cell-body volumes of these neurons are significantly increased in foragers compared to freshly eclosed ants and interior workers. Quantification of mRNA expression levels revealed a stage-related change in the expression of allatostatin-A and corazonin mRNA in the brain. Given the presence of the neuropeptides in major control centers of the brain and the neurohemal organs, these mRNA-changes strongly suggest an important modulatory role of both neuropeptides in the behavioral maturation of *Cataglyphis* ants.

KEYWORDS
allatostatin-A, *Cataglyphis*, corazonin, division of labor, neuropeptides, social insects, tachykinin

Abbreviations: AL, antennal lobe; AMMC, antennal mechanosensory and motor center; Ast-A, allatostatin-A; CA, calyces; CANP, central adjoining neuropils; CB, central body; CBR, cell body rind; CO, collar; Crz, corazonin; CX, central complex; FLA, flange; INP, inferior neuropils; ir, immunoreactive; JH, juvenile hormone; KC, Kenyon cell; LA, lamina; LH, lateral horn; LO, lobula; ME, medulla; MB, mushroom body; NGS, normal goat serum; PBS, phosphate-buffered saline; PED, pedunculus; PER, proboscis extension reflex; PRW, prow; qPCR, quantitative real-time polymerase chain reaction; RCC, retrocerebral complex; SMP, superior medial protocerebrum; sNPF, short neuropeptide F; TK, tachykinin; TRP, tachykinin-related peptide; VG, vitellogenin; VL, vertical lobe; VLNP, ventrolateral neuropils; VMNP, ventromedial neuropils.

1 | INTRODUCTION

Insect societies often comprise large numbers of individuals (Hölldobler & Wilson, 1990; Wilson, 1971), and the organization within social-insect colonies is highly sophisticated and requires a species-specific and flexible task allocation. Some species exhibit distinct polymorphic worker castes devoted to specific tasks, for example, minor and major workers in leaf-cutting ants (Hughes et al., 2003; Wilson, 1980, 1984). However, most social insect species lack task-specific polymorphic worker castes. Instead, individual workers show a high degree of behavioral flexibility and different behavioral phenotypes are rather associated with the age (temporal polyethism) than with a specific morph (Hölldobler & Wilson, 1990; Robinson, 1992; Robinson, 2002). Ants of the genus *Cataglyphis* (Foerster 1850) represent prominent examples for a marked temporal polyethism. *Cataglyphis* workers undergo distinct behavioral transitions. Newly emerged ants (callows), recognizable by their pale and soft cuticle, behave very sluggishly. Then, workers go through several interior phases inside the darkness of the nest. During the first 2 weeks, interior workers (interior I) serve as food storage for the colony (repletes) before they become more active (interior II) and accomplish tasks such as brood care or nest maintenance. The most drastic change, the interior-forager transition, happens after about 4 weeks when the ants leave the nest for the first time (Schmid-Hempel & Schmid-Hempel, 1984; reviewed by Wehner & Rössler, 2013). In order to calibrate their visual navigational systems, the ants first perform learning walks for 2–3 days close to the nest entrance before they finally start to forage solitarily (Fleischmann et al., 2017; Fleischmann et al., 2018; for reviews, see Grob et al., 2019; Rössler, 2019). The interior-forager transition is accompanied by fundamental changes in behavior. Whereas interior workers predominantly rely on olfactory and tactile cues inside the dark nest, foragers navigate on far-ranging foraging trips under bright sunlight mostly using visual compass cues (Ronacher, 2008; reviewed by Wehner & Rössler, 2013; Buehlmann et al., 2014; Huber & Knaden, 2015). The interior-forager transition is associated with high levels of structural synaptic plasticity in two visual pathways of the ants' brains (Grob et al., 2017; Schmitt et al., 2016; Stieb et al., 2010; Stieb et al., 2012). Recently, a detailed atlas of all brain neuropils and major connecting fiber systems in *Cataglyphis nodus* was published (Habenstein et al., 2020). This was complemented by a comprehensive peptidomic analysis of the *C. nodus* brain (Habenstein et al., 2021). Based on this profound knowledge on the behavioral transitions, brain anatomy, neuroplastic changes, and neuropeptide inventory, *C. nodus* ants are well-suited experimental models to address the potential role of neuropeptides in modulating intrinsic mechanisms underlying age-related behavioral plasticity.

Neuropeptides play crucial roles throughout an insect's life. They are involved in physiological and developmental processes and in the modulation of many essential behaviors (for reviews, see Fricker, 2012; Kastin, 2013; Nässel & Zandawala, 2019). Recent studies suggest that the neuropeptides allatostatin-A (Ast-A), tachykinin (TK), and corazonin (Crz) act as regulators of behavioral plasticity in social insects (Gospocic et al., 2017; Han et al., 2021; Pratavieira et al., 2014; Schmitt et al., 2017; Takeuchi et al., 2003). Age-related fluctuations of Ast-A and/or TK have been revealed in honeybees (Pratavieira et al., 2014; Takeuchi et al., 2003) and in the ant *Cataglyphis fortis* (Schmitt et al., 2017). Ast-A is a major regulator of the biosynthesis of juvenile hormone (JH) in many insects (for reviews, see Weaver & Audsley, 2009; Verlinden et al., 2015). However, a clear evidence for an allatoregulatory role is missing in *Cataglyphis*. In honeybees, Ast-A induces shifts in the stress reactivity and modulates appetitive olfactory memory (Urlacher et al., 2016; Urlacher et al., 2019). Ast-A as well as TK-related peptides (TRP) are suspected to further modulate aggressive behavior in bees (Pratavieira et al., 2018). TK signaling modulates locomotion and general activity levels (Kahsai et al., 2010; Winther et al., 2006), olfactory sensitivity (Gui et al., 2017; Jung et al., 2013; Ko et al., 2015; Winther et al., 2006), and nociception (Im et al., 2015). Although most of these studies were conducted in *Drosophila*, the similarities in the location of tachykinergic neurons in the antennal lobes (ALs) and the central complex (CX) may indicate similar functions in *Cataglyphis* (Habenstein et al., 2021; Schmitt et al., 2017). Whereas TK and Ast-A have been suggested to be involved in behavioral transitions in closely related *C. fortis* (Schmitt et al., 2017), Crz remained largely neglected in previous studies. Crz is a highly conserved neuropeptide and omnipresent in most insect species (Predel et al., 2007). In *Drosophila*, the endocrine corazonergic pathway is known to alter stress responses and metabolism (Johnson, 2017; Kapan et al., 2012; Kubrak et al., 2016; Zandawala et al., 2021). In addition, Crz signaling is important for the development of moth larvae (Kim et al., 2004; Tanaka, Hua, et al., 2002) and induces morphological changes in locusts, which are associated with behavioral transitions (Maeno et al., 2004; Sugahara et al., 2018; Tanaka, Zhu, et al., 2002; Tawfik et al., 1999). The effect of Crz on developmental processes is not restricted to insects, as similar effects of Crz on growth and maturation could be found in bristle worms (Andreatta et al., 2020). Gospocic et al. (2017) suggested that Crz is an important regulator of the sexual and behavioral differentiation in the ponerine ant *Harpegnathos saltator*. Higher Crz levels were found in workers compared to queens (or pseudoqueens). Moreover, worker-specific hunting behavior could be induced by experimental increase of Crz levels.

In the present study, we investigated the spatial expression patterns of Ast-A, TK, and Crz in callows, interior workers, and foragers of the ant *C. nodus*. We compared general innervation patterns and cell body volumes of peptidergic neurons across different behavioral stages using immunohistochemistry. In addition, we analyzed the mRNA levels of the three neuropeptides in the brain. The results show that expression levels and soma sizes particularly of Ast-A and Crz relate to the behavioral stage. This strongly suggests the involvement of these neuropeptides as modulators during behavioral maturation of *Cataglyphis* workers.

2 | MATERIALS AND METHODS

2.1 | Animals

C. nodus nests were located in the Strofylia National Park, Greece (38°15′N, 21°37′E). To be able to differentiate foragers from interior workers with high accuracy, foragers were marked outside the nest

using acrylic paint (Motip Lackstift Acryl, MOTIP DUPLI GmbH, Haßmersheim, Germany) over at least three consecutive days before the nests were excavated. Afterward, all unmarked animals were considered to be either interior workers or callows. Callows were discriminated from interior workers by their pale cuticle. To ensure that callows and interior workers were never exposed to sunlight, the nest was excavated during night using red light. After excavation, the ants were kept in complete darkness in large plastic boxes with permanent access to water and honey water. Animals of different behavioral stages were collected arbitrarily out of the boxes and brains were dissected within 30 h after nest excavation. Dissections of the brains from ants of different behavioral stages were pseudo-randomized to avoid effects of potential daytime-dependent changes of neuropeptide expressions.

For the expression analyses, ant colonies were transferred to the University of Würzburg. In the laboratory, the ants were kept in a dark cabinet within a climate chamber at a constant temperature (28°C) and relative humidity (30%). The colonies had permanent access through a light trap connection into a foraging arena with a 12 h/12 h day/night cycle. During the 12-h light cycle, light was generated by UV-emitting fluorescent tubes (Repti Glo 2.0/10.0, Exo Terra, Holm, Germany). In the foraging arena, the animals had an infinite supply of water and were fed with honey water (1:2) and dead arthropods twice a week. The animals were allowed to acclimate for 48 h. Thereafter, all ants in the foraging arena were marked on three consecutive days and considered as foragers. In the following, all unmarked ants were classified as interior workers since no callows had remained in the colony after the transport to Würzburg.

2.2 | Primary antibodies

For immunolabeling, the following primary antibodies were used: anti-Ast-A (*H. Agricola*, Jena BioScience, Jena, Germany); anti-Crz (J.A. Veenstra, Université Bordeaux I, Bordeaux, France); anti-TK (LemTRP-1, D.R. Nässel, Stockholm University, Stockholm, Sweden); and anti-synapsin (SYN-ORF1, E. Buchner, University of Würzburg, Germany) (Table 1).

The polyclonal anti-Ast-A antibody was raised in rabbit and conjugated to thyroglobulin with glutaraldehyde. The specificity of the antiserum has been verified by a competitive enzyme-linked immunosorbent assay (ELISA) (Vitzthum et al., 1996) and its affinity was demonstrated in diverse insect species (e.g., Carlsson et al., 2013; Kahsai & Winther, 2011; Kreissl et al., 2010) including *Cataglyphis* ants (Schmitt et al., 2017).

The polyclonal Crz antiserum was raised in rabbit and coupled to bovine serum albumin. The specificity of the antibody was characterized by ELISA (Veenstra, 1991; Veenstra & Davis, 1993). The antibody was used to study the immunoreactivity to Crz in different arthropods (e.g., Hansen et al., 2001; Hou et al., 2017; Roller et al., 2003).

The polyclonal antibody to TK was raised in rabbit, conjugated to bovine serum albumin, and the specificity was characterized by preabsorbing with synthetic *Leucophaea maderae* TRP-1 (Winther & Nässel, 2001). The antibody has been used for immunohistochemistry in various insects (e.g., Kahsai & Winther, 2011; Neupert et al., 2012; Siju et al., 2014; Winther et al., 2003) including *Cataglyphis* (Habenstein et al., 2021; Schmitt et al., 2017).

To visualize synapse-rich neuropils, we used a monoclonal antibody to synapsin. The presence of synapsin in most synaptic terminals is highly conserved across invertebrate species (Hofbauer et al., 2009; Klagges et al., 1996). The antibody was raised in mice against fusion proteins of glutathione-*S*-transferase and *Drosophila* SYN1 protein (Klagges et al., 1996). The specificity has been verified in *Drosophila* (Godenschwege et al., 2004; Klagges et al., 1996) and in the honeybee *Apis mellifera* (Pasch et al., 2011). The antiserum was used for a variety of neuroanatomical studies in diverse arthropods (e.g., Groh & Rössler, 2011; Heinze & Reppert, 2012; Immonen et al., 2017; von Hadeln et al., 2018) including *Cataglyphis* ants (Habenstein et al., 2020; Schmitt et al., 2016; Schmitt et al., 2017; Stieb et al., 2012).

2.3 | Immunohistochemistry

Animals were anesthetized on ice and decapitated under red light. The head capsule was opened between the compound eyes and the

TABLE 1 Primary antibodies

Antibody	Immunogen	Manufacturer; species; clonality; Cat #; RRID	Dilution
Allatostatin-A	APSGAQRLYGFGLa coupled to thyroglobulin	H.J. Agricola, Jena BioScience, Jena, Germany; rabbit; polyclonal; Cat # Ast-A, RRID:AB_2313972	1:2000
Corazonin	pQTFQYSRGWTNa coupled to bovine serum albumin	J.A. Veenstra, Université Bordeaux I, Bordeaux, France; rabbit; polyclonal; Cat # anti-corazonin, RRID: AB_2532101	1:1000
Synapsin	*Drosophila* Synapsin glutathione-*S*-transferase fusion protein	E. Buchner, Theodor-Boveri-Institute, University of Würzburg, Germany; mouse; monoclonal; Cat # 3C11 (SYNORF1); RRID: AB_528479	1:50
Tachykinin	APSGFLGVRa coupled to bovine serum albumin	D.R. Nässel, Stockholm University; Stockholm; Sweden; rabbit; polyclonal; Cat # LemTRP-1, RRID: AB_2315469	1:2500

brain was covered with ice-cold physiological ant saline (126.6 mM NaCl, 6.7 mM KCl, 1.5 mM $CaCl_2$, 0.8 mM Na_2HPO_4, 0.4 mM KH_2PO_4, 4.8 mM TES, and 3.2 mM trehalose; pH 7.0). The brains were removed and fixated in 4% formaldehyde in phosphate-buffered saline (PBS) overnight at 4°C. Thereafter, the brains were rinsed in PBS (3 × 10 min), stored in PBS in the dark at 4°C for up to 3 days, and subsequently transferred in a cooler to Würzburg. In Würzburg, samples were stored at 4°C until further processing for up to two more days. To facilitate the penetration of the antibodies, the brains were treated with PBS containing Triton-X (PBST; 2% PBST for 10 min, 0.5% PBST for 3 × 10 min). Subsequently, the brains were preincubated in 0.5% PBST with 2% normal goat serum (NGS) for 1 h at 4°C before the brains were incubated in the primary antibody solution (2% NGS in 0.5% PBST, either Ast-A, Crz or TK, dilution see Table 1) for 4 days at 4°C. After rinsing in PBS (3 × 10 min), the brains were transferred into the anti-synapsin antibody solution (2% NGS in 0.2% PBST, Table 1) to incubate for another 4 days at 4°C. Thereafter, brains were again rinsed in PBS (3 × 10 min) followed by incubation in the secondary antibodies Alexa Fluor 488 goat anti-rabbit (1:250; RRID: AB_143165, Thermo Fisher Scientific, Waltham, MA) and CF633 goat anti mouse (1:250; Biotrend Chemikalien GmbH, Köln, Germany) in PBS containing 1% NGS for 3 days at 4°C. Brains were washed in PBS (3 × 10 min), dehydrated through an ascending ethanol series (30, 50, 70, 90, 95, 100, and 100% for 10 min each step) and finally cleared in methyl salicylate (M-2047; Sigma Aldrich, Steinheim, Germany).

2.4 | Laser scanning confocal microscopy, image processing, and data analysis

Imaging of the brain samples was performed with a confocal laser scanning microscope (Leica TCS SP8, Leica Microsystems AG, Wetzlar, Germany). For scans of the whole brain, we used a 20× glycerol immersion objective (Leica HC PL APO 20.0 × 0.75 NA) with a step size of 5 µm in z-direction. For detailed scans of individual brain regions or neurons, we used a 63× glycerol immersion objective (Leica HCX PL APO 63.0 × 1.3 NA) with a step size of 1 µm in z-direction. All image stacks were scanned at a resolution of 1024 × 1024 pixels and processed using ImageJ (ImageJ 1.52p; Wayne Rasband, NIH, Bethesda, MD) and CorelDRAW X8 (Version 20.0.0.633, Corel Corporation, Ottawa, Canada). To improve the quality of images, contrasts were adjusted in ImageJ if necessary. For volume calculations of Crz positive cell bodies, image stacks were analyzed using the software Amira 2019.1 (FEI, Visualization Sciences Group, Hillsboro, OR; http://thermofisher.com/amira-avizo). The step size of the z-axis was corrected according to deviations caused by the immersion medium (1.05 for glycerol). The cell bodies of interest were manually labeled in each layer of the image stack. Thereafter, the three-dimensional structure was reconstructed, and the volume was measured applying the respective tools of the Amira software. To compare the volumes of the corazonergic somata between different brains, we averaged the volume of all corazonergic cell bodies of each brain hemisphere. In some cases (8 out of 65 brains), the cell bodies of one hemisphere were damaged or the quality of confocal images was not sufficient for analyzing the volumes. In those cases, we used only the volume of the corazonergic somata of one hemisphere.

2.5 | RNA extraction and cDNA synthesis

- *Preparation in Greece*: Ants were chosen arbitrarily from the colony according to their behavioral stage. Then, ants were anesthetized on ice, the head was removed, and a small window was cut into the head capsule to allow the penetration of RNAlater stabilization solution (Thermo Fisher Scientific) into the brain tissue. The samples were stored in the RNAlater solution in the dark at 4°C for up to 3 days before they were transferred in a cooler to Germany.
- *Preparation in the laboratory*: Ants were collected arbitrarily from the colony according to their behavioral stage and immediately snap-frozen in liquid nitrogen. Samples were stored in a freezer at −80°C until the brain was dissected.

All brains were dissected in RNAlater solution, transferred into a reaction tube and snap-frozen in liquid nitrogen. Samples were stored at −80°C until RNA extraction. For RNA extraction, the brains were homogenized in 750 µl TriFast (peqGOLD, VWR, Radnor, PA) with the TissueLyzer LT (QIAGEN, Venlo, Netherlands) at 40 Hz for 3 min using stainless steel beads (5 mm). After 5 min incubation, 150 µl chloroform was added and mixed with the solution. Subsequently, the samples were centrifuged, and the aqueous phase was transferred in a perfectBind RNA column (peqGOLD total RNA Kit, VWR). Further RNA extraction was carried out according to the manufacturer instructions of the peqGOLD total RNA kit. RNA was resolved in H_2O and precipitated with 4 M lithium chloride and ethanol at 4°C overnight. After centrifugation, the RNA pellet was washed with ethanol and dissolved in H_2O adjusted to the respective RNA concentration.

Synthesis of the cDNA was performed using the QuantiTect Reverse Transcription Kit (QIAGEN). About 500 ng of the RNA (in 8 µl H_2O) were mixed with the buffer solution (2 µl gDNA wipeout buffer in 4 µl H_2O) and preincubated for 2 min at 42°C. Thereafter, 1 µl Quantiscript reverse transcriptase (RT), 4 µl Quantiscript RT buffer, and 1 µl RT primer mix were added and the solution was incubated at 42°C for 15 min before the reaction was terminated at 95°C for 3 min. The cDNA solution was cooled at 4°C and 30 µl H_2O was added before the samples were stored at −20°C until usage.

2.6 | Quantitative real-time polymerase chain reaction

Quantitative real-time polymerase chain reaction (qPCR) analysis was performed using Rotor Gene Q (Qiagen, Hilden, Germany). Genes of interest and the reference gene were analyzed in duplex runs. Primer and TaqMan probes (TIB MOLBIOL, Berlin, Germany) used for qPCR are listed in Table 2. Each individual sample was analyzed in triplicates. Each reaction contains 5 µl cDNA, 10 µl Biozym Blue Probe qPCR Mix

(Biozym Scientific GmbH, Hessisch Oldendorf, Germany), 0.4 μl of each primer (each 20 μM) and TaqMan probe (each 10 μM), and 2.4 μl water. Initial denaturation was performed at 95°C for 2 min. Thereafter, 40 cycles including denaturation (95°C for 5 s) and annealing/extension (60°C for 30 s) phases were carried out. Neuropeptide expression levels were determined relative to transcripts of elongation factor-1 alpha (EF1 α) using the ΔΔCt method. EF1 α was shown to be a suitable reference gene in brains of honeybees (Lourenço et al., 2008; Reim et al., 2013) and several ant species (Moreira et al., 2017; Ratzka et al., 2011). Therefore, we decided to use this gene in *C. nodus*. We calculated and compared the absolute copy number of EF1a. Here, we observed no differences ($p_{Greece} = 0.59$, $\chi^2 = 1.056$, Kruskal–Wallis test; $p_{lab} = 0.432$, $Z = 0.893$, $U = 23.00$, Mann–Whitney *U* test) in all data sets and thus, defined this gene as stable.

2.7 | Statistical analyses

Statistical analyses were performed using SPSS statistic software package (IBM Corp.; IBM SPSS Statistics for Windows, Version 25.0.0.1, Armonk, NY). Normality was tested using the Shapiro–Wilk-test. As not all data sets were normally distributed, we used nonparametric tests for all statistical analyses. Data sets with more than two groups were tested by using the Kruskal–Wallis test ($\alpha = .05$). To analyze significant differences between the groups, post hoc pairwise comparisons were performed using the Mann–Whitney *U* test with Bonferroni correction. For all data sets with two behavioral groups, we used the Mann–Whitney *U* test ($\alpha = .05$).

2.8 | Nomenclature

We followed the unified nomenclature rules for insect brains (Ito et al., 2014). To identify neuropils of the central brain, we used the three-dimensional atlas of the *C. nodus* brain as a reference (Habenstein et al., 2020) (see also https://www.insectbraindb.org to access 3D reconstructions of the *C. nodus* brain).

3 | RESULTS

3.1 | Ast-A, Crz, and TK immunoreactivity in *Cataglyphis* workers

To compare the localization of neuropeptides in *Cataglyphis* brains across different behavioral stages, we used immunohistological stainings with antibodies specific for Ast-A, Crz, and TK. Close visual inspection did not reveal any obvious differences in the general distribution and branching patterns of Ast-A-, Crz-, and TK-like immunoreactivity (Ast-A-ir, Crz-ir, and TK-ir) among callows, interior workers, and foragers. Across all three behavioral stages, Ast-A-ir is localized in numerous neurons of the brain with arborizations in important primary sensory neuropils such as the AL and the optic lobes (OL, Figure 1(a,f)). We found Ast-A-ir scattered across the entire volumes of virtually all AL glomeruli (Figure 1(a,d)). In the lobula (LO) and medulla (ME), Ast-A-ir neurons are only present in very distinct neuropil layers. In contrast, branches of Ast-A-ir neurons were found across the entire lamina neuropil (Figure 1(f)). Ast-A-ir is also present in prominent high-order integration centers of the brain (Figure 1(a–c,e)). Ast-A-ir neurons innervate the central body (CB), but not the protocerebral bridge and the noduli. Ast-A-ir was present in different subunits of the mushroom body (MB) such as the pedunculus (PED), the collar (CO), and a subset of extrinsic MB neurons of the vertical lobe (VL, Figure 1(a–c,e)). The neurons arborizing in the VL project into the protocerebral-calycal tract (PCT, Figure 1(b)). In honeybees, the neurons of the PCT provide GABAergic feedback to the MB calyces (Grünewald, 1999; Haehnel & Menzel, 2010). Our staining revealed Ast-A-ir neurons also beyond the major neuropils in brain regions with less

TABLE 2 Oligonucleotides used for quantitative real-time PCR

Name	Direction	Sequence	Concentration (μM)
Allatostatin-A	Sense	5′-TTCCCTATGCCGAACCTGTA-3′	20
	Antisense	5′-ATAGCGAGGATAAACGGACG-3′	20
	TM	5′-Cy5-CCGATACCGAACGAGAACGGTCG-BBQ-3′	10
Corazonin	Sense	5′-AACGGTGATCTCAACAGACTGAA-3′	20
	Antisense	5′-GGATTATCAGCGGTTGTTCGTC-3′	20
	TM	5′-YAK-ATGCTGATACACGGAAGCACCGAC-BBQ-3′	10
Elongation factor-1 alpha	Sense	5′-CCAGGACAGATCAGCAACG-3′	20
	Antisense	5′-TCCTTAATCTCGGCGAACTTG-3′	20
	TM	5′-6FAM-ACCGGTTCTCGATTGCCATACCG-BBQ-3′	10
Tachykinin	Sense	5′-GGTACTCGCGGCAAGTTGAA-3′	20
	Antisense	5′-CCTCTCATGCCCTGAAAACC-3′	20
	TM	5′-YAK-CTCGTCGAGCAATGATTTCCTTGCCT-BBQ-3′	10

Abbreviation: PCR, polymerase chain reaction.

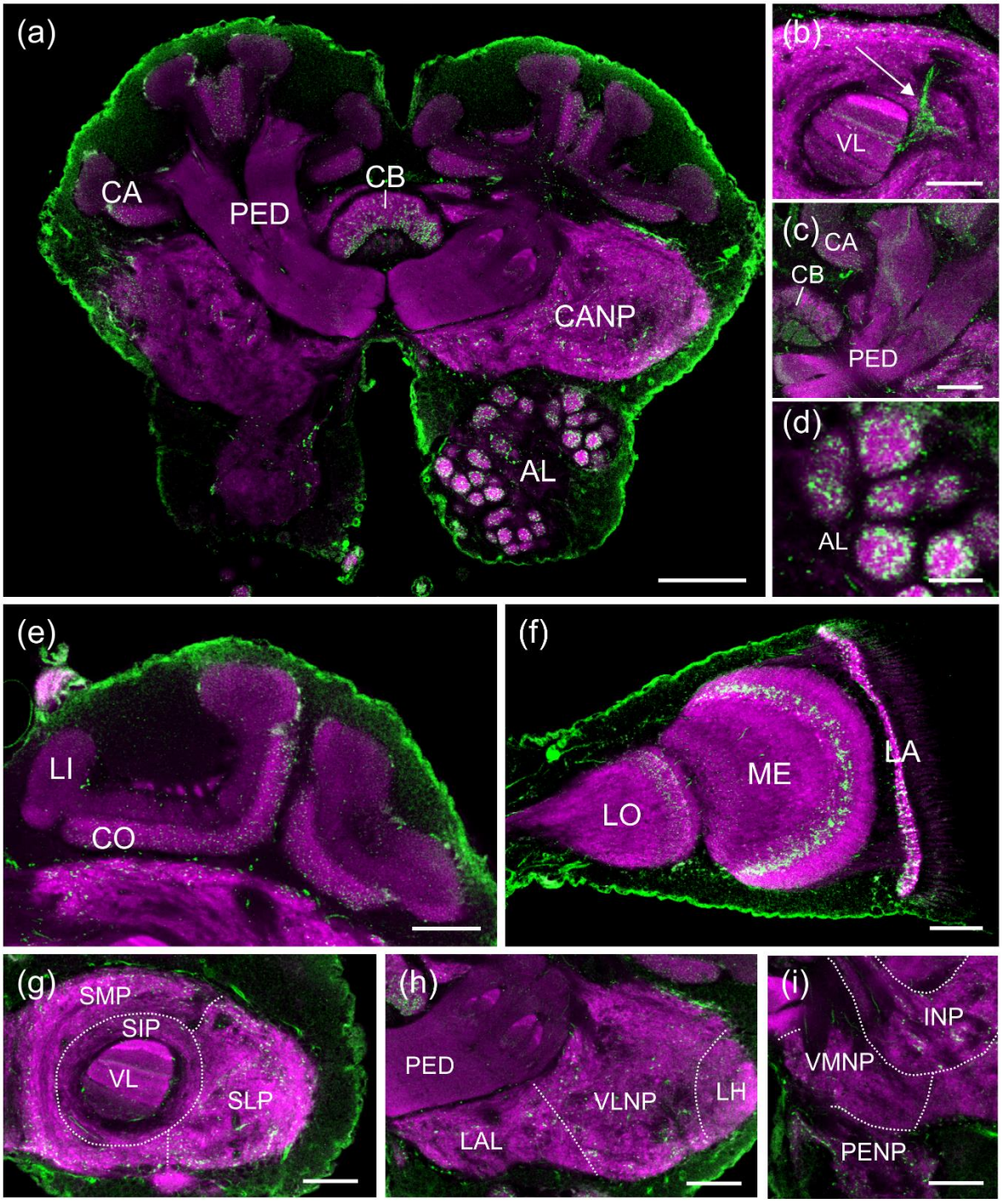

FIGURE 1 Immunofluorescence staining of allatostatin-A (Ast-A; green) and synapsin (magenta) in *Cataglyphis nodus* brain. (a) Overview of Ast-A-immunoreactivity (−ir) in the central brain. Ast-A-ir neurons are present in the central body (CB), the collar (CO) of the mushroom body calyx (CA), the antennal lobes (AL), and across the central adjoining neuropils (CANP). (b) The vertical lobe (VL) is innervated by a layer of Ast-A positive neurons. Ast-A-ir neurons connect the VL with the CA by the protocerebral-calycal tract (white arrow; z-projection from a stack of four optical sections, 5 μm step size). (c) Pattern of Ast-A-ir in the pedunculus (PED). (d) Higher magnification image of the Ast-A-ir distribution in the AL glomeruli. (e) Ast-A-ir in the CA. Ast-A innervation of the CA was restricted to the visual CO and absent in the lip (LI). (f) Overview of Ast-A-ir in the optic lobes. Lobula (LO), medulla (ME), and lamina (LA) are innervated by a layer of Ast-A-ir neurites. (g–i) Ast-A-ir in the CANP. (g) Ast-A-ir is present in all superior neuropils which consist of superior lateral protocerebrum (SLP), the superior intermediate protocerebrum (SIP), and the superior medial protocerebrum (SMP). (h) Pattern of Ast-A-ir in the lateral accessory lobe (LAL), the ventrolateral neuropils (VLNP), and the lateral horn (LH). (i) Ast-A-ir in the inferior neuropils (INP), the periesophageal neuropils (PENP), and the ventromedial neuropils (VMNP). Scale bars = 100 μm (a); 50 μm (b,c,e–i); and 20 μm (d) [Color figure can be viewed at wileyonlinelibrary.com]

distinct boundaries, known as central adjoining neuropils (CANP) (Habenstein et al., 2020). Our detailed brain atlas (Habenstein et al., 2020) enabled us to assign branching patterns to neuropils within central brain regions that have not been accessible in a previous study on Ast-A neurons in the closely related ant *C. fortis* (Schmitt et al., 2017). In particular, Ast-A-ir is present in the lateral accessory lobe, the superior neuropils (SNP), the inferior neuropils, the ventrolateral neuropils (VLNP), the lateral horn (LH), and less pronounced also in more posterior neuropils, such as in the ventromedial neuropils (VMNP) and the periesophageal neuropils (Figure 1(a,g–i)). We found no Ast-A-ir in the antennal mechanosensory and motor center (AMMC). Numerous cell bodies of the Ast-A-ir neurons are dispersed across the entire cell body rind (CBR). The distribution of TK-ir neurons did not reveal any obvious differences between the three behavioral stages. Similar to the Ast-A-ir, innervation by numerous TK-ir neurons was present in major sensory input regions, high-order processing centers and extensively in the CANP (Figure 2). We found very dense TK-ir across the entire volume of virtually all AL glomeruli (Figure 2(a,c)). In the ME and LO, TK-ir is present only in distinct layers. However, in contrast to the Ast-A-ir pattern, we found no TK-ir in the LA (Figure 2(d)). Similar to the pattern found in Ast-A-ir neurons in the CX, TK-ir is restricted to the CB and absent in the protocerebral bridge and noduli. The PED is intensely innervated by TK-ir neurons, which is reflected in labeling of multiple layers in the MB VL (Figure 2(a,b)). TK-ir was found in very prominent ventral and several distinct dorsal layers of the VL (Figure 2(b,f)). In the honeybee, the ventralmost layer is known as the gamma lobe receiving input from Type II (clawed) Kenyon cells (KCs) and more dorsal layers include terminal branching areas of Type I (spiny) KCs with dendritic arborizations in visual and olfactory parts of the MB calyx (Strausfeld, 2002). By contrast, Ast-A-ir neurons are not present in the gamma lobe and innervate only a single dorsal layer of the VL (Figure 1(b)). As we did not find any Ast-A- and TK-ir in KC cell bodies, we assume that all labeling within the MB neuropil is from MB extrinsic neurons. Another difference of both neuropeptide distributions was visible in posterior CANPs. We found more arborizations of TK-ir neurons in these regions including dense innervation of the AMMC (Figure 2(e)). Similar to Ast-A, numerous TK-ir cell bodies distribute all across the entire CBR. A particularly prominent cluster of TK positive cell bodies is present in the lateral cluster of AL neurons (Figure 2(c)).

In contrast to the labeling of Ast-A and TK, Crz-ir neurons show very different and distinct branching patterns. They are restricted to a very small number of neurons forming a tight cluster in each brain hemisphere. Each cluster consists of four cell bodies, located in the pars lateralis (Figure 3(a,d)), a region housing neurosecretory cells in insects (Veelaert et al., 1998; Siegmund & Korge, 2001; reviewed by Raabe, 2012). The Crz-ir neurons extend projections into the superior medial protocerebrum (SMP) and the flange (FLA, Figure 3(a–c)). In addition, one axon bundle per hemisphere projects into the ipsilateral retrocerebral complex (RCC, Figure 3(c,e,f)), a major neurohemal organ in insects (Gade et al., 1997; Predel, 2001). The rest of the central brain, including sensory input regions and high-order processing and integration sites, did not show any Crz-ir. Like the other two neuropeptides, Crz-ir neurons did not exhibit obvious differences in their branching patterns between callows, interior workers, and foragers.

Despite consistent general branching patterns of Ast-A-, TK-, and Crz-ir neurons in ants of different behavioral stages, we analyzed potential differences in the volume of cell bodies. This was possible in the case of Crz-ir neurons due to the relatively large size of the cell bodies and their small overall number. We reconstructed the three-dimensional structure of the four Crz-ir somata in callows, interior workers, and foragers to compare their volumes. Foragers displayed significantly larger Crz-ir somata than callows ($p < .001$, $Z = 4.424$, $\chi^2 = 20.345$) and interior workers ($p < .001$, $Z = 4.422$, $\chi^2 = 19.417$, Figure 4). To exclude seasonal or colony related factors, the experiment was repeated for interior workers and foragers from another *C. nodus* colony at a different time of the year (June instead of August). Likewise, corazonergic cell-body volumes were significantly ($p < .001$, $Z = 3.971$, $U = 151.0$) larger in foragers (mean volume $9.22 \pm 2.28 \times 10^3$ µm, $n = 13$) compared to interior workers (mean volume $= 4.97 \pm 1.11 \times 10^3$ µm, $n = 12$, data not shown).

3.2 | Quantitative real-time PCR comparison of neuropeptide mRNA expression

To investigate potential differences at the level of gene expression, we compared the mRNA expression levels of TK, Ast-A, and Crz in ants of the three behavioral stages. To measure mRNA levels as close to the natural conditions as possible, we conducted the experiments on ants collected in their natural habitat within the Strofylia National Park (Greece). This revealed neuropeptide-specific differences between mRNA expression levels in the three behavioral stages (Figure 5). Ast-A mRNA expression was significantly lower in interior workers compared to both callows ($p = .047$, $Z = 2.414$, $\chi^2 = 11.00$) and foragers ($p = .005$, $Z = 3.12$, $\chi^2 = 12.542$, Figure 5(a)). In contrast, TK mRNA expression levels remained stable throughout the different behavioral stages ($p = .788$, $\chi^2 = 0.477$, Figure 5(b)). The largest change in relative mRNA expression levels was found for Crz with more or less similar expression levels in callows and interior workers ($p = 1.00$, $Z = 0.864$, $\chi^2 = 3.938$), but a significant increase in foragers compared to callows ($p = .002$, $Z = 3.433$, $\chi^2 = 16.50$) and interior workers ($p = .005$, $Z = 3.124$, $\chi^2 = 12.562$). Interestingly, the median of the relative expression value for Crz in foragers is almost twice as high as in the other behavioral stages (Figure 5(c)).

To minimize artificially generated errors (e.g., changed mRNA production caused by stress during excavation of the nest), we repeated the experiment using the same colony after it was transferred to constant conditions in our climate chamber in Würzburg. Since no more callows were present in the colony after this transition, only interior workers and foragers were used for this part of the expression analysis. The analyses confirmed all results from the measurements under natural colony conditions. Foragers and interior workers displayed similar TK expression levels ($p = .876$, $Z = 0.244$, $U = 19.00$). In contrast, both Crz ($p = .018$, $Z = 2.355$, $U = 32.00$) and Ast-A ($p = .018$, $Z = 2.355$, $U = 3.00$) expression was significantly higher in foragers compared to interior workers with Crz showing the highest difference in expression levels (Figure 6).

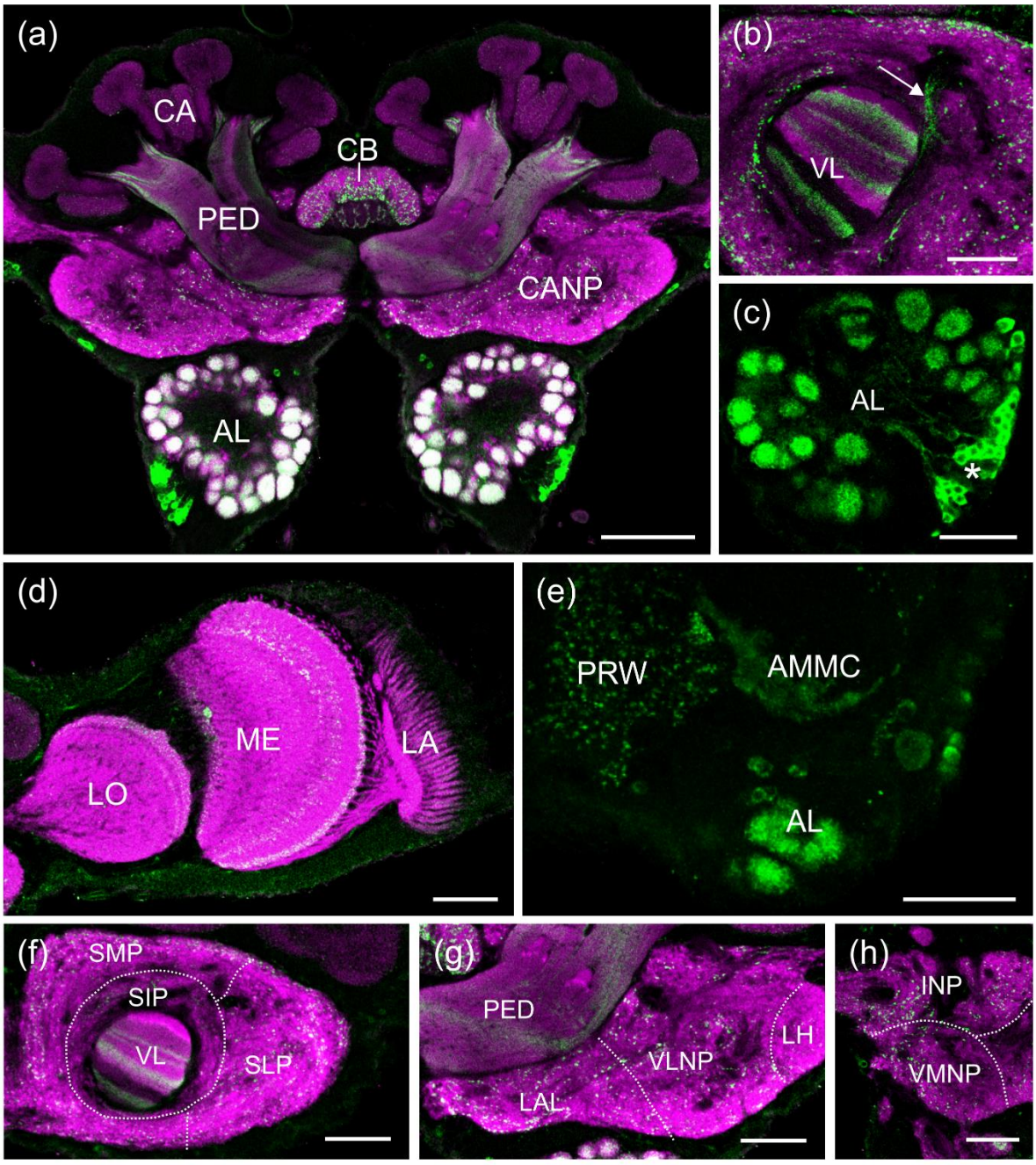

FIGURE 2 Immunofluorescence staining of tachykinin (TK; green) and synapsin (magenta) in the *Cataglyphis* brain. (a) Overview of TK-immunoreactivity (−ir) in the central brain. Innervation of TK-ir neurons was found in the upper and lower unit of the central body (CB), the pedunculus (PED), the antennal lobes (AL), and the central adjoining neuropils (CANP). (b) TK-ir neurons innervate several layers of the vertical lobe (VL) and project into the protocerebral-calycal tract (white arrow). (c) Dense pattern of TK-ir throughout AL glomeruli. Numerous TK-ir cell bodies (asterisk) in the lateral cluster of AL neurons project into all glomeruli of the AL. (d) TK-ir in the lobula (LO) and medulla (ME) of the optic lobes. No staining was found in the lamina (LA). (e–h) TK-ir in the CANP. (e) TK-ir in the periesophageal neuropils (z-projection of six optical sections, 5 μm step size). TK-ir was found in the antennal mechanosensory and motor center (AMMC) and the prow (PRW). (f) TK is present in all superior neuropils (SNP) and the VL. The SNP comprise the superior lateral protocerebrum (SLP), the superior intermediate protocerebrum (SIP), and the superior medial protocerebrum (SMP). (g) TK-ir is present in the in the lateral accessory lobe (LAL), the ventrolateral neuropils (VLNP), and the lateral horn (LH). (h) TK-ir neurons innervate the inferior neuropils (INP) and the ventromedial neuropils (VMNP). Scale bars = 100 μm (a) and 50 μm (b–h). CO, collar [Color figure can be viewed at wileyonlinelibrary.com]

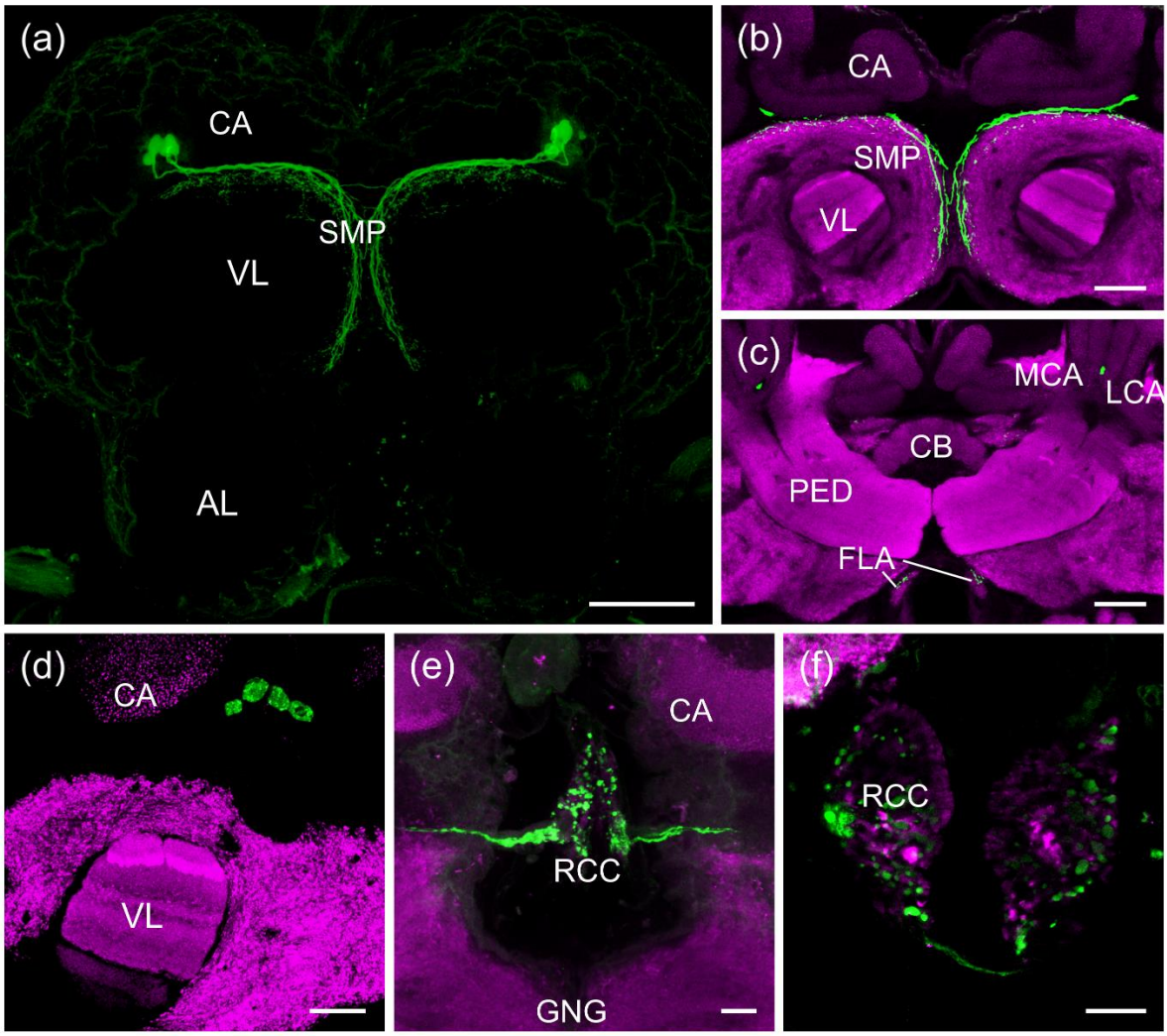

FIGURE 3 Corazonin-immunoreactivity (Crz-ir, green) in the brain of *Cataglyphis nodus*. Anti-synapsin (magenta) highlights synapse-rich brain neuropils. (a) Crz-ir in the anterior part of the central brain (z-projection of 18 optical sections, step size 5 μm). Each brain hemisphere contains a cluster of four corazonergic somata in the region of the pars lateralis. Crz-ir neurons project into the medial protocerebrum. (b) Innervation pattern of Crz-ir neurons in the superior medial protocerebrum (SMP). (c) Crz-ir neurons project into the flange (FLA). One neuron bundle per hemisphere runs in between the medial (MCA) and lateral calyx (LCA) of the mushroom bodies to posterior brain regions (z-projection from 3 optical sections, 5 μm step size). (d) Typical cluster of the total of four somata in the region of the pars lateralis (z-projection of three optical sections, 2 μm step size). (e) Crz-ir neurons leave the posterior brain and project into the retrocerebral complex (RCC) (z-projection of 22 optical images, 1 μm step size). (f) Pattern of Crz-ir in the RCC. Scale bars = 100 μm (a); 50 μm (b,c); and 25 μm (d–f). AL, antennal lobes; CB, central body; GNG, gnathal ganglion; PED, pedunculus; VL, vertical lobe [Color figure can be viewed at wileyonlinelibrary.com]

4 | DISCUSSION

4.1 | Distribution of Ast-A, TK, and Crz in the *Cataglyphis* brain

Ast-A and TK belong to the most abundant neuropeptides in the *Cataglyphis* brain. Both have multiple paracopies within the respective prepropeptide (Habenstein et al., 2021) and, as shown in our present work, extensively innervate major portions of the ant's brain, with differences in individual neuropils as described in the results section. They are present in high-order processing centers as well as in major visual, antennal mechanosensory, and olfactory neuropils (Figures 1 and 2) which is in line with previous studies in the closely related ant *C. fortis* (Schmitt et al., 2017) and with data from mass spectrometric analyses in *C. nodus* (Habenstein et al., 2021). Both TK- and Ast-A-ir neurons innervate the CB of the CX. The CX is implicated in processing sky-polarization information in various insects (reviewed by Homberg et al., 2011; el Jundi et al., 2014) and plays a role in path

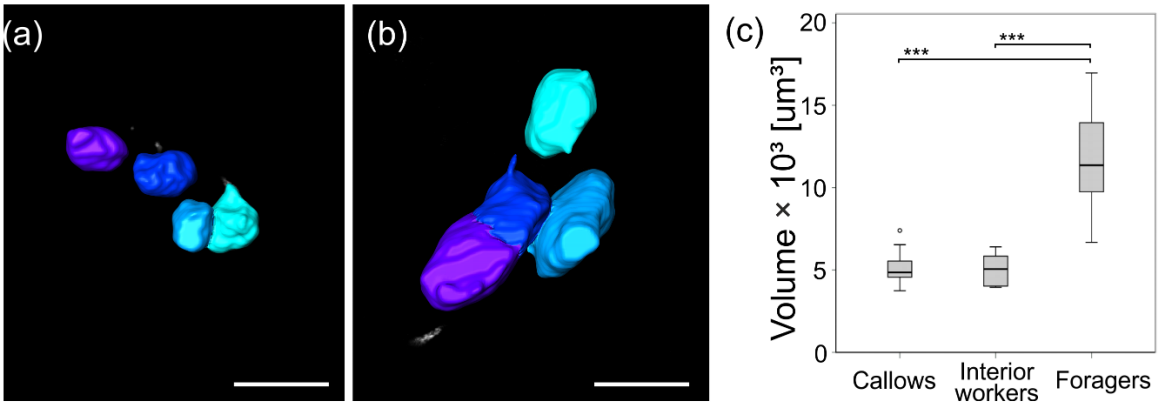

FIGURE 4 Volumes of corazonergic somata increase during behavioral maturation of *Cataglyphis* ants. Colors of individual cell bodies were assigned randomly in (a) and (b). (a) Example of a three-dimensional reconstruction of the corazonin-immunoreactive (Crz-ir) cell bodies of one brain hemisphere of an interior worker. (b) Example of a three-dimensional reconstruction of Crz-ir cell bodies of one brain hemisphere of a forager. (c) Volume changes of corazonergic cell bodies in the pars lateralis of callows ($n = 14$), interior workers ($n = 14$), and foragers ($n = 12$). The average volume of the somata is significantly increased in foragers. In c), volumes have been calculated from the four corazonergic cell bodies per hemisphere. Volumes of cell bodies in the two brain hemispheres were averaged. Boxes indicate 25th and 75th percentiles and the solid line represents the median of the data. Whiskers extend to all data points within 1.5 times of the interquartile length from the median. Outliers are shown as circle. For statistics, Kruskal–Wallis test with Bonferroni correction was used. Significant different data are indicated by an asterisk ($\alpha = .05$). Scale bars = 20 μm [Color figure can be viewed at wileyonlinelibrary.com]

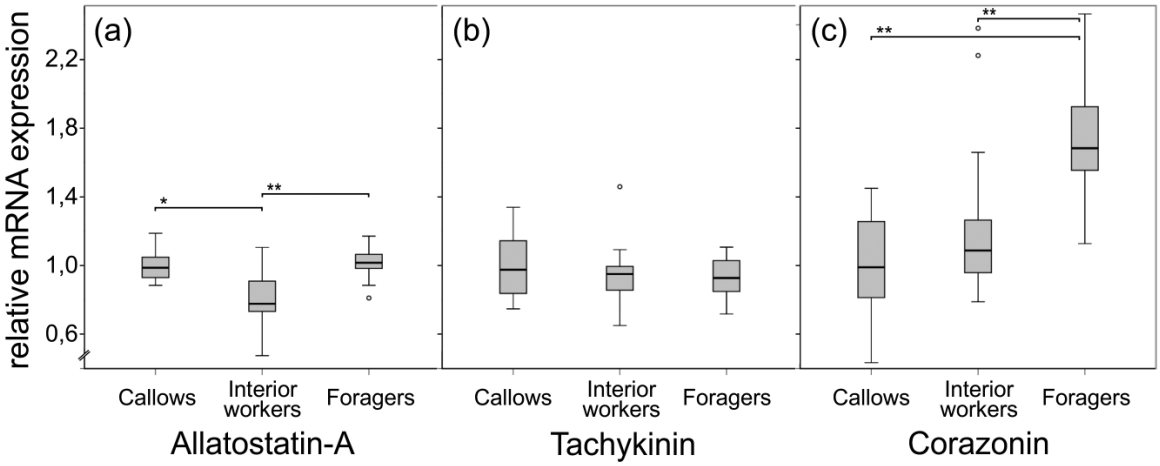

FIGURE 5 Changes of allatostatin-A (Ast-A), tachykinin (TK), and corazonin (Crz) expression in brains of ants at different behavioral stages (field study). (a) Ast-A expression in callows ($n = 8$), interior workers ($n = 16$), and foragers ($n = 12$). Ast-A expression is significantly lower in interior workers. (b) TK expression in callows ($n = 8$), interior workers ($n = 16$), and foragers ($n = 12$). TK expression remains stable throughout all behavioral stages. (c) Crz expression in callows ($n = 8$), interior workers ($n = 16$), and foragers ($n = 12$). Crz expression is significantly increased in foragers. For all neuropeptides, expression level of callows was set to one to determine relative changes compared with other behavioral stages. Boxes indicate 25th and 75th percentiles and the solid line represents the median of the data. Whiskers extend to all data points within 1.5 times of the interquartile length from the median. Outliers are shown as circle. For statistics, the Kruskal–Wallis test with Bonferroni correction was used. Significant different data are indicated by an asterisk ($\alpha = .05$)

integration (Heinze et al., 2018; Pfeiffer & Homberg, 2014; Ritzmann et al., 2012; Strausfeld & Hirth, 2013). Furthermore, the CX is involved in coordinating motor output. For example in *Drosophila*, short neuropeptide F (sNPF) and TK neurons in the CX were demonstrated to control locomotor activity. Moreover, TK-deficient individuals avoided central zones of an open arena supporting the hypothesis that TK is implicated in spatial orientation (Kahsai et al., 2010).

Using the three-dimensional atlas of the *Cataglyphis* brain as a reference (Habenstein et al., 2020), we were also able to map TK- and Ast-A-ir in less well-known CANP. In addition to the AL glomeruli and subregions of the MBs, we found TK- and Ast-A-ir in the LH, the

VLNP, and the SIP—neuropils involved in primary and high-order olfactory processing (Galizia & Rössler, 2010; Habenstein et al., 2020). Interestingly, treatments with Ast-A lead to dose-dependent impairments of associative olfactory learning in honeybees (Urlacher et al., 2016). Ast-A and TK might exert this function on intrinsic MB neurons (KCs) leading to effects on olfactory memory formation. Modulation at the level of the LH may provide the substrate for orchestrating the behavioral significance or sensitivity for olfactory stimuli, as it was demonstrated in fruit flies (Gui et al., 2017; Winther et al., 2006; Winther & Ignell, 2010) and the American cockroach (Jung et al., 2013). In addition to the OL, we also found innervation by TK- and Ast-A-ir neurons of CANPs involved in processing of visual and antennal mechanosensory input. In particular, VLNP and VMNP are important target regions of visual fiber bundles from the OL in *C. nodus* (Habenstein et al., 2020). AMMC, VLNP, and VMNP additionally receive antennal mechanosensory projections (Grob et al., 2021) and potentially gustatory input (only AMMC) from taste hairs from the antennae, as shown in *A. mellifera* (Haupt, 2007). The input of visual (VMNP, VLNP), mechanosensory (VMNP, VLNP, AMMC), olfactory (VLNP), and gustatory cues (AMMC) renders these neuropils to multimodal sensory integration centers indicating that Ast-A and TK in these neuropils may exert modulatory effects on multisensory processing.

The spatial distribution of Crz is largely conserved in insect brains (e.g., Predel et al., 2007; Roller et al., 2003; Settembrini et al., 2011; Veenstra & Davis, 1993; Wen & Lee, 2008). Corazonergic cell bodies are often located in the region of the pars lateralis and exhibit projections to the SMP and the RCC. This was also found in the honeybee and termites (Verleyen et al., 2006; Závodská et al., 2009). Similarly, in *C. nodus*, we found a cluster of four Crz-ir neurons with cell bodies located in the pars lateralis and projections to the SMP and the RCC. In addition, neurites extend into the FLA, a small subregion within the CANP. Whether this is also the case in other insects analyzed so far cannot be conclusively judged due to the lack of detailed brain atlases of the central protocerebral neuropils. As an important neurohemal organ, the RCC produces and releases hormones such as the adipokinetic hormone or JH (Diederen et al., 2002; Goldsworthy et al., 1972; Noriega, 2014; Tobe & Pratt, 1974; Tobe & Stay, 1985). JH together with the egg yolk precurser protein vitellogenin (VG) have been implicated in orchestrating the timing of behavioral transitions in social Hymenoptera (reviewed by Hamilton et al., 2017). The synthesis of JH in the corpora allata of the RCC is mediated via allatoregulatory neuropeptides from neurosecretory cells from the brain (Tobe & Stay, 1985). Although studies in other insects could demonstrate an inhibitory effect of allatostatins and stimulatory effects of allatotropins on JH biosynthesis, the underlying mechanisms seem to be complex and may vary between different species (reviewed by Stay, 2000; Bendena et al., 2020). Recent studies therefore started to speculate about the participation of further neuropeptides such as sNPF or Crz in regulating JH biosynthesis (Bendena et al., 2020; Johnson, 2017). However, so far no evidence exists in the case of Crz (Johnson, 2017). Interestingly, Crz acts antagonistically to VG in *Harpegnathos* ants and in *Drosophila* (Gospocic et al., 2017). An antagonistic relationship between JH and VG was shown to be involved in behavioral maturation of honeybee workers (reviewed by Harwood et al., 2017). Crz might act on similar pathways, which makes the potential role of an interplay between Crz, JH, and VG in behavioral maturation in social insects a highly interesting target for future studies.

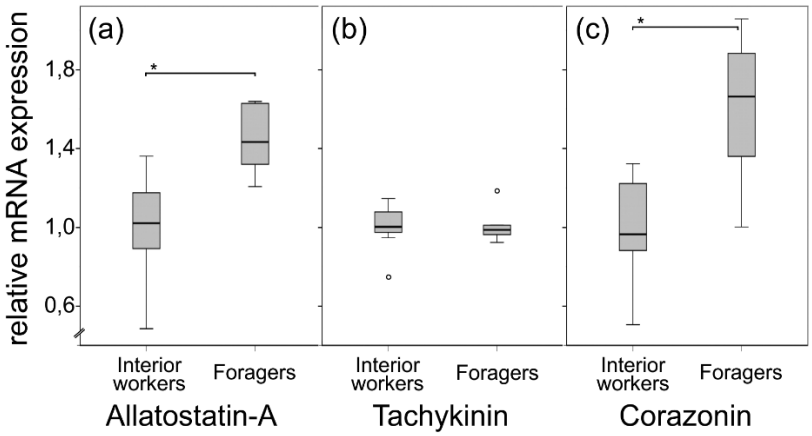

FIGURE 6 Changes of allatostatin-A (Ast-A), tachykinin (TK), and corazonin (Crz) expression in brains of interior workers and foragers (laboratory study). (a) Ast-A expression in interior workers and foragers. Ast-A expression is significantly increased in foragers. (b) TK expression in interior workers and foragers. No significant difference of the TK expression was found. (c) Crz expression in interior workers and foragers. Crz expression is significantly increased in foragers. For all neuropeptides, expression level of interior workers was set to one to determine the relative changes compared with foragers. Boxes indicate 25th and 75th percentiles and the solid line represents the median of the data. Whiskers extend to all data points within 1.5 times of the interquartile length from the median. Outliers are shown as circle. For statistics, the Mann–Whitney *U* test was used. Significant different data are indicated by an asterisk ($\alpha = .05$)

4.2 | Changes in neuropeptide expression at different behavioral stages

We had focused on Ast-A, TK, and Crz as candidate modulators of the behavioral transitions in *Cataglyphis* ants. We hypothesized if these neuropeptides act as modulators of behavioral stage transitions in adult workers, this should be reflected in changes of neuropeptide expression patterns between respective stages. In the case of Ast-A and Crz, we found clearly increased expression levels in foragers suggesting a regulatory role associated with behavioral maturation. In contrast, TK expression levels remained unchanged in *C. nodus* brains. This is different in the honeybee, where TK brain expression is upregulated in foragers (Han et al., 2021; Takeuchi et al., 2003). Manipulation experiments further indicate that TK modulates response thresholds of the proboscis extension response (PER) in a stage specific manner: Whereas TK injection decreased PER responsiveness, TK knockdown had an opposite effect (Han et al., 2021). Injection of TK and Ast-A in another study induced aggressive behavior in 7-day-old honeybee workers (Pratavieira et al., 2018). Typically, aggressive behavior is attributed to older honeybee workers compared to younger stages (Breed et al., 1990; Pearce et al., 2001; Rittschof et al., 2018). Similar observations were made in *Cataglyphis cursor* (Nowbahari & Lenoir, 1989). Schmitt et al. (2017) demonstrated slight alterations of TK innervation patterns in the CB during early stages (between Days 7 and 14) in *C. fortis* ants raised under controlled laboratory conditions. This may be related to an early transition between more or less motionless interior I- and highly mobile interior II stages in *C. fortis* (Schmid-Hempel & Schmid-Hempel, 1984). In our present work using freshly excavated natural colonies, we were not able to differentiate between these early interior substages and rather compared the three major behavioral stages—callows, interior workers, and foragers, in which we did not find significant changes in TK expression. Similarly, the TK distribution was not different between nurse and forager honeybees (Takeuchi et al., 2004). This suggests that the changes in TK innervation of the CB observed by Schmitt et al. (2017) may reflect an age-specific transition or sensitive phase during early adult development. Future work may need to focus on potential changes of TK expression at higher temporal resolution.

The changes seen in both Crz expression and expansion of Crz-ir cell body volumes suggest that this neuropeptide is a robust candidate involved in the orchestration of the interior-forager transition in *Cataglyphis*. In various insect species, Crz is associated with reproductive behavior and the control of developmental processes (e.g., Choi et al., 2005; Gospocic et al., 2017; Hou et al., 2018; Imura et al., 2020; Kim et al., 2004; Lee et al., 2008; Sugahara et al., 2018). The high concordance of findings in diverse insect taxa suggests a relatively early emergence of an ancient corazonergic pathway in the insect nervous system. Accordingly, Crz signaling could be a conserved trait that co-opted the establishment of age-related polyethism in social insects, both in Hymenoptera and Isoptera (Gospocic et al., 2017). Our finding on changes in volume of Crz-ir cell bodies together with increased expression levels in foragers further support this idea. Together with the substantial volume increase of Crz-ir cell bodies, the expression results indicate an increase of Crz also at the peptide level. However, this still needs to be confirmed in future studies, for example, using quantitative mass spectrometric approaches. Our data suggest that shifts in Crz expression levels can be attributed to the transition from interior worker to forager (nurse-forager transition), as both the cell body volumes and mRNa expression levels do not differ between callows and interior workers. This indicates that Crz may potentially alter hormone release and physiological processes during the interior-forager transition, and thus might contribute substantially to the underlying behavioral switches. However, whether the increase in Crz expression is causal in triggering the behavioral switch or rather a consequence of changes in behavior between interior workers and foragers still requires future manipulation experiments, for example, neuropeptide injections in defined behavioral phenotypes. Although this remains speculative in *Cataglyphis*, a potentially important role of Crz in regulating behavioral transitions is supported by results from Crz injections inducing a forager-like behavior in the ponerine (basal) ant species *H. saltator* (Gospocic et al., 2017). However, due to the large phylogenetic distance between the two ant species future manipulation in *Cataglyphis* are necessary to confirm this.

Leaving the social environment and darkness of the nest for the first time is probably the most far-reaching behavioral decision in the life of social insects. Accordingly, the correct timing of this transition is most important for the ecological success of a colony. Furthermore, the transition needs to be flexible and adjustable to the specific needs of a colony. This requires the control of a variety of external and intrinsic feedback mechanisms. Crz appears to be one of the key players in these complex species-specific systems, which is most likely orchestrated by further neuropeptide modulators, hormones, and biogenic amines.

5 | CONCLUSION

This study revealed the distribution of the neuropeptides Ast-A, Crz, and TK in major neuropils and less-well known central neuropils of the brain in *C. nodus* worker ants. Although differences are present between the distribution of Ast-A- and TK-ir, their wide distribution in major sensory neuropils and high-order integration centers suggests potential roles in modulating a diverse range of behavioral processes. Both Ast-A and Crz expression levels increase at the interior-forager transition, whereas TK expression levels remain unchanged. This correlates with a volumetric increase of Crz-ir cell bodies indicating a related increase in the amounts of neuropeptide. Both correlations are suggestive of a role of Crz- and Ast-A in age-related polyethism in *Cataglyphis* ants. In the light of these results, future experimental manipulations of Crz- and Ast-A levels are highly promising in revealing the specific function and causal role of these neuropeptides in modulating behavioral transitions of the ants.

ACKNOWLEDGMENTS

The authors thank the Greek government and the management board of the Strofylia National Park for the permission to perform their research in the park and to transfer *Cataglyphis* ants to Germany. The

authors are very grateful for the administrative help from Vasiliki Orfanou, Georgia Karamperou, and Christos Georgiadis and their support during their fieldwork. The authors especially thank all field assistants in the years 2018 and 2019—the study would not have been possible without arduous work even in extreme heat or during nest excavations throughout the night. The authors also thank Yasemin Brückner and Clara Tritscher for the reconstruction of neurons in Amira. Special thanks go to Kornelia Grübel (University of Würzburg) for her support with confocal-image acquisition and Susanne Neupert for suggesting volume measurements on Crz-ir cell bodies. The authors further thank E. Buchner and C. Wegener for providing the synapsin antibody, J. A. Veenstra for the kind gift of the Crz antisera, and D. Nässel for kindly providing them with TK and Ast-A antibodies. This study was supported by the German Research Foundation (DFG), DFG Ro1177/7-1 and DFG equipment grant INST 93/829-1, both to W. R. Open Access funding enabled and organized by Projekt DEAL.

CONFLICT OF INTEREST

The authors declare no conflicts of interest.

AUTHOR CONTRIBUTIONS

Wolfgang Rössler, **Jens Habenstein**, and **Markus Thamm**: Contributed to study concept and design. **Jens Habenstein**: Performed the preparations and acquisition of data. **Jens Habenstein**: Wrote the first draft of the manuscript. **Wolfgang Rössler** and **Markus Thamm**: Critically reviewed and edited the manuscript. **Wolfgang Rössler**: Obtained funding. All authors contributed to data analyses and interpretations and approved the final version of the manuscript.

PEER REVIEW

The peer review history for this article is available at https://publons.com/publon/10.1002/cne.25166.

DATA AVAILABILITY STATEMENT

The data that support the findings of this study are available from the authors upon reasonable request.

ORCID

Jens Habenstein https://orcid.org/0000-0003-3589-6436
Markus Thamm https://orcid.org/0000-0003-0480-2206
Wolfgang Rössler https://orcid.org/0000-0002-5195-8214

REFERENCES

Andreatta, G., Broyart, C., Borghgraef, C., Vadiwala, K., Kozin, V., Polo, A., Bileck, A., Beets, I., Schoofs, L., Gerner, C., & Raible, F. (2020). Corazonin signaling integrates energy homeostasis and lunar phase to regulate aspects of growth and sexual maturation in Platynereis. *Proceedings of the National Academy of Sciences of the United States of America*, *117*(2), 1097–1106.

Bendena, W. G., Hui, J. H., Chin-Sang, I., & Tobe, S. S. (2020). Neuropeptide and microRNA regulators of juvenile hormone production. *General and Comparative Endocrinology*, *295*, 113507.

Breed, M. D., Robinson, G. E., & Page, R. E. (1990). Division of labor during honey bee colony defense. *Behavioral Ecology and Sociobiology*, *27*(6), 395–401.

Buehlmann, C., Graham, P., Hansson, B. S., & Knaden, M. (2014). Desert ants locate food by combining high sensitivity to food odors with extensive crosswind runs. *Current Biology*, *24*(9), 960–964.

Carlsson, M. A., Schäpers, A., Nässel, D. R., & Janz, N. (2013). Organization of the olfactory system of Nymphalidae butterflies. *Chemical senses*, *38*(4), 355–367.

Choi, Y. J., Lee, G., Hall, J. C., & Park, J. H. (2005). Comparative analysis of Corazonin-encoding genes (Crz's) in Drosophila species and functional insights into Crz-expressing neurons. *Journal of Comparative Neurology*, *482*(4), 372–385.

Diederen, J. H., Oudejans, R. C., Harthoorn, L. F., & van der Horst, D. J. (2002). Cell biology of the adipokinetic hormone-producing neurosecretory cells in the locust corpus cardiacum. *Microscopy Research and Technique*, *56*(3), 227–236.

el Jundi, B., Pfeiffer, K., Heinze, S., & Homberg, U. (2014). Integration of polarization and chromatic cues in the insect sky compass. *Journal of Comparative Physiology A*, *200*(6), 575–589.

Fleischmann, P. N., Grob, R., Müller, V. L., Wehner, R., & Rössler, W. (2018). The geomagnetic field is a compass cue in Cataglyphis ant navigation. *Current Biology*, *28*(9), 1440–44. e2.

Fleischmann, P. N., Grob, R., Wehner, R., & Rössler, W. (2017). Species-specific differences in the fine structure of learning walk elements in Cataglyphis ants. *Journal of Experimental Biology*, *220*(13), 2426–2435.

Fricker, L. D. (2012). Neuropeptides and other bioactive peptides: From discovery to function. In *Colloquium series on neuropeptides* (pp. 1–122). Morgan & Claypool Life Sciences.

Gade, G., Hoffmann, K.-H., & Spring, J. H. (1997). Hormonal regulation in insects: Facts, gaps, and future directions. *Physiological Reviews*, *77*(4), 963–1032.

Galizia, C. G., & Rössler, W. (2010). Parallel olfactory systems in insects: Anatomy and function. *Annual Review of Entomology*, *55*, 399–420.

Godenschwege, T. A., Reisch, D., Diegelmann, S., Eberle, K., Funk, N., Heisenberg, M., Hoppe, V., Hoppe, J., Klagges, B. R. E., Martin, J. R., Nikitina, E. A., Putz, G., Reifegerste, R., Reisch, N., Rister, J., Schaupp, M., Scholz, H., Schwarzel, M., Werner, U., … Buchner, E. (2004). Flies lacking all synapsins are unexpectedly healthy but are impaired in complex behaviour. *European Journal of Neuroscience*, *20*(3), 611–622.

Goldsworthy, G., Johnson, R., & Mordue, W. (1972). In vivo studies on the release of hormones from the corpora cardiaca of locusts. *Journal of Comparative Physiology*, *79*(1), 85–96.

Gospocic, J., Shields, E. J., Glastad, K. M., Lin, Y., Penick, C. A., Yan, H., Mikheyev, A., Linksvayer, T., Garcia, B., Berger, S., Liebig, J., Reinberg, D., & Bonasio, R. (2017). The neuropeptide corazonin controls social behavior and caste identity in ants. *Cell*, *170*(4), 748–759.

Grob, R., Fleischmann, P. N., Grübel, K., Wehner, R., & Rössler, W. (2017). The role of celestial compass information in Cataglyphis ants during learning walks and for neuroplasticity in the central complex and mushroom bodies. *Frontiers in Behavioral Neuroscience*, *11*, 226.

Grob, R., Fleischmann, P. N., & Rössler, W. (2019). Learning to navigate—How desert ants calibrate their compass systems. *e-Neuroforum*, *25*(2), 109–120.

Grob, R., Tritscher, C., Grübel, K., Stigloher, C., Groh, C., Fleischmann, P. N., et al. (2021). Johnston's organ and its central projections in Cataglyphis desert ants. *Journal of Comparative Neurology*, *529*(8), 2138–2155.

Groh, C., & Rössler, W. (2011). Comparison of microglomerular structures in the mushroom body calyx of neopteran insects. *Arthropod Structure & Development*, *40*(4), 358–367.

Grünewald, B. (1999). Physiological properties and response modulations of mushroom body feedback neurons during olfactory learning in the honeybee, *Apis mellifera*. *Journal of Comparative Physiology A*, *185*(6), 565–576.

Gui, S.-H., Jiang, H.-B., Xu, L., Pei, Y.-X., Liu, X.-Q., Smagghe, G., & Wang, J. J. (2017). Role of a tachykinin-related peptide and its receptor in modulating the olfactory sensitivity in the oriental fruit fly,

Bactrocera dorsalis (Hendel). *Insect Biochemistry and Molecular Biology*, *80*, 71–78.

Habenstein, J., Amini, E., Grübel, K., el Jundi, B., & Rössler, W. (2020). The brain of Cataglyphis ants: Neuronal organization and visual projections. *Journal of Comparative Neurology*, *528*(18), 3479–3506.

Habenstein, J., Schmitt, F., Liessem, S., Ly, A., Trede, D., Wegener, C., Predel, R., Rössler, W., & Neupert, S. (2021). Transcriptomic, peptidomic and mass spectrometry imaging analysis of the brain in the ant *Cataglyphis nodus*. *Journal of Neurochemistry*.

Haehnel, M., & Menzel, R. (2010). Sensory representation and learning-related plasticity in mushroom body extrinsic feedback neurons of the protocerebral tract. *Frontiers in Systems Neuroscience*, *4*, 161.

Hamilton, A., Shpigler, H., Bloch, G., Wheeler, D. E., & Robinson, G. E. (2017). Endocrine influences on insect societies. *Hormones, Brain, and Behavior*, 421–451.

Han, B., Wei, Q., Wu, F., Hu, H., Ma, C., Meng, L., et al. (2021). Neuromodulation of behavioral specialization: Tachykinin signaling inhibits task-specific behavioral responsiveness in honeybee workers. *eLife*, *10*, e64830.

Hansen, I., Sehnal, F., Meyer, S., & Scheller, K. (2001). Corazonin gene expression in the waxmoth Galleria mellonella. *Insect Molecular Biology*, *10*(4), 341–346.

Harwood, G. P., Ihle, K. E., Salmela, H., & Amdam, G. (2017). Regulation of honeybee worker (*Apis mellifera*) life histories by vitellogenin. *Hormones, Brain, and Behavior*, 403–420.

Haupt, S. S. (2007). Central gustatory projections and side-specificity of operant antennal muscle conditioning in the honeybee. *Journal of Comparative Physiology A*, *193*(5), 523–535.

Heinze, S., Narendra, A., & Cheung, A. (2018). Principles of insect path integration. *Current Biology*, *28*(17), R1043–R1058.

Heinze, S., & Reppert, S. M. (2012). Anatomical basis of sun compass navigation I: The general layout of the monarch butterfly brain. *Journal of Comparative Neurology*, *520*(8), 1599–1628.

Hofbauer, A., Ebel, T., Waltenspiel, B., Oswald, P., Chen, Y.-C., Halder, P., et al. (2009). The Wuerzburg hybridoma library against Drosophila brain. *Journal of Neurogenetics*, *23*(1–2), 78–91.

Hölldobler, B., & Wilson, E. O. (1990). *The ants*. Harvard University Press.

Homberg, U., Heinze, S., Pfeiffer, K., Kinoshita, M., & el Jundi, B. (2011). Central neural coding of sky polarization in insects. *Philosophical Transactions of the Royal Society B: Biological Sciences*, *366*(1565), 680–687.

Hou, Q.-L., Chen, E.-H., Jiang, H.-B., Yu, S.-F., Yang, P.-J., Liu, X.-Q., Park, Y., Wang, J. J., & Smagghe, G. (2018). Corazonin signaling is required in the male for sperm transfer in the oriental fruit fly *Bactrocera dorsalis*. *Frontiers in Physiology*, *9*, 660.

Hou, Q.-L., Jiang, H.-B., Gui, S.-H., Chen, E.-H., Wei, D.-D., Li, H.-M., et al. (2017). A role of corazonin receptor in larval-pupal transition and pupariation in the oriental fruit fly *Bactrocera dorsalis* (Hendel) (Diptera: Tephritidae). *Frontiers in Physiology*, *8*, 77.

Huber, R., & Knaden, M. (2015). Egocentric and geocentric navigation during extremely long foraging paths of desert ants. *Journal of Comparative Physiology A*, *201*(6), 609–616.

Hughes, W. O., Sumner, S., van Borm, S., & Boomsma, J. J. (2003). Worker caste polymorphism has a genetic basis in Acromyrmex leaf-cutting ants. *Proceedings of the National Academy of Sciences of the United States of America*, *100*(16), 9394–9397.

Im, S. H., Takle, K., Jo, J., Babcock, D. T., Ma, Z., Xiang, Y., & Galko, M. J. (2015). Tachykinin acts upstream of autocrine hedgehog signaling during nociceptive sensitization in Drosophila. *eLife*, *4*, e10735.

Immonen, E. V., Dacke, M., Heinze, S., & el Jundi, B. (2017). Anatomical organization of the brain of a diurnal and a nocturnal dung beetle. *Journal of Comparative Neurology*, *525*(8), 1879–1908.

Imura, E., Shimada-Niwa, Y., Nishimura, T., Hückesfeld, S., Schlegel, P., Ohhara, Y., et al. (2020). The Corazonin-PTTH neuronal axis controls systemic body growth by regulating basal ecdysteroid biosynthesis in *Drosophila melanogaster*. *Current Biology*, *30*(11), 2156–65. e5.

Ito, K., Shinomiya, K., Ito, M., Armstrong, J. D., Boyan, G., Hartenstein, V., Harzsch, S., Heisenberg, M., Homberg, U., Jenett, A., Keshishian, H., Restifo, L. L., Rössler, W., Simpson, J. H., Strausfeld, N. J., Strauss, R., Vosshall, L. B., & Insect Brain Name Working Group. (2014). A systematic nomenclature for the insect brain. *Neuron*, *81*(4), 755–765.

Johnson, E. C. (2017). Stressed out insects II. Physiology, behavior, and neuroendocrine circuits mediating stress responses. *Hormones, Brain, and Behavior*, 465–481.

Jung, J. W., Kim, J.-H., Pfeiffer, R., Ahn, Y.-J., Page, T. L., & Kwon, H. W. (2013). Neuromodulation of olfactory sensitivity in the peripheral olfactory organs of the American cockroach, *Periplaneta americana*. *PLoS One*, *8*(11), e81361.

Kahsai, L., Martin, J. R., & Winther, A. M. (2010). Neuropeptides in the Drosophila central complex in modulation of locomotor behavior. *Journal of Experimental Biology*, *213*(Pt 13), 2256–2265.

Kahsai, L., & Winther, Å. M. (2011). Chemical neuroanatomy of the Drosophila central complex: Distribution of multiple neuropeptides in relation to neurotransmitters. *Journal of Comparative Neurology*, *519*(2), 290–315.

Kapan, N., Lushchak, V., Luo, J., & Nässel, D. R. (2012). Identified peptidergic neurons in the Drosophila brain regulate insulin-producing cells, stress responses and metabolism by coexpressed short neuropeptide F and corazonin. *Cellular and Molecular Life Sciences*, *69*(23), 4051–4066.

Kastin, A. (2013). *Handbook of biologically active peptides*. Academic Press.

Kim, Y.-J., Spalovská-Valachová, I., Cho, K.-H., Zitnanova, I., Park, Y., Adams, M. E., et al. (2004). Corazonin receptor signaling in ecdysis initiation. *Proceedings of the National Academy of Sciences of the United States of America*, *101*(17), 6704–6709.

Klagges, B. R., Heimbeck, G., Godenschwege, T. A., Hofbauer, A., Pflugfelder, G. O., Reifegerste, R., et al. (1996). Invertebrate synapsins: A single gene codes for several isoforms in Drosophila. *Journal of Neuroscience*, *16*(10), 3154–3165.

Ko, K. I., Root, C. M., Lindsay, S. A., Zaninovich, O. A., Shepherd, A. K., Wasserman, S. A., Kim, S. M., & Wang, J. W. (2015). Starvation promotes concerted modulation of appetitive olfactory behavior via parallel neuromodulatory circuits. *eLife*, *4*, e08298.

Kreissl, S., Strasser, C., & Galizia, C. G. (2010). Allatostatin immunoreactivity in the honeybee brain. *Journal of Comparative Neurology*, *518*(9), 1391–1417.

Kubrak, O. I., Lushchak, O. V., Zandawala, M., & Nässel, D. R. (2016). Systemic corazonin signalling modulates stress responses and metabolism in Drosophila. *Open Biology*, *6*(11), 160152.

Lee, G., Kim, K.-M., Kikuno, K., Wang, Z., Choi, Y.-J., & Park, J. H. (2008). Developmental regulation and functions of the expression of the neuropeptide corazonin in *Drosophila melanogaster*. *Cell and Tissue Research*, *331*(3), 659–673.

Lourenço, A. P., Mackert, A., dos Santos, C. A., & Simões, Z. L. P. (2008). Validation of reference genes for gene expression studies in the honey bee, *Apis mellifera*, by quantitative real-time RT-PCR. *Apidologie*, *39*(3), 372–385.

Maeno, K., Gotoh, T., & Tanaka, S. (2004). Phase-related morphological changes induced by [His7]-corazonin in two species of locusts, Schistocerca gregaria and *Locusta migratoria* (Orthoptera: Acrididae). *Bulletin of Entomological Research*, *94*(4), 349–357.

Moreira, A. C., dos Santos, A. M., Carneiro, R. L., Bueno, O. C., & Souza, D. H. F. (2017). Validation of reference genes in leaf-cutting ant *Atta sexdens* rubropilosa in different developmental stages and tissues. *International Journal of Environment, Agriculture and Biotechnology*, *2*(2), 238725.

Nässel, D. R., & Zandawala, M. (2019). Recent advances in neuropeptide signaling in Drosophila, from genes to physiology and behavior. *Progress in Neurobiology*, *179*, 101607.

Neupert, S., Fusca, D., Schachtner, J., Kloppenburg, P., & Predel, R. (2012). Toward a single-cell-based analysis of neuropeptide expression in *Periplaneta americana* antennal lobe neurons. *Journal of Comparative Neurology*, *520*(4), 694–716.

Noriega, F. G. (2014). Juvenile hormone biosynthesis in insects: What is new, what do we know, and what questions remain? *International Scholarly Research Notices*, *2014*, 1–16.

Nowbahari, E., & Lenoir, A. (1989). Age-related changes in aggression in ant *Cataglyphis cursor* (Hymenoptera, Formicidae): Influence on intercolonial relationships. *Behavioural Processes*, *18*(1–3), 173–181.

Pasch, E., Muenz, T. S., & Rössler, W. (2011). CaMKII is differentially localized in synaptic regions of Kenyon cells within the mushroom bodies of the honeybee brain. *Journal of Comparative Neurology*, *519*(18), 3700–3712.

Pearce, A., Huang, Z., & Breed, M. (2001). Juvenile hormone and aggression in honey bees. *Journal of Insect Physiology*, *47*(11), 1243–1247.

Pfeiffer, K., & Homberg, U. (2014). Organization and functional roles of the central complex in the insect brain. *Annual Review of Entomology*, *59*, 165–184.

Pratavieira, M., da Silva Menegasso, A. R., Garcia, A. M., dos Santos, D. S., Gomes, P. C., Malaspina, O., et al. (2014). MALDI imaging analysis of neuropeptides in the Africanized honeybee (*Apis mellifera*) brain: Effect of ontogeny. *Journal of Proteome Research*, *13*(6), 3054–3064.

Pratavieira, M., Menegasso, A. R. D. S., Esteves, F. G., Sato, K. U., Malaspina, O., & Palma, M. S. (2018). MALDI imaging analysis of neuropeptides in africanized honeybee (*Apis mellifera*) brain: Effect of aggressiveness. *Journal of Proteome Research*, *17*(7), 2358–2369.

Predel, R. (2001). Peptidergic neurohemal system of an insect: Mass spectrometric morphology. *Journal of Comparative Neurology*, *436*(3), 363–375.

Predel, R., Neupert, S., Russell, W. K., Scheibner, O., & Nachman, R. J. (2007). Corazonin in insects. *Peptides*, *28*(1), 3–10.

Raabe, M. (2012). *Recent developments in insect neurohormones*. Springer Science & Business Media.

Ratzka, C., Liang, C., Dandekar, T., Gross, R., & Feldhaar, H. (2011). Immune response of the ant *Camponotus floridanus* against pathogens and its obligate mutualistic endosymbiont. *Insect Biochemistry and Molecular Biology*, *41*(8), 529–536.

Reim, T., Thamm, M., Rolke, D., Blenau, W., & Scheiner, R. (2013). Suitability of three common reference genes for quantitative real-time PCR in honey bees. *Apidologie*, *44*(3), 342–350.

Rittschof, C. C., Vekaria, H. J., Palmer, J. H., & Sullivan, P. G. (2018). Brain mitochondrial bioenergetics change with rapid and prolonged shifts in aggression in the honey bee, *Apis mellifera*. *Journal of Experimental Biology*, *221*(8), jeb176917.

Ritzmann, R. E., Harley, C. M., Daltorio, K. A., Tietz, B. R., Pollack, A. J., Bender, J. A., et al. (2012). Deciding which way to go: How do insects alter movements to negotiate barriers? *Frontiers in Neuroscience*, *6*, 97.

Robinson, G. E. (1992). Regulation of division of labor in insect societies. *Annual Review of Entomology*, *37*, 637–665.

Robinson, G. E. (2002). Genomics and integrative analyses of division of labor in honeybee colonies. *The American Naturalist*, *160*(S6), S160–S172.

Roller, L., Tanaka, Y., & Tanaka, S. (2003). Corazonin and corazonin-like substances in the central nervous system of the Pterygote and Apterygote insects. *Cell and Tissue Research*, *312*(3), 393–406.

Ronacher, B. (2008). Path integration as the basic navigation mechanism of the desert ant *Cataglyphis fortis* (Forel, 1902) (Hymenoptera: Formicidae). *Myrmecological News*, *11*, 53–62.

Rössler, W. (2019). Neuroplasticity in desert ants (Hymenoptera: Formicidae)–importance for the ontogeny of navigation. *Myrmecological News*, *29*, 1–20.

Schmid-Hempel, P., & Schmid-Hempel, R. (1984). Life duration and turnover of foragers in the ant Cataglyphis bicolor (Hymenoptera, Formicidae). *Insectes Sociaux*, *31*(4), 345–360.

Schmitt, F., Stieb, S. M., Wehner, R., & Rössler, W. (2016). Experience-related reorganization of giant synapses in the lateral complex: Potential role in plasticity of the sky-compass pathway in the desert ant *Cataglyphis fortis*. *Developmental Neurobiology*, *76*(4), 390–404.

Schmitt, F., Vanselow, J. T., Schlosser, A., Wegener, C., & Rossler, W. (2017). Neuropeptides in the desert ant *Cataglyphis fortis*: Mass spectrometric analysis, localization, and age-related changes. *Journal of Comparative Neurology*, *525*(4), 901–918.

Settembrini, B. P., de Pasquale, D., Postal, M., Pinto, P. M., Carlini, C. R., & Villar, M. J. (2011). Distribution and characterization of Corazonin in the central nervous system of *Triatoma infestans* (Insecta: Heteroptera). *Peptides*, *32*(3), 461–468.

Siegmund, T., & Korge, G. (2001). Innervation of the ring gland of *Drosophila melanogaster*. *Journal of Comparative Neurology*, *431*(4), 481–491.

Siju, K., Reifenrath, A., Scheiblich, H., Neupert, S., Predel, R., Hansson, B. S., et al. (2014). Neuropeptides in the antennal lobe of the yellow fever mosquito, *Aedes aegypti*. *Journal of Comparative Neurology*, *522*(3), 592–608.

Stay, B. (2000). A review of the role of neurosecretion in the control of juvenile hormone synthesis: A tribute to Berta Scharrer. *Insect Biochemistry and Molecular Biology*, *30*(8–9), 653–662.

Stieb, S. M., Hellwig, A., Wehner, R., & Rössler, W. (2012). Visual experience affects both behavioral and neuronal aspects in the individual life history of the desert ant *Cataglyphis fortis*. *Developmental Neurobiology*, *72*(5), 729–742.

Stieb, S. M., Muenz, T. S., Wehner, R., & Rossler, W. (2010 May). Visual experience and age affect synaptic organization in the mushroom bodies of the desert ant *Cataglyphis fortis*. *Developmental Neurobiology*, *70*(6), 408–423.

Strausfeld, N. J. (2002). Organization of the honey bee mushroom body: Representation of the calyx within the vertical and gamma lobes. *Journal of Comparative Neurology*, *450*(1), 4–33.

Strausfeld, N. J., & Hirth, F. (2013). Deep homology of arthropod central complex and vertebrate basal ganglia. *Science*, *340*(6129), 157–161.

Sugahara, R., Tanaka, S., Jouraku, A., & Shiotsuki, T. (2018). Identification of a transcription factor that functions downstream of corazonin in the control of desert locust gregarious body coloration. *Insect Biochemistry and Molecular Biology*, *97*, 10–18.

Takeuchi, H., Yasuda, A., Yasuda-Kamatani, Y., Kubo, T., & Nakajima, T. (2003). Identification of a tachykinin-related neuropeptide from the honeybee brain using direct MALDI-TOF MS and its gene expression in worker, queen and drone heads. *Insect Molecular Biology*, *12*(3), 291–298.

Takeuchi, H., Yasuda, A., Yasuda-Kamatani, Y., Sawata, M., Matsuo, Y., Kato, A., Tsujimoto, A., Nakajima, T., & Kubo, T. (2004). Preprotachykinin gene expression in the brain of the honeybee *Apis mellifera*. *Cell and Tissue Research*, *316*(2), 281–293.

Tanaka, S., Zhu, D.-H., Hoste, B., & Breuer, M. (2002). The dark-color inducing neuropeptide,[His7]-corazonin, causes a shift in morphometic characteristics towards the gregarious phase in isolated-reared (solitarious) *Locusta migratoria*. *Journal of Insect Physiology*, *48*(11), 1065–1074.

Tanaka, Y., Hua, Y.-J., Roller, L., & Tanaka, S. (2002). Corazonin reduces the spinning rate in the silkworm, *Bombyx mori*. *Journal of Insect Physiology*, *48*(7), 707–714.

Tawfik, A. I., Tanaka, S., de Loof, A., Schoofs, L., Baggerman, G., Waelkens, E., et al. (1999). Identification of the gregarization-associated dark-pigmentotropin in locusts through an albino mutant. *Proceedings of the National Academy of Sciences of the United States of America*, *96*(12), 7083–7087.

Tobe, S. S., & Pratt, G. E. (1974). The influence of substrate concentrations on the rate of insect juvenile hormone biosynthesis by corpora allata of the desert locust in vitro. *Biochemical Journal*, *144*(1), 107–113.

Tobe, S. S., & Stay, B. (1985). Structure and regulation of the corpus allatum. *Advances in Insect Physiology*, *18*, 305–432.

Urlacher, E., Devaud, J.-M., & Mercer, A. R. (2019). Changes in responsiveness to allatostatin treatment accompany shifts in stress reactivity in young worker honey bees. *Journal of Comparative Physiology A*, *205*(1), 51–59.

Urlacher, E., Soustelle, L., Parmentier, M. L., Verlinden, H., Gherardi, M. J., Fourmy, D., Mercer, A. R., Devaud, J. M., & Massou, I. (2016). Honey bee allatostatins target galanin/somatostatin-like receptors and modulate learning: A conserved function? *PLoS One*, *11*(1), e0146248.

Veelaert, D., Schoofs, L., & de Loof, A. (1998). Peptidergic control of the corpus cardiacum-corpora allata complex of locusts. In *International review of cytology* (pp. 249–302). Elsevier.

Veenstra, J. A. (1991). Presence of corazonin in three insect species, and isolation and identification of [His7] corazonin from *Schistocerca americana*. *Peptides*, *12*(6), 1285–1289.

Veenstra, J. A., & Davis, N. T. (1993). Localization of corazonin in the nervous system of the cockroach *Periplaneta americana*. *Cell and Tissue Research*, *274*(1), 57–64.

Verleyen, P., Baggerman, G., Mertens, I., Vandersmissen, T., Huybrechts, J., van Lommel, A., et al. (2006). Cloning and characterization of a third isoform of corazonin in the honey bee *Apis mellifera*. *Peptides*, *27*(3), 493–499.

Verlinden, H., Gijbels, M., Lismont, E., Lenaerts, C., Broeck, J. V., & Marchal, E. (2015). The pleiotropic allatoregulatory neuropeptides and their receptors: A mini-review. *Journal of Insect Physiology*, *80*, 2–14.

Vitzthum, H., Homberg, U., & Agricola, H. (1996). Distribution of dip-allatostatin I-like immunoreactivity in the brain of the locust Schistocerca gregaria with detailed analysis of immunostaining in the central complex. *Journal of Comparative Neurology*, *369*(3), 419–437.

von Hadeln, J., Althaus, V., Häger, L., & Homberg, U. (2018). Anatomical organization of the cerebrum of the desert locust Schistocerca gregaria. *Cell and Tissue Research*, *374*(1), 39–62.

Weaver, R., & Audsley, N. (2009). Neuropeptide regulators of juvenile hormone synthesis: Structures, functions, distribution, and unanswered questions. *Annals of the New York Academy of Sciences*, *1163*(1), 316–329.

Wehner, R., & Rössler, W. (2013). Bounded plasticity in the desert ant's navigational tool kit. In *Handbook of Behavioral Neuroscience* (pp. 514–529). Elsevier.

Wen, C. J., & Lee, H. J. (2008). Mapping the cellular network of the circadian clock in two cockroach species. *Archives of Insect Biochemistry and Physiology*, *68*(4), 215–231.

Wilson, E. O. (1971). *The insect societies*. Belknap Press.

Wilson, E. O. (1980). Caste and division of labor in leaf-cutter ants (Hymenoptera: Formicidae: Atta). *Behavioral Ecology and Sociobiology*, *7*(2), 157–165.

Wilson, E. O. (1984). The relation between caste ratios and division of labor in the ant genus Pheidole (Hymenoptera: Formicidae). *Behavioral Ecology and Sociobiology*, *16*(1), 89–98.

Winther, A., & Nässel, D. (2001). Intestinal peptides as circulating hormones: Release of tachykinin-related peptide from the locust and cockroach midgut. *Journal of Experimental Biology*, *204*(7), 1269–1280.

Winther, Å. M., Acebes, A., & Ferrús, A. (2006). Tachykinin-related peptides modulate odor perception and locomotor activity in Drosophila. *Molecular and Cellular Neuroscience*, *31*(3), 399–406.

Winther, Å. M., & Ignell, R. (2010). Local peptidergic signaling in the antennal lobe shapes olfactory behavior. *Fly*, *4*(2), 167–171.

Winther, Å. M., Siviter, R. J., Isaac, R. E., Predel, R., & Nässel, D. R. (2003). Neuronal expression of tachykinin-related peptides and gene transcript during postembryonic development of Drosophila. *Journal of Comparative Neurology*, *464*(2), 180–196.

Zandawala, M., Nguyen, T., Balanyà Segura, M., Johard, H. A., Amcoff, M., Wegener, C., et al. (2021). A neuroendocrine pathway modulating osmotic stress in Drosophila. *PLoS Genetics*, *17*(3), e1009425.

Závodská, R., Wen, C.-J., Sehnal, F., Hrdý, I., Lee, H.-J., & Sauman, I. (2009). Corazonin-and PDF-immunoreactivities in the cephalic ganglia of termites. *Journal of Insect Physiology*, *55*(5), 441–449.

How to cite this article: Habenstein, J., Thamm, M., & Rössler, W. (2021). Neuropeptides as potential modulators of behavioral transitions in the ant *Cataglyphis nodus*. *Journal of Comparative Neurology*, 1–16. https://doi.org/10.1002/cne.25166

6 Discussion

6.1 General discussion

Cataglyphis desert ants have been a target of neuroethological studies for several decades [Wehner, 2019]. Thanks to meticulous work, much is known about the behavior and navigational skills of the thermophilic desert ants. *Cataglyphis* workers have a behavioral ontogeny with a marked sequence of age-related behaviors [Schmid-Hempel and Schmid-Hempel, 1984; reviewed by: Rössler, 2019]. In the present thesis, I wanted to elaborate the neuronal basis of behavioral changes in these charismatic ants, especially with respect to the temporal polyethism of the worker caste. Despite many studies on *Cataglyphis* ants, the structure and function of major brain regions are still unknown. Therefore, the thesis aimed to create a three-dimensional brain atlas including a detailed description of previously undescribed brain regions of the central protocerebrum. Applying immunohistochemistry and tracing with different fluorescent markers, a total of 33 synapsin-rich brain neuropils and 30 fiber bundles could be identified in the brain. Traceable boundaries allow a precise assignment of these neuropils. This can be used in the future to study their neurochemistry, physiology (e.g., by live-imaging techniques), and development in more detail.

My thesis focuses on investigating the potential role of neuropeptides in controlling the behavioral maturation. The three-dimensional brain atlas offers the possibility to allocate the neuropeptides to individual neuropils, including previously unknown neuropils in the central brain. However, this requires prior knowledge of which neuropeptides are present in the brain. In the second part of this thesis, I therefore did a comprehensive analysis using state of the art techniques to detect and map the complement of neuropeptides in the *Cataglyphis* brain. So far, a comprehensive neuropeptidome only existed for a single ant species, the carpenter ant *Camponotus floridanus* [Schmitt et al., 2015]. In *Cataglyphis*, only a few neuropeptides had been identified in the work of Schmitt et al. (2017). Therefore, transcriptome analyses were

performed to predict and subsequently characterize peptides in the brain of *Cataglyphis nodus* ants by using mass spectrometrical approaches. This resulted in the most comprehensive neuropeptidome of a hymenopteran species so far. In a further step, the spatial distribution of a total of 35 peptides was visualized by high-resolution MALDI-MSI on thin brain cryosections. The novel combination of MALDI-MSI data and the three-dimensional *Cataglyphis* brain atlas provides a unique tool for studying neuropeptides in insect brains at a high spatial resolution.

In the third part of this thesis, the expression of Ast-A, Crz, and TK during the behavioral maturation of *Cataglyphis* workers was studied. These neuropeptides were selected based on some knowledge of their function in other insects including social Hymenoptera. By applying immunohistochemistry and qPCR analyses, I characterized the neuropeptide distribution patterns and mRNA expression levels in callows, interior workers, and foragers. I revealed task related Ast-A and Crz mRNA levels and a substantial enlargement of the corazonergic cell bodies during the interior-forager transition. Compared with similar findings in other social insects, these results suggest a modulatory role of these neuropeptides in the temporal polyethism of *Cataglyphis* ants. The results of my thesis further demonstrate that *Cataglyphis* is an excellent experimental model to study the intrinsic mechanisms underlying the dynamic behavioral phenotypes of social insects.

6.2 The *Cataglyphis* brain

6.2.1 Brain structure

For a long time, insect research mainly focused on major brain neuropils such as the MB, the CX, the AL, and the OL. Due to new functional insights, a greater awareness of the importance of CANP emerged. Simultaneously, the introduction of a systematic nomenclature for insect brains has defined precise criteria that allow the mapping of the CANP across species [Ito et al., 2014]. Nevertheless, detailed three-dimensional

brain atlases of the CANP only exist in the fruit fly *Drosophila melanogaster* [Ito et al., 2014], the monarch butterfly *Danaus plexippus* [Heinze and Reppert, 2012], the dung beetle *Scarabaeus lamarcki* [Immonen et al., 2017], the ant *Cardiocondyla obscurior* [Bressan et al., 2015], and the desert locust *Schistocerca gregaria* [von Hadeln et al., 2018]. These neuronal atlases provide the basis for a cross-species understanding of insects' brain structure, its development, and its functionality. Here, the brain of *C. nodus* ants was reconstructed and reproducible boundaries within CANP were defined (see Manuscript I). To allow comparisons with other insects, three-dimensional data of the *Cataglyphis* brain are available online at the Insect Brain Database website (https://www.insectbraindb.org/). The general structure and overall layout of the *Cataglyphis* brain is similar compared to that of other Hymenoptera [e.g., Brandt et al., 2005; Ribi et al., 2008; Bressan et al., 2015; Groothuis et al., 2019]. The enlarged MB is a typical feature of hymenopteran brains [Brandt et al., 2005; Farris, 2013; Bressan et al., 2015; Farris, 2016] which is also reflected in the brain of *C. nodus*. As in other hymenopteran species [e.g., Brandt et al., 2005; Bressan et al., 2015; Groothuis et al., 2019], the orientation of the *Cataglyphis* brain is rotated by 90 degrees relative to its body axis compared to other insects such as dipterans, lepidopterans, and coleopterans [e.g., el Jundi et al., 2009; Huetteroth et al., 2010; Heinze and Reppert, 2012; Ito et al., 2014; Immonen et al., 2017]. Apart from that and different size ratios of individual neuropils, many similarities to other insect brains can be found in *Cataglyphis*. In all species studied so far, the CANP can be subdivided into superior neuropils, inferior neuropils, ventromedial neuropils (VMNP), ventrolateral neuropils (VLNP), and the periesophageal neuropils. Additionally, the lateral complex, the lateral horn (LH), and the AOTU are present in the investigated insect brains [Heinze and Reppert, 2012; Ito et al., 2014; Immonen et al., 2017; von Hadeln et al., 2018]. Only in a few brain regions, the *Cataglyphis* brain differs from that of the fruit flies *Drosophila melanogaster* [Ito et al., 2014]. For instance, wedge and posterior optic tubercle could not be found in *Cataglyphis*. Furthermore, the ventral complex and the clamp could not be further divided into their subneuropils. However, this could also be attributable to the different methods and genetic tools that were used in *Drosophila* research.

Future studies should therefore investigate these brain neuropils in more detail. Due to the high resolution of the protocerebral neuropils, new anatomical [Grob et al., 2021] and neuropeptidomic studies [Habenstein et al., 2021] could already use the brain atlas very efficiently.

6.2.2 Sensory pathways

Olfactory pathways have been described in detail for various insect species [reviewed by: Galizia and Rössler, 2010]. After olfactory information is received by the AL, it is transmitted via projection neurons to higher processing centers of the brain. These projection neurons extend their neurites along a set of antennal lobe tracts (ALT), with the number of ALTs differing across insect species. In *C. nodus*, five ALTs exist: the medial (m-ALT), the lateral, and three thinner mediolateral ALTs (ml-ALT). The ml-ALTs project to the superior intermediate protocerebrum, the VLNP, and the LH. The l-ALT and m-ALT run in opposite directions and exhibit arborizations into the MB calyx lip and the LH. This assembly of five ALTs and a dual olfactory pathway to the MBs seems to be conserved across hymenopteran species [Kirschner et al., 2006; Zube et al., 2008; Galizia and Rössler, 2010; Brill et al., 2015]. The dual olfactory system allows for parallel transmission of different odor properties including parallel processing and temporal (coincidence) coding of different odor attributes [Brill et al., 2013; Brill et al., 2015]. At the same time, the parallel pathway may play a crucial role in olfactory learning and memory processing. Studies suggest that one pathway might be responsible for experience-independent learning and one for experience-dependent learning [Peele et al., 2006; reviewed by: Galizia and Rössler, 2010; Rössler and Brill, 2013]. The advantages of a dual olfactory pathway might be beneficial for the specifically high demands on sophisticated olfactory processing in a social insect's life. Living in large insect societies, colony members have to recognize their nestmates by complex patterns of cuticular hydrocarbon cues [Hölldobler and Wilson, 1990]. In addition, *Cataglyphis* foragers use olfactory cues to locate their prey [Steck et al., 2011;

Buehlmann et al., 2014] and pinpoint their way back to their nest [Steck et al., 2009]. During their foraging runs, the ants can learn and discriminate a variety of odors and are able to store them in a lifelong memory [Huber and Knaden, 2018].

In contrast to the olfactory pathways, a comprehensive and detailed overview of all visual tracts is only described in a few insect species, such as bees [Hertel et al., 1987; Paulk and Gronenberg, 2008; Paulk et al., 2009] and the cockroach *Leucophaea maderae* [Reischig and Stengl, 2002]. In *Cataglyphis*, previous studies exclusively focused on two major visual tracts - the anterior superior optic tract (ASOT) and the anterior optic tract (AOT) [Grob et al., 2017; Rössler, 2019]. The ASOT has been described only in bees [Mobbs, 1984; Hertel et al., 1987; Ehmer and Gronenberg, 2002] and ants [Gronenberg, 1999; Ehmer and Gronenberg, 2004; Yilmaz et al., 2016; Grob et al., 2017]. In *Cataglyphis*, the ASOT is suggested to transmit visual information from the panoramic scenery to the ipsilateral and contralateral MB collar [Rössler, 2019]. This assumption is consistent with functional studies on other ant species, showing that lesions of MB calyces and vertical lobes impair the visual memory in navigational tasks [Buehlmann et al., 2020; Kamhi et al., 2020]. The AOT is a highly conserved visual tract across insects and relays celestial information, such as polarization patterns or chromatic cues, to the AOTU [e.g., Homberg et al., 2011; Pfeiffer and Kinoshita, 2012; Held et al., 2016; el Jundi et al., 2018; Sancer et al., 2019]. In the present thesis, I described the posterior optic commissure (POC), the inferior optic commissure (IOC), and the serpentine optic commissure in *Cataglyphis* for the first time. These visual pathways are very similar to those identified in honey bee brains [Hertel and Maronde, 1987; Hertel et al., 1987]. Moreover, I localized a previously unknown tract in the anterior region of the *Cataglyphis* brain – the optical calycal tract (OCT). The OCT forms a direct connection between the OL and the ipsilateral CO of the MB calyx. However, which visual information the tract transmits and if the tract is also present in other ant species still needs to be investigated. In this study, anterograde tracing of the visual tracts was combined with the generation of a three-dimensional brain atlas (see above). Using this new methodological approach, the projections of the visual

pathways could be assigned to individual brain neuropils. This was especially beneficial to assign the POC and IOC neurons, as the commissures exhibit many thin ramifications into the posterior central protocerebrum. POC and IOC extensively innervate the VLNP and VMNP (for more details see Manuscript I) as shown analogously in bumblebees [Paulk et al., 2008; Paulk et al., 2009] and the honey bee *Apis mellifera* [Hertel and Maronde, 1987; Hertel et al., 1987; Maronde, 1991]. In both bee species, VLNP and VMNP receive diverse visual information, ranging from chromatic cues up to detection of movement [Hertel et al., 1987; Maronde, 1991; Paulk et al., 2009]. The high similarities of the visual circuitry in *C. nodus* brains suggests that this is also likely to be the case in *Cataglyphis* ants. Recent studies additionally assigned antennal mechanosensory input to the AMMC, VLNP, and VMNP in *Cataglyphis* by using this elaborated three-dimensional *Cataglyphis* brain atlas [Grob et al., 2021]. This result further emphasizes the importance of the CANPs as multimodal sensory processing centers in *Cataglyphis* and illustrates the possibilities in the application of the neuronal atlas. The three-dimensional atlas also helps to understand the potential role of neuropeptides in the CANP (see discussion in chapter 6.3.2 and Manuscript III) and allows to compare the situation with that of other insects.

6.3 Neuropeptides in the brain of *Cataglyphis*

6.3.1 The neuropeptidome of *Cataglyphis nodus*

Recent advances in research have shown how neuropeptides control the behavioral output of insects [Fricker, 2012; Kastin, 2013; Nässel and Zandawala, 2019]. Until today, new neuropeptides are continuously being discovered and novel signaling pathways described. This highlights the need for ongoing research to unravel the neuromodulatory effects of various neuropeptides. To reach a deeper understanding of the physiological functionality of numerous neuropeptides on insect behavior, an overview of all neuropeptides in the central nervous system and their structural

assembly by amino acid sequences is necessary. In Hymenoptera, detailed neuropeptidomic studies have been performed only in the honey bee *Apis mellifera* [Hummon et al., 2006], the parasitic wasp *Nasonia vitripennis* [Hauser et al., 2010], and the carpenter ant *Camponotus floridanus* [Schmitt et al., 2015]. The present thesis aimed to obtain a comprehensive neuropeptidome in *C. nodus* ants. Combining Q-Exactive Orbitrap MS with direct tissue profiling by MALDI-TOF MS, I identified 71 peptides encoded on 49 neuropeptide-, neuropeptide-like-, and protein hormone prepropeptide genes in *C. nodus* ants (see Manuscript II). The neuropeptidome revealed many parallels to other hymenopteran species. For example, peptides of the families Ast-A, Ast-C, calcitonin-like diuretic hormone-31, Crz, myosuppressin, orcokinin, SIFamide, short neuropeptide F, and TK are present in the brain of all studied hymenopteran species [Hummon et al., 2006; Hauser et al., 2010; Schmitt et al., 2015]. Comparing exclusively the ants *C. nodus* with *C. floridanus*, the list of matches becomes even longer. This indicates that the prepropeptide genes of these two ant species are conserved to a large extend. However, some neuropeptides were identified in *C. nodus* which are not present in the *C. floridanus* neuropeptidome. Adipokinetic hormone, agatoxin-like-peptide, crustacean cardioactive peptide, elevenin, fliktin, inotocin, insulin-like peptide, Ion transport peptide-like, NVP-like peptides, pyrokinin, sulfakinin, and trissin are prominent neuropeptides identified exclusively in the *C. nodus* brain. On the other hand, HUGIN/PBAN pyrokinins are only present in *C. floridanus* and not in *C. nodus*. The higher number of identified neuropeptides in *C. nodus* can probably be related to the increasing capacities of modern MS analyzers and software tools/data bases to predict the prepropeptide genes rather than to large deviations in the ant genomes. Although the total number of peptides characterized is somewhat higher than in other hymenopteran species, it is likely that still not all neuropeptides were identified in the *Cataglyphis* brain. For instance, the brain was analyzed only in the range of 600 - 10,000 Da in the experiments. Neuropeptides with an ion mass below or above that range are therefore not included in the neuropeptidome. In addition, the transcription of some neuropeptides depends on the developmental stage of an insect, e.g., as it is known for the eclosion hormone [Truman, 1992]. To encounter stage-

related neuropeptides in the brain, neuropeptidomic studies have to be performed at all developmental stages.

By using direct tissue profiling and MSI, numerous peptides encoded on a total of 41 genes have been spatially assigned in the brain of *Cataglyphis*. Hereby, the coexistence of peptides that derived from up to 27 different genes was demonstrated within single brain regions or neuropils (see Manuscript II). This illustrates the complex local interaction of a multitude of neuromodulators, whose influence on the central nervous system is in many cases still unknown. To disentangle the interplay between neuropeptides with respect to behavioral and physiological processes, comprehensive studies on individual neuropeptides will be necessary in the future. The increasing number of sequenced ant genomes [e.g., Nygaard et al., 2011; Smith et al., 2011a; Smith et al., 2011b; Wurm et al., 2011; Oxley et al., 2014; Bohn et al., 2021] and neuropeptidome datasets available online could be a first step towards generating new genomic approaches to properly address this issue in the future.

6.3.2 Distribution of allatostatin-A, corazonin and tachykinin in the brain

A crucial question of the present thesis was whether the neuropeptide candidates Ast-A, Crz, and TK are localized in areas of the *Cataglyphis* brain in which neuromodulation could induce relevant behavioral changes. MSI provides information about the spatial distribution of neuropeptides with high resolution on thin brain sections. In *Cataglyphis*, it enabled the simultaneous localization of up to 32 peptides on a single brain slice. Since the method works independently of antibodies, it is particularly valuable for peptides where no antibody exists. However, appropriate neuronal markers are needed to assign the ion signals to individual brain neuropils which are not separated by prominent glial borders. The staining of filamentous actin was only possible on consecutive cryosections (see Manuscript II), making MSI an unsuitable tool for high spatial resolution studies of neuropeptides within individual neuropils

belonging to the CANP group. Therefore, Ast-A, Crz, and TK were instead localized by immunohistochemistry (see Manuscript III).

The neuronal composition of corazonergic neurons in the brain is largely conserved across insects [Predel et al., 2007]. Four Crz-immunoreactive (-ir) cell bodies per hemisphere are found in the *pars lateralis* of the *Cataglyphis* brain, with axons branching into the medial protocerebrum and the RCC. This is identical to findings in the closely related honey bee *Apis mellifera* [Verleyen et al., 2006]. My newly developed three-dimensional brain atlas allowed an even more precise assignment of the Crz-ir branching in the CANP in *Cataglyphis*. Here, the staining revealed that superior medial protocerebrum and flange are innervated by Crz-ir neurons. However, the relevance of these neuropils in the insect brain is still unclear. This once again exemplifies the gaps in our current knowledge about the CANPs, which needs to be addressed in the future. Of particular interest for the present research question are the conserved projections of corazonergic neurons into the RCC. Important hormones such as JH and PTTH are synthesized and released in the RCC [Agui et al., 1980; Nijhout, 1998; Noriega, 2014]. The connection from the central brain to the neurohemal organs could be an important element in controlling behavior. Previous studies already associated neurosecretory cells with JH release and linked them to the behavioral maturation of honey bees [Wheeler et al., 2015]. Whether Crz is involved in JH synthesis has not yet been sufficiently investigated across insects, but has recently been speculated [Johnson, 2017]. In *Harpegnathos saltator*, an antagonistic relationship between Crz and VG was demonstrated [Gospocic et al., 2017]. Given the complex mutual interaction of VG and JH in social Hymenoptera [e.g., Robinson and Vargo, 1997; Amsalem et al., 2014; Azevedo et al., 2016; Harwood et al., 2017], this could indicate an indirect effect of Crz on JH. Innervation of the RCC by corazonergic neurons would allow involvement in hormone release in *Cataglyphis* ants, but whether Crz affects the synthesis of VG or JH in *Cataglyphis* needs to be shown in future manipulation experiments.

Ast-A and TK neurons are virtually omnipresent in the *Cataglyphis* brain. Both neuropeptides were found at different extents in all important high order processing centers, sensory input regions as well as in the CANP (for a detailed discussion see Manuscript III). Their presence in a variety of neuropils suggests a multifunctionality of these neuropeptides in *Cataglyphis*. This would be consistent with the pleiotropic actions of TK and Ast-A shown in other insects [for reviews see: Bendena et al., 1999; Nässel et al., 2019a; Nässel et al., 2019b]. However, functional studies with TK and Ast-A in ants are missing. Therefore, the role of neuropeptides can only be speculated based on findings in other insects. For instance, the presence of neuropeptides in the CX might suggest a modulation on locomotor output. This is consistent with studies in *Drosophila melanogaster*, demonstrating a modulatory role of CX TK neurons on locomotor behavior [Kahsai et al., 2010]. Neuropeptides could also modulate behavioral output in a more indirect way. Neuromodulation of sensory input and its integration within the MB, AMMC, VLNP, or the VMNP could alter the sensitivity to a given stimulus. TK, for example, has been shown to regulate the PER response in a task-specific manner in honey bees [Han et al., 2021]. Unfortunately, the study does not answer the question if this change is a result of an altered sensitivity to the gustatory stimuli or if it occurs more downstream in the motor control centers. It is therefore important to find out what role Ast-A and TK play in the brain of *Cataglyphis*. Future studies need to show if neuropeptides might alter the sensitivity to important olfactory cues (e.g., signaling pheromones) or modulate behavioral decisions in important motor control centers and thus, contribute significantly to behavioral transitions in *Cataglyphis*.

The revealed innervation by Ast-A, Crz, and TK neurons in the central brain of *Cataglyphis* renders these neuropeptides as suitable candidates for such neuromodulations.

6.4 Neuropeptides are potential regulators of the temporal polyethism

Behavioral stage transitions of social insects are accompanied by far-reaching changes on neuronal, physiological, and behavioral levels. In particular, the transition from indoor to outdoor duties requires a completely different behavioral repertoire. This includes not only the core tasks (e.g., nursing or foraging) but also significantly affects locomotor activity [e.g., Ben-Shahar, 2005; Stieb et al., 2012], response sensitivity to a specific stimuli [e.g., Robinson, 1987a; Muscedere et al., 2012], phototaxis [e.g., Wehner et al., 1972; Menzel and Greggers, 1985; Southwick and Moritz, 1987], aggression levels [e.g., Robinson, 1987a; Nowbahari and Lenoir, 1989; Pearce et al., 2001; Rittschof et al., 2018], or the circadian rhythm [e.g., Bloch, 2010; Mildner and Roces, 2017; Beer and Bloch, 2020]. It is therefore not surprising that the control of temporal polyethism is a highly complex process involving diverse neuromodulators [reviewed by: Hamilton et al., 2017]. Whereas the role of JH has been extensively studied for several decades [for reviews see: Robinson, 1987b; Fahrbach, 1997; Hamilton et al., 2017], neuropeptides only recently came into focus. The three neuropeptides Ast-A, Crz, and TK have emerged as suitable candidates for modulating temporal polyethism [e.g., Pratavieira et al., 2014; Gospocic et al., 2017; Schmitt et al., 2017; Han et al., 2021]. In this thesis, I demonstrated that these neuropeptides are present in brain regions of *C. nodus* that potentially modulate physiological processes underlying task specific behaviors (see discussion 6.3.2 and Manuscript III). Employing immunohistochemistry and qPCR analyses, I further screened the brains of callows, interior workers, and foragers in search for any qualitative or quantitative stage-specific changes. For TK, no differences were found between the three major behavioral stages of *Cataglyphis* workers. In contrast, Ast-A and Crz mRNA expression levels are related to the task of the individual. Here, increased Crz and Ast-A mRNA levels in foragers hint towards higher translation rates of bioactive neuropeptides than in interior workers. In case of Crz, a significant enlargement of the cell bodies after the interior-forager transition additionally supports this assumption. A putative behavioral stage-related release of neuropeptides would suggest a concomitant neuromodulation

in a task-specific manner by the neuropeptides in the brain. However, evidence on the quantity of the respective neuropeptides at different behavioral stages remains to be provided in the future. In the same line, it should be noted that the mRNA quantifications were performed on whole brains, which could mask local changes in individual neurons or neuropils. In *C. fortis* ants, a modified innervation pattern by TK-ir neurons in the brain of 7- and 14-day-old workers was detected in certain subunits of the CX [Schmitt et al., 2017]. This example illustrates, that changes can occur in sensitive developmental phases at the level of brain neuropils or even individual neurons, which are not fully covered by the methodological approaches of the present study (for a more detailed discussion see Manuscript III).

The challenge for future studies is therefore to reproduce the changes of Crz and Ast-A in individual neuropils or neurons and to investigate their causal effects on the behavior at a high temporal resolution. Nowadays, diverse quantitative techniques (e.g., mass spectrometry) allow comparison of signal molecules down to the level of single cells [DeLaney et al., 2018; Diesner and Neupert, 2018] and could therefore provide an appropriate tool to investigate the neuropeptide expression in the *Cataglyphis* brain in more detail. Many further questions need to be addressed in the future in order to better understand the role of neuropeptides in behavioral transitions. This could for example be achieved by future local injections of neuropeptides, RNAi knockdowns, or gene editing approaches like CRISPR-Cas9 mediated knockouts. By using these methods, the effect of the neuropeptides on certain behaviors as well as on the biosynthesis of other neuromodulators can be tested. For instance, manipulation experiments in *Harpegnathos* ants and honey bees have demonstrated that the injection of neuropeptides or interfering RNAs is a suitable tool to address the causal impact of neuropeptides on behavior or the titer of VG [Gospocic et al., 2017; Pratavieira et al., 2018; Han et al., 2021]. These results highlight the potential of neuropeptides to act on behavioral traits associated with temporal polyethism. Considering the findings from this thesis, Ast-A and Crz are highly

promising candidates that should be further investigated in careful manipulation experiments in *Cataglyphis*.

6.5 Conclusion and Outlook

Over the last decades, *Cataglyphis* desert ants have been established as an important experimental model for studying behavior in insects [for reviews see: Wehner and Rössler, 2013; Wehner, 2019]. Besides their stunning navigational abilities, the task allocation among *Cataglyphis* workers has become a focus of research. The combination of behavioral and neuroanatomical studies has yielded unique insights into the behavioral maturation and the accompanying neuronal changes in the brain of the social insects [reviewed by: Rössler, 2019]. In this study, I investigated the neuronal basis of temporal polyethism in *C. nodus* ants. By providing an extensive neuropeptidomic data set and a three-dimensional brain atlas, I have established an unprecedented framework for in-depth studies of neuropeptides in a hymenopteran species. This opens up new possibilities for a better understanding of the behavior and the underlying physiological processes in *Cataglyphis* ants. In addition, my anatomical studies are raising awareness of the importance of previously disregarded brain regions. For instance, the complex sensory neurocircuitry in the *Cataglyphis* brain highlights the role of some CANPs as important multimodal convergence and integration centers. This should serve as an incentive to study the functioning of individual neuropils more thoroughly. Calcium imaging or genomic tools such as the expression of immediate early genes can be used to screen neuronal activity in individual brain neuropils [Gobel and Helmchen, 2007; Sommerlandt et al., 2019]. This could help to map brain areas involved in a particular behavioral output or processing specific sensory stimuli. The largely conserved general layout of insect brains suggests similar neuronal properties of individual brain neuropils. Comparative studies across species might therefore additionally help to improve our understanding of distinct quantitative and qualitative differences in the neuronal architecture and participation

of specific neuropils in neuronal processes. The neuroanatomical mapping and tracing of sensory input tracts together with mapping neuropeptides greatly helps for a general understanding of the input and its potential modulation in previously unknown brain areas. However, for a general understanding of functional aspects of these less well-known neuropils, functional studies are necessary in the future to also understand the mechanisms of modulation by neuropeptides.

The presence of more than 50 bioactive neuropeptides distributed across a small brain illustrates the complexity of neuromodulation of physiological and behavioral processes. What role do all these neuropeptides have in controlling individual behavior, physiology, and development? How do different neuromodulators such as biogenic amines, JH, and neuropeptides interact with each other? What is the influence of age, nutrition, or metabolism on modulatory systems in social insects? To disentangle these different parameters, innovative studies using integrative research approaches are necessary. This includes localizing the peptidergic neurons and their release sites, elaborating quantitative differences in age- or stage-specific features of the peptidergic signaling pathways, revealing mutual correlations with other neuromodulators, and finally, finding out their direct influence on behavior by careful manipulation experiments in combination with appropriate behavioral assays. The latter can be realized via injections of the neuropeptides or interfering RNAs into the hemolymph, as it has already been shown in bees and ants [Gospocic et al., 2017; Pratavieira et al., 2018; Han et al., 2021]. Although the application of CRISPR-Cas9 is still very difficult and very inefficient in most social insects due to complex reproduction cycles, it might be a promising tool for the future. Here, one could alternatively use clonal ants such as *Cataglyphis cursor* [Lenoir et al., 1988] or ponerine ants with substitute queens [Peeters et al., 2000]. For example, knockouts of the *orco* gene have already been performed in the clonal ants *Ooceraea biroi* [Trible et al., 2017] and *Harpegnathos saltator* ants [Yan et al., 2017]. However, it remains problematic that knockouts in embryos already influence the early development of the animals, which could lead to undesirable side effects. Therefore, a conditional knockout would

be more advantageous, but so far this is only feasible in ants with an injection of mRNAi. Such manipulation experiments can be applied to investigate the effect on the biosynthesis of important neuromodulators of the temporal polyethism (e.g., JH and VG) and the behavior of the animals. If a neuropeptide is involved in the interior-forager transition, a manipulation of the peptide titer should induce changes of the behavioral output of the individuals. For example, locomotion [Ben-Shahar, 2005; Stieb et al., 2012], aggression [Nowbahari and Lenoir, 1989; Pearce et al., 2001; Rittschof et al., 2018], or phototaxis [Wehner et al., 1972; Southwick and Moritz, 1987] are increased in exterior workers compared to interior workers in social insects. Neuronal activity in the brain could also change significantly when neuropeptide concentrations are up- or down-regulated. So far, manipulation experiments have focused mainly on behavioral effects and have not yet identified the underlying physiological changes in the brain [Gospocic et al., 2017; Pratavieira et al., 2018; Han et al., 2021]. Electrophysiological recordings could be used to detect modifications even in single neurons [Scanziani and Häusser, 2009]. In vivo calcium imaging, on the other hand, allows to examine whole brain regions for changes in neuronal activity patterns [Gobel and Helmchen, 2007; Grewe et al., 2010].

My thesis revealed a most comprehensive account of neuropeptides in an ant brain, their structural composition, and their distribution. Furthermore, from the multitude of neuropeptides in the *Cataglyphis* brain, Ast-A, Crz, and TK were identified as candidates, potentially involved in temporal polyethism. For Ast-A and Crz, stage-specific mRNA expression levels were detected for the first time in *Cataglyphis*. In addition, I provided new insights into a task-related neuroplasticity of individual neurons in the case of corazonergic neurons. It is now necessary to investigate the effect of the neuropeptides on behavior and physiological processes using the above-mentioned methodology approaches. In the view of my results, Crz and Ast-A are promising candidates that could play specific roles in the modulation of temporal polyethism.

Abbreviations

AL	antennal lobe
ALT	antennal lobe tract
AMMC	antennal mechanosensory and motor center
AOT	anterior optic tract
AOTU	anterior optic tubercle
ASOT	anterior superior optic tract
Ast-A	allatostatin-A
CANP	central adjoining neuropils
CBU/CBL	upper/lower unit of the central body
CO	collar
Crz	corazonin
CX	central complex
IOC	inferior optic commissure
Ir	immunoreactive
JH	juvenile hormone
LA	lamina
LH	lateral horn
LI	lip
LO	lobula
LX	lateral complex
MALDI-TOF	matrix-assisted laser desorption/ionization time-of-flight
MB	mushroom body
ME	medulla
ML	medial lobe

MS	mass spectrometry
MSI	mass spectrometry imaging
PED	pedunculus
PER	proboscis extension response
POC	posterior optic commissure
PTTH	prothoracicotropic hormone
OCT	optical calycal tract
OL	optic lobe
qPCR	quantitative real-time polymerase chain reaction
RCC	retrocerebral complex
TK	tachykinin
VG	vitellogenin
VL	vertical lobe
VLNP	ventrolateral neuropils
VMNP	ventromedial neuropils

Bibliography

Agosti D. Review and reclassification of Cataglyphis (Hymenoptera, Formicidae). Journal of Natural history. 1990;24(6):1457-505.

Agui N, Bollenbacher W, Granger N, Gilbert L. Corpus allatum is release site for insect prothoracicotropic hormone. Nature. 1980;285(5767):669-70.

Ament SA, Chan QW, Wheeler MM, Nixon SE, Johnson SP, Rodriguez-Zas SL, Foster LJ, Robinson GE. Mechanisms of stable lipid loss in a social insect. Journal of Experimental Biology. 2011;214(22):3808-21.

Amsalem E, Malka O, Grozinger C, Hefetz A. Exploring the role of juvenile hormone and vitellogenin in reproduction and social behavior in bumble bees. BMC evolutionary biology. 2014;14(1):1-13.

Azevedo DO, de Paula SO, Zanuncio JC, Martinez LC, Serrão JE. Juvenile hormone downregulates vitellogenin production in Ectatomma tuberculatum (Hymenoptera: Formicidae) sterile workers. Journal of Experimental Biology. 2016;219(1):103-08.

Beer K, Bloch G. Circadian plasticity in honey bees. The Biochemist. 2020;42(2):22-26.

Ben-Shahar Y. The foraging gene, behavioral plasticity, and honeybee division of labor. Journal of Comparative Physiology A. 2005;191(11):987-94.

Bendena W, Donly B, Tobe S. Allatostatins: a growing family of neuropeptides with structural and functional diversity. Annals of the New York Academy of Sciences. 1999;897(1):311-29.

Bendena WG, Hui JH, Chin-Sang I, Tobe SS. Neuropeptide and microRNA regulators of juvenile hormone production. General and comparative endocrinology. 2020;295:113507.

Bloch G. The social clock of the honeybee. Journal of biological rhythms. 2010;25(5):307-17.

Bohn J, Halabian R, Schrader L, Shabardina V, Steffen R, Suzuki Y, Ernst UR, Gadau J, Makałowski W. Genome assembly and annotation of the California harvester ant Pogonomyrmex californicus. G3. 2021;11(1):1-9.

Bolton B. An online catalog of the ants of the world. Version. 5.21. 2020.

Bonabeau E, Theraulaz G, Deneubourg J-L. Fixed response thresholds and the regulation of division of labor in insect societies. Bulletin of Mathematical Biology. 1998;60(4):753-807.

Boulay R, Aron S, Cerdá X, Doums C, Graham P, Hefetz A, Monnin T. Social life in arid environments: the case study of Cataglyphis ants. Annual review of entomology. 2017;62:305-21.

Brandt R, Rohlfing T, Rybak J, Krofczik S, Maye A, Westerhoff M, Hege HC, Menzel R. Three-dimensional average-shape atlas of the honeybee brain and its applications. Journal of Comparative Neurology. 2005;492(1):1-19.

Bressan J, Benz M, Oettler J, Heinze J, Hartenstein V, Sprecher SG. A map of brain neuropils and fiber systems in the ant Cardiocondyla obscurior. Frontiers in neuroanatomy. 2015;8:166.

Brill MF, Meyer A, Rössler W. It takes two—coincidence coding within the dual olfactory pathway of the honeybee. Frontiers in Physiology. 2015;6:208.

Brill MF, Rosenbaum T, Reus I, Kleineidam CJ, Nawrot MP, Rössler W. Parallel processing via a dual olfactory pathway in the honeybee. Journal of Neuroscience. 2013;33(6):2443-56.

Buehlmann C, Graham P, Hansson BS, Knaden M. Desert ants locate food by combining high sensitivity to food odors with extensive crosswind runs. Current Biology. 2014;24(9):960-64.

Buehlmann C, Graham P, Hansson BS, Knaden M. Desert ants use olfactory scenes for navigation. Animal Behaviour. 2015;106:99-105.

Buehlmann C, Hansson BS, Knaden M. Desert ants learn vibration and magnetic landmarks. Plos one. 2012;7(3):e33117.

Buehlmann C, Wozniak B, Goulard R, Webb B, Graham P, Niven JE. Mushroom bodies are required for learned visual navigation, but not for innate visual behavior, in ants. Current Biology. 2020;30(17):3438-43. e2.

Carlsson MA, Diesner M, Schachtner J, Nässel DR. Multiple neuropeptides in the Drosophila antennal lobe suggest complex modulatory circuits. Journal of Comparative Neurology. 2010;518(16):3359-80.

Cerdá X. Behavioural and physiological traits to thermal stress tolerance in two Spanish desert ants. Etología. 2001;9:15-27.

Chen J, Reiher W, Hermann-Luibl C, Sellami A, Cognigni P, Kondo S, Helfrich-Forster C, Veenstra JA, Wegener C. Allatostatin A Signalling in Drosophila Regulates Feeding and Sleep and Is Modulated by PDF. PLoS Genetics. 2016 Sep;12(9):e1006346.

Christ P, Reifenrath A, Kahnt J, Hauser F, Hill SR, Schachtner J, Ignell R. Feeding-induced changes in allatostatin-A and short neuropeptide F in the antennal lobes affect odor-mediated host seeking in the yellow fever mosquito, Aedes aegypti. PloS one. 2017;12(11):e0188243.

Collett M, Collett TS. Path integration: combining optic flow with compass orientation. Current Biology. 2017;27(20):R1113-R16.

Collett TS, Zeil J. Insect learning flights and walks. Current Biology. 2018;28(17):R984-R88.

Dahanukar A, Hallem EA, Carlson JR. Insect chemoreception. Current opinion in neurobiology. 2005;15(4):423-30.

DeLaney K, Buchberger AR, Atkinson L, Gründer S, Mousley A, Li L. New techniques, applications and perspectives in neuropeptide research. Journal of Experimental Biology. 2018;221(3).

Deveci D, Martin FA, Leopold P, Romero NM. AstA signaling functions as an evolutionary conserved mechanism timing juvenile to adult transition. Current Biology. 2019;29(5):813-22. e4.

Diesner M, Neupert S. Quantification of biogenic amines from individual GFP-labeled Drosophila cells by MALDI-TOF mass spectrometry. Analytical chemistry. 2018;90(13):8035-43.

Duarte A, Pen I, Keller L, Weissing FJ. Evolution of self-organized division of labor in a response threshold model. Behavioral ecology and sociobiology. 2012;66(6):947-57.

Ehmer B, Gronenberg W. Segregation of visual input to the mushroom bodies in the honeybee (Apis mellifera). Journal of Comparative Neurology. 2002;451(4):362-73.

Ehmer B, Gronenberg W. Mushroom body volumes and visual interneurons in ants: comparison between sexes and castes. Journal of Comparative Neurology. 2004;469(2):198-213.

el Jundi B, Huetteroth W, Kurylas AE, Schachtner J. Anisometric brain dimorphism revisited: implementation of a volumetric 3D standard brain in Manduca sexta. Journal of Comparative Neurology. 2009;517(2):210-25.

el Jundi B, Pfeiffer K, Heinze S, Homberg U. Integration of polarization and chromatic cues in the insect sky compass. Journal of Comparative Physiology A. 2014;200(6):575-89.

el Jundi B, Warrant EJ, Pfeiffer K, Dacke M. Neuroarchitecture of the dung beetle central complex. Journal of Comparative Neurology. 2018;526(16):2612-30.

Fahrbach SE. Regulation of age polyethism in bees and wasps by juvenile hormone. Advances in the Study of Behaviour. 1997;26:285-316.

Fahrbach SE, Van Nest BN. Synapsin-based approaches to brain plasticity in adult social insects. Current opinion in insect science. 2016;18:27-34.

Farris SM. Evolution of complex higher brain centers and behaviors: behavioral correlates of mushroom body elaboration in insects. Brain, Behavior and Evolution. 2013;82(1):9-18.

Farris SM. Insect societies and the social brain. Current opinion in insect science. 2016;15:1-8.

Field LH, Matheson T. Chordotonal organs of insects. Advances in insect physiology. 1998;27:1-228.

Fittkau EJ, Klinge H. On biomass and trophic structure of the central Amazonian rain forest ecosystem. Biotropica. 1973:2-14.

Fleischmann PN, Christian M, Müller VL, Rössler W, Wehner R. Ontogeny of learning walks and the acquisition of landmark information in desert ants, Cataglyphis fortis. Journal of Experimental Biology. 2016;219(19):3137-45.

Fleischmann PN, Grob R, Müller VL, Wehner R, Rössler W. The geomagnetic field is a compass cue in Cataglyphis ant navigation. Current Biology. 2018;28(9):1440-44. e2.

Fleischmann PN, Grob R, Wehner R, Rössler W. Species-specific differences in the fine structure of learning walk elements in Cataglyphis ants. Journal of Experimental Biology. 2017;220(13):2426-35.

Fricker LD. Neuropeptides and other bioactive peptides: from discovery to function. Colloquium Series on Neuropeptides: Morgan & Claypool Life Sciences; 2012. p. 1-122.

Galizia CG, Rössler W. Parallel olfactory systems in insects: anatomy and function. Annual review of entomology. 2010;55:399-420.

Gehring WJ, Wehner R. Heat shock protein synthesis and thermotolerance in Cataglyphis, an ant from the Sahara desert. Proceedings of the National Academy of Sciences. 1995;92(7):2994-98.

Giray T, Giovanetti M, West-Eberhard MJ. Juvenile hormone, reproduction, and worker behavior in the neotropical social wasp Polistes canadensis. Proceedings of the National Academy of Sciences USA. 2005;102(9):3330-5.

Gobel W, Helmchen F. In vivo calcium imaging of neural network function. Physiology. 2007;22(6):358-65.

Gospocic J, Shields EJ, Glastad KM, Lin Y, Penick CA, Yan H, Mikheyev AS, Linksvayer TA, Garcia BA, Berger SL. The neuropeptide corazonin controls social behavior and caste identity in ants. Cell. 2017;170(4):748-59. e12.

Grewe BF, Langer D, Kasper H, Kampa BM, Helmchen F. High-speed in vivo calcium imaging reveals neuronal network activity with near-millisecond precision. Nature methods. 2010;7(5):399-405.

Grob R, Fleischmann PN, Grübel K, Wehner R, Rössler W. The role of celestial compass information in Cataglyphis ants during learning walks and for neuroplasticity in the central complex and mushroom bodies. Frontiers in behavioral neuroscience. 2017;11:226.

Grob R, Tritscher C, Grübel K, Stigloher C, Groh C, Fleischmann PN, Rössler W. Johnston's organ and its central projections in Cataglyphis desert ants. Journal of Comparative Neurology. 2021;529(8):2138-55.

Gronenberg W. Modality-specific segregation of input to ant mushroom bodies. Brain, Behaviour and Evolution. 1999;54(2):85-95.

Gronenberg W. Subdivisions of hymenopteran mushroom body calyces by their afferent supply. Journal of Comparative Neurology. 2001;435(4):474-89.

Gronenberg W. Structure and function of ant (Hymenoptera: Formicidae) brains: strength in numbers. Myrmecological News. 2008;11:25-36.

Gronenberg W, Hölldobler B. Morphologic representation of visual and antennal information in the ant brain. Journal of Comparative Neurology. 1999;412(2):229-40.

Groothuis J, Pfeiffer K, El Jundi B, Smid HM. The Jewel Wasp Standard Brain: Average shape atlas and morphology of the female Nasonia vitripennis brain. Arthropod structure & development. 2019;51:41-51.

Gui S-H, Jiang H-B, Xu L, Pei Y-X, Liu X-Q, Smagghe G, Wang J-J. Role of a tachykinin-related peptide and its receptor in modulating the olfactory sensitivity in the oriental fruit fly, Bactrocera dorsalis (Hendel). Insect biochemistry and molecular biology. 2017;80:71-78.

Guidugli KR, Nascimento AM, Amdam GV, Barchuk AR, Omholt S, Simões ZL, Hartfelder K. Vitellogenin regulates hormonal dynamics in the worker caste of a eusocial insect. FEBS letters. 2005;579(22):4961-65.

Habenstein J, Thamm M, Rössler W. Neuropeptides as potential modulators of behavioral transitions in the ant Cataglyphis nodus. Journal of Comparative Neurology. 2021;529(12):3155-70.

Hamilton A, Shpigler H, Bloch G, Wheeler DE, Robinson GE. Endocrine influences on insect societies. Hormones, Brain, and Behavior. 2017. p. 421-51.

Han B, Wei Q, Wu F, Hu H, Ma C, Meng L, Zhang X, Feng M, Fang Y, Rueppell O. Tachykinin signaling inhibits task-specific behavioral responsiveness in honeybee workers. Elife. 2021;10:e64830.

Harwood GP, Ihle KE, Salmela H, Amdam G. Regulation of honeybee worker (Apis mellifera) life histories by vitellogenin. Hormones, Brain, and Behavior. 2017. p. 403-20.

Hauser F, Neupert S, Williamson M, Predel R, Tanaka Y, Grimmelikhuijzen CJ. Genomics and peptidomics of neuropeptides and protein hormones present in the parasitic wasp Nasonia vitripennis. Journal of proteome research. 2010;9(10):5296-310.

Heinze S, Reppert SM. Anatomical basis of sun compass navigation I: the general layout of the monarch butterfly brain. Journal of Comparative Neurology. 2012;520(8):1599-628.

Held M, Berz A, Hensgen R, Muenz TS, Scholl C, Rössler W, Homberg U, Pfeiffer K. Microglomerular synaptic complexes in the sky-compass network of the honeybee connect parallel pathways from the anterior optic tubercle to the central complex. Frontiers in behavioral neuroscience. 2016;10:186.

Hentze JL, Carlsson MA, Kondo S, Nässel DR, Rewitz KF. The neuropeptide allatostatin A regulates metabolism and feeding decisions in Drosophila. Scientific reports. 2015;5(1):1-16.

Hergarden AC, Tayler TD, Anderson DJ. Allatostatin-A neurons inhibit feeding behavior in adult Drosophila. Proceedings of the national academy of sciences. 2012;109(10):3967-72.

Hertel H, Maronde U. Processing of visual information in the honeybee brain. Neurobiology and Behavior of Honeybees. Springer; 1987. p. 141-57.

Hertel H, Schäfer S, Maronde U. The physiology and morphology of visual commissures in the honeybee brain. Journal of Experimental Biology. 1987;133(1):283-300.

Hölldobler B. Multimodal signals in ant communication. Journal of Comparative Physiology A. 1999;184(2):129-41.

Hölldobler B, Wilson EO. The ants. Harvard University Press; 1990.

Hölldobler B, Wilson EO. The superorganism: the beauty, elegance, and strangeness of insect societies. WW Norton & Company; 2009.

Homberg U, Heinze S, Pfeiffer K, Kinoshita M, el Jundi B. Central neural coding of sky polarization in insects. Philosophical Transactions of the Royal Society B: Biological Sciences. 2011;366(1565):680-87.

Honkanen A, Adden A, da Silva Freitas J, Heinze S. The insect central complex and the neural basis of navigational strategies. Journal of Experimental Biology. 2019;222(Suppl_1):jeb188854.

Huang Z-Y, Robinson G. Seasonal changes in juvenile hormone titers and rates of biosynthesis in honey bees. Journal of Comparative Physiology B. 1995;165(1):18-28.

Huber R, Knaden M. Desert ants possess distinct memories for food and nest odors. Proceedings of the National Academy of Sciences. 2018;115(41):10470-74.

Huetteroth W, El Jundi B, El Jundi S, Schachtner J. 3D-reconstructions and virtual 4D-visualization to study metamorphic brain development in the sphinx moth Manduca sexta. Frontiers in Systems Neuroscience. 2010;4:7.

Hughes WO, Sumner S, Van Borm S, Boomsma JJ. Worker caste polymorphism has a genetic basis in Acromyrmex leaf-cutting ants. Proceedings of the national Academy of Sciences. 2003;100(16):9394-97.

Hummon AB, Richmond TA, Verleyen P, Baggerman G, Huybrechts J, Ewing MA, Vierstraete E, Rodriguez-Zas SL, Schoofs L, Robinson GE. From the genome to the proteome: uncovering peptides in the Apis brain. Science. 2006;314(5799):647-49.

Hurlbert AH, Ballantyne F, Powell S. Shaking a leg and hot to trot: the effects of body size and temperature on running speed in ants. Ecological Entomology. 2008;33(1):144-54.

Im SH, Takle K, Jo J, Babcock DT, Ma Z, Xiang Y, Galko MJ. Tachykinin acts upstream of autocrine Hedgehog signaling during nociceptive sensitization in Drosophila. Elife. 2015;4:e10735.

Immonen EV, Dacke M, Heinze S, el Jundi B. Anatomical organization of the brain of a diurnal and a nocturnal dung beetle. Journal of Comparative Neurology. 2017;525(8):1879-908.

Ito K, Shinomiya K, Ito M, Armstrong JD, Boyan G, Hartenstein V, Harzsch S, Heisenberg M, Homberg U, Jenett A. A systematic nomenclature for the insect brain. Neuron. 2014;81(4):755-65.

Jackson DE, Ratnieks FL. Communication in ants. Current biology. 2006;16(15):R570-R74.

Jassim O, Huang ZY, Robinson GE. Juvenile hormone profiles of worker honey bees, Apis mellifera, during normal and accelerated behavioural development. Journal of Insect Physiology. 2000;46(3):243-49.

Johnson EC. Stressed Out Insects II. Physiology, Behavior, and Neuroendocrine Circuits Mediating Stress Responses. Hormones, Brain, and Behavior. 2017. p. 465-81.

Jung JW, Kim J-H, Pfeiffer R, Ahn Y-J, Page TL, Kwon HW. Neuromodulation of olfactory sensitivity in the peripheral olfactory organs of the American cockroach, Periplaneta americana. PloS one. 2013;8(11):e81361.

Kahsai L, Martin JR, Winther AM. Neuropeptides in the Drosophila central complex in modulation of locomotor behavior. Journal of Experimental Biology. 2010;213(Pt 13):2256-65.

Kamhi JF, Barron AB, Narendra A. Vertical lobes of the mushroom bodies are essential for view-based navigation in Australian Myrmecia ants. Current Biology. 2020;30(17):3432-37. e3.

Kapan N, Lushchak V, Luo J, Nässel DR. Identified peptidergic neurons in the Drosophila brain regulate insulin-producing cells, stress responses and metabolism by coexpressed short neuropeptide F and corazonin. Cellular and Molecular Life Sciences. 2012;69(23):4051-66.

Kastin A. Handbook of biologically active peptides. Academic press; 2013.

Kim Y-J, Spalovská-Valachová I, Cho K-H, Zitnanova I, Park Y, Adams ME, Žitňan D. Corazonin receptor signaling in ecdysis initiation. Proceedings of the National Academy of Sciences. 2004;101(17):6704-09.

Kirschner S, Kleineidam CJ, Zube C, Rybak J, Grünewald B, Rössler W. Dual olfactory pathway in the honeybee, Apis mellifera. Journal of comparative neurology. 2006;499(6):933-52.

Knaden M, Tinaut A, Stoekl J, Cerda X, Wehner R. Molecular phylogeny of the desert ant genus Cataglyphis (Hymenoptera: Formicidae). Myrmecological News. 2012;12:123- 32.

Knaden M, Wehner R. Ant navigation: resetting the path integrator. Journal of Experimental Biology. 2006;209(1):26-31.

Ko KI, Root CM, Lindsay SA, Zaninovich OA, Shepherd AK, Wasserman SA, Kim SM, Wang JW. Starvation promotes concerted modulation of appetitive olfactory behavior via parallel neuromodulatory circuits. Elife. 2015;4:e08298.

Kreissl S, Strasser C, Galizia CG. Allatostatin immunoreactivity in the honeybee brain. Journal of Comparative Neurology. 2010;518(9):1391-417.

Kubrak OI, Lushchak OV, Zandawala M, Nässel DR. Systemic corazonin signalling modulates stress responses and metabolism in Drosophila. Open biology. 2016;6(11):160152.

Kühn-Bühlmann S, Wehner R. Age-dependent and task-related volume changes in the mushroom bodies of visually guided desert ants, Cataglyphis bicolor. Journal of Neurobiology. 2006;66(6):511-21.

Lebhardt F, Ronacher B. Interactions of the polarization and the sun compass in path integration of desert ants. Journal of Comparative Physiology A. 2014;200(8):711-20.

Lebhardt F, Ronacher B. Transfer of directional information between the polarization compass and the sun compass in desert ants. Journal of Comparative Physiology A. 2015;201(6):599-608.

Lenoir A, Querard L, Pondicq N, Berton F. Reproduction and dispersal in the ant Cataglyphis cursor (Hymenoptera: Formicidae). Psyche. 1988;95(1-2):21-44.

Lin X, Smagghe G. Roles of the insulin signaling pathway in insect development and organ growth. Peptides. 2019;122:169923.

Maeno K, Gotoh T, Tanaka S. Phase-related morphological changes induced by [His7]-corazonin in two species of locusts, Schistocerca gregaria and Locusta migratoria (Orthoptera: Acrididae). Bulletin of entomological research. 2004;94(4):349.

Maronde U. Common projection areas of antennal and visual pathways in the honeybee brain, Apis mellifera. Journal of Comparative Neurology. 1991;309(3):328-40.

Matthews RW, Matthews JR. Insect behavior. Springer Science & Business Media; 2009.

McMeeking RM, Arzt E, Wehner R. Cataglyphis desert ants improve their mobility by raising the gaster. Journal of theoretical biology. 2012;297:17-25.

Menzel R. Memory dynamics in the honeybee. Journal of Comparative Physiology A. 1999;185(4):323-40.

Menzel R. Searching for the memory trace in a mini-brain, the honeybee. Learning & Memory. 2001;8(2):53-62.

Menzel R, Greggers U. Natural phototaxis and its relationship to colour vision in honeybees. Journal of Comparative Physiology A. 1985;157(3):311-21.

Mersch DP. The social mirror for division of labor: what network topology and dynamics can teach us about organization of work in insect societies. Behavioral Ecology and Sociobiology. 2016;70(7):1087-99.

Mildner S, Roces F. Plasticity of daily behavioral rhythms in foragers and nurses of the ant Camponotus rufipes: influence of social context and feeding times. PloS one. 2017;12(1):e0169244.

Mitchell B, Itagaki H, Rivet MP. Peripheral and central structures involved in insect gustation. Microscopy research and technique. 1999;47(6):401-15.

Mobbs P. Neural networks in the mushroom bodies of the honeybee. Journal of insect physiology. 1984;30(1):43-58.

Müller M, Wehner R. Wind and sky as compass cues in desert ant navigation. Naturwissenschaften. 2007;94(7):589-94.

Muscedere ML, Johnson N, Gillis BC, Kamhi JF, Traniello JF. Serotonin modulates worker responsiveness to trail pheromone in the ant Pheidole dentata. Journal of Comparative Physiology A. 2012;198(3):219-27.

Nässel DR. Functional roles of neuropeptides in the insect central nervous system. Naturwissenschaften. 2000;87(10):439-49.

Nässel DR, Pauls D, Huetteroth W. Neuropeptides in modulation of Drosophila behavior: how to get a grip on their pleiotropic actions. Current opinion in insect science. 2019a;36:1-8.

Nässel DR, Winther AM. Drosophila neuropeptides in regulation of physiology and behavior. Progress in Neurobiology. 2010;92(1):42-104.

Nässel DR, Zandawala M. Recent advances in neuropeptide signaling in Drosophila, from genes to physiology and behavior. Progress in Neurobiology. 2019.

Nässel DR, Zandawala M, Kawada T, Satake H. Tachykinins: neuropeptides that are ancient, diverse, widespread and functionally pleiotropic. Frontiers in Neuroscience. 2019b;13:1262.

Neupert S, Fusca D, Schachtner J, Kloppenburg P, Predel R. Toward a single-cell-based analysis of neuropeptide expression in Periplaneta americana antennal lobe neurons. Journal of Comparative Neurology. 2012;520(4):694-716.

Nijhout HF. Insect hormones. Princeton University Press; 1998.

Noriega FG. Juvenile hormone biosynthesis in insects: what is new, what do we know, and what questions remain? International Scholarly Research Notices. 2014;2014:967361.

Norman VC, Hughes WO. Behavioural effects of juvenile hormone and their influence on division of labour in leaf-cutting ant societies. Journal of Experimental Biology. 2016;219(1):8-11.

Nowbahari E, Lenoir A. Age-related changes in aggression in ant Cataglyphis cursor (Hymenoptera, Formicidae): influence on intercolonial relationships. Behavioural processes. 1989;18(1-3):173-81.

Nygaard S, Zhang G, Schiøtt M, Li C, Wurm Y, Hu H, Zhou J, Ji L, Qiu F, Rasmussen M. The genome of the leaf-cutting ant Acromyrmex echinatior suggests key adaptations to advanced social life and fungus farming. Genome research. 2011;21(8):1339-48.

Okamoto N, Yamanaka N. Nutrition-dependent control of insect development by insulin-like peptides. Current opinion in insect science. 2015;11:21-30.

Oxley PR, Ji L, Fetter-Pruneda I, McKenzie SK, Li C, Hu H, Zhang G, Kronauer DJ. The genome of the clonal raider ant Cerapachys biroi. Current Biology. 2014;24(4):451-58.

Pankiw T, Page Jr RE. Response thresholds to sucrose predict foraging division of labor in honeybees. Behavioral ecology and sociobiology. 2000;47(4):265-67.

Paulk AC, Dacks AM, Phillips-Portillo J, Fellous J-M, Gronenberg W. Visual processing in the central bee brain. Journal of Neuroscience. 2009;29(32):9987-99.

Paulk AC, Gronenberg W. Higher order visual input to the mushroom bodies in the bee, Bombus impatiens. Arthropod Structure & Development. 2008;37(6):443-58.

Paulk AC, Phillips-Portillo J, Dacks AM, Fellous J-M, Gronenberg W. The processing of color, motion, and stimulus timing are anatomically segregated in the bumblebee brain. Journal of Neuroscience. 2008;28(25):6319-32.

Pearce A, Huang Z, Breed M. Juvenile hormone and aggression in honey bees. Journal of Insect Physiology. 2001;47(11):1243-47.

Peele P, Ditzen M, Menzel R, Galizia CG. Appetitive odor learning does not change olfactory coding in a subpopulation of honeybee antennal lobe neurons. Journal of Comparative Physiology A. 2006;192(10):1083-103.

Peeters C, Liebig J, Hölldobler B. Sexual reproduction by both queens and workers in the ponerine ant Harpegnathos saltator. Insectes Sociaux. 2000;47(4):325-32.

Pfeffer SE, Wittlinger M. Optic flow odometry operates independently of stride integration in carried ants. Science. 2016;353(6304):1155-57.

Pfeiffer K, Homberg U. Organization and functional roles of the central complex in the insect brain. Annual review of entomology. 2014;59:165-84.

Pfeiffer K, Kinoshita M. Segregation of visual inputs from different regions of the compound eye in two parallel pathways through the anterior optic tubercle of the bumblebee (Bombus ignitus). Journal of Comparative Neurology. 2012;520(2):212-29.

Pratavieira M, da Silva Menegasso AR, Garcia AM, Dos Santos DS, Gomes PC, Malaspina O, Palma MS. MALDI imaging analysis of neuropeptides in the Africanized honeybee (Apis mellifera) brain: effect of ontogeny. Journal of proteome research. 2014 Jun 6;13(6):3054-64.

Pratavieira M, Menegasso ARdS, Esteves FG, Sato KU, Malaspina O, Palma MS. MALDI imaging analysis of neuropeptides in africanized honeybee (Apis mellifera) brain: effect of aggressiveness. Journal of proteome research. 2018;17(7):2358-69.

Predel R, Neupert S, Russell WK, Scheibner O, Nachman RJ. Corazonin in insects. Peptides. 2007;28(1):3-10.

Reischig T, Stengl M. Optic lobe commissures in a three-dimensional brain model of the cockroach Leucophaea maderae: A search for the circadian coupling pathways. Journal of Comparative Neurology. 2002;443(4):388-400.

Ribi W, Senden TJ, Sakellariou A, Limaye A, Zhang S. Imaging honey bee brain anatomy with micro-X-ray-computed tomography. Journal of Neuroscience Methods. 2008;171(1):93-97.

Rittschof CC, Vekaria HJ, Palmer JH, Sullivan PG. Brain mitochondrial bioenergetics change with rapid and prolonged shifts in aggression in the honey bee, Apis mellifera. Journal of Experimental Biology. 2018;221(8): jeb176917.

Robinson GE. Effects of a juvenile hormone analogue on honey bee foraging behaviour and alarm pheromone production. Journal of Insect Physiology. 1985;31(4):277-82.

Robinson GE. Modulation of alarm pheromone perception in the honey bee: evidence for division of labor based on hormonall regulated response thresholds. Journal of Comparative Physiology A. 1987a;160(5):613-19.

Robinson GE. Regulation of honey bee age polyethism by juvenile hormone. Behavioral ecology and sociobiology. 1987b;20(5):329-38.

Robinson GE. Regulation of division of labor in insect societies. Annual Review of Entomology. 1992;37:637-65.

Robinson GE, Page RE, Strambi C, Strambi A. Hormonal and genetic control of behavioral integration in honey bee colonies. Science. 1989;246(4926):109-12.

Robinson GE, Vargo EL. Juvenile hormone in adult eusocial Hymenoptera: gonadotropin and behavioral pacemaker. Archives of Insect Biochemistry and Physiology: Published in Collaboration with the Entomological Society of America. 1997;35(4):559-83.

Roller L, Tanaka Y, Tanaka S. Corazonin and corazonin-like substances in the central nervous system of the Pterygote and Apterygote insects. Cell and tissue research. 2003;312(3):393-406.

Ronacher B. Path integration as the basic navigation mechanism of the desert ant Cataglyphis fortis (Forel, 1902)(Hymenoptera: Formicidae). Myrmecological News. 2008;11:53-62.

Rössler W. Neuroplasticity in desert ants (Hymenoptera: Formicidae)–importance for the ontogeny of navigation. Myrmecological News. 2019;29:1-20.

Rössler W, Brill MF. Parallel processing in the honeybee olfactory pathway: structure, function, and evolution. Journal of Comparative Physiology A. 2013;199(11):981-96.

Rössler W, Groh C. Plasticity of synaptic microcircuits in the mushroom-body calyx of the honey bee. Honeybee neurobiology and behavior. 2012:141-53.

Rössler W, Zube C. Dual olfactory pathway in Hymenoptera: evolutionary insights from comparative studies. Arthropod structure & development. 2011;40(4):349-57.

Ruano F, Tinaut A, Soler, José J. High surface temperatures select for individual foraging in ants. Behavioral Ecology. 2000;11(4):396-404.

Sancer G, Kind E, Plazaola-Sasieta H, Balke J, Pham T, Hasan A, Munch LO, Courgeon M, Mathejczyk TF, Wernet MF. Modality-Specific Circuits for Skylight Orientation in the Fly Visual System. Current Biology. 2019;29(17):2812-25.e4.

Scanziani M, Häusser M. Electrophysiology in the age of light. Nature. 2009;461(7266):930-39.

Schmid-Hempel P, Schmid-Hempel R. Life duration and turnover of foragers in the antCataglyphis Bicolor (Hymenoptera, Formicidae). Insectes sociaux. 1984;31(4):345-60.

Schmitt F, Stieb SM, Wehner R, Rössler W. Experience-related reorganization of giant synapses in the lateral complex: Potential role in plasticity of the sky-compass pathway in the desert ant Cataglyphis fortis. Developmental neurobiology. 2016;76(4):390-404.

Schmitt F, Vanselow JT, Schlosser A, Kahnt J, Rossler W, Wegener C. Neuropeptidomics of the carpenter ant Camponotus floridanus. Journal of Proteome Research. 2015;14(3):1504-14.

Schmitt F, Vanselow JT, Schlosser A, Wegener C, Rossler W. Neuropeptides in the desert ant Cataglyphis fortis: Mass spectrometric analysis, localization, and age-related changes. Journal of Comparative Neurology. 2017;525(4):901-18.

Schultz TR. In search of ant ancestors. Proceedings of the National Academy of Sciences. 2000;97(26):14028-29.

Schulz DJ, Huang Z-Y, Robinson GE. Effects of colony food shortage on behavioral development in honey bees. Behavioral Ecology and Sociobiology. 1998;42(5):295-303.

Shorter JR, Tibbetts EA. The effect of juvenile hormone on temporal polyethism in the paper wasp Polistes dominulus. Insectes sociaux. 2009;56(1):7-13.

Smith CD, Zimin A, Holt C, Abouheif E, Benton R, Cash E, Croset V, Currie CR, Elhaik E, Elsik CG. Draft genome of the globally widespread and invasive Argentine ant (Linepithema humile). Proceedings of the National Academy of Sciences. 2011a;108(14):5673-78.

Smith CR, Smith CD, Robertson HM, Helmkampf M, Zimin A, Yandell M, Holt C, Hu H, Abouheif E, Benton R. Draft genome of the red harvester ant Pogonomyrmex barbatus. Proceedings of the National Academy of Sciences. 2011b;108(14):5667-72.

Sommer S, Wehner R. Leg allometry in ants: extreme long-leggedness in thermophilic species. Arthropod structure & development. 2012;41(1):71-77.

Sommerlandt FM, Brockmann A, Rössler W, Spaethe J. Immediate early genes in social insects: a tool to identify brain regions involved in complex behaviors and molecular processes underlying neuroplasticity. Cellular and Molecular Life Sciences. 2019;76(4):637-51.

Song W, Veenstra JA, Perrimon N. Control of lipid metabolism by tachykinin in Drosophila. Cell reports. 2014;9(1):40-47.

Southwick EE, Moritz RF. Social control of air ventilation in colonies of honey bees, Apis mellifera. Journal of insect physiology. 1987;33(9):623-26.

Steck K, Hansson BS, Knaden M. Smells like home: Desert ants, Cataglyphis fortis, use olfactory landmarks to pinpoint the nest. Frontiers in Zoology. 2009;6(1):1-8.

Steck K, Hansson BS, Knaden M. Desert ants benefit from combining visual and olfactory landmarks. Journal of Experimental Biology. 2011;214(8):1307-12.

Stieb SM, Hellwig A, Wehner R, Rössler W. Visual experience affects both behavioral and neuronal aspects in the individual life history of the desert ant Cataglyphis fortis. Developmental neurobiology. 2012;72(5):729-42.

Stieb SM, Muenz TS, Wehner R, Rossler W. Visual experience and age affect synaptic organization in the mushroom bodies of the desert ant Cataglyphis fortis. Developmental Neurobiology. 2010 May;70(6):408-23.

Stone T, Webb B, Adden A, Weddig NB, Honkanen A, Templin R, Wcislo W, Scimeca L, Warrant E, Heinze S. An anatomically constrained model for path integration in the bee brain. Current Biology. 2017;27(20):3069-85. e11.

Sugahara R, Tanaka S, Jouraku A, Shiotsuki T. Identification of a transcription factor that functions downstream of corazonin in the control of desert locust gregarious body coloration. Insect biochemistry and molecular biology. 2018;97:10-18.

Sullivan JP, Fahrbach SE, Robinson GE. Juvenile hormone paces behavioral development in the adult worker honey bee. Horm Behav. 2000;37(1):1-14.

Szyszka P, Galkin A, Menzel R. Associative and non-associative plasticity in Kenyon cells of the honeybee mushroom body. Frontiers in Systems Neuroscience. 2008;2:3.

Tanaka S, Zhu D-H, Hoste B, Breuer M. The dark-color inducing neuropeptide,[His7]-corazonin, causes a shift in morphometic characteristics towards the gregarious phase in isolated-reared (solitarious) Locusta migratoria. Journal of Insect Physiology. 2002a;48(11):1065-74.

Tanaka Y, Hua Y-J, Roller L, Tanaka S. Corazonin reduces the spinning rate in the silkworm, Bombyx mori. Journal of insect physiology. 2002b;48(7):707-14.

Tawfik AI, Tanaka S, De Loof A, Schoofs L, Baggerman G, Waelkens E, Derua R, Milner Y, Yerushalmi Y, Pener MP. Identification of the gregarization-associated dark-pigmentotropin in locusts through an albino mutant. Proceedings of the National Academy of Sciences. 1999;96(12):7083-87.

Theraulaz G, Bonabeau E, Denuebourg J. Response threshold reinforcements and division of labour in insect societies. Proceedings of the Royal Society of London Series B: Biological Sciences. 1998;265(1393):327-32.

Toth AL, Kantarovich S, Meisel AF, Robinson GE. Nutritional status influences socially regulated foraging ontogeny in honey bees. Journal of Experimental Biology. 2005;208(24):4641-49.

Toth AL, Robinson GE. Worker nutrition and division of labour in honeybees. Animal behaviour. 2005;69(2):427-35.

Trible W, Olivos-Cisneros L, McKenzie SK, Saragosti J, Chang N-C, Matthews BJ, Oxley PR, Kronauer DJ. Orco mutagenesis causes loss of antennal lobe glomeruli and impaired social behavior in ants. Cell. 2017;170(4):727-35. e10.

Truman JW. The eclosion hormone system of insects. Progress in brain research. 1992;92:361-74.

Turner-Evans DB, Jayaraman V. The insect central complex. Current Biology. 2016;26(11):R453-R57.

Urlacher E, Devaud J-M, Mercer AR. Changes in responsiveness to allatostatin treatment accompany shifts in stress reactivity in young worker honey bees. Journal of Comparative Physiology A. 2019;205(1):51-59.

Urlacher E, Soustelle L, Parmentier ML, Verlinden H, Gherardi MJ, Fourmy D, Mercer AR, Devaud JM, Massou I. Honey Bee Allatostatins Target Galanin/Somatostatin-Like Receptors and Modulate Learning: A Conserved Function? PLoS One. 2016;11(1):e0146248.

Veenstra JA. Isolation and structure of corazonin, a cardioactive peptide from the American cockroach. FEBS letters. 1989;250(2):231-34.

Veenstra JA, Davis NT. Localization of corazonin in the nervous system of the cockroach Periplaneta americana. Cell and tissue research. 1993;274(1):57-64.

Verleyen P, Baggerman G, Mertens I, Vandersmissen T, Huybrechts J, Van Lommel A, De Loof A, Schoofs L. Cloning and characterization of a third isoform of corazonin in the honey bee Apis mellifera. Peptides. 2006;27(3):493-99.

Verlinden H, Gijbels M, Lismont E, Lenaerts C, Broeck JV, Marchal E. The pleiotropic allatoregulatory neuropeptides and their receptors: A mini-review. Journal of insect physiology. 2015;80:2-14.

von Hadeln J, Althaus V, Häger L, Homberg U. Anatomical organization of the cerebrum of the desert locust Schistocerca gregaria. Cell and tissue research. 2018;374(1):39-62.

Wang C, Chin-Sang I, Bendena WG. The FGLamide-allatostatins influence foraging behavior in Drosophila melanogaster. PloS one. 2012;7(4):e36059.

Weaver R, Audsley N. Neuropeptide regulators of juvenile hormone synthesis: structures, functions, distribution, and unanswered questions. Annals of the New York Academy of Sciences. 2009;1163(1):316-29.

Wehner R. The ant's celestial compass system: spectral and polarization channels. Orientation and communication in arthropods. Springer; 1997. p. 145-85.

Wehner R. Desert ant navigation: how miniature brains solve complex tasks. Journal of Comparative Physiology A. 2003;189(8):579-88.

Wehner R. The Cataglyphis Mahrèsienne: 50 years of Cataglyphis research at Mahrès. Journal of Comparative Physiology A. 2019;205(5):641-59.

Wehner R, Harkness RD, Schmid-Hempel P. Foraging strategies in individually searching ants. Fischer; 1983.

Wehner R, Herrling P, Brunnert A, Klein R. Periphere Adaptation und zentralnervöse Umstimmung im optischen System von Cataglyphis bicolor (Formicidae, Hymenoptera). Revue suisse de zoologie. 1972:197-228.

Wehner R, Müller M. The significance of direct sunlight and polarized skylight in the ant's celestial system of navigation. Proceedings of the National Academy of Sciences. 2006;103(33):12575-79.

Wehner R, Räber F. Visual spatial memory in desert ants, Cataglyphis bicolor (Hymenoptera: Formicidae). Experientia. 1979;35(12):1569-71.

Wehner R, Rössler W. Bounded Plasticity in the Desert Ant's Navigational Tool Kit. Handbook of Behavioral Neuroscience. 2013;22:514-29.

Wehner R, Wehner S. Parallel evolution of thermophilia: daily and seasonal foraging patterns of heat-adapted desert ants: Cataglyphis and Ocymyrmex species. Physiological entomology. 2011;36(3):271-81.

Wheeler MM, Ament SA, Rodriguez-Zas SL, Southey B, Robinson GE. Diet and endocrine effects on behavioral maturation-related gene expression in the pars intercerebralis of the honey bee brain. Journal of Experimental Biology. 2015;218(24):4005-14.

Whitfield CW, Cziko A-M, Robinson GE. Gene expression profiles in the brain predict behavior in individual honey bees. Science. 2003;302(5643):296-99.

Willot Q, Gueydan C, Aron S. Proteome stability, heat hardening and heat-shock protein expression profiles in Cataglyphis desert ants. Journal of Experimental Biology. 2017;220(9):1721-28.

Wilson EO. Caste and division of labor in leaf-cutter ants (Hymenoptera: Formicidae: Atta). Behavioral ecology and sociobiology. 1980;7(2):157-65.

Wilson EO. The relation between caste ratios and division of labor in the ant genus Pheidole (Hymenoptera: Formicidae). Behavioral Ecology and Sociobiology. 1984;16(1):89-98.

Winther ÅM, Acebes A, Ferrús A. Tachykinin-related peptides modulate odor perception and locomotor activity in Drosophila. Molecular and cellular neuroscience. 2006;31(3):399-406.

Wittlinger M, Wehner R, Wolf H. The ant odometer: stepping on stilts and stumps. Science. 2006;312(5782):1965-67.

Wolf H, Wittlinger M, Pfeffer SE. Two distance memories in desert ants—Modes of interaction. PloS one. 2018;13(10):e0204664.

Wurm Y, Wang J, Riba-Grognuz O, Corona M, Nygaard S, Hunt BG, Ingram KK, Falquet L, Nipitwattanaphon M, Gotzek D. The genome of the fire ant Solenopsis invicta. Proceedings of the National Academy of Sciences. 2011;108(14):5679-84.

Yack JE. The structure and function of auditory chordotonal organs in insects. Microscopy research and technique. 2004;63(6):315-37.

Yan H, Opachaloemphan C, Mancini G, Yang H, Gallitto M, Mlejnek J, Leibholz A, Haight K, Ghaninia M, Huo L. An engineered orco mutation produces aberrant social behavior and defective neural development in ants. Cell. 2017;170(4):736-47. e9.

Yang A. Seasonality, division of labor, and dynamics of colony-level nutrient storage in the ant Pheidole morrisi. Insectes Sociaux. 2006;53(4):456-62.

Yilmaz A, Lindenberg A, Albert S, Grübel K, Spaethe J, Rössler W, Groh C. Age-related and light-induced plasticity in opsin gene expression and in primary and secondary visual centers of the nectar-feeding ant Camponotus rufipes. Developmental neurobiology. 2016;76(9):1041-57.

Závodská R, Wen C-J, Sehnal F, Hrdý I, Lee H-J, Sauman I. Corazonin-and PDF-immunoreactivities in the cephalic ganglia of termites. Journal of insect physiology. 2009;55(5):441-49.

Zube C, Kleineidam CJ, Kirschner S, Neef J, Rössler W. Organization of the olfactory pathway and odor processing in the antennal lobe of the ant Camponotus floridanus. Journal of Comparative Neurology. 2008;506(3):425-41.

Danksagung

Eine Doktorarbeit ist weit mehr als nur ein wissenschaftliches Werk, das zu Papier gebracht wurde. Eine Doktorarbeit ist vielmehr ein ganzer Lebensabschnitt, in dem man Höhen wie Tiefen durchläuft und welcher einen für das weitere Leben prägt. Meine persönlichen Erfahrungen werden mir hierbei immer in gutem Gedächtnis bleiben und mir hoffentlich den Weg in eine positive Zukunft ebnen. Dass ich diesen Lebensabschnitt erfolgreich bewältigen konnte, habe ich auch der hilfreichen Unterstützung einiger wichtigen Personen zu verdanken.

An erster Stelle möchte ich **Wolfgang Rössler** danken. Wolfgang, durch dich wurde mir dieser unvergessliche Lebensabschnitt überhaupt erst ermöglicht. Du hast mich vor gut 6 Jahren mit deiner Vorlesung über die Navigation in *Cataglyphis* Ameisen erstmals für dieses Thema faszinieren können. Du hast mir die Chance eröffnet, mich an deinem Lehrstuhl in dieses großartige Thema einzuarbeiten und diese Faszination über diese winzigen Multitalente mit dir zu teilen. Ich danke dir, dass du mir stets mit deiner Erfahrung eine große Hilfe warst und mir gleichzeitig den nötigen Freiraum gewährt hast mich als Wissenschaftler zu verwirklichen.

Durch die umfangreiche Expertise von **Susanne Neupert** konnte ich bereits seit meiner Masterarbeit im Bereich der Massenspektrometrie unheimlich profitieren. Susanne, durch die Zusammenarbeit mit dir ist ein großartiges Projekt entstanden, das tieferen Einblick in die Welt der Neuropeptide bei *Cataglyphis* Ameisen ermöglicht. Was mir persönlich noch viel wichtiger ist - während der intensiven Zusammenarbeit in Köln, auf Konferenzen oder mit einem Gläschen Wein auf der alten Mainbrücke, konnte ich dich als Mensch kennenlernen und schätzen.

Christian Wegener stellt einen schier unendlichen Fundus an Wissen über Neuropeptide in Insekten dar. Christian, danke, dass du mir bei meinem Weg stets mit Rat und Tat zur Seite gestanden hast. Vielen Dank für die ertragreiche Zusammenarbeit und dass du mir dabei immer ein offenes Ohr geliehen hast.

Ein großer Dank geht auch an **Franzi**, die mich während meiner Masterarbeit betreut hat und mir den Einstieg in meine Zeit als Doktorand erleichtert hat. Franzi, durch dich konnte ich mich für diese wunderbaren Tiere begeistern und viel für meinen weiteren Werdegang lernen.

Vielen Dank möchte ich all meinen fantastischen Zimmerkollegen/-innen aussprechen. Mit **My** konnte ich meine ersten Schritte in der Forschung gehen. Unvergessen bleibt die gemeinsame Zeit, als wir beide noch in der wissenschaftlichen Kinderstube steckten. Ob im Büro, Göttingen, Australien oder auch mal Abseits der Arbeit – es war immer eine schöne Zeit mit dir. **Conny**, durch dich habe ich viel gelernt und noch heute Blicke ich ein klein wenig neidisch auf deine ausgezeichneten Fähigkeiten unter dem Bino. Am meisten werde ich aber unsere langen Diskussionen über Gott und die Welt vermissen. Neben meinen Dank möchte ich dir auch alles Gute in deiner neuen Rolle als Oma wünschen. **Nadine** und **Katja**, ich bin sehr froh, dass ich euch beide kennen- und schätzen lernen durfte. Ich werde immer auf eine angenehme Zeit samt großartigen Gesprächen zurückblicken. **Emad**, auch wenn ich dir das ein oder andere Mal „I told you“ sagen musste, hast du mit deiner akribischen Arbeit den Grundstock für unsere gemeinsame Publikation gelegt. Gerne erinnere ich mich an Griechenland zurück, als wir zusammen in der Sonne geschwitzt aber auch viel gelacht haben. Mit einem weinenden Auge werde ich irgendwann auf die einmalige Zeit mit euch allen zurückblicken. Diese Hilfsbereitschaft und freundliche Atmosphäre ist nicht selbstverständlich und hat mir viel während dieses Lebensabschnittes gegeben.

Bester Dank geht auch an **Robin** und **Pauline**. Durch die Forschung an unseren geliebten Sechsbeinern durfte ich euch beide näher kennenlernen und auf eine schöne gemeinsame Zeit zurückblicken. Auch möchte ich der gesamten **AG Rössler** für eine wunderbare Arbeitsatmosphäre danken. Mit **Claudi**, **Tom**, **Schmalz**, **Martin**, **Mira, Anne** und **Ayse** durfte ich wunderbare Menschen kennenlernen, die mir bei sämtlichen Problemen zur Seite standen und gleichzeitig auch mal für ein Bierchen Abseits der Arbeitszeit zu haben waren. Gleiches gilt für den Rest der **Zoologie II** - vielen Dank euch allen für die wunderschöne Zeit!

Ich bedanke mich auch bei **Basil** und **Markus**. Ihr beide wart jeweils in einem Projekt wichtiger Ansprechpartner für mich und ich konnte viel durch euer Wissen lernen. Zudem danke ich allen weiteren Co-Autoren. Danke **Reinhard**, **Sander**, **Alice** und **Dennis** für die Zusammenarbeit im MSI Projekt. Danke auch an die komplette **AG Predel** in Köln, die mich immer wunderbar „beherbergt“ hat und mit denen ich eine schöne Zeit verbringen durfte. Danke an die Kollaborateure in Griechenland. Ohne **Christos Georgiadis** von der Universität Athen, **Maria** und **Olga** aus dem Schinias Nationalpark sowie **Vasiliki** und **Georgia** aus dem Strofylia Nationalpark hätte sich mir die wunderbare Welt der *Cataglyphis* Ameisen in ihren natürlichen Lebensraum in Griechenland nicht erschlossen.

Ein besonderer Dank gilt allen, die mir bei der Versorgung der Ameisen geholfen haben. Danke **Viviana** und **Daniela**. Gleiches gilt für alle Studenten, die ich betreuen durfte und/oder die mich mit hervorragenden Daten versorgt haben. Neben **Emad** gilt dies insbesondere für **Alex**, **Yasemin, Clara** und **Sousan**. Ganz nebenbei seid ihr alle sehr feine Zeitgenossen, mit denen es Spaß gemacht hat zu arbeiten. Natürlich möchte ich auch allen danken, die in Griechenland geholfen haben Ameisen zu markieren und die bei nächtlichen Ausgrabungsaktionen gefühlt um den Verstand gekommen sind.

Nicht zuletzt möchte ich mein gesamtes privates Umfeld danken. Den vergangenen Lebensabschnitt konnte ich nur durch die Unterstützung durch **Freunde** und **Familie** bewältigen. Ihr wart in guten wie in schlechten Zeiten immer für mich da und habt mir geholfen den Kopf auch mal von der Arbeit freizubekommen. **Adi, Kilian** und **Armin**, danke, dass ihr euch die Zeit genommen habt diese Arbeit nochmal Korrektur zu lesen. Ein besonderer Dank geht an **Vanessa**. Du hast mich immer unterstützt und mich durch Lob und Tadel zu Höchstleistungen angespornt. Ich bin mir sicher, dass wir auch in Zukunft alle Hürden gemeinsam bewältigen. Selbstverständlich gebührt meinen **Eltern** das wohl größte Dankeschön. Nicht nur, dass es mich ohne euch überhaupt nicht gäbe. Nein, ihr habt mir schon immer auf all meinen Wegen eure volle Unterstützung und Liebe gewährt. Danke, ohne euch wäre das alles niemals möglich gewesen!

List of publications

Peer-reviewed articles

Habenstein J, Thamm M, Rössler W. Neuropeptides as potential modulators of behavioral transitions in the ant *Cataglyphis nodus*. Journal of Comparative Neurology. 2021;529(12):3155-3170.

Habenstein J, Schmitt F, Liessem S, Ly A, Trede D, Wegener C, Predel R, Rössler W, Neupert S. Transcriptomic, peptidomic and mass spectrometry imaging analysis of the brain in the ant *Cataglyphis nodus*. Journal of Neurochemistry. 2021;158(2):391-412

Habenstein J, Amini E, Grübel K, el Jundi B, Rössler W. The brain of *Cataglyphis* ants: neuronal organization and visual projections. Journal of Comparative Neurology. 2020;528(18):3479-506.

Lyutova R, Selcho M, Pfeuffer M, Segebarth D, Habenstein J, Rohwedder A, Frantzmann F, Wegener C, Thum AS, Pauls D. Reward signaling in a recurrent circuit of dopaminergic neurons and peptidergic Kenyon cells. Nature communications. 2019;10(1):1-14.

Poster presentations

Habenstein J, Amini E, Thamm M, el Jundi B, Neupert S, Rössler W. Neuropeptides as potential modulators of the behavioral-stage transitions in the ant *Cataglyphis nodus*. 14th Göttingen Meeting of the German Neuroscience Society (2021). Virtual conference.

Habenstein J, Schmitt F, Amini E, Thamm M, Predel R, Wegener C, Neupert S, Rössler W. Neuropeptides in *Cataglyphis* desert ants and their role as potential modulators of behavior. 13th Göttingen Meeting of the German Neuroscience Society (2019). Göttingen, Germany.

Habenstein J, Schmitt F, Thamm M, Predel R, Wegener C, Neupert S, Rössler W. Neuropeptides as potential modulators of the behavioral-stage transitions in the desert ant *Cataglyphis noda*. International Congress of Neuroethology (2018). Brisbane, Australia.

Habenstein J, Schmitt F, Ly A, Trede D, Predel R, Wegener C, Rössler W, Neupert S. Identification and localization of neuropeptides in the brain of *Cataglyphis* desert ants using imaging mass spectrometry. European Mass Spectrometry Conference (2018). Saarbrücken, Germany.

Habenstein J, Schmitt F, Predel R, Wegener C, Rössler W, Neupert S. Identification and localization of neuropeptides in the brain of *Cataglyphis* desert ants using imaging mass spectrometry. 12th Göttingen Meeting of the German Neuroscience Society (2017). Göttingen, Germany.

ORAL PRESENTATIONS

Habenstein J. Neuropeptides in Cataglyphis desert ants and their role as potential modulators of behavior. 30th NeuroDoWo (2019). Würzburg, Germany.

Habenstein J. Neuromodulatory influences on behavioral stage transitions in *Cataglyphis* desert ants. Guest talk at the Institut für Biologie 1, Zoologie (2017). Freiburg, Germany.

Habenstein J. Neuromodulatory influences on behavioral stage transitions in *Cataglyphis* desert ants. *Cataglyphis* workshop (2017). Würzburg, Germany.

Habenstein J, Neupert S, Schmitt F, Predel R, Wegener C, Rössler W. Identification and localization of neuropeptides in the brain of *Cataglyphis* desert ants using mass spectrometry imaging. 14th Rauischholzhausen Seminar (2016). Development and Plasticity of the insect nervous system.